MACQUARIE UNIVERSITY SYDNEY

Proteomics of adipose derived cells and secretions

Implications for renal failure

Michael John Medynskyj

Bachelor of Biomedical Science - Honours

Supervised by

VC Innovation fund fellow

Dr Benjamin R. Herbert PhD

Macquarie University Sydney

Faculty of Science, Department of Chemistry and Biomolecular Sciences

Submitted for review: July 2012

Final submission: April 2013

Table of Contents

Abstract

Adipose tissue is now viewed as an important endocrine organ through the actions of adipokines; and a source of multipotent adult mesenchymal stem cells termed adipose derived stem cells, or ADSCs. Adipokines, the term used for the protein secretions from adipose tissue, have been shown to have broad ranging effects on the body and have been shown to be involved in the pathogenesis or amelioration of disease processes. The paracrine effects of secretions from ADSCs have been shown to be the major driving force behind the therapeutic benefits of ADSC treatments in most cases. The work described here utilised protein secretion preparations derived from rodent and human adipose tissue produced *in vitro* to assess the potential of a secretion mixture as a therapeutic agent for renal disease. Renal disease is a growing problem world-wide with relatively little improvement in treatment regimens or drug effectiveness in the past twenty years.

This thesis combines knowledge from the growing field of adipose cell-derived regenerative medicine and novel xenogeneic applications of proteomic techniques to test the effects of adipose tissue secretions on renal cells. Xenogeneic cell-based assays were developed to test the effects of the human adipose secretions on rodent primary renal cells (PRCs) and Madin-Darby canine kidney cells (MDCK cells). Novel applications of multiplexed cytokine assays were combined with quantitative proteomic analysis in order to gain a complex and meaningful understanding of the effects of the secretions on primary and immortalised renal cells. Simultaneous analysis of the secretory response to treatment by the PRCs and the uptake of human adipose secretions by the cells were performed, providing novel data on biological effects of the adipose secretions and the relevance of certain cytokines within the preparation. Proteomic analysis indicate broad suppression of TGF-β signalling pathways, increased resistance to apoptosis, altered cytoskeletal organisation and increased mitotic potential in the treated renal cell populations; effects that appear beneficial to the recovery from renal disease processes.

Declaration

The work presented within this thesis is original and of my own conduction. It was begun at the University of Technology Sydney in 2008 and was then transferred (with myself) to Macquarie University Sydney in early 2010 through all formal and necessary channels. It has not been submitted for the award of any other degree or diploma at any other university or institution.

Candidate:

Michael John Medynskyj

Signed:

.....

Acknowledgments

This thesis is dedicated to all of the people who have helped, inspired and invested in me. You have made it possible for me to complete something I never thought myself capable of and for that, I thank you all.

To Mum and Tony, thanks for supporting me through all my long years at university and providing me with the drive to finally get it done. Mum, you always let me be me and *always* did what was best; you are truly a strong woman. I love you and I am proud of you.

To Dad, Nancy and Matthew, thanks for the faith in me, the pride in your eyes and in your voice and the hundreds of hot meals provided on those Monday evenings (yum!). Dad, you have always seen more in me than I saw in myself and have always pushed me to go further. Thank you all for that love, faith and vision, I love you.

To Lizzy, the little pixie, your positive attitude and light heartedness, deep soul and tremendous creativity has been a huge inspiration to me. Thanks for always being you and always being an amazing sister. You're "the duck's guts!"

To Dr Ben Herbert, taking Honours with you at UTS changed my life forever. You made me see science for what it really is. Working in your labs has been the best experience of my life so far. Your humorous approach to life and 'unconventional' approach to supervision have made my years at UTS and MQU unforgettable. You are not just a supervisor, you are a dear friend. I look forward to your continued success and hope to continue to learn from you for as long as possible.

To Dr Graham Vesey, I thank you for the amazing opportunities you have given me over the years and for the continued investment in me in the form of employment and scholarships over the course of this project. Your (and Bens) investment made all this work possible. Your work ethic drives those around you to excel and has made me want more from life and my career. I have learned a lot from you and look forward to continuing to do so in the future.

To everyone at Regeneus Ltd., thanks for the chance to better myself and learn from you all. Not everyone is so lucky to have such friendly and intelligent co-workers and friends.

I would like to acknowledge and thank Macquarie University for supporting me through the award of a Macquarie University Research Excellence Scholarship (MQRES). My attendance would not have been possible without this funding. Human tissue samples were also obtained under approval of the Macquarie University Human Ethics Research Committee, approval reference # 5201100385.

To Cameron Hill, your friendship and guidance has been instrumental in shaping the way I see things in the lab. Thanks for always being cool and always having great technical tips and suggestions. Our discussions of computer games and internet culture (mostly failblog.org) have been hugely entertaining.

Thanks to Edmond Breen for all the assistance with statistical analysis. The insight I had into your world of math fascinated and scared me.

To Dr Matthew Padula, thanks for the great memories at UTS of Mass spec, beer, 'cactus juice', metal music screaming out of the lab and the mountain biking sessions. You're a cool dude and a passionate scientist.

To Sinead Blaber, thanks for your sharp mind, keen sense of humour and for just being a good friend. You have a very bright future ahead! P.s. your fear of tape is still hilarious.

To Rebecca Webster, cheers for the support, understanding and great sense of humour; working with you has never been dull and probably never will be.

To Mitchell Burrett, thanks for never being politically correct (especially at work!) and always being a kind and considerate friend.

To Michael Sivell, those two years or so where we were like best friends were the craziest and most entertaining I have ever had. I will never forget the mistake I made; and for it, I am sorry. You are a talented scientist and have the guts to use that talent, I have no doubt you will go very far.

To Jerran Santos, thanks for the crazy times, the pub "craw!s" and great beer and KFC fuelled adventures. We've had some amazing times!

To Katherine, Peter and everyone else at the UTS and Macquarie labs; thanks for the laughs, the support and for providing a great environment for science and social adventures.

To Rennick, Chris and Audrey, my best friends; thanks for all the support, good times and belief that I would get there eventually. I could not have done this without your help, you are family to me. Stay cool!

Finally, to Elia Gina Madonna; thanks for making these last months of thesis writing manageable. Your love, support, quirkiness, humour and the occasional kick up the bum have made it possible for me to get through this without going completely insane. I Love you.

Chapter 1: Introduction

The role of adipose tissue secreted proteins in stem-cell based regenerative medicine: Implications for renal failure

1.1 Introduction:

Adipose tissue (fat) performs a large range of functions in the mammalian body. There are two major types of adipose tissue, brown and white. Brown adipose tissue is present predominantly in bone marrow and serves as a rapid source of heat due to high levels of mitochondria and the brown fat mitochondria-specific protein uncoupling protein 1 [1]. White adipose tissue (WAT) has been viewed as primarily responsible for the storage and release of energy in the form of triacylglycerol. In the past ten to fifteen years, the conventional view on WAT has been expanded to include an array of secretory proteins that have systemic endocrine effects. These endocrine proteins, usually termed adipokines, are key players in whole-body homeostasis with established links to cardiovascular health, insulin resistance and sensitivity, pro and anti-inflammatory states, kidney function and of course, energy storage and release. WAT has also been identified as a rich source of mesenchymal stem cells (MSC) termed adipose derived stem cells (ADSC), also called adipose stromal cells (ASC). ADSCs have been shown to aid in the amelioration of a large number of diseases both *in vitro* and *in vivo*; these actions have been heavily associated with the ADSC secretory repertoire of bioactive proteins and cytokines.

In general, the investigation of white adipose tissue (WAT) has centred on the connection between circulating adipokine levels in different disease states with a view to establishing a causative or predicitive link between a particular adipose tissue secreted factor and a given disease. However, increasing investigation of these factors has shown a growing number of them have beneficial effects on cell stress, blood pressure, insulin sensitivity, atherosclerosis inhibition, angiogenesis and immune responses. When combined with the already sizeable knowledge on the beneficial effects of stem cell secretions it is logical to propose that an *in vitro* preparation of WAT and ADSC protein secretions may prove to be beneficial when administered to a tissue in a given disease state. This chapter

will elaborate on the functions and effects of some major adipokines and ADSC secretions with a distinct view to their relation to renal failure. Renal failure is a disease which has had little significant improvement in therapeutic management in the last 20 years and whose prevalence is expected to rise exponentially in humans and animals due to increasing levels of obesity and diabetes in the developed world.

Research into regeneration of damaged tissues has found adult stem cells in many more tissues and organs than was thought to be the case a decade ago. Adipose tissue has become known as a major source of mesenchymal ADSCs [2]. These are similar in many respects to the MSCs sourced from the bone marrow stroma, termed bone marrow mesenchymal stem cells (BMSC); or commonly just referred to as MSC. Technologies utilising MSCs from bone marrow and adipose tissue are currently being used for academic and therapeutic applications in conditions like arthritis [3], myocardial infarction [4-6], stroke [7], multiple sclerosis [8], acute ischemic renal failure [9], liver cirrhosis [10], hair growth [11] and wound healing [12-14]. The ADSCs present in WAT are part of the family of mesenchymal stem cells very similar to BMSC. Bone marrow has been the conventional and most investigated source of MSCs in the literature, and their use in research and some therapeutics continue to this day. ADSCs have very similar functionality to BMSCs, but are present at up to 500 times more per gram of tissue, a great boon to the researcher and clinician alike. The reason for the relatively high level of ADSCs in WAT is currently unknown; however it is possible that they are linked to the need for WAT to remain plastic as a tissue on the whole. WAT functions to expand and contract in size depending on stored lipid levels and food availability; thus requiring the ability to change its connective tissue properties and its blood supply to cope with increased demand for oxygen in times of prosperity and an increased ability to dispose of unnecessary cells or blood vessels in times of famine. This may also explain the high levels of tissue macrophages within WAT, perhaps aiding in connective tissue remodelling in times of feast; and in excess cell disposal during famine.

Both BMSCs and ADSCs are capable of *in vitro* differentiation into adipogenic, osteogenic, chondrogenic and myogenic lineages [2]. White adipose tissue as a source of cells is easier to obtain, requiring common liposuction techniques rather than the painful extraction of bone marrow aspirate. ADSCs present a major advantage over bone marrow MSCs because no cell culture is required to obtain a therapeutic dose of cells. This reduces

treatment times, reduces possible changes to the cells during *in vitro* manipulation and allows for autologous cell-based therapy without expansion. The discovery of high yield adult mesenchymal stem cells in adipose tissue has led to the utilisation of WAT as a source of 'point-of care' cell-based regenerative treatments for both animals and humans [8].

Recent findings have demonstrated that ADSC secretions can have beneficial effects on tissue regeneration and wound healing [12,13], suggesting that protein or metabolite secretions from these cells contribute significantly to their ability to aid tissue regeneration and resolving of inflammation. It is clear from the literature that implanted adult mesenchymal stem cells home to the site of injury or inflammation and secrete a range of immune-modulating cytokines and trophic factors. Their secretions appear to be regulated by local stimuli at the implant site or their engraftment site after homing. The secretome is defined as the complement of secreted proteins from a cell population or tissue. When secretome studies are performed *in vitro*, the culture media, oxygen level, culture confluence and other factors can significantly alter the secretion profile of ADSCs [11].

White adipose tissue has been identified as a key endocrine organ, secreting a wide range of proteins dubbed 'adipokines'. The discovery of adipokines (defined here as the complement of proteins released from whole WAT); and ADSCs, have sparked a great deal of interest in WAT and have been the major driving force behind a recent explosion in adipokine research. Many investigations into the secretome of adipocytes, whole WAT and ADSCs have been conducted with a view to understanding the therapeutic or pathologic 'value' of one particular secreted protein to a given disease [15-18]. Not surprisingly, the results of these studies have been varied and interestingly, little overlap between whole WAT secretions and ADSC secretions has been demonstrated. This is likely a result of differences in the secretion levels of the ADSCs compared to other cells within WAT. Adipokines have been shown to affect insulin sensitivity/resistance [19-21], inflammation [22,23], appetite [24], energy storage and expenditure [25], reproduction [24], blood pressure [26,27], angiogenesis [28] and many other bodily processes.

Mesenchymal stem cells, in the form of ADSCs and BMSCs have been successfully used to treat many different diseases in the literature both *in vitro* and *in vivo*. In the 1980's and 1990's many studies attempted to treat animal models of organ damage or chronic

failure, with a stem cell differentiation-based hypothesis. That is, the target organ required 'regeneration' and the implanted ADSCs or BMSCs would be able to differentiate *in vivo* and substantially drive the replacement of damaged or lost cells of the target organ. The conventional theories of mesenchymal stem cell therapeutics are derived from embryonic and haematopoietic stem cells; and centre on the differentiation of the injected stem cells into cells of the damaged tissue. However, growing evidence suggests that in many cases this is not the case. Proteins secreted by ADSCs or BMSCs have been shown to induce tissue repair to a level comparable to actual stem cell transplants; and indeed in experiments where preparations of secretions have been compared to treatments with stem cells, little to no evidence of stem cell differentiation is commonly observed [9,13,29,30].

As adipose tissue is an organ that does not mobilise cells throughout the body to perform its numerous functions, it is therefore logical that the functions of WAT other than lipid storage are completed via its *secretome*. There have been several studies linking adipose tissue with actions of the hypothalamus and immune system [31-33]. Adipokines have been found to have influences on body weight [34], inflammation [31,32], blood clotting [35], insulin resistance and sensitivity [36], diabetes and atherosclerosis [18]. It has been reported that there are up to 50 adipokines, including putative identifications; relatively few with characterised functions [37,38]. In the area of secreted proteins or factors and their effects on pain and inflammation, it is now known that the secretions of mesenchymal stem cells have positive effects on inflammation and cellular stress [30,39-42], although the exact mechanisms are not fully understood. In general, the very broad literature on MSCs and their secretions describes positive effects on reducing inflammation, promoting angiogenesis, accelerating wound healing and decreasing cell death after ischemia [13,30,39-42]. Many of these demonstrate a 'repair at a distance' effect. Both BMSCs and ADSCs have been described as factories for cytokines and other bioactive secretions [43] and also as trophic mediators [44]. Trophic mediators are cells capable of influencing surrounding cells directly or indirectly using secretions, whilst not inducing a phenotypic change within themselves. This ability makes these cells important candidates for cell-based therapeutic tools, potentially capable of administering beneficial protein secretions to a diseased tissue at appropriate bioactive levels. A crucial aspect of MSC therapeutics is the context and location dependant nature of

the secretome. The secretome can vary depending on tissue oxygenation, local tissue stress, inflammation and the presence/activity of local or invading immune cells [44].

1.2 The use of ADSCs and BMSCs to treat diseases: evidence for secretions as the effectors

Togel *et al* [9] tested the effectiveness of bone marrow-derived MSC treatment to rats with induced acute renal failure. The group noted that MSC treated animals had significantly improved renal function, lower cell death and higher cell proliferation indices. The group did establish that a number of MSCs did remain within the kidneys using *in vivo* fluorescence tracking however found no evidence of MSC differentiation into either tubular or endothelial cells within the treated kidneys three days post-treatment. Togel *et al* [9] observed a decreased level of pro-inflammatory cytokines interleukin 1 beta (IL-1β), tumour necrosis factor alpha (TNF-α) and interferon gamma (IFN-γ) while also noting a dramatic increase in a range of anti-inflammatory cytokines, including interleukin-10 (IL-10), basic fibroblast growth factor (bFGF), transforming growth factor-alpha (TGF-α) and B-cell lymphoma-2 protein (Bcl-2). The lack of differentiation of MSCs observed and the apparent modulation of the local immune system through altered cytokine expression in the MSC treated kidneys indicates a key role for cellular secretions in tissue regeneration. Togel *et al.* conducted an exhaustive investigation into the presence of MSCs in not only the kidney, but also the lungs, liver spleen and bone marrow; using *in vivo* live-cell imaging techniques, sex-mismatched host and donor cells for FISH immunofluorescent staining, and PCR-detection of Y-chromosome containing donor MSCs. After twenty-four hour post-infusion, the only tissue with detectable levels of MSC was the lung. This has led to the groups' assertion that the differentiation of the MSCs into functional cells of the kidney is not the primary mode of repair at least in the short term, indicating that the MSC secretions play a major role in post-ischemic acute renal damage recovery. The significance of secretory factors is also supported by other notable scientists in the field like Professor Arnold Caplan [45,46].

Further work completed by Togel *et al* [29] has expanded on the view that the secretory actions of infused MSCs are the primary motivators of renal tissue repair post-injury. The group assessed the effect of infused murine primary MSC into kidneys subjected to acute ischemia/reperfusion (I/R) injury after 24 hours and at 5 days post-injury. The group identified that MSC infusion results in a 'rapid' (24hr) recovery from I/R injury over fibroblast

treated controls. The group did not identify any engrafted MSC within the treated kidneys at twenty-four hours and only low levels at five days (approximately one cell per tissue section). They also stated that the levels of MSC identifiable within these kidneys using tissue sectioning and immunofluorescent staining do not account for the increase in renal function of these animals, indicating an integral role of MSC secretions. Furthermore, Togel *et al* [29] conducted *in vitro* testing of MSC secretions on primary murine aortic endothelial cells, as a model for the secretions effects on endothelial cells of the kidney. The group identified a significant stimulatory effect on the growth of the aortic endothelial cells at five days treatment. They also demonstrated a significant anti-apoptotic effect on the cells over control media after twenty-four hours treatment with ATP depletion agent antimycin A. This is an example of how MSC secretions can be produced *in vitro* for therapeutic use.

The infusion of ADSCs and MSCs has been shown to be an effective treatment for many diseases in recent studies. Due to the growing body of evidence that suggests that cellular secretions are the major effecting force behind these benefits, the question must be asked: is it possible to produce the secretions *in vitro*, administer them to a diseased tissue and observe the same or similar effects as ADSC/MSC infusion?

In an attempt to elucidate the effects of *in vitro* produced secretions, Oh *et al* [13] assessed the effects of administered GFP labelled mesenchymal stem cells (MSC) and MSC conditioned media (MSC-CM) on chemically burnt rodent corneas *in vivo*. Whilst they concluded that treatment with MSCs produced the most beneficial effect on decreased corneal neovascularisation, they also observed a dose-dependent benefit from using MSC-CM treatments which was significantly better than non-treated controls. These findings suggest that much of the corneal recovery is driven through secretory cross-talk between the MSCs and the insulted tissue, indicating that treatment of tissue trauma may be possible using repeat administration of stem cell secretions. This shows that MSCs are capable of producing cytokines at bioactive levels *in vitro* and that they are able to be utilised effectively *in vivo*, an important finding.

Furthermore, Shabbir *et al* [30] demonstrated that MSCs have been shown to greatly increase the recovery of experimental animals in induced myocardial infarction. However, Shabbir *et al* [30] also state that the myocardial recruitment and engraftment of the MSCs

after administration is too low to explain the functional recovery observed in the heart. That is, the number of MSCs recruited to the infarctions site was far less than required to actually replace the number of dead cells within the tissue. Shabbir *et al* [30] tested the trophic ability of transplanted MSCs by treating TO2 cardiomyopathic hamsters with repeated doses of isolated porcine MSCs injected intramuscularly into the leg, or with repeat doses of porcine MSC conditioned media (MSC-CM) produced *in vitro*. The group was able to show that the injected cells remained at their site of injection, so no possibility of differentiation of the MSCs to replace the damaged heart tissue was present; there was also no host immune reaction to the implanted porcine cells reported. Results for both the MSC treated group and the MSC-CM treated group showed marked functional recovery over non-treated controls. This demonstrates how important the secretory component of stem cell therapy is to the regenerative process. Additionally, it demonstrates the effectiveness of xenogeneic MSC-based secretion treatments and shows that implanted MSCs are able to evade a host immune response and still provide appropriate secretory signals to promote healing, even when administered in a xenogeneic fashion. Xenogeneic MSC administration is now well documented in many animal models to be safe and effective as reviewed by Arnold Caplan [47]. This opens up many potential avenues of investigation *in vitro,* and is of particular importance to the work reported in later chapters of this thesis where a preparation of human adipose secretions have been used to treat rodent and canine renal cells *in vitro*.

1.3 The study of white adipose tissue (WAT):

Two important areas of research have arisen out of the study of adipose tissue. The first is the study of increased adiposity, adipokine expression levels and their possible links with diseases. These include cardiovascular disease [48], atherosclerosis [18], hypertension [49], asthma [50,51] and allergic sensitisation [52]; and the collection of symptoms loosely labelled the 'metabolic syndrome' *i.e.* the combination of obesity, high cholesterol, hypertension, insulin resistance; and pro-thrombotic and pro-inflammatory states [53]. The second research branch is being conducted for a different purpose; cells from WAT stromal vascular fraction, individual ADSC populations have been isolated and utilised to ameliorate a number of disease states in both clinical and laboratory settings. Examples include myocardial infarction [5,6,30], multiple sclerosis [8], acute ischemia/reperfusion and experimentally induced renal failure [9,42,54-56], arthritis [3,57], ischemic limb disease [58] and recovery from high dose

chemotherapy [40]. Current research is investigating how the same tissue can have both beneficial and detrimental effects through the secretion of both pro-inflammatory and anti-inflammatory proteins. The secretome of WAT has been found to swing to a pro-inflammatory state in obese humans and animals [53,59]; whereas anti-inflammatory adipokines have been found to be secreted at comparatively higher levels in non-obese subjects. Adipose tissue is now commonly referred to as a pro-inflammatory endocrine organ because of the significantly increased circulating levels of IL-6, MCP-1, and TNF-α that are associated with increasing obesity.

1.4 Adipokines:

Kershaw and Flier [60], Fain *et al* [15] and Frayn *et al* [25] acknowledge the presence and contribution of the non-adipocyte cells in adipose tissue. They also indicate that the heterogeneity of WAT and the presence of different secretory cells is what make WAT a true endocrine organ. The findings of Fain *et al*. state that over 90% of the secretions from adipose tissue detected were derived from non-adipocyte cells. Weisberg *et al* [61] have shown macrophages to be the major source of tumour necrosis factor alpha (TNF-α) produced by WAT and contributors to approximately fifty percent of WAT derived interleukin-6 (IL-6). Macrophages have been found to constitute up to ten percent of the stromal vascular fraction (SVF) of WAT [62]. The level of macrophages in WAT has been shown to be positively correlated with increasing obesity, which partially explains the increased levels of circulating pro-inflammatory factors found in obese subjects.

A short list of some of the proteins that have been identified as adipokines from WAT in the literature has been provided in table 1. This critical review will explore the functions of the adipokines that have been shown to positively or negatively affect the pathogenesis of renal failure and its associated diseases.

Table 1: Proteins described as major adipokines and ADSC secretions in the literature.

Adipokine name:	Function(s):	References:
Adiponectin	Anti-inflammatory, insulin sensitising properties. Circulating levels decrease with increasing obesity. Anti-atherogenic properties. Production is inhibited by TNF-α and IL-6. Inhibits the functions of TNF-α *in vivo*. Induces the production of anti-inflammatory cytokines IL-10 and IL-1Ra. Widely acknowledged cardio-protective effects.	15,35,36,59,63-66
Leptin	Many and varied roles in energy storage, localisation and expenditure; actions on hypothalamus and wound healing. Obese subjects have increased circulating leptin levels.	15,26,59,63,67-71
Resistin	Implicated in regulation of blood glucose, diabetes and atherosclerosis pathology. Elevated in patients with end-stage renal disease (ESRD).	59,72-74
Tumour necrosis factor alpha (TNF-α)	Major pro-inflammatory cytokine. May have immunomodulatory role in resolution of inflammatory responses. Elevated circulating levels in obese subjects.	15,35,59
Interleukin 6 (IL-6)	Pro-inflammatory cytokine. IL-6 deficient mice develop obesity. Increased expression is induced by TNF-α.	35,59,75,76
Interleukin 1β (IL-1 β)	Pro-inflammatory cytokine. Expressed rapidly after tissue damage. Induces CRP production, neutrophil, insulin and cortisol release.	15,18,77-79
Adrenomedullin	Possible cardioprotective and anti-microbial actions. Dose dependant anti-inflammatory actions.	38,80-84
Interleukin 10 (IL-10)	Important immunomodulatory cytokine. Regulation of TNF-α, IFN-γ and IL-6 expression in monocytes.	15,85-88
Monocyte chemoattractant protein 1 (MCP-1)	Expressed by adipocytes and increased in circulation in obesity. Chemoattractant for monocytes and T-lymphocytes. Increases the expression of monocyte adhesion molecules on endothelial cells and monocytes to increase tissue invasion capability. Some implications in tissue damage by inflammatory cells in cardiovascular and renal diseases.	59,89-91
Plasminogen activator inhibitor 1 (PAI-1)	Belongs to the serine protease inhibitor family. Key regulator of fibrinolysis. Also inhibits cell adhesion to extracellular matrix. Stimulatory and inhibitory roles in angiogenesis.	15,35,92
Visfatin	May have insulin mimetic effects. Increases expression of IL-6 in monocytes. Down-regulated by IL-6 and TNF-α in adipocytes *in vitro*.	59,93-95
Hepatocyte growth factor (HGF)	Integral growth factor in liver regeneration. Effects on regeneration of many other organs. Expressed in almost all developing epithelial tissues in embryogenesis. Angiogenic factor. Significant effects on renal regeneration in a range of renal failure models.	15,96-100
Vascular endothelial growth factor (VEGF)	Expression induced by hypoxia, some cytokines and activated oncogenes. Induces endothelial cell proliferation and endothelial cell, monocyte, and pericyte migration. Holds anti-apoptotic properties. Some anti-inflammatory effects through actions on local dendritic cells.	15,101-103
Vaspin	Member of the serine protease inhibitor family. Insulin sensitising effects. Circulating levels increased in obesity. Can decrease the expression of leptin, resistin and TNF-α while increasing adiponectin synthesis.	21,104

1.4.1 Adiponectin:

Adiponectin has high potential from a treatment and tissue regeneration perspective. Adiponectin is an anti-inflammatory and insulin sensitising adipokine secreted from adipocytes [105]. Circulating adiponectin levels are reduced in states of obesity; thus it has been investigated for links between obesity and obesity associated diseases. These include cardiovascular disease [63,105], atherosclerosis [53], type 2 diabetes [106] asthma [51,107] and other allergic sensitisations [108]. The anti-atherogenic properties of adiponectin stem from its ability to inhibit the adhesion of macrophages to endothelial cells even when they are stimulated by TNF-α, which aids in the process of macrophage-endothelial cell adhesion. Adiponectin also inhibits the transformation of infiltrated macrophages to foam cells in the blood vessel intima [109]. It has been found to inhibit the expression of vascular cell adhesion molecule 1 (VCAM-1) mRNA [110], the protein product of which aids in the adhesion of leukocytes to endothelial cells so they can infiltrate the vessel wall; this process is associated with endothelial injury and atheromatous lesions. Ouchi *et al*. [109] found that adiponectin accumulates in the subendothelial space in a damaged carotid artery model, and that treatment with adiponectin dose-dependently decreases class A macrophage scavenger receptor (MSR) ligand binding and uptake of oxidised LDL. Accumulation of oxidised LDL is a hallmark of foam cell transformation and a classic histological marker of developing atherosclerosis [111]. It has therefore been postulated that adiponectin has a prominent role in the prevention of atherosclerosis. Adiponectin has also been found to induce the synthesis of decorin in cultured vascular smooth muscle cells. Decorin is proposed to suppress atherogenesis through mechanisms that are yet to be fully determined [66] and is also implicated in regulation of TGF-β signalling and therefore may be beneficial for the recovery of the kidney post-injury [112].

The apparent relationship between adiponectin and atherosclerosis is significant in the context of renal disease because atherosclerosis, among other cardiovascular symptoms, commonly developed in patients suffering renal failure and is a leading cause of mortality in these patients [113]. Zoccali *et al*. [114] conducted research into adiponectin levels of patients suffering from end-stage renal disease (ESRD) compared to matched healthy controls. They found that adiponectin was positively correlated with HDL cholesterol levels which is cardio-protective and inversely related to body mass index (BMI), plasma leptin, insulin and

triglyceride levels. Because of the relationships between adiponectin levels and cardio-protective and non cardio-protective substances, it was concluded that adiponectin was a likely protectant of the cardiovascular system during ESRD [114]. Shen *et al.* [115] found that the increased adiponectin and adiponectin receptor levels in ESRD patients are likely not explained by a shift in isoform expression or a change in the expression of the adiponectin receptor. They also postulated that the up-regulation of this protein-receptor axis may be a beneficial effect struggling to curb a damaging and growing pro-inflammatory response [115].

Pischon *et al*. [116] have identified that high adiponectin levels are associated with a lower risk of heart attack in men; and furthermore, Ouchi *et al.* [63] showed that people who suffer from coronary artery disease exhibit significantly lower serum adiponectin levels when compared to age, sex and body mass index (BMI) matched controls. These results show the possibility of a strong link between adiponectin expression and overall cardiovascular health.

Secretion of adiponectin is inhibited by the pro-inflammatory adipokines TNF-α and IL-6 [117,118]. Serum adiponectin is decreased in sufferers of diabetes mellitus type 2. Many sufferers of type 2 diabetes suffer from obesity and thus exhibit higher circulating IL-6 and TNF-α levels, the likely cause of the decreased adiponectin. However as adiponectin has insulin sensitising activity, there may be more specific underlying mechanisms at work as part of the type 2 diabetes pathogenesis. Sympathetic nervous system activation of adipocytes through the β-adrenergic receptor has also been found to significantly reduce the expression of adiponectin [119,120]. This is potentially important in the context of renal disease as sympathetic over activity has also been found to be an important symptom in patients suffering from renal failure [121].

Additionally, adiponectin also suppresses the nuclear factor-κB (NFκB) induction of TNF-α and interferon-γ (IFN-γ), which are pro-inflammatory cytokines; and induces the production the anti-inflammatory IL-10 and interleukin 1 receptor antagonist (IL-1Ra) [122]. These are potentially protective effects in the case of renal disease whereby an increasing spiral of inflammation is commonly observed.

1.4.2 Leptin:

Leptin is encoded by the obese (*ob*) gene, initially named so because its expression levels were found to correlate positively with obesity. Mice with '*ob/ob*' genotype ($^{-/-}$), grow to be vastly obese, have decreased energy expenditure and suffer from reproductive deficiency [68]. Administration of leptin to these *ob/ob* obese mice results in weight loss [123], leading to the hypothesis that leptin is primarily involved in roles linked with energy storage, localisation and expenditure [124]. Further research by Stephens *et al.* [125] had shown that leptin decreases the expression of neuropeptide Y (NPY) in the hypothalamus, which lowers appetite and increases energy expenditure. However leptin has been found to have a much broader range of biological actions, including roles in reproduction, glucose and insulin metabolism, lipolysis, sympathetic nerve activity, immune response, haematopoiesis, angiogenesis and the hypothalamic-pituitary-adrenal axis (HPA) [126]. The actions of this protein are clearly extremely complex and are still being investigated today; the actions of this protein will be discussed in the context of other adipokines and possible association with tissue regeneration and renal failure. For a more comprehensive review on the range of peripheral actions of leptin please see Margetic *et al.* [24].

Leptin has been found to significantly accelerate skin wound healing when administered to injured *ob/ob* mice, which have a non-functional leptin protein, compared to *db/db* mice that have a non-functional leptin receptor (Ob-R) [71]. The mechanism of this beneficial effect has not been fully identified; however this does indicate that activation of the leptin receptor plays a prominent role in the effects of leptin on wound healing. This is potentially important in the context of renal failure as a high affinity Ob-R has been found in the rodent kidney in specific areas of the inner medulla and associated with vascular structures in the corticomedullary region [127]. Leptin receptors have also been identified in bovine kidney membranes [128]. Acute changes to free serum leptin concentration have been postulated to be buffered by other forms bound to plasma proteins or bound to proteins associated with endothelial cell surfaces [128], dulling the effects of any sudden increase or decrease in leptin concentration. In a study by Murad *et al* [129], leptin was shown to be synthesised after four hours in mouse wound cells and maintained in all phases of the healing process. Abrogation of leptin activity by administration of leptin specific antibodies

disrupted the healing process, resulting in poorer re-epithelialisation, thinner granulation tissue, and thinner matrix density [129].

It has been shown that renal sympathetic nerve activity (RSNA) can be stimulated by infusion of Leptin into WAT and that this infusion does not cause acute changes in blood pressure; however chronic infusion over a period of three to four days did result in an increase in blood pressure [27]. Higher RSNA is an important contributor to the control of blood pressure by the kidneys as it causes higher renal blood flow (RBF), glomerular filtration rate (GFR), sodium excretion and renin expression [27]. In contrast to the ability of leptin to increase blood pressure when present in chronically high levels, it has also been found to induce vasorelaxation through both nitric oxide (NO) synthase induction and endothelium-derived hyperpolarising factor (EDHF) dependant on artery type [26]. Lembo *et al.* [26] explained this contradiction of function by postulating that the concomitant increase in sympathetic nervous activity by leptin counteract the more direct vasorelaxation effects of the protein.

Research into atherosclerosis has led to the implication of leptin and other adipokines in its pathogenesis. Kralisch *et al.* [130] found that secreted factors from primary cultured human adipocytes contributed to an increase in monocyte adhesion to cultured endothelial cells, and also led to an increased NFκB transcription factor activity. NFκB is viewed to play a central role in the induction of pro-inflammatory gene expression. NFκB activation has also been found to occur in the development of progressive renal inflammatory disease [131]. However, functional NFκB is made up of two dimers named p65 and p50; the heterodimer p65/p50, has been found to be active in the induction phase of damage during inflammatory renal disease whereas the p50/p50 homodimer is the predominant variant during the second phase of NFκB activation during resolution of the disease [131]. Further findings by Panzer *et al.* [131] show that p50 subunit knockout mice exhibit prolonged renal inflammation, higher levels of leukocyte invasion and connective tissue damage and reduced overall survival. These are potentially important discoveries as Kralisch *et al.* [130] only performed NFκB assays looking for p65 variants of the transcription factor, meaning that no assessment of the levels of the resolution p50 homodimers was completed. Furthermore, adipocytes are also a known source of monocyte chemoattractant protein-1 (MCP-1) which is known to induce increased monocyte adhesion to endothelial cell surfaces *in vitro* and *in vivo* [90] and may be the cause of the effects of the adipose tissue conditioned

media observed by Kralisch *et al* [130]. The large range of biological effects of leptin and its *in vivo* effects on wound healing make it a promising potential treatment, worth investigating for application to a variety of diseases including renal failure.

1.4.3 Resistin:

Resistin has been classified as an adipokine since its discovery by three independent groups in 2000 and 2001 [19,73,74], its synonyms are 'found in inflammatory zone 1' (FIZZ1) [74] and 'adipose secretory factor (ADSF)' [73]. Research into resistin has predominantly been centred around the possible roles of the protein in regulation of blood glucose and diabetes [19,132], and atherosclerosis [133,134]. Other researchers have focused on locating possible sites of action in various tissues and sought to identify resistin receptors in these tissues [72]. For reviews on the state of research into resistin and its proposed actions please see Steppan and Lazar [135] or Rea and Donnelly [136].

Resistin has been reported by some researchers as positively correlated with adiposity in both mice and humans [133]; others however highlight the fact that there have been mixed results in this field of analysis [136]. This is a continuing area of discussion and may prove critical to studies relating the function and expression of resistin to type 2 diabetes. In mice, resistin is predominantly expressed by adipocytes [19], whereas expression in humans has been found to be greater in macrophages [72].

Initial research into the basic biology of resistin does not necessarily reveal any overt relationships with renal failure. However, adipokines including resistin, TNF-α, IL-6 and MCP-1; have been found to be elevated significantly in patients suffering from end-stage renal disease (ESRD) [137]. C-reactive protein (CRP) levels were also found to be four-fold higher in these patients. The altered secretion of these adipokines found by Roubicek *et al.* [137] were ultimately attributed to the increased level of immune cells located in the WAT of these patients. These findings are supported by other studies which have noted an increased number of tissue macrophages in obese subjects [59]. Axelsson *et al.* [138] also noted that serum resistin levels were strongly associated with GFR and inflammatory biomarkers in patients with mild to moderate and advanced renal functional impairment. Axelsson *et al*. [138] proposed that the homeostasis of resistin occurs through clearance into the urine, and therefore patients with impaired renal function have a lessened ability to maintain proper

resistin levels. Whether resistin does or does not contribute further to the pathogenesis of renal failure is a topic which still requires further research.

1.4.4 Tumor necrosis factor-alpha (TNF-α):

Tumour necrosis factor-alpha is a major pro-inflammatory cytokine that plays a role in many protective and pathological processes [139,140]. For a current review on TNF-α expression in WAT and its effects, see Cawthorn and Sethi [141]. Levels of TNF-α increase with rising adiposity [142], this could be attributed to the concomitant increase in infiltrated macrophages that occurs in obese subjects [61]. Curat *et al.* [62] found that macrophages constitute up to ten percent of the stromal vascular fraction (SVF) of WAT in obese patients. A possible common link between renal failure and the secretion of adipokines has arisen from the observation of the immunodeficiency which exists in renal failure despite an increasing activation of most immunocompetent cells [143]. Descamps-Latscha *et al.* [143] observed that the progression of uraemia was associated with a gradual increase in immune cell activation markers; in particular neopterin, a monocyte cell-specific marker. This is significant as a progressive accumulation of monocytes in adipose tissue also occurs in obesity [61,137] leading to a progressive increase in circulating TNF-α and other pro-inflammatory cytokines similar to that observed in renal failure [143]. The findings of Pereira *et al.* [144] have indicated that the increase in pro-inflammatory markers and concomitant decrease in immune response is possibly linked to the presence of higher levels of receptor antagonists for these pro-inflammatory cytokines. The soluble form of the p55 TNF-α receptor (TNFsRp55) which neutralises active circulating TNF-α; has been found to be elevated significantly in patients with chronic renal failure compared to healthy controls; the levels of the interleukin 1 receptor antagonist (IL-1Ra) were also found to be significantly increased when compared to control subjects [144]. However, this study failed to show a statistically significant elevation of the actual cytokines IL-1 and TNF-α in ESRD patients, even though many other studies have shown this to be the case.

There has also been suggestions that TNF-α may hold anti-inflammatory, or at least immunomodulatory effects, as opposed to the classical view of this protein as only a pro-inflammatory cytokine. In their study of TNF-α deficient mice (TNF-$\alpha^{-/-}$), Marino *et al*. [145] showed that these mice exhibited a delayed, vigorous and disorganised response to *C. parvum* infection which lead to the animals death; whereas control TNF-$\alpha^{+/+}$ mice exhibited a

prompt and organised response and survived infection [145]. The contribution of TNF-α and other pro-inflammatory cytokines to the progression of renal failure is very complex; it is becoming exceedingly clear that the increased levels of pro-inflammatory cytokines in diseases like ESRD arise from a currently unknown, but very fundamental change in the homeostasis network of these proteins.

1.4.5 Interleukin-6 (IL-6):

Interleukin-6 is a pro-inflammatory cytokine that is secreted by WAT; its expression has been found to correlate positively with increased adiposity [75,146]. Mice deficient in IL-6 develop mature onset obesity which is partly ameliorated by IL-6 replacement therapy [147]. These knockout mice also exhibit increased leptin levels which may be a compensatory symptom of the IL-6 deficiency [147]. Circulating IL-6 levels are a well known regulator of hepatic C-reactive protein (CRP) expression [76], which is an important marker when attempting to assess systemic inflammation [18]. IL-6 also impacts the secretion of other adipokines in a similar manner to TNF-α. Adiponectin mRNA and protein levels are shown to be decreased by up to fifty percent and twenty-five percent respectively in 3T3-L1 adipocytes treated with the cytokine compared to non-treated controls [117]. Expression of IL-6 is also induced by TNF-α which possibly aids in the formation of a pro-inflammatory positive reinforcement loop resulting in the increased systemic pro-inflammatory state which is well documented to be associated with obesity.

Interleukin-6 has been implicated in the progression of atherosclerosis, like TNF-α, via the autocrine and paracrine activation of infiltrated monocytes which then stimulate the deposition of fibrinogen [76], as TNF-α, CRP and IL-6 are all increased in abundance in states of obesity and ESRD. IL-6 has been found to be a primary stimulator of both TNF-α and CRP. It is possible that the increased expression of these proteins in obesity and ESRD is due primarily to the increased levels of IL-6 expression in macrophages.

1.4.6 Interleukin 1β (IL-1 β):

Interleukin 1β is a major pro-inflammatory cytokine produced by monocytes in the defence against many infectious agents. The most likely reason that it has been reported as an adipokine is the increase in monocyte invasion of adipose tissue with increasing adiposity. IL-1β is expressed rapidly after tissue damage [77] and has been shown to induce fever, slow

wave sleep, the synthesis of CRP in the liver, cortisol, insulin release and the release of neutrophils [18,78]. For a comprehensive review on the contribution of IL-1 to disease biology see Dinarello [79]. The other form of IL-1 is IL-1α, this is primarily an intracellular form and is not commonly found in circulation or body fluids [79]. IL-1β appears to be the primary cytokine for inducing the acute responses to local tissue injury or infection [18,79]. There is little discussion of the circulating levels of IL-1β during renal failure; however the increased levels of CRP and other pro-inflammatory cytokines during renal failure have been reported extensively. As IL-1β is an inducer of CRP, it may be an important factor in the progression of the disease.

1.4.7 Adrenomedullin (AM):

Adrenomedullin was first identified from a pheochromocytoma by Kitamura *et al*. [80] and has since been identified to be expressed and have actions in adrenal glands, lung, kidney, heart, spleen duodenum and submandibular glands [148] and has subsequently been reported in almost every organ in the body [149]. The myocardium and vascular endothelium are widely regarded as the major sources of AM [82]; however very few studies that have assessed the distribution of AM production throughout the body have actually included adipose tissue in their analyses as a potential source. Harmancey *et al*. [38] is one exception, and identified the production of AM mRNA in human adipocytes at higher levels than known positive control sources such as human right auricle cells. This finding implies that adipose tissue is a significant source of circulating AM and indeed may even be the primary source of circulating systemic AM levels. The absence of adipose tissue analysis in experiments screening for AM expression is a classic example of the traditional view of adipose tissue as nothing more than an energy store. This view is gradually changing due to discoveries like those documented by Harmancey *et al.* [38], Zuk *et al*. [150] and Caplan *et al* [151]. Analysis of whether circulating levels of AM are increased or decreased in obese patients will provide important insights into obesity and its associated complications; however, to the best of our knowledge such experimental works have yet to be published.

AM was originally described as a protein with potent and long lasting hypotensive actions [80]. It has been implicated in a more broad cardioprotective role [81] and is postulated to hold intrinsic antimicrobial activity in the lung due to its presence in respiratory mucus [149]. AM has been found to be induced by many factors including hypoxia [81,149,152-155], oxidative

stress [153], anaemia [155], mechanical stress [149], activation of the renin-angiotensin system, sympathetic nervous system activation and inflammatory processes [81,83,152,156]. For broader reviews on AM characteristics and function see Hamid and Baxter [82] and Ishimitsu *et al*. [83].

Adrenomedullin has been found to be induced by the presence of pro-inflammatory cytokines TNF-α, IL-1β and IL-6 [81,152,157] and is also able to induce the down-regulation of these cytokines in a dose-dependent manner [152]. Temmesfeld-Wollbrück *et al*. [156] found that AM is able to protect rats from septic shock induced by administration of *Staphylococcus aureus* α-toxin. The animals treated with AM exhibited a seven percent mortality rate compared to fifty-three percent in saline treated controls. This was postulated to be due to a reduction in the level of vascular permeability in AM treated animals, allowing better hemodynamic regulation [156]. Adrenomedullin also protects against ischemia/reperfusion (I/R) injury in the rat gut and brain through decreased pro-inflammatory marker levels, increased NO production and glial cell survival in the brain [152,153]. Administered AM also protects against I/R injury in the mouse kidney likely through its NO stimulating activity and subsequent increase of renal blood flow [158]. Adrenomedullin has been found to also decrease the level of reactive oxygen species in cultured mesangial cells and macrophages indicating a further possible renoprotective function during states of heightened TNF-α, IL-1β and IL-6 expression like those observed in renal failure. Circulating AM is increased in cases of hypertension during renal failure [159]. This is significant as hypertension is an important cardiovascular risk factor in the pathogenesis of renal failure.

1.4.8 Interleukin 10 (IL-10):

Interleukin 10 is widely regarded as an important anti-inflammatory cytokine. It has roles in inhibiting the activation of macrophages, down-regulating the responses of T helper type 1 responses [85], and roles in the regulation of TNF-α, IFN-γ and IL-6 expression in monocytes [86-88]. It has wide and varying effects across the immune system and is even able to provide stimulatory signals to B cells and activated $CD8^+$ T lymphocytes [85]. Interleukin 10 has been found to inhibit the production of IL-6 through inhibition of the NFκB transcription factor [86]. This is significant as TNF-α and IFN-γ are also controlled through NFκB activation (discussed earlier). Thus inhibition of NFκB by IL-10 likely constitutes a major inflammatory regulation point for multiple proteins of the pro-inflammatory response [160].

Simmons *et al.* [161] noted increased IL-10 serum levels and a concomitant increase in TNF-α, IL-6 and IL-8 in non-surviving sufferers of acute renal failure. This indicates the possibility that IL-10 over-expression is due to compensatory stimulation via increased levels of TNF-α, which is known to stimulate IL-10 production [88]. Alternately, the over-expression may be part of the pathogenic process indicating aberrant inflammatory cytokine control. Choi *et al*. [162] and Mu *et al.* [163] have both investigated the over-expression of IL-10 by using adenovirally administered and expressed IL-10 in glomerulosclerosis and chronic renal disease respectively. IL-10 levels were elevated by up to twelve times normal levels [163] and resulted in decreased proteinuria [162,163], serum creatinine [163], TGF-1β [162]; and decreased renal infiltration by immune cells [163]. The infiltration of immune cells has been shown to be associated with occurrence of glomerulosclerosis [162,163]. These results demonstrate the potential renoprotective effects of IL-10 over-expression and provide insight into the findings of Simmons *et al.* [161] where IL-10 was seen to be increased along with TNF-α, IL-6 and IL-8; indicating that IL-10 over-expression is likely a compensatory beneficial effect.

1.4.9 Monocyte chemoattractant protein 1 (MCP-1):

Monocyte chemoattractant protein 1, also called JE in mice, is commonly known as a potent inducer of monocyte chemotaxis. In the mouse, JE has been described as the most prominent mRNA transcript induced in 3T3 fibroblasts in response to exposure to platelet derived growth factor (PDGF) [164]. Rollins *et al* [164] were the first to describe a structural analysis of the JE gene, while investigating the reaction of fibroblasts to PDGF. MCP-1 is also secreted by adipocytes and pre-adipocytes *in vitro* and *in vivo*; with pre-adipocytes exhibiting higher secretion levels than mature adipocytes [89]. Circulating MCP-1 levels are increased in obese humans and reduced after weight loss or cachexia [90]. Adipocytes have been identified as the major source of MCP-1 from within adipose tissue [90]. Besides its chemotactic effects on monocytes, MCP-1 also induces the production of IL-1 and IL-6 in human peripheral blood monocytes and increases their expression of cell surface adherence molecules shown to aid in tissue infiltration [165]. MCP-1 is also capable of attracting an activated subset of memory T-lymphocytes to sites in a dose dependant manner *in vitro* [91]. The MCP-1 gene is also insulin responsive, and increased MCP-1 expression in obesity has been linked to higher circulating insulin levels during type II diabetes [166] and addition of MCP-1 to adipocytes *in vitro* results in the reduction of insulin stimulated glucose uptake [166].

As monocytes can constitute up to ten percent of the stromal vascular fraction of adipose tissue in obese humans, it is logical to suspect that the expression of MCP-1 by adipocytes serves multiple purposes:

A. To accumulate immune cells capable of tissue remodelling; essential in an expanding and shrinking tissue, depending on food availability.
B. To reduce the capability of the organism to store yet more energy in situations of obesity where excess has been reached long ago.
C. To accumulate immune cells in a commonly exposed and insulatory tissue where exposure to the elements and injury are more common.

MCP-1 has been extensively investigated for potential roles in almost every disease where excessive inflammation is cited as the driving force behind the bulk of the pathology, especially in more chronic disorders like rheumatoid arthritis, atherosclerosis and chronic kidney disease. To this end, studies have been conducted to examine the effects of MCP-1 over-expression in a tissue-specific [167] and systemic scale [168]. Gunn *et al.* [167] utilised a transgenic mouse model to over-express the human MCP-1 gene in alveolar epithelial cells. The mice developed significantly higher numbers of infiltrated leukocytes within the lung; these results correspond to *in vitro* tissue invasion models demonstrating a similar effect. However, Gunn *et al* [167] reported that despite the increased pro-inflammatory presence, no other signs of pro-inflammatory processes were evident. The transgenic mice did exhibit a greater sensitivity to external pro-inflammatory stimuli like LPS over controls, showing a kind of inflammatory alertness. This study indicated the possibility that MCP-1 is the agent responsible for the recruitment of inflammatory cells to a particular site, but is not the agent which then activates their destructive actions. Using other transgenic mouse models, Gu *et al* [168] analysed the effects of MCP-1 over expression on a systemic and a localised scale. When induced on a more systemic scale, using over expression in multiple organs including breast, lung and kidney, they noted a lack of inflammatory infiltration into the mouse organs at any age. These transgenic mice were essentially healthy and long-lived, in a protected pathogen-free *in vitro* environment. However these mice did exhibit an increased susceptibility to intracellular pathogens like *Listeria monocytogenes* compared to non-transgenic controls, indicating a possible system-wide shift towards a Th2 type response [168]. In contrast to the findings of Gunn *et al* [167], Gu *et al* [168] also demonstrated that a more

specific expression of MCP-1 to islets of the pancreas does result in the heavy leukocyte invasion in accordance with previously reported *in vitro* models.

Expression of MCP-1 in atherosclerotic lesions of humans and rabbits has implicated it in the pathogenesis of atherosclerosis, as monocyte invasion and subsequent accumulation of oxidised LDL are keystones for the pathogenesis of this disease [169]. However, no implication of MCP-1 in the activation of the monocytes in this process was presented. Thus MCP-1 may not incite the pathogenic response, but may only be responsible for the recruitment of the inflammatory cells. In relation to renal disease, it has been shown that the presence of albumin and transferring proteins can induce proximal tubule epithelial cells to secrete MCP-1 [170]. This implicates MCP-1 in the pathogenesis of chronic renal failure (CRF) by promoting an inflammatory presence in the renal interstitium [170]. A role for MCP-1 has also been implied in cases of diabetic glomerulosclerosis, where high serum glucose levels can cause chronic progressive renal damage [171]. Albumin non-enzymatically modified with glucose due to high glucose concentration has been shown to increase the expression of the MCP-1 gene and protein *in vitro* in a dose-dependent manner [171]. The same study also revealed that urinary albumin levels correlated closely with urinary MCP-1 levels. No data was presented on the effects of MCP-1 on monocytes once they had invaded renal tissue however. In a study of the inflammatory phase of crescentic nephritis, Lloyd *et al* [172] analysed the roles of regulated upon T-cells expressed and secreted (RANTES) and MCP-1. Their results implicate MCP-1 as a major driver of not only the recruitment of inflammatory cells to the kidney, but also in their activation. Neutralising antibodies to MCP-1 in an *in vivo* mouse crescentic nephritis model demonstrated a significant decrease in the level of glomerular crescent formation and in deposition of type-I collagen [172]. The strong association that MCP-1 has with many diseases, including renal disease implies that the administration of MCP-1 exogeneously in a renal failure model will not result in a beneficial outcome unless the presence of other anti-inflammatory cytokines is considered.

1.4.10 Plasminogen activator inhibitor 1 (PAI-1):

Plasminogen activator inhibitor -1 is a member of the serine protease inhibitor (serpin) gene family. Its primary function has been shown to be the inhibition of fibrin clot breakdown (fibrinolysis) during haemostasis. PAI-1 expression has been identified as perhaps one of the most tightly regulated in the body [173]. The biological half-life of PAI-1 is

reported to be between ten minutes in the blood *in vivo* and up to two hours *in vitro*, which is most likely a part of the mechanism of its regulation, as over-inhibition of fibrinolysis can result in severe thrombotic complications. PAI-1 is produced by endothelial cells, smooth muscle cells, adipocytes, spleen cells and the liver [174]. In lean mice, adipose tissue presents only a very small source of circulating PAI-1 levels, with adipocytes and stromal cells showing no detectable mRNA signal, whilst the smooth muscle cell signal is barely detectable [175]. However plasma levels of PAI-1 increase in obesity [176], with the elevated circulating TNF-α level, a known stimulator of PAI-1 production, touted as the most likely cause [175].

The actions of PAI-1 reach beyond the inhibition of fibrinolysis. Evidence shows PAI-1 has an involvement as an inhibitor of cell attachment to extracellular matrix protein vitronectin through competition with vitronectin receptor $\alpha_v\beta_3$ on smooth muscle cells [92]. PAI-1 displays a dichotomous effect toward angiogenesis; normal physiological levels seem to stimulate angiogenesis whereas higher levels inhibit it [174]. In a Matrigel implant assay, wild-type mice injected with low level PAI-1 demonstrated increased angiogenesis by up to three times, whilst high levels inhibited angiogenesis almost completely [28]. This effect may be due to changes in the ability of certain angiogenic cell populations to adhere to the site and begin angiogenesis at different local PAI-1 levels. Some angiogenic cells may be able to resist the effects of PAI-1 presence at lower levels by up-regulating vitronectin receptor expression. Elevated PAI-1 levels have been associated with almost every type of aggressive renal disease, especially those characterised by some form of renal fibrosis [177,178]. The mechanisms relating to the role of PAI-1 in kidney fibrogenesis are not completely understood, but it is suspected that the inhibition of fibrolysis alone is not the complete story. For a review on the subject see Eddy and Fogo [177].

The relatively short lifespan of PAI-1 means it may not be in its active conformation within an *in vitro* preparation of WAT secretions that has been produced, stored, and defrosted for use as a potential therapeutic treatment.

1.4.11 Visfatin:

Visfatin was identified by Fukuhara *et al* [20], as an adipokine that is increased in the plasma of obese humans and mice and is expressed in visceral fat at significantly greater levels than subcutaneous fat [20]. In the same study, it was also shown to have potential

insulin mimetic effects. Visfatin has since been shown to be identical to a protein previously cloned and described by Samal *et al* [179] as pre-B-cell colony-enhancing factor. In response, the work of Fukuhara *et al* [20] has since been retracted. The work of Fukuhara *et al* [20] has however, sparked a new research interest in Visfatin/pre-B-cell colony-enhancing factor as a novel adipokine and its possible role in many of the obesity related diseases like type 2 diabetes and the metabolic syndrome [93,94,180-182].

Visfatin plasma levels have been widely reported to be positively correlated to BMI and body fat percentage in humans and mice [181]. However, contention still exists as to whether the increased levels of visfatin in obese subjects is actually secreted by WAT or by other sources, as there have been many other cells capable of visfatin production previously identified. Visfatin is expressed in the liver, bone marrow, human foetal membranes and muscle as well as tissue macrophages [183] and isolated adipocytes [184]. There are some conflicting results regarding the increased expression of visfatin in visceral fat over subcutaneous fat. Fukuhara *et al* [20] and Kralisch *et al* [95] both show a clear difference between the two fat sources in visfatin production in mice. Subsequent studies by other groups however, have shown that there appears to be no difference in visfatin secretion between visceral and subcutaneous adipose tissue. Perhaps more importantly, some do not show a correlation between visceral adiposity and plasma visfatin levels [180,181]. When comparing visfatin release from WAT macrophages to individual WAT adipocytes, Curat *et al* [183] found the macrophages to be a greater source of the adipokine as assessed by RT-PCR.

Visfatin has been touted as a pro-inflammatory adipokine due to its ability to greatly increase the expression of inflammatory cytokine IL-6 in human monocytes [93]. In the same study visfatin was also found to increase pro-inflammatory TNF-α, IL-1β and anti-inflammatory cytokines IL-10 and interleukin-1 receptor antagonist (IL-1Ra), to different degrees. Visfatin expression was found to be inhibited by the presence of IL-6 and TNF-α in 3T3-L1 adipocytes [94,95], indicating a negative feedback loop link to these pro-inflammatory processes. In CKD, Yilmaz *et al* [185] found serum visfatin to be elevated in human patients with CKD stages 3,4 and 5 compared to healthy controls. They also showed a strong correlation between serum visfatin levels and endothelial dysfunction and estimated glomerular filtration rate (eGFR). However, they did not assess urine visfatin levels in either the CKD cohort or the controls, so no data on whether visfatin is regulated by the kidneys

was obtained. To our knowledge, no study has assessed the visfatin level in the urine of renal disease sufferers. As there was a significant correlation between eGFR levels and serum visfatin, it will be important to investigate whether the decreased renal functional capacity is the cause or the symptom of higher serum visfatin.

1.4.12 Hepatocyte growth factor (HGF):

Hepatocyte growth factor, also called scatter factor [186] is a widely expressed growth factor initially identified for its role in the remarkable regenerative capacity of the mammalian liver, giving rise to its name. In rats with two-thirds hapectomy, serum HGF levels are seen to rise fifteen to twenty-fold [96]. The HGF receptor is a tyrosine kinase receptor, c-met; and has been observed in the epithelium of almost every adult mammalian tissue [96] and in many of the developing epithelial tissues of embryonic mice [187]. HGF is secreted in its inactive form by tissue stromal cells and fibroblasts; it remains locally bound to extracellular matrix until cleaved into α and β subunits by urokinase [188]. Active HGF is formed by association of the now separated αβ subunits, activation can be inhibited by the presence of PAI-1 [188]. In studies of mouse embryological development, c-met and HGF RNA have been identified in almost all epithelial tissues including muscle, intestine, liver, lung, pancreas, teeth, nasal cavity and the kidney [187]. This implicated HGF as a crucial factor in the regulation of growth of these tissues. HGF was identified to be produced by mesenchymal cells in close proximity to developing epithelial cells positive for the c-met HGF receptor [187]. In an investigation by Sonnenberg *et al* [187] no evidence was found that HGF was an inducer of new epithelia. However, due to the close relationship between the developing epithelial structures and the HGF secreting mesenchymal cells, it was theorised that existing epithelia respond to HGF to form tubular epithelial structures. In a study by Schmidt *et al* [189] using $HGF^{-/-}$ mice, it was found that the $HGF^{-/-}$ genotype resulted in death between embryonic days 13 and 16.5. However, morphological analysis of the major organs showed no observable defects, except in the liver and placenta which showed marked reduction in overall liver size and a more loose liver cellular structure and defects in the development of the labyrinth layer of the placenta [189]. The lack of defects in the epithelial tissues of the $HGF^{-/-}$ mice contrast with the prevalence of its expression in these developing tissues found in the Sonnenberg *et al* [187] paper.

HGF is also an angiogenic factor, promoting the proliferation of human endothelial cells *in vitro* [97]. Bussolino *et al* [97] utilised Boyden chamber and checkerboard analysis to find that HGF induced both chemokinesis and chemotaxis of human endothelial cells. They also used slow-release HGF implants into rabbit corneas to show a significant dose-dependent effect on induced angiogenesis and inferred a positive effect on wound healing based on an *in vitro* wound healing assay with significant re growth of a human endothelial cell monolayer [97]. HGF over-expression via gene therapy significantly reduced induced liver cirrhosis *in vivo* in rats treated with toxin dimethylnitrosamine [190]. The rats administered with HGF gene therapy showed a seventy percent reduction in liver fibrosis over controls, demonstrating a profound effect on a pathological state which is already well under-way.

In the mouse kidney, the c-met receptor and HGF is detected at embryological day 11.5 (E11.5) [98]. HGF has been shown to be responsible for the induction of branching tubule formation in *in vitro* renal cell models using Madin-Darby Canine Kidney (MDCK) cells, a canine distal tubule epithelial cell line commonly used as a model for renal epithelial cells [191,192]. Branching tubule morphogenesis was also noted in an investigation by Santos *et al* [98], using embryonic kidney organs co-cultured with MDCK cells. In this case monoclonal antibodies to HGF abrogated the morphogenic effects caused by the presence of embryonic kidney, furthermore anti-HGF serum significantly reduced the *in vitro* growth of embryonic kidneys in organ culture compared to non-immune sera treated controls [98]. This provides further evidence for a key role of HGF in kidney development that is in almost direct contrast to the results shown by Schmidt *et al* [189] detailing no aberrant renal development in the absence of HGF.

In renal disease models, HGF has been found to significantly affect the recovery of the kidney after many different types of insults in models of both acute and chronic renal failure. Cisplatin, a common anti-tumour drug with known nephrotoxic effects, was used by Kawaida *et al* [99] to induce acute renal failure in mice and administration of exogenous human HGF to these mice demonstrated improved blood urea nitrogen and serum creatinine over control animals. In the same study, using $HgCl_2$ to induce renal damage, HGF-treated mice exhibited increased DNA synthesis, an indirect measure of cellular proliferation. This increased proliferation was mostly confined to the outer medulla, where damage to the tubular cells was most obvious [99], indicating a pivotal role of HGF in renal

regeneration. Furthermore, in a unilateral nephrectomy renal damage model by Kawaida *et al* [99], increased proliferation of the cortex tubular cells was observed in HGF treated kidneys compared to controls. In a folic acid administration model of acute renal failure, Liu *et al* [193] observed a significant and rapid increased abundance of circulating HGF levels and kidney c-met expression. Plasma HGF rose by up to sixteen-fold post-injection of folic acid [193]. As a model of chronic renal failure, Mizuno *et al* [100] treated ICGN strain mice with exogenous HGF and noted almost complete prevention of fibrosis when compared to non-treated controls. They also noted higher DNA synthesis levels in the kidneys of HGF treated mice and a significant down-regulation of TGF-β positive, α-smooth muscle actin expressing myofibroblasts, which are widely regarded as key cells in the formation of fibrosis [100]. Yang and Liu [194] also noted reduced fibrosis and lower TGF-β positive myofibroblast levels as a result of HGF administration, this time in a unilateral obstruction renal failure model. HGF is a potent regenerator of not only the liver, but also the kidney, and represents a potentially key cytokine in the effectiveness of WAT secretions in the treatment of disease.

1.4.13 Vascular endothelial growth factor (VEGF):

VEGF is essential to the induction and maintenance of vasculature formation during embryological development [195,196]. It is a protein with six identified isoforms produced from alternative splicing of the human VEGF gene: $VEGF_{121}$, $VEGF_{145}$, $VEGF_{165}$, $VEGF_{183}$, $VEGF_{189}$ and $VEGF_{206}$. Isoforms 121, 165 and 189 are the most abundantly expressed [101,197]. Studies have been conducted investigating the role of VEGF in embryological vascular development, its association with tumour growth angiogenesis, immune inhibition and metastasis, and also for its role in other pathologies like wound healing. It is a major stimulator of angiogenesis through its activity on endothelial cells, pericytes and vascular smooth muscle cells [101,103,198]. Its identified effects include the increased proliferation and migration of pericytes [103], endothelial cells and smooth muscle cells [103,198], the inhibition of apoptosis in endothelial cells [199], increased vascular permeability [198], and the inhibition of dendritic cell maturation [102,200]. VEGF has been identified as a cytokine essential to the proper embryological growth and development of mammalian tissues, whose major stimulation of expression lies in tissue hypoxia [103]. Other stimulators of VEGF expression are cytokines like epidermal growth factor, transforming growth factor β (TGF-β), platelet derived growth factor (PDGF), insulin-like growth factor I (IGF-I), angiotensin II, interleukin-1β (IL-1β) and interleukin-6 (IL-6) [197].

Because of the many splice variants of VEGF and the differing roles it plays in the development and maintenance of mammalian tissues, the set of receptors found to respond to VEGF are also many. They usually share cross-reactivity with multiple VEGF splice variants and also with other cytokines like placental growth factor (PIGF). The difference in VEGF activity is, therefore, achieved through the expression of certain isoforms at specific sites and the presence of cells that have the correct set of VEGF receptors to produce a certain effect. This is an extremely complex area of research which is still being explored. For reviews on the splice variants of VEGF and their receptors see Robinson and Stringer (2001) [201] and Neufeld *et al* (1999) [101].

VEGF is essential to the normal functioning of the mammalian kidney [202]. The distribution of expression of the growth factor and its receptors demonstrate a complex and intricate web of effects that are still being investigated today. The main VEGF producing cells within the kidney are glomerular podocytes [203], proximal and distal tubule epithelial cells [204] and collecting duct cells [204,205]. The major site of VEGF binding has been identified as the glomeruli, where glomerular endothelial cells express high levels of VEGFR-2. VEGFR-2 was also detected on cortical and reno-medullary interstitial cells and endothelial cells of peritubular capillaries [204]. The close situational relationship between podocyte and endothelial cells and the roles of the epithelial cells further down the nephrons proximal and distal tubules and collecting duct have led to theories regarding the involvement of VEGF in the tight regulation of glomerular permeability. This is still being investigated however, VEGF levels have been identified as associated with certain renal pathologies. For a more in-depth analysis of the role of VEGF in kidney disease see Schrijvers, Flyvbjerg and De Vriese (2004)[197].

1.4.14 Vaspin:

Vaspin is an obesity associated, insulin sensitising adipokine first identified by Hida *et al* [21]. It bears homology similarities to serine protease inhibitors and has thus been classified as part of the serine protease inhibitor family (serpins). However no common proteases have been found to be inhibited by vaspin, including trypsin, elastase, urokinase, factor Xa, collagenase and dipeptidyl peptidase [21], leaving its exact mode of action unknown. Most groups have identified that circulating vaspin serum levels are significantly elevated in females [104,206]. There is some contention as to whether vaspin levels are increased in obese

patients; groups measuring the relationship between body mass index (BMI) and vaspin serum protein or mRNA levels found significant correlations showing an association between increased vaspin levels and higher BMI [21,206,207]. However, Seeger *et al* [104] identified a negative correlation between waist to hip ratio and serum vaspin levels. This may be due to differences in the way that waist to hip ratio and BMI are calculated.

Hida *et al* [21] also investigated the effect of vaspin on the expression of a small set of other known adipokines, leptin, resistin, TNF-α and adiponectin. The group found that intraperitoneal injections of recombinant human vaspin had significant effects on these adipokines in male CRL:CD-1 (ICL) mice fed with a high fat, high sucrose (HFHS) chow to induce obesity. They found vaspin administration had significantly decreased the expression of leptin, resistin and TNF-α; whereas it significantly increased the expression of adiponectin [21]. The decreased expression of TNF-α in adipose tissue in response to vaspin demonstrates a possible usefulness to the suppression of inflammation elsewhere in the body. Further work needs to be done to explore the effects of vaspin on other inflammatory cytokine producing cells and tissues. However, it does shed some light on the use of *in vitro* produced adipokines as potentially effective treatments.

Due to identified associations between other adipokine levels and states of renal failure, Seeger *et al* [104] analysed the relationship between vaspin serum concentration and renal function. Diabetic and non-diabetic chronic haemodialysis (CD) patients versus non-CD controls with a GFR of >50 ml/minute were compared. They found serum vaspin levels showed no significant difference between CD patients and control patients, meaning that renal elimination is not a likely method of vaspin serum concentration control. More investigation of vaspin functions and effects are required in order to fully understand any possible role it may have in the pathogenesis or resolution of renal failure.

1.5 Conclusions and experimentation:

WAT and ADSC secretions contain a complex and potent mix of pro- and anti-inflammatory proteins with roles in both the resolution and exacerbation of various mammalian pathologies. Taken together, the combination of the anti-inflammatory, anti-apoptotic, angiogenic and growth promoting effects of adiponectin, leptin, adrenomedullin, IL-10, HGF and VEGF may indeed prove useful in the treatment of renal disease. This will

depend upon the nature of the *in vitro* preparation of the WAT secretions, namely the concentration and expansion of anti-inflammatory secreting cells like ADSCs and on the presence of other as-yet unidentified secreted proteins from both WAT and ADSCs.

Choice of the proteomic techniques used:

Current technologies are not sufficient to identify every secreted low-abundance protein from WAT, ADSCs or indeed any other complex protein mixture. Functional assaying for the beneficial effects of a WAT secretion preparation is possible however, regardless of its protein complement. That is, the limits of current proteomic techniques may prevent the identification of every protein within a complex mixture, but they do allow for the assessment of the effects of such a mix as a whole on a given cell population. As such, this thesis held a biologically targeted focus, rather than an exploration of the different proteomic techniques available. This thesis was not designed to identify every protein within the adipose secretion mix, nor was it designed to identify every quantitative change in protein expression in the treated renal cells. The priority was to obtain large, global-scale proteomic datasets that would provide an overview of the systems at play when a population of renal cells (PRCs or MDCK cells) were treated with an adipose tissue secretion preparation.

Isobaric tags for relative and absolute quantitation (iTRAQ) was the method selected for the comparison of treated and control populations of PRCs and MDCKs. This is a technique which is well established in the literature. This approach provided the project with the ability to identify large numbers of proteins from a relatively small amount of sample. The samples to be compared in an iTRAQ analysis are run through the LC-MS stages in parallel, enabling direct relative quantification of protein abundances and simultaneous identification of these proteins [208]. This reduces variability in the analysis by eliminating run-to-run variation in the LC-MS/MS stages. iTRAQ analysis does not bias the isolation or analysis of a sample based on protein hydrophobicity, isoelectric point or molecular weight [209]. These advantages are tempered however by the loss of potentially important information on post-translational modifications to the analysed proteins. iTRAQ also has a limited ability to compare presence/absence abundance changes between groups. Run-to-run comparisons can also be problematic in an iTRAQ experiment unless an internal

standard sample is used, reducing the number of channels in the 4- or 8- plex system that are available for sample analysis.

All current proteomic technologies entail a range of advantages and disadvantages that must be taken into account in the final analysis. Two major alternatives to the iTRAQ approach chosen include 1-dimensional (1-DE) and 2-dimensional (2-DE) electrophoresis based approaches. The 1-DE approach typically entails the resolution of a single protein sample per lane followed by the excision of bands, in-gel enzymatic digestion and finally, identification of the proteins via LC-MS/MS. This approach is robust and can cope with very high sample concentrations. However the sample size required for comprehensive protein identifications and the number of technical replicates required can be high to account for variation in peptide extraction efficiency from the gel and variances in LC-MS/MS runs. This technique also does not readily allow for the analysis of post-translational modifications in the identified proteins.

Two-dimensional electrophoresis based approaches typically involve the fractionation of the protein samples firstly by isoelectric point and then by molecular weight. This approach provides a highly informative and distinct protein spot patterns for each sample that enable the use of image analysis software tools for identification of differentially expressed proteins. These proteins are typically excised from the gels and identified using in-gel enzymatic digestion and LC-MS/MS based approaches. This technique is powerful in that it is inherently able to highlight protein isoforms produced by post-translational modifications. The gel image can provide clear information on the quality of the sample preparation used, making troubleshooting fast and directed to a specific problem [210]. However, this approach can be relatively sample intensive and identification and visualisation of proteins that are of low abundance in the gels can be problematic. Typical 2-DE preparation methods are not suited well to the separation and fractionation of hydrophobic proteins. The total number of proteins identified in a 2-D gel is typically lower than the total number identified in a 1-DE or LC-MS/MS based approach. The use of immobilised pH gradients also restricts the view of the sample proteome to only those proteins whose isoelectric point fall within the selected range [210].

Preparation of the adipose tissue-derived secretions:

I proposed a WAT preparation method, utilising partial-digest and tissue culture techniques designed to enhance and expand the ADSC cell population from adipose tissue whilst also retaining the other cellular components from adipose tissue *in vitro*. The partial-digest of the human WAT secretion preparation allows for the concentration of plastic adherent stromal-vascular cells from the WAT, whilst also allowing for the culture of individual adipocytes and small adipose tissue clusters. This resulted in a mixed cell culture/organ culture *in vitro* scenario, allowing the liberated ADSCs to adhere to the plastic flask surface and proliferate, while also allowing for the survival of the adipocytes and other cells of the SVF over the incubation period. Preliminary work also included the use of a crude organ culture method for the production of rodent adipose tissue secretions. My own work and that of others in the group indicated that mixed populations of cells produced more complex secretion profiles, which were considered the most likely to have therapeutic efficacy.

Experimental overview of the subsequent chapters:

Chapter 2 details the preliminary experiments conducted while at the University of Technology Sydney during the initial stages of this project. These experiments were designed to assess the effects of rat adipose tissue secretions produced using an organ culture method, on cultured primary rat renal cells using 2-D electrophoresis (2-DE) techniques. The chapter also demonstrates novel applications of the biotin-avidin system to detect the binding of adipose tissue secretions to the primary renal cells, indicating a possible interaction between the cells and the secretions.

To test the effects of the human adipose tissue secretions and the human adipose tissue secretion preparations, two *in vitro* assay systems using primary rat kidney cells and Madin-Darby canine kidney (MDCK) cells were used.

In Chapter 3, the human adipose secretion preparation was then used to treat preparations of plastic adherent, primary rat kidney cells and MDCK cells as *in vitro* models of the mammalian kidney. In the primary renal cells, changes to the primary renal cell proteome were analysed using isobaric tag for relative and absolute quantification (iTRAQ), comparing the proteomes of treated and non-treated controls. As an interesting and novel

side-experiment, changes in the cytokine profile of both the rat primary cell secretome and the human adipose secretions were monitored over a time-course using BioPlex™ multiplexed cytokine assay technology. As the treatment of the primary cells was xenogeneic in nature, detection of both the human and rat cytokines from within the same flasks was possible using the rat and human Bio-Plex™ cytokine assay kits. This allowed for the simultaneous measurement of the changes to the primary renal cell secretions in response to the treatment and the decline in human cytokines from the treatment media over time as the primary cells utilised them.

Chapter 4 assessed the effects of the human adipose secretions on the proteome of MDCK cells also using iTRAQ analysis. MDCK cells represented a population of cells from a different portion of the nephron to the primary rat renal cells, thus providing a more rounded view as to the effects of the adipose secretions on the mammalian kidney as a whole.

Both the rat PRCs and the canine MDCK cells displayed an increased abundance of proteins involved in apoptosis resistance and suppression of transforming growth factor beta signalling despite the differences in the cell type, position in the nephron and species. Both of these effects have been shown in the literature to be beneficial to the recovery of the kidney during disease processes and will be explored in detail in the following chapters.

Chapter 2: Prologue

This chapter details a major portion of the body of work completed at the University of Technology Sydney (UTS) during the first 1.5 years of my PhD. Dr Ben Herbert and I started the project with an idea to work towards using adipose derived stem cells as a treatment for renal failure. This project was the first one to be undertaken as part of the relationship between Regeneus Ltd and UTS (and later Macquarie University) and soon spawned another 3 PhD projects as we realised the potential for adipose stem cell treatments from our own experiences and from the explosion of studies appearing in the literature. Because the project was the first of its kind within the group and indeed within the entire university, our initial approach to some aspects of the project and the scientific questions it posed was perhaps a little naive. We had little experience at the time with mammalian cell culture (I had none), and were only beginning to understand the mechanisms by which stem cells actually exert their beneficial effects in transplant scenarios.

The first 8 months or so of the project consisted mainly of exploratory experiments: learning how to enzymatically digest fat, how to get adipose derived stem cells into culture and just how to culture primary mammalian cells in general. As our knowledge increased about the subject matter to do with adult stem cells and about the practicalities of clinical treatments, we came to realise that the secretions and/or conditioned media from the adipose stem cells tended to yield results similar to those of the actual cell transplantations. In some cases, complex mixtures of cytokines i.e. conditioned media, may be more practical and desirable in-clinic over a personalised autologous treatment that requires surgery for every patient. As our understanding of fat increased, we also came to an understanding of the existence of adipokines and the potential benefit of some adipokines to the healing process.

Our focus then shifted away from the culture of adipose stem cells and toward the production of adipose tissue secretions for use in in vitro cell-based assays. For this study we focused on in vitro kidney cells in order to gain some understanding of how a preparation of adipose secretions would affect cells in culture. The goal was to understand whether an in vitro cell-based assay could be used as a reasonable surrogate for renal failure – and by extension, perhaps how conditioned media may be administered to animals in a renal failure

model. Like I said before, we were ambitious. Renal failure is an area where little improvement has been made in treatment in the last twenty years and is also an area expected to grow exponentially with the increasing prevalence of diabetes, heart disease and obesity worldwide, so the potential rewards for a successful novel treatment were, and still are, attractive.

The initial attempts described in this chapter detail the original methods of producing secretions using a type of primary organ culture. The initial methods were since replaced with a partial digest method used for the work in the subsequent chapters of the thesis. As our understanding and competency at cell culture techniques was minimal at the time, the organ culture (undigested fat) technique was used for this work. Also, as a consequence of my limited cell culture experience at the time, the contamination of preparations was a bit of a problem; making already scarce fat samples an even more precious commodity.

From the animals used as a source of fat, we also removed the kidneys and processed them in order to obtain a plastic adherent renal cell population in culture used as our in vitro kidney cell model. We utilised this type of methodology based on professional advice from a colleague of Dr Herbert's at the time who is an expert in cell biology and genomics, Professor George Miklos. Our decision to choose a primary cell line instead of an immortalised line at first was in line with all of Regeneus Ltd's previous translational approach to medicine, meaning that any results would ideally be directly translatable into clinical trials. In addition, my growing understanding of primary cell culture suggested that the cells would be difficult to grow and the culture process would likely induce a stress response, which may be similar to chronic renal failure. However, due to the shortage of animal samples during our time at UTS and the difficulty in the culturing of the primary renal cells (due mainly to inexperience on my part), we migrated to a cell-line type approach. The Vero cell line is an African Green Monkey kidney cell line and was donated to us from a fellow researcher at UTS, Dr Michael Johnson and was selected for no other reason. The use of African Green Monkey cells was what I now see as our first dalliance with xenogeneic treatments, which we further adapted and refined in the other two major data chapters of this thesis with the use of human fat tissue and rat or canine-derived renal cell types. It also marked the start of our real change in focus in some ways away from a pure renal failure focus and toward the use and development of cell-based assay systems to test the effect of the secretions on target cells in

order to generate preliminary data for indications of therapeutic use. The methods described in the later chapters of this thesis represent the use of two different renal cell lines and assay systems used to identify possible indications of the adipose tissue secretions for renal failure. However, the methods may be adapted in future studies for use in other organ disease systems.

In 2010 our group moved from UTS to Macquarie University. The experiences and experiments from my time at UTS provided us with an opportunity to learn the proteomics and cell culture techniques that made the other two data chapters of this thesis both conceptually and practically possible.

Chapter 2: Preliminary primary renal cell and adipose tissue secretion biotinylation experiments

2.1 Introduction:

It is well established that mesenchymal stem cells (MSCs) are present in a high frequency within adipose tissue [211] and that these stem cells may illicit beneficial therapeutic effects in many diseases [3,10,13,57,212], including renal failure [9,29,41,42,55]. A key test to determine the identity of MSCs in culture is commonly referred to as the tri-lineage differentiation. Cells *in vitro* can be differentiated into chondrocytes, adipocytes and osteoblasts, thus confirming their functionality as MSCs [213]. Their behaviour after *in vivo* transplantation however, is quite different. It is now clear that differentiation of these stem cells into specialised cells of the recipient tissue is not likely to be the primary mechanism of tissue repair [9,13,30]. As discussed in the introduction to this thesis, secretion of trophic factors has been cited as the most likely cause for the broad applicability of stem cell therapy to many types of diseases. Adipokines secreted by adipose tissue have also been associated with tissue repair in some cases, although these adipokines tend to be secreted at higher levels in lean individuals rather than obese ones [36,65,71,153,157]. By taking this information together, it was logical to conclude that if a preparation of adipose tissue secretions were produced, it may have a beneficial effect on a range of disease states. Indeed, the conditioned media of adipose stem cells prepared *in vitro* has been shown to have beneficial therapeutic properties not dissimilar to those of an actual adipose stem cell transplant [13]. In this way, it was hypothesised that a preparation of conditioned media that contained the secretions of the entire population of cells from adipose tissue, including MSCs, may provide an improved set of secretions that would yield a positive effect on cells of a target tissue. The reciprocal signalling in a mixed population of adipose tissue cells was considered likely to produce a more complex secretion mixture than any single population of cells.

This chapter details the initial investigations of the effects of primary renal cell (PRC) responses to adipose tissue secretions derived from rat fat using 2-D gel based proteomic techniques. The chapter also details novel experiments designed to try to detect the proteins within the secretions that interact with the PRCs *in vitro* using avidin-biotin chemistry and a prototype cell-based assay system.

The method for producing the secretion mixture from the adipose tissue utilised a simple form of organ culture that involved incubation of intact pieces of adipose tissue in culture media for twenty-four hours. Initial characterisation using proteomics demonstrated that this process generated a very complex conditioned media, containing many hundreds of rat proteins. The fat was washed to remove blood proteins before the secretion production process, however residual plasma proteins were inevitable because of the very high concentrations of proteins such as albumin and their tendency to bind other proteins. The goal of these experiments was to use a primary cell as a biological filter and to provide a functional sorting mechanism that would display a subset of important proteins on the cell surface after incubation. In this way, I hypothesised that a significant enrichment of the biologically active proteins from the secretion mixture could be detected.

Primary cells were selected for use in these experiments because they represent the closest *in vitro* model of the kidney and will inevitably display the least number of changes induced by cell culture exposure and immortalisation techniques. The primary cells were considered important because they were closer to a true *in vivo* cell type. Primary mesangial cell preparations were produced as described by Menè and Stoppacciaro [214], with some simplifications. Plastic adherence was used as the primary mode of cell selection in these experiments. Literature theory and data on primary cell culture seems to indicate that in general, many current *in vitro* cell culture techniques possess an inherent factor of low-level cellular stress. The inevitable shifts in temperature, exposure to low serum protein concentrations, high concentrations of growth factors (when using ten percent foetal bovine serum), a lack of cell-cell contact, lack of three-dimensional structure, repeated exposure to high concentrations of proteases like trypsin and repeated exposure to nutrients and cellular waste through feeding and incubation cycles are all potential sources of stress to a cell *in vitro*. The fact that modern culture techniques lead to successful cell cultivation means that these stresses are able to be handled by most cells. However two major questions arise: When do these cells experience all of these stresses *in vivo*? When are these cells required to complete such high levels of proliferation *in vivo*? The answers to these questions remain unknown. However, situations where many of these conditions may arise concurrently are embryogenesis, pathogenesis and cancer. The processes governing tissue genesis, cancer and successful reconstruction are often the same. During pathogenesis, local tissue cells can

be exposed to altered oxygen tensions, elevated free radical levels, pro- and anti-inflammatory stimuli, pro- and anti- apoptotic stimuli, elevated immune cell presence, pro-fibrotic processes and changes to the extracellular matrix (ECM).

It was hypothesised that changes to the PRC proteome after treatment with adipose tissue secretions would yield protein expression information that related to the effects of the secretions on cells of the kidney. It was also theorised that labelling the secretion proteins prior to treatment with the PRCs and using the PRCs as a sort of novel 'biological filter' would serve to enrich and highlight the biologically relevant proteins from this complex preparation.

2.2 Aims:

1. To identify the effects of adipose tissue secretions on the mammalian kidney using proteomics techniques.
2. To identify the proteins from the rat adipose tissue secretions that bind to the PRCs using adapted biotin labelling and capture techniques.

2.3 Materials and Methods:

Animal ethics approval: All use of animal tissues in this chapter was subjected to review and approval by the University of Technology Sydney Animal Care and Ethic Committee (UTS ACEC). Applicable approval numbers: 2008-190 and 2008-190A.

2.3.1 Combined materials list for all experiments:

Materials required:

- Sonicator 3000 Ultrasonic probe – Misonix Inc. Farmingdale NY USA.
- Quantity One® image acquisition and analysis software - Bio-Rad Pty. Ltd. Hercules CA USA.
- Pharos FX™ PLUS gel scanner - Bio-Rad Pty. Ltd. Hercules CA USA.
- Protean IEF Cell, isoelectric focusing apparatus - Bio-Rad Pty. Ltd. Hercules CA USA.
- QSTAR Elite™ Mass Spectrometer – Applied Biosystems / MDS SCIEX.
- TEMPO™ NanoLC – Eksigent, Dublin, CA USA.
- Criterion™ Precast gel 4 - 12% Bis-Tris IPG+1 comb, 11 cm, 1.0 mm - Bio-Rad Pty. Ltd. Hercules CA USA.
- Criterion™ 1-Dimensional precast 12-well, 4 - 12% Bis-Tris 11 cm, 1.0 mm, polyacrylamide gels - Bio-Rad Pty. Ltd. Hercules CA USA.
- Criterion™ 1-Dimensional precast 26-well, 4 - 12% Bis-Tris 11 cm, 1.0 mm, polyacrylamide gels - Bio-Rad Pty. Ltd. Hercules CA USA.
- Criterion™ gel resolving apparatus - Bio-Rad Pty. Ltd. Hercules CA USA.
- CaptAvidin™ agarose magnetic beads (C-21386) - Life Technologies Corporation, Wilmington DE USA.
- Orbital shaker.
- Immobilised pH gradient (IPG) strips [4 - 7 pH] Linear - Bio-Rad Pty. Ltd. Hercules CA USA.
- Immobilised pH gradient (IPG) strips [3 - 10 pH] Linear - Bio-Rad Pty. Ltd. Hercules CA USA.
- 11 cm IPG strip rehydration/equilibration tray - Proteome Systems Ltd. Sydney NSW Australia
- IPG wicks - Proteome Systems Ltd. Sydney NSW Australia.
- 25 cm^2 plastic culture flasks, filter cap - Nalge Nunc International. Rochester NY USA.

- 75 cm^2 plastic culture flasks, filter cap - Nalge Nunc International. Rochester NY USA.
- Cell-scrapers – Nalge Nunc International. Rochester NY USA.
- Incubator (37°C, 5% CO_2) – Sanyo North America Corporation, San Diego CA USA.
- Disposable PD-10 Desalting Columns - GE Healthcare Fairfield CT USA.
- Protease inhibitor cocktail tablets, cOmplete Cocktail Tablets – Roche Diagnostics Australia Pty. Ltd. Castle Hill NSW Australia.
- Syringe filters, 0.2 µm pore size. Millex-GP Filter unit 33 mm – Millipore Corporation. Billerica, MA USA.
- ChemiDoc™ XRS+ gel/blot imaging apparatus - Bio-Rad Pty. Ltd. Hercules CA USA.
- Dithiothreitol (DTT) - Bio-Rad Pty. Ltd. Hercules CA USA.
- Precision Plus Protein™ Unstained Standards - Bio-Rad Pty. Ltd. Hercules CA USA.
- Semi-dry blotting apparatus - Bio-Rad Pty. Ltd. Hercules CA USA.
- PVDF Immobiline-P Membrane, 0.45 µm pore size - Millipore Corporation. Billerica, MA USA.
- Extra thick blot paper.
- Plastic roller.
- Vivaspin 500, 3000 Da cut-off filter – Sartorius-Stedim Biotech S.A. Aubagne Cedex, France.

Solutions required:

- Gel fixing solution – 40% Methanol, 10% Acetic acid (*v/v*).
- IPG equilibration solution – 6 M Urea, 0.25 M Tris-HCl pH 6.8, bromophenol blue, 10% SDS (*w/v*).
- MES gel resolving buffer – 50 mM Tris-base pH 8.8, 50 mM 2-(N-morpholino)ethanesulfonic acid, 1 mM EDTA; 0.1% SDS.
- Flamingo™ fluorescent protein stain - Bio-Rad Pty. Ltd. Hercules CA USA.
- Orange G tracking dye solution – Proteome Systems Ltd. Sydney NSW Australia.
- 7 M Urea, 2 M Thiourea, 1% C7BzO (*w/v*) solution (UTC7 solution).
- 7 M Urea, 2 M Thiourea, 1% C7BzO (*w/v*), 40 Mm Tris (UTC7 Tris solution) supplemented with protease inhibitor cocktail.
- Tributylphosphine (TBP), 200 mM stock – Sigma-Aldrich, St Louis MO USA.
- Acrylamide, 1 M stock – Sigma-Aldrich, St Louis MO USA.
- Dithiothrietol (DTT) solution, 50 mM stock - Bio-Rad Pty. Ltd. Hercules CA USA.
- Paraffin oil.
- Coomassie blue G250 staining solution 1.
- Coomassie blue G250 staining solution 2 (50% Ammonium sulphate).
- Coomassie destaining solution, 1% Acetic acid (*v/v*).
- 10% Methanol, 7% Acetic acid solution.
- Acetonitrile, LC-MS grade.
- 100 mM Ammonium bicarbonate (NH_4HCO_3) solution.
- 50 mM Ammonium bicarbonate / 50% Acetonitrile solution (*v/v*).
- Trypsin solution: 12.5 ng/µL Trypsin in 50 mM NH_4HCO_3 – Trypsin Gold, Mass spectrometry grade – Promega Corporation, Madison WI USA.
- Ficoll-Paque™ – GE Healthcare Fairfield CT USA.
- Phosphate Buffered Saline solution (PBS) 1x concentration; made using PBS tablets, 100 mL – Amresco LLC, Solon OH USA.
- EZ-Link® Sulfo-NHS-Biotin labelling reagent – Thermo Scientific, Rockford IL USA.
- ExtrAvidin®–HRP conjugated biotin specific probe - Sigma-Aldrich, St Louis MO USA.
- ExtrAvidin®-Peroxidase blot solution: 50 mL blocking solution supplemented with 50 µL ExtrAvidin®-Peroxidase (1:1000 dilution of stock).

- Glycine solution, 1 M stock – Glycine *ReagentPlus®* >99% (TLC) - Sigma-Aldrich, St Louis MO USA.
- CaptAvidin™ binding/washing solution: 50 mM citrate phosphate buffer, pH 4.0.
- CaptAvidin™ bead elution buffer: 50 mM sodium carbonate-HCl buffer, pH 10.6.
- Dithiothreitol stock solution (DTT), 1 M.
- NuPAGE® LDS Sample Buffer (4x) – Life Technologies Corporation, Wilmington DE USA.
- Buffer 1, 10x Stock: 400 mM Amino-caporic acid and 250mM Tris.
- Buffer 2, 10x Stock: 250 mM Tris.
- Buffer 3, 10x Stock: 3 M Tris.
- Washing solution - 40% ethanol (*v/v*), 10% acetic acid (*v/v*) in Milli-Q H_2O.
- 20% Sodium dodecyl-sulphate solution (*w/v*).
- 100% methanol.
- Blocking solution: 5% non-fat milk powder in Phosphate buffered saline (PBS) containing 0.1% (*v/v*) Tween-20.
- PBS-Tween 20 solution: PBS containing 0.1% (*v/v*) Tween-20.
- TBS wash solution: 50 mM Tris, 500 mM NaCl, 0.1% Tween 20 (*v/v*) titrated to pH 9 with 1 M HCl solution.
- Novex® ECL Chemiluminescent substrate Reagents A and B - Life Technologies Corporation, Wilmington DE USA.

2.3.2 Production of rat adipose tissue secretions:

The donor rats were euthanised according to UTS ACEC approved protocols using CO_2 asphyxiation prior to visceral fat pad excision. All animals were male Sprague-Dawley strain rats of twelve weeks of age (mean peak weight age) and were obtained under UTS ACEC approval. After euthanasia, the peri-renal and epididymal fat pads were harvested and placed into sterile mincing pots where they were minced using sterile small surgical scissors until pieces were approximately 2–3 mm^3 in size. The minced fat was then washed using sterile PBS solution at 37°C and placed into sterile 50 mL tubes up to the 10 mL graduation. The fat was suspended in 40 mL of DMEM-F12 (1:1) media supplemented with 1% antibiotic/antimycotic (ABAM) (*v/v*). The tubes were then capped and incubated at 37°C on a rotating wheel at 10 rpm for 24 hours. After the incubation, the tubes were assessed for any signs of microbial contamination using macroscopic and microscopic examination. All contaminated samples were disposed of, whilst non-contaminated samples were harvested from the tubes. The tubes were centrifuged at 1200 x g for 10 minutes to pellet any liberated cells and cause the free lipid and fat pieces to form layers at the top of the tube. The free lipid layer and fat piece layers were removed and discarded carefully. The intranatant (in-between cellular pellet and upper fat and free lipid layers) was then harvested into new 50 mL tubes and re-centrifuged at 1200 x g for 10 minutes. Any remaining lipid, fat or cellular debris was discarded while the conditioned media was harvested into new tubes and frozen at -22°C for future use.

2.3.3 Isolation and culture of rat primary renal cells (PRCs):

From the same rats used as donors to produce the rat adipose tissue secretions, the kidneys were also harvested. Once excised, the kidneys from one rat were placed onto a sterile petri-dish and were removed of their membranes using sterile forceps, the membranes were discarded. The kidneys were then placed into a sterile mincing pot together and minced using sterile small surgical scissors until pieces were approximately 2-3 mm^3 in size. The minced kidneys were then placed into a 50 mL tube containing 10 mL DMEM-F12 supplemented with 0.2% Collagenase enzyme (*w/v*). The tissue was allowed to digest at 37°C for 2 hours in a water bath with manual agitation every 5 - 10 minutes. Once the incubation period was complete, the undigested kidney pieces were strained from the cell suspension using a crude method with a sterile scalpel blade pressed against the top of

the tube while pouring the contents into a fresh 50 mL tube. The strained sample was centrifuged at 1000 x g for 10 minutes and the supernatant was removed and discarded. The cell pellet was resuspended in DMEM/F12 medium and carefully layered onto a bed of Ficoll-Paque^{TM} in a ratio of 3 mL Ficoll-Paque: 4 mL cell suspension. The layered cell suspension was centrifuged at 500 x g for 20 minutes at room temperature. Once centrifugation was complete, the cells at the interface of the Ficoll and the DMEM/F12 solution were harvested carefully into a sterile 15 mL tube, where they were washed with an additional 10 mL of DMEM/F12 solution, mixed and centrifuged again. The cell pellet was then suspended in 2 mL primary renal cell culture media containing DMEM/F12 supplemented with 50% Foetal Bovine Serum (FBS) (*v/v*) and 1% ABAM (*v/v*). The 2 mL cell suspension was then used to seed a 25 cm^2 plastic culture flask with filter cap and incubated at 37°C 5% CO_2 for up to two weeks, with daily microscopic observation.

The success of a given flask of renal derived cells was judged based on the presence of plastic adherent cells in the surface of the flask upon light microscopic examination after the first media change of a culture at day five to seven. Generally, success was low due mostly to the use of an excessive initial cell inoculum. Those flasks that yielded plastic adherent cells were retained at 37°C 5% CO_2 and maintained in culture with media changes every three to four days until used in experiments. No sub-culturing was completed using these cells due to the operator's inexperience in mammalian cell culture (explained in part in the Prologue to this chapter).

2.3.4 Culture of Vero cells:

When first seeding the Vero cells into culture from a frozen stock, the cells were defrosted in a 37°C water bath with gentle manual agitation and then quickly placed into a sterile 15 mL tube containing standard cell culture medium which consisted of DMEM/F12 (1:1), supplemented with 10% (*v/v*) FBS and 1% ABAM (*v/v*). The cells were mixed gently within the medium and then distributed into 75 cm^2 size flasks to form monolayer cultures. Once confluency was reached the media was removed, the cells were washed twice with 10 mL pre-warmed plain DMEM/F12 media and then trypsinised off the surface of the flasks. Once the cells were no longer attached to the flask surface they were suspended in 10 mL DMEM/F12 media and transferred into a 15 mL tube (one per flask). The tubes were then centrifuged at 500 x g for 10 minutes to pellet the Vero cells, after which the supernatant

was removed and the cells were re-suspended in 10 mL standard cell culture medium. The 10 mL of cell suspension was then used to seed three new T75 flasks using 3 mL of cell suspension each. The flasks were then topped up with another 12 mL of standard culture medium, mixed gently and then placed back in the incubator at 37°C 5% CO_2.

Cultures were checked macroscopically and microscopically for signs of contamination and for confluency every one to two days. Media was changed every three to four days or earlier as required during the culture and expansion stages of Vero culture. Once the desired amount of cells had been cultured, any excess cells were discarded according to proper procedures and the desired number of flasks was maintained after culture splitting until required for treatment with the adipose tissue secretions and proteomic analysis.

2.3.5 Biotin labelling of rat adipose tissue secretions:

The adipose tissue secretions were derived from rat tissue, while the renal cells being treated with the secretions were also of rat descent; this made distinction between the fat-derived proteins and the renal cell-derived proteins impossible in standard label-free proteomic approaches. Biotin labelling of the adipose secretions was chosen as a way to form a distinction between rat derived fat secretions and rat renal cell proteins when the two are mixed in culture during the treatment of the renal cells. It was thought that this would enable some identification of not only some form of interaction between the fat secretions and the renal cells but also may provide a means to pull these interacting proteins back out from the renal cells, enrich them and then identify them using mass spectrometric techniques.

The rat adipose secretions were first put through a PD10 disposable buffer exchange column using PBS as the wash and elution buffers in order to remove excess free primary amines from the original secretion solution (DMEM/F12). The PD10 column elution fraction was collected into a 15 mL tube and then mixed with 40 µL of EZ-Link® Sulfo-NHS-Biotin labelling reagent stock (5 mg/mL stock concentration) to provide excess biotin for reaction to the protein secretions. The tube was incubated at room temperature for sixty minutes and then the reaction was quenched by the addition of 50 µL of a 1 M glycine stock and fifteen minute incubation at room temperature.

2.3.6 Treatment of PRCs with biotinylated rat adipose tissue secretions:

The biotinylated secretions were added to PBS solution and FBS in the ratio 5:2:3 respectively. This gave a final concentration of FBS in the mixture of 30% (*v/v*), which matched the FBS concentration within the standard PRC growth medium being used and also provided a source of blocking protein to inhibit non-specific protein binding between the PRCs and the biotinylated secretions. The adipose secretion mix was then filtered through a 0.2 µm syringe filter and then placed in a water bath to warm to 37°C prior to use. All culture and liquid manipulations were completed inside a biological class II safety cabinet.

The PRC culture flasks to be treated with the biotinylated adipose secretions were drained of growth medium and washed gently with PBS solution that had been filtered through a 0.2 µm syringe filter and then pre-warmed to 37°C. Once washed, 2 mL of the biotinylated secretion mix was added to each flask, the flask was gently rocked to allow for circulation of the solution over the cells and then the flasks were incubated at 37°C 5% CO_2 for twenty minutes to allow any proteins to bind to the cells.

After the incubation, the flasks were removed from the incubator and the secretion mix was removed from the flasks and retained inside a 15 mL tube. The flasks were washed out twice with 5 mL pre-warmed PBS solution; each lot of PBS used to wash the flasks was collected into a separate 15 mL tube and labelled 'W1', 'W2', 'W3' *etc* and were retained for use in the western blot analysis to be performed at a later stage. After two washes inside the flask, the cells were scraped off the surface of the flask into a new 15 mL tube using a cell-scraper and PBS solution to wash out the remaining cells from the flask into the tube. The 15 mL tube was then filled to the 10 mL graduation with PBS and the cells were gently suspended and mixed to further wash them. The tubes were then centrifuged at 1000 x g for 10 minutes. The supernatant was retained in a separate tube labelled 'W3' and the wash step described here repeated twice more, with each of the washes being retained as 'W4' and 'W5' respectively. After the final wash the cells were left in the 15 mL tube and frozen as a dry pellet along with the wash samples and an aliquot of the initial biotinylated secretion mix; at -22°C until future use in western blotting experiments.

2.3.7 Western blotting of 1-D and 2-D gels:

Separated proteins were transferred onto 0.45 µm Immobilon-P Transfer Membrane (PVDF) following a semi-dry method similar to the one developed by Khyse-Anderson [215]. During the electrophoresis stage of the 1-D or 2-D gel resolution, seven blot papers and one membrane were cut to the size of the gel to be blotted. The three buffers required for the blot procedure were then prepared and cooled to 4°C as described below:

- Buffer 1: (200 mL total required per gel) 20mL of 10x stock, 20mL of 100% methanol and 500 µL of 20% SDS made up to 200 mL final volume with Milli-Q H_2O.
- Buffer 2: (100 mL total required per gel) 10mL of 10x stock and 20mL of 100% methanol made up to 100 mL final volume with Milli-Q H_2O.
- Buffer 3: (50 mL total required per gel) 5 mL of 10x stock made up to 50 mL final volume with Milli-Q H_2O.

100 mL of buffer 1 was decanted into a clean plastic tray. All of buffer two and buffer three were decanted into additional individual clean plastic trays. Two blot papers were then placed into the tray containing buffer 1, four placed into the tray containing buffer 2 and one placed into the tray containing buffer 3. The membrane was then placed into a clean tray containing 100% methanol. The membrane was soaked in the methanol until completely wet before being transferred to the tray containing buffer 2 underneath the four blot papers that were soaking in this tray already.

Upon the completion of the 1-D or 2-D gel electrophoresis resolution, the gel was removed from its cassette and placed in a clean plastic tray containing Milli-Q H_2O for two minutes. The H_2O was then decanted from the plastic tray and replaced with 100 mL of buffer 1 and was incubated at room temperature for a further five minutes. When equilibrated, the blot stack was assembled in a bottom-up manner as shown in **Figure 2.1**.

When the gel was placed onto the membrane it was carefully inspected to ensure that there were no air bubbles trapped between the gel and the membrane which would have prevented the transfer of protein. Once the stack was assembled it was carefully rolled with a plastic roller to remove excess buffer and any residual air bubbles. The blotting cassette was then closed and the instrument programmed to transfer at 300 mA (constant) for twenty-five minutes at 4°C (inside a cold room).

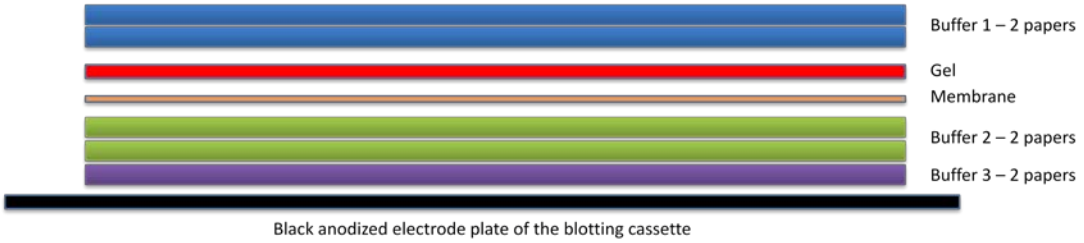

Figure 2.1: Bottom-up Western blot stack configuration used in the protocol described in this chapter.

The membrane was then incubated with blocking solution for a minimum of one hour at 4°C and then washed with washing solution for twenty minutes. The ExtrAvidin®-Peroxidase blot solution was then added to the membrane and allowed to bind to any biotinylated proteins present on the membrane from the sample for one hour at room temperature. The membrane was then washed four times with wash solution over a minimum period of ninety minutes. At the end of the wash procedure, the Novex® ECL substrate reagents A and B were mixed in equal proportions inside a foil-covered 15 mL tube just before the membrane was ready for development and washing was completed. Once washed extensively, the membrane was then removed from the wash solution and placed face-down on a sheet of plastic wrap where the development reagent mix was poured onto the membrane and sealed in with it using the plastic wrap. The membrane was then developed immediately using the ChemiDoc™ XRS+ gel/blot imaging apparatus and Quantity One® image acquisition and analysis software.

2.3.8 The use of CaptAvidin™ beads to recover and identify interacting biotinylated adipose secretion proteins:

The initial step of this experiment was to capture and purify the interacting proteins from the biotinylated adipose secretions. To achieve this, CaptAvidin™ beads were utilised to capture the interacting proteins from a lysate of treated PRCs. This should have allowed for the removal of non-interacting non-biotinylated proteins through wash steps and then elution of the interacting proteins using a pH change-induced conformational change in the avidin-biotin binding site, a unique property of the CaptAvidin™ system.

The CaptAvidin™ beads were mixed thoroughly with a vortex and then 300 µL of bead slurry was removed and placed into a 1.7 mL tube. The tube was centrifuged at 1000 x g for five minutes and the storage buffer was removed and discarded. The beads were then

washed three times in 500 µL CaptAvidin™ binding/washing solution pH 4 in order to remove traces of storage solution and re-equilibrate the beads to pH 4 in order to create appropriate biotin-avidin binding conditions. After the final bead washing step, 300 µL of biotinylated secretion treated PRC lysate was prepared for addition to the beads; 270 µL of biotinylated secretion treated PRC lysate was added to the bead pellet and mixed thoroughly using a vortex. The remaining 30 µL was retained for use as the 'Pre-treatment' sample as an example of the sample prior to exposure to the beads.

The sample was allowed to bind for two hours at room temperature with the tube attached to a rotating wheel set on slow rotation to allow for mixing throughout the binding process. Once binding was complete the tube was centrifuged at 1000 x g for ten minutes and the unbound supernatant was collected and retained in a labelled tube. The beads were then washed twice with 300 µL of CaptAvidin™ binding/washing solution pH 4, using a centrifugation step of 1000 x g for ten minutes for each step. The elution buffer (pH 10.6) was then added to the bead pellet (300 µL) and the beads were suspended and incubated at room temperature for one hour on the rotating wheel as described earlier. The sample was centrifuged at 700 x g for ten minutes and the first elution sample was collected into a labelled tube. A further two elution steps were performed in a similar manner to that just described, however the incubation time for elutions were shortened to twenty minutes each. Once all elution samples had been collected, they were pooled and concentrated from 900 µL to a final volume of 30 µL using centrifugation at 8000 x g inside a 3000 Da cut-off filter.

The pre-treatment, unbound and the concentrated elution fraction samples were then reduced and alkylated by adding TBP and acrylamide solutions to the samples to a final concentration of 10 mM each and incubated at room temperature for ninety minutes. The process was quenched by the addition of 10 mM DTT. The samples were then aliquotted and frozen at -22°C for future use. One aliquot of the samples was retained for assessment using 1-D electrophoresis. In preparation for 1-DE, NuPAGE LDS buffer (4x) was added to the sample in a ratio of 1:3 respectively. The sample was mixed well using a vortex and then incubated at 95-100°C for five minutes. The sample was then centrifuged at 20 000 x g for ten minutes. During this time the precast Criterion™ 12-well 1-D gel, resolving apparatus and resolving buffer were prepared according to the product manuals. The sample was

loaded into one well of a Criterion™ 1-D pre-cast 12-well, 4 - 12% Bis-Tris 11 cm, 1.0 mm, polyacrylamide gel, 5 µL Precision Plus Protein™ Unstained Standards were also added to one lane. The sample was resolved at 150 V (constant) until the dye front reached the bottom of the gel, at which time it was placed into 100 mL of gel fixing solution and onto an orbital shaker on slow rotation for a minimum of thirty minutes. The gel was then stained with Flamingo™ fluorescent protein stain overnight at room temperature while covered in foil to prevent photobleaching. The next day, the gel was scanned using the Pharos FX™ PLUS gel scanner and Quantity One® 1-D image acquisition and analysis software in order to assess the protein load present within each elution sample.

2.3.9 Treatment of PRCs with rat adipose tissue secretions for 2-D gel based analysis:

The selected flasks of PRCs for use in the differential display experiment were first drained of growth media and washed gently with 5 mL pre-warmed (37°C) DMEM/F12 media using a sterile transfer pipette to wash the media up and down the surface of the flasks. The wash media was removed and the flasks were split into two equal groups; control and treated. The control group received 2 mL of control PRC growth media per flask (DMEM/F12 supplemented with 30% FBS (*v/v*) and 1% ABAM (*v/v*)). The treated group received 2 mL of media containing adipose secretions per flask, which consisted of rat adipose secretions mixed with DMEM/F12 media and FBS and ABAM to a final concentration of 30% and 1% (*v/v*) respectively. All media preparations had been filtered through a 0.2 µm syringe filter prior to use and were pre-warmed to 37°C. The control and treated flasks were then gently tipped to mix the media around within the flasks and then incubated for three days at 37°C 5% CO_2.

2.3.10 Isolation of PRC/Vero cell proteins for 2-D electrophoresis:

Culture flasks of cells to be used in proteomic experiments, PRCs or Vero cells, were washed twice with PBS solution supplemented with a protease inhibitor cocktail (one tablet per 50 mL PBS) inside the flasks after the treatment or control media had been drained off and discarded. The cells from one flask were then scraped off using a cell scraper and washed into a sterile 15 mL tube using PBS solution and a transfer pipette. The tube was then filled to 10 mL volume with more PBS (and protease inhibitor) and the cells were gently mixed by inversion to further wash them of FBS and other non-cell derived proteins that may hinder the proteomic analysis. The tube was then centrifuged at 1000 x g for ten minutes

and the supernatant was discarded. The wash step was then repeated twice more using a further 10 mL PBS (and protease inhibitor cocktail) to make the total number of washes per flask equal five.

Once washed, the cell pellet was suspended in 3 mL UTC7 Tris/protease inhibitor solution using a pipette tip to break up any cell clumps. The cells in suspension were then lysed using an ultrasonic probe with six bursts of thirty seconds with the probe in total and a minimum of thirty seconds on ice between each burst. The cell lysate was then set up for reduction and alkylation of the proteins by the addition of TBP and acrylamide stocks to a final concentration of 10 mM each. The tube was then incubated at room temperature for ninety minutes with occasional mixing; the reduction/alkylation was quenched by the addition of 10 mM DTT. Once reduced and alkylated, the sample was then transferred into three 2 mL tubes and centrifuged at 21,000 x g for twenty minutes to remove any cellular debris. The original 15 mL tube was retained and used to pool the supernatants from the centrifugation step (this minimised protein loss due to interaction with plastic surfaces). The re-combined sample was then acetone precipitated using a five-fold volume of acetone to protein solution. Citric acid was added to samples in order to induce precipitation of the proteins as necessary, but in extremely small increments. The sample was incubated at room temperature for thirty minutes and then centrifuged at 3,200 x g for ten minutes. The supernatant was carefully removed and discarded. The protein pellet was re-suspended in UTC7 solution ready for a 1-DE based protein assay, protein load equalisation and isoelectric focusing at protein loads of 3 mg/mL for the PRC samples and 4.2 mg/mL for the Vero cell samples.

2.3.11 One-dimensional gel protein quantification assay and sample protein equalisation:

Prior to resolving the samples via 1-D isoelectric focusing and then 2-D PAGE, total protein loads between the samples required equalisation to allow for accurate comparisons to be made between replicates and test and control groups. NuPAGE LDS sample buffer (4x) was added to small aliquots of each control or treated sample and mixed thoroughly using a pipette and vortex. The samples were then heated to 95° C for 10 minutes to ensure that the sample buffer and proteins from each sample were properly interacting. The samples were then diluted in series one-in-two along side a BSA protein standard at a starting concentration of 4.2 mg/mL. NuPAGE LDS sample buffer (1x) solution was used to dilute

each sample and standard at each stage of the dilution series. The samples and standards were vortexed and centrifuged for 10 seconds each prior to every subsequent dilution step. The diluted samples and standards were then heated to 95° C for 10 minutes.

The samples were loaded into a pre-cast 26-well one-dimensional Criterion gel and resolved at 120 Volts until each sample had only just entered the gel. It was important to prevent the proper resolution of the different proteins in each sample into bands that would interfere with the densitometry analysis of each sample as a single protein band. See **Figure 2.2** for demonstration of how far the samples were resolved into each well of the gel in a properly run assay. The gel was then fixed with fixing solution for a minimum of thirty minutes while rotating on an orbital shaker. The fixing solution was removed and the gel was stained with Flamingo fluorescent protein stain solution for ninety minutes while protected from light with a foil wrapping.

The gel was then imaged on the Pharos FX^{TM} PLUS gel scanner at 100 nm resolution using the QuantityOne^{TM} scanning software. The bands in the gel image were then labelled as either Standard (Std) or Unknown (U) and the concentrations of each of the standards were typed into the input sections for each band. A properly run and labelled 1-D protein assay gel image appears similar to the one featured in **Figure 2.2**.

A standard curve was constructed using the densitometric analysis of the standard dilution series in the gel image from **Figure 2.2**. This was done by selecting the Volume Analysis tool and then selecting the Std Curve application in the subsequent window which appeared. The standard curve R-squared value was checked to ensure that it was above 0.95, if the R-squared value was below 0.95, the assay was considered inaccurate and was repeated. The standard curve was also used to ensure that an adequate number of unknown sample dilutions were inside the ranges of the standard dilutions. If this was not found to be the case, then the assay was repeated using further dilutions of the samples or standards. As an example, the standard curve for the samples/standards in **Figure 2.2** has been featured in **Figure 2.3**.

Once it was confirmed that the R-squared value and that the unknown samples fell within the standard curve limits, the volume analysis tool was used to obtain the densitometric data output for each unknown sample. This data appears in the form shown in

Figure 2.4. This data allowed for the back-calculation of the concentration of each unknown sample. Once the concentration of each sample was known, the samples were equalised by dilution of the most concentrated samples to the same concentration as the least concentrated sample.

Figure 2.2: Gel image of a properly run 1-D gel protein quantification assay with appropriate sample labels

Figure 2.2: Gel image of a properly run 1-D gel protein quantification assay with appropriate sample labels. Samples and standards have only just entered the gel without further resolution. The gel has been stained with Flamingo protein stain and scanned using a Pharos FX™ PLUS gel scanner. QuantityOne™ software was used to perform densitometry on each of the bands to determine the volume of each sample/standard at each dilution. **(U)** Treated/control samples of unknown concentration. **(Std)** Standards of a known concentration used in the construction of a standard curve, as demonstrated in **Figure .**

Figure 2.3: A graphical representation of the standard dilution series samples from the gel in **Figure 2.2**.

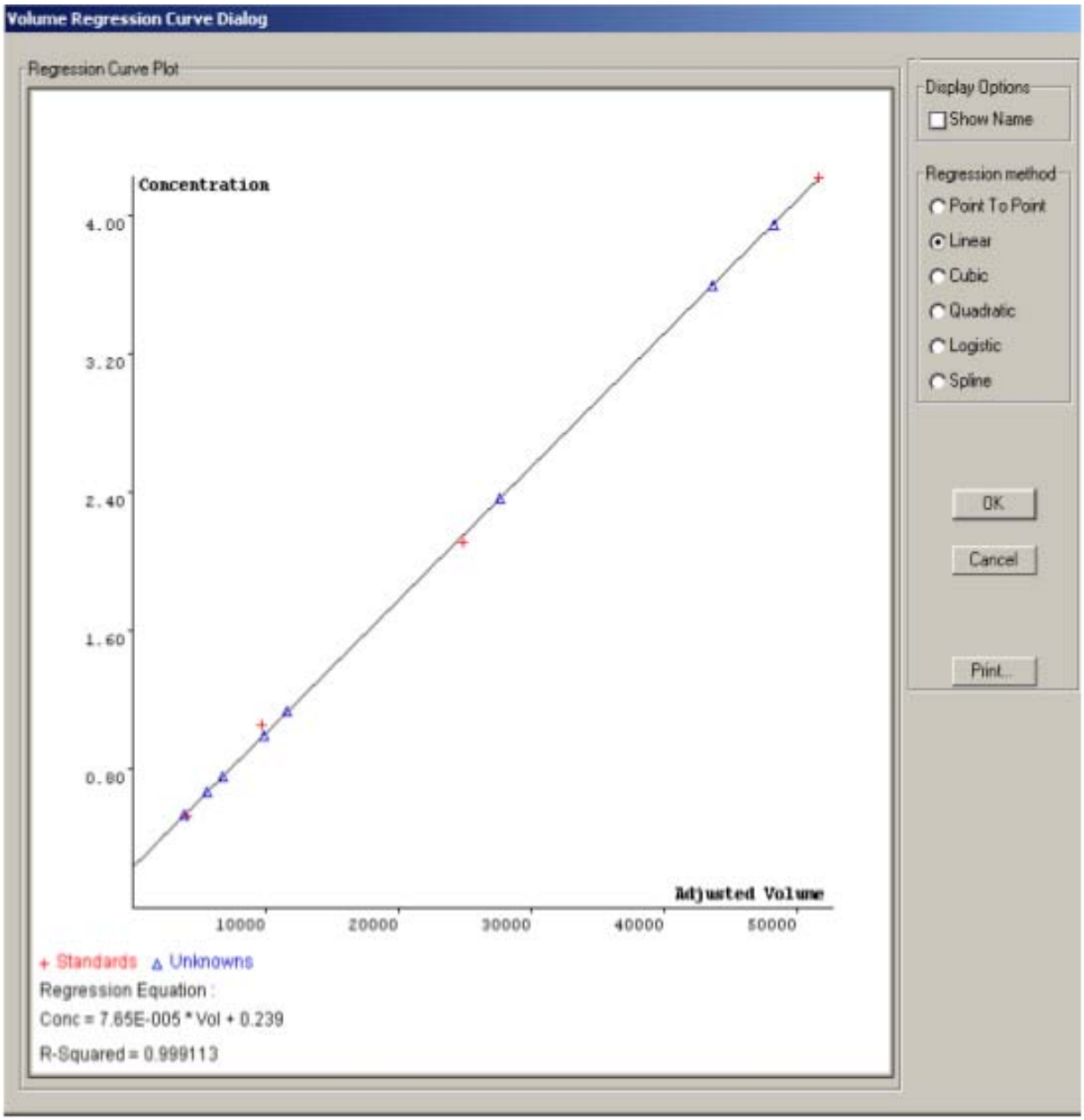

Figure 2.3: A graphical representation of the standard dilution series samples from the gel in **Figure 2.2**. The R-squared value is featured at the bottom of the figure (0.999113), indicating that the standard curve in this example is highly linear. The samples of unknown concentration are all seen to fit into the ranges of the standard curve, indicating that the starting standard concentration and subsequent dilution series selected is suitable for establishing the protein load in the unknown samples.

Figure 2.4: QuantityOne™ data output showing the detected volume data output for every standard and unknown sample band included in the assay.

Index	Name	Adj. Vol. CNT*mm2	Concentration
1	Std1	51632.77930	4.200000000000
2	Std2	24849.17429	2.100000000000
3	Std3	9761.376789	1.050000000000
4	Std4	4188.050825	0.525000000000
5	U1	43708.88831	3.583609226418
6	U2	11664.49389	1.131257181384
7	U3	6818.240642	0.760374245745
8	U4	3890.177281	0.536290055551
9	U5	48311.81778	3.935870634539
10	U6	27660.35628	2.355417804704
11	U7	9912.172946	0.997152357842
12	U8	5622.592334	0.668871484417

R-Squared = 0.999113
Background Subtraction Method: Local
data units: Counts (CNT)

Figure 2.4: QuantityOne™ data output showing the detected volume data for every standard and unknown sample band included in the assay. The unknown sample data is measured against the standards in the standard curve by the QuantityOne™ software. This data can then be used to back-calculate the concentration of the original samples, thereby enabling equalisation of the total protein load of each sample by dilution of the most concentrated sample(s) to the same concentration as the least concentrated sample.

2.3.12 Isoelectric Focusing (IEF) of isolated proteins:

In preparation for IEF, the selected immobilised pH gradient (IPG) strips were rehydrated with 100 µL of UTC7 solution in the gel-side down orientation within a strip rehydration/equilibration tray. The strips were incubated at room temperature for a minimum of forty minutes, or until the entire 100 µL of UTC7 solution had been absorbed into the strips.

Once rehydration was complete the strips were placed into an 11 cm IPG running tray, also in the face down position; with dampened IPG wicks placed under the strips at both ends. The strips and wicks were then covered in paraffin oil in preparation for loading with the sample in a process known as active rehydration.

The control and treated PRC or Vero protein samples were then defrosted and sonicated in a sonic bath for five minutes to fully re-suspend the sample. The samples were then centrifuged at 20,000 x g for ten minutes to remove any extraneous cellular debris or protein aggregates which may have been present within the samples. Tracking dye was then added to the samples in the ratio of 10 µL dye per 1 mL of sample. The samples were mixed thoroughly and then 150 µL of the sample was loaded underneath and IPG strip along the entire centre of the strip so that none touched the wicks at either end. The location and orientation of each strip and sample was planned and recorded carefully in order to track each different sample, which at this point all essentially looked identical.

Once loaded the lid was placed onto the running tray and it was placed carefully into the resolving bay of the Protean IEF cell where it was connected to the positive and negative electrodes and the machine was programmed for the focusing method of choice. The method used here involved a three step gradual increase of voltage and a reciprocal decrease in applied current to provide optimum focusing.

<u>Phase 1 setting:</u>

- Current limit: 75 µA per strip.
- Zero hours voltage = 100 V per strip ramped in a logarithmic fashion to 2950 V at five hours.

Phase 2 settings:

- Current limit: 49.5 µA per strip.
- Five hours voltage = 2950 V per strip ramped to 10000 V at eight hours in a linear fashion.

Phase 3 settings:

- Current limit: 29 µA per strip.
- Eight hours voltage = 10000 V per strip maintained constantly for a minimum of four hours.

2.3.13 Two-dimensional PAGE:

The IPG strips were left to focus until they had reached 115000 Volt-hours, at which point they were removed from the Protean IEF apparatus and placed into a clean equilibration tray, covered in 10 mL equilibration solution and incubated at room temperature on an orbital shaker for twenty minutes (and no longer).

During the equilibration, the precast gel, resolving buffer and gel resolving apparatus were prepared. For each IPG strip being equilibrated a single Criterion™ Precast gel 4 - 12% Bis-Tris IPG+1 comb gel was prepared and placed into the gel resolving apparatus, which was then filled with 500 mL 1x MES resolving buffer including the upper reservoir of the gel.

The strips were then removed from the equilibration solution and placed into the upper chamber of the precast gel in a 'positive to positive' orientation described on the casting surrounding the gel. Once orientated, 5 µL Precision Plus Protein™ Unstained Standards was added to each gel in the separate standards well. The lid of the apparatus was put into place and the gel was resolved at 150 V (constant) until the tracking dye reached the bottom of the gel.

Once the electrophoresis was complete, each gel was placed into a clean fixing tray containing 100 mL gel fixing solution for a minimum of forty minutes. The gels were then stained with 100 mL of Flamingo™ fluorescent protein stain overnight on an orbital shaker with the gel covered in foil to prevent photo-bleaching.

2.3.14 Gel imaging and analysis using PDQuest™ image analysis software:

The gels were scanned using the PharosFX™ gel imager and Quantity One® image acquisition and analysis software using the correct pre-set wavelength and PMT voltage settings for the Flamingo™ protein stain within the software. Gels were scanned using identical settings in terms of scanner sensitivity (low, medium or high) and resolution (50 µm) for all gels within one differential display experiment.

The differential comparison of spots between gels was then completed using the scan files, which were loaded into PDQuest™ image analysis software. Image analysis was completed according to the software instruction manual. The software compared the relative intensities of corresponding spots in each gel to conduct a two sample t-test assuming non-equal variances on these spots to generate a *p*-value related to the null-hypothesis that there is no change in protein intensity; and therefore no change in protein level between the two conditions.

2.3.15 Spot cutting and MS identification of selected proteins:

The gels containing the desired protein spots were stained with Coomassie blue G250 in order to allow for the easy visual identification of the spot pattern and the desired spots in order for manual excision of the spots from the gel. Each gel was washed twice with dH_2O for ten minutes in a gel staining tray to wash off excess Flamingo™ protein stain. Coomassie stain reagents 1 and 2 were combined in a ratio of 4:1 respectively and then added to the gels (100 mL total per gel), which were then covered and placed on an orbital shaker at room temperature overnight to stain.

The Coomassie stained gels were then detained using 1% Acetic acid solution until the background staining was gone and the protein spots were clearly visible. The destained gels were placed on a white light illuminator with water added to prevent gel distortion due to dehydration. For all replicate gels within a set, all control PRC gels for example; the target spots were excised from all of the gels within the set and combined in the same labelled 600 µL tube containing 200 µL of a solution containing 10% methanol and 7% Acetic acid to further destain the protein spots of Coomassie stain. The spot cuts were left to destain for up to two hours with regular changes to the 10% methanol, 7% Acetic acid solution to enhance the destaining.

The destain solution was then removed and the spot cuts were washed twice with 200 µL of 100 mM NH_4HCO_3 solution for five minutes per wash. The spot cuts were then washed twice with 50 mM NH_4HCO_3 / 50% ACN solution for five minutes each wash. The cuts were then further dehydrated by treatment with 100 µL ACN, at which point the gel pieces appeared as small shrivelled white lumps within the tubes. If this did not occur in the first wash, the ACN was changed and the dehydration step repeated. Once dehydrated, the ACN was removed from the tubes and the pieces were allowed to air dry for ten to fifteen minutes. Once dried, 30 µL of trypsin solution was added to each tube and allowed to soak into the gel pieces at 4°C for thirty minutes. The tubes were then topped up with 20 - 40 µL of 50 mM NH_4HCO_3 and then placed into a 37°C incubator overnight to digest.

Once the digestion incubation was complete, the digestion solution from each tube was removed and collected into clean, labelled 600 µL tubes and then put aside. To the gel pieces, 50% ACN 2% Formic acid solution was added and incubated at room temperature for twenty minutes. The solution was then removed and pooled with the corresponding tube digest solution samples put aside earlier. The pooled digest solutions were then placed into a vacuum evaporator at 30°C until the total sample volumes were reduced to approximately 20 µL each. The sample tubes were then centrifuged at 20000 x g for ten minutes and then 15 µL was loaded into labelled auto-sampler tubes for MS processing and protein identification. Alternately, samples were frozen at -22°C inside the original 600 µL tubes for future MS identification.

The auto-sampler tubes were placed in the rack of the Eksigent AS-1 auto-sampler connected to the TEMPO™ nanoLC system. Due to the high level of variables one can control during MS protocols, many parameter settings must be recorded as methodological data. The following paragraphs are a detailed recollection of the settings by the creator of the protocol used, Dr Matthew Padula, UTS in an unpublished personal communication.

10 µL of the sample was loaded at 20 µL/minute with 2% ACN, 0.2% Formic acid (Solvent A) onto a C18 reversed-phase trap column connected to a 10-way switching valve. After washing the trap for two minutes, the 10-way valve was switched and the peptides washed off the trap at 500 nL/minute onto a New Objective IntegraFrit column (75 µm ID x 100 mm) packed with ProteoPrep 2 C18 resin. At the moment of switching, a gradient

program was started to elute bound peptides from the column and into the source of a QSTAR Elite hybrid quadrupole-time-of-flight mass spectrometer (Applied Biosystems/MDS SCIEX). This program consisted of the following phases:

1. *5 - 30% solvent B (98% ACN, 0.2% Formic acid) over 8 minutes.*
2. *30 - 80% solvent B over 2 minutes.*
3. *80% solvent B for 2 minutes.*
4. *80 - 5% solvent B for 3 minutes.*
5. *Re-equilibration for 10 minutes in solvent A prior to the next sample.*

Eluted peptides flowed from the column into a MicroIonSpray II-mounted 75 µm ID emitter tip that tapered to 15 µm. Charged peptides were then ionised by nanoelectrospray with 2300 V into the source of the QSTAR which then preformed an Intelligent Data Acquisition (IDA) experiment. Briefly, a mass range of 375 – 1500 Da was continuously scanned until a peptide of charge state 2^+ - 5^+ was detected with and intensity of more than 100 counts/second. This precursor peptide was then selected, fragmented and the product ion fragments measured over a mass range of 100 – 1500 Da. The mass of the precursor peptide was then excluded for 45 seconds so that lower abundance peptides would also be fragmented and analysed. (Dr Matthew Padula, UTS, *personal communication,* 2008).

2.4 Results:

The experimental work-flow for this chapter is outlined in a flow-chart detailing the variants of labelled and non-labelled rat adipose tissue secretions and their use on the PRCs *in vitro*. This work-flow can be seen in **Figure 2.5**.

2.4.1 Changes to the PRC proteome in response to treatment with rat adipose secretions:

After successful culture of the rat PRCs and obtaining a successful batch of rat adipose secretions, the PRCs were treated with the secretions for three days and subjected to proteome analysis using the protocols described in section 2.3. The three day treatment time was decided upon for two reasons: to give the PRC proteome the maximum amount of time to change and cause down-stream network-wide effects on the cell; and because initial unpublished clinical data typically showed a significant improvement in patients treated for osteoarthritis using adipose stem cells (ASCs) after a three day period. These factors influenced the decision to use three days as a suitable timepoint to utilise for the indicative experiments planned in this section of the chapter.

Overall, it was only possible to produce two control and two treated PRC 2-D gels for this comparison because of the low numbers of rat kidneys and the difficulty of successful PRC culture at the time. These four gels were derived from eight individual flasks of PRCs (two per gel). Therefore the small number of biological and technical replicate gels for this type of experiment was only enough to derive indicative results which were not subjected to a full statistical analysis between biological replicates. **Figure 2.6** shows control and treated gels from a single biological replicate typical of the resolution and quality obtained for each sample. The circled proteins are those that were quantitatively changed between control and treated PRCs with a detected expression difference of two-fold or greater using the PDQuest^{TM} image analysis software. The successful protein identifications from the circled spots in **Figure 2.6** are detailed in **Table 2.1**. As minimal replicate gels were available for each condition, the ability to detect the identity of the fainter spots using in-gel tryptic digestion and LC/MS based identification techniques was diminished.

2.4.2 Detection of the interaction of rat adipose secretions with PRCs:

The difficulty in obtaining and culturing PRCs was a significant impediment. The key issue was the requirement for hundreds of micrograms of protein per 2-D gel to enable MS

analysis and identification of differentially expressed proteins. A comprehensive strategy using 2-DE based detection of PRC proteome changes in response to adipose secretion treatment was not likely to be successful within the timeframe and budget of the project. Attention was turned to detecting the factors within the adipose secretions that may be responsible for some of the regenerative effects of adipose secretions noted in the literature. The use of biotin-avidin chemistry was selected due to the wide literature base, the strong affinity of the biotin-avidin interaction and the commercial availability of labelling kits. In addition, the hypothesis was that biotin labelling of the secretions would not result in significant functional change in the labelled proteins (based on manufacturer's information, see Materials and Methods). The relatively short treatment time of twenty minutes, compared to three days in the previous PRC experiment, was used in this work to avoid any loss of labelled cytokine through PRC metabolism of the labelled secretion proteins. A short treatment of twenty minutes provided enough time for the PRCs to bind to the selected labelled proteins and/or internalise these proteins in order for them to be detected in suitable levels using western blot analysis. The short incubation time also allowed for a snapshot of the PRC interacting proteins at the very start of the induction of changes to the treated PRCs.

In summary, the complete mixture of rat adipose secretions was biotinylated and used to treat PRCs in culture. After washing of the PRCs to remove unbound proteins, the cells were solubilised and the proteins separated by 1-D or 2-D electrophoresis. The separated proteins were transferred to PVDF membrane by semi-dry electroblotting and the biotinylated proteins detected by probing with avidin-HRP conjugate and chemiluminescence. **Figure 2.7** details a typical western blot obtained from the short-term treatment of one flask of PRCs with a biotin labelled preparation of adipose secretions. The lanes marked 'Treated PRCs' indicate the lanes that contain the whole PRC lysate and proteins from the adipose secretions that were present in the cell lysate after extensive washing of the cells. The 'W1-W4' lanes indicate how washing of the PRCs after treatment resulted in depletion of the 'non-interacting' proteins. There were five wash steps in total performed on the cells but only the first three were ran on the gel, indicating an even lower level of biotinylated proteins in the wash samples and an even greater depletion of 'non-interacting' proteins than is shown in **Figure 2.7**. The pattern and density of the 'T' lane in

Figure 2.7 indicates that proteins have possibly bound to or internalised by the PRCs during the incubation.

2.4.3 Attempts to identify the proteins that may be interacting with the PRCs *in vitro*:

Following the promising results in **Figure 2.7**, attempts were made to further utilise the biotin-avidin interaction for the isolation, enrichment and identification of the proteins that may be interacting with the PRCs as seen in **Figure 2.7** (lane T). CaptAvidin^{TM} magnetic agarose beads were selected based on their ability to bind and release biotin-labelled substances following a pH change that results in a conformational change in the avidin binding site for the biotin molecule. Theoretically this would have enabled the addition of the PRC lysate containing biotinylated adipose secretion proteins and the recovery and enrichment of these proteins on the beads. However as shown in **Figure 2.8**, the yield of biotinylated proteins off the beads was very low and did not result in a protein yield large enough to allow for protein identification using a gel-based approach.

Figure 2.5: Experimental flow diagram used to describe the different uses of the donor rat tissues. Adipose tissue and kidneys were extracted from the euthanised rats for varying applications. The adipose tissue was used for the production of conditioned media using a crude organ culture method as described in **Section 2.3.2**. The kidneys were processed to produce a mixed plastic adherent primary renal cell population as described in **Section 2.3.3**. The conditioned media contained a mixture of different adipose secreted proteins. The secretion preparations were then either used to treat PRCs directly for 2-DE analysis as in **Section 2.3.9;** or were biotinylated and then used to treat the PRCs as in **Section 2.3.6**. The PRCs treated with biotinylated adipose secretions were then used in western blot and CaptAvidin^{TM}-based experiments in order to assess and investigate the interaction of the secretions with the PRCs *in vitro*.

Figure 2.5: Brief experimental work-flow for the work completed in Chapter 2.

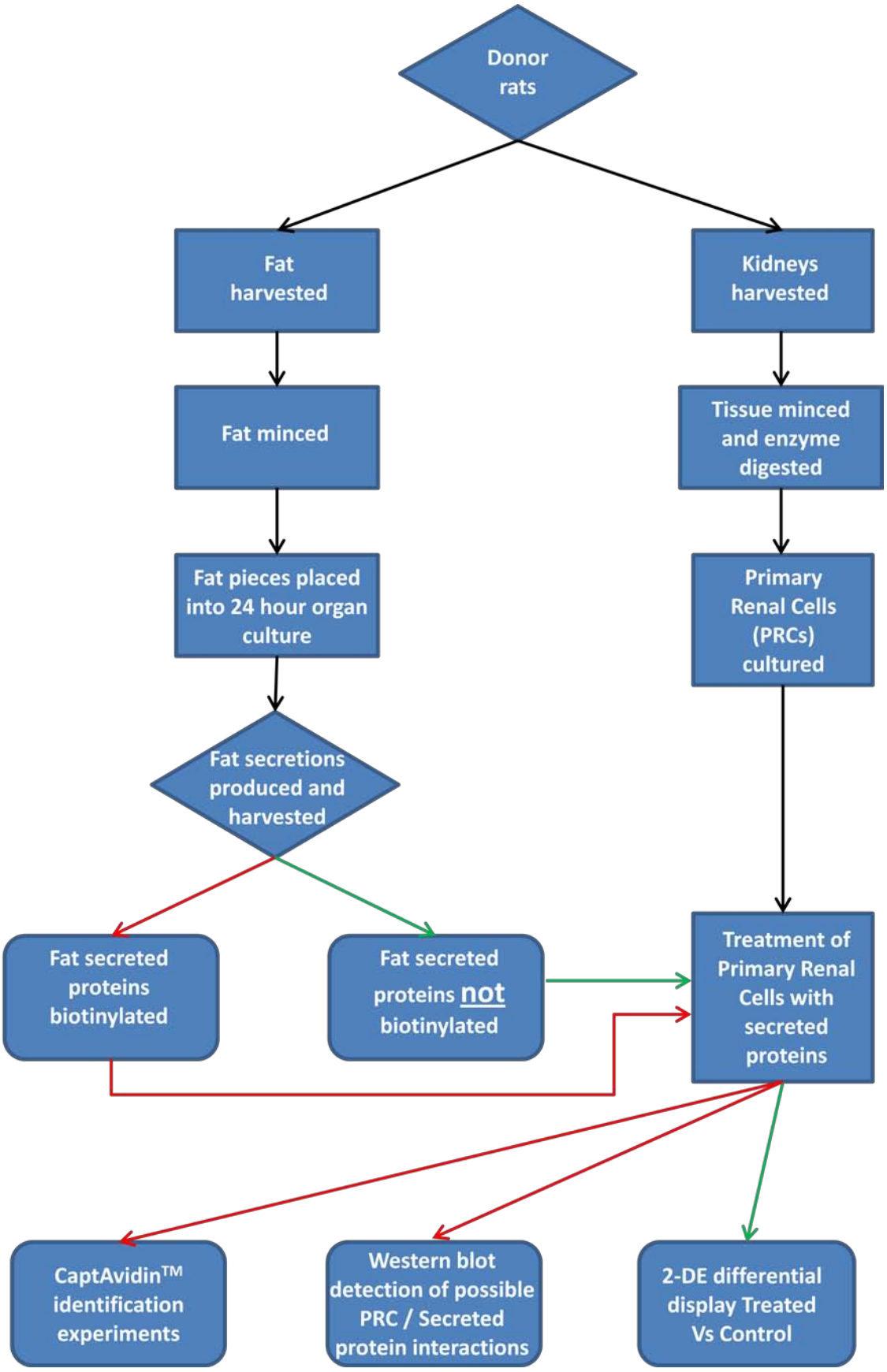

Following on from these technical issues regarding the experiments around **Figure 2.8**, it was decided to take another approach utilising two different 2-D gels of proteins from PRCs that had been treated with the biotinylated secretions. The first gel was prepared at a low protein load (~2.0 - 2.5 mg/mL protein concentration) and subsequently subjected to western blotting and probed in the same way as the blot in **Figure 2.7**. This was done in order to display the 'interacting' biotinylated proteins from the adipose secretions and their approximate positions on a 2-D gel, shown in **Figure 2.9**. The second treated PRC 2-D gel was completed using a preparative protein concentration (~6 mg/mL) and resolved, fixed and stained as in a normal 2-D gel preparation techniques described previously in the materials and methods section. Our laboratory had successfully used this approach before. The principle used was that unique spot patterns within the biotinylated protein blot, shown here in **Figure 2.9**, would be visible in the preparative 2-D gel version and would therefore allow a means of preliminary identification of the 'interacting' proteins using standard spot excision, in-gel tryptic digestion and MS identification techniques. The preparative protein gel images however were not included in this chapter as the staining did not reveal patterns which could be matched to the spot pattern shown in the avidin probed blots, **Figure 2.9**. This is likely to be a result of the difference in detection sensitivity of the Flamingo™ fluorescent protein stain (approx. 1 ng per spot) compared to the 1 pg detection sensitivity of the amplifying signal from streptavidin-HRP probed western blot system. In addition, the Flamingo™ stain detects the total protein load on the gel, whereas the blot detects only the labelled proteins. In this case the two different detection systems produced images which could not be readily matched.

2.4.4 The use of Vero cells as a replacement renal cell line for *in vitro* study of adipose secretion induced renal cell responses:

Due to the lack of a consistent source of rat PRCs, an alternate source of renal cells was sought in the form of an immortalised cell line. The Vero cell line was made available through a kind donation of Dr Michael Johnson at the University of Technology Sydney. The work on Vero cells was completed in the final months at UTS just before the move to Macquarie University. The Vero cells were grown and treated with rat adipose secretions in the same way as the PRCs were treated in **Figure 2.6**. The treated and control Vero cell groups consisted of four 25 cm^2 flasks each that yielded enough protein to suitably load and

resolve two 2-D gels per treated or control condition, providing results that are indicative, but not statistically significantly for changes between the treated and control groups. **Figure 2.10** displays two typical gel images obtained from the 2-DE analysis of the treated and control groups, with annotations of protein spots observed as differentially expressed between the two groups using PDQuest™ image analysis software. **Table 2.2** provides the protein identification information for most of the annotated spots from **Figure 2.10**, with three exceptions due to low spot intensity resulting in unsuccessful identification. By analysing the functions of the identified proteins in **Table 2.2**, the preliminary Vero cell results indicate possibly a more organised cytoskeletal structure in the control cells than the treated Vero cells and an increased propensity for mitosis, energy production and use in the treated Vero cells.

Completion of more technical replicates of the Vero cell treatment would have been advantageous to confirm the identifications and obtain statistically significant results. Also, additional experiments may have enabled the identification of some of the less intense protein spots; however due to the move to Macquarie University after the completion of the first set of experiments this was not accomplished. The move allowed for the re-evaluation of the project and for the implementation of alternative techniques for PRC cell culture, a renewed source of PRCs rather than Vero cells and also the introduction of different techniques that required much lower protein concentrations and therefore enabled the generation of very large datasets. These advances are discussed in the following chapters of this thesis.

Figure 2.6 A and B: Control and treated PRC proteomes compared using 2-DE.

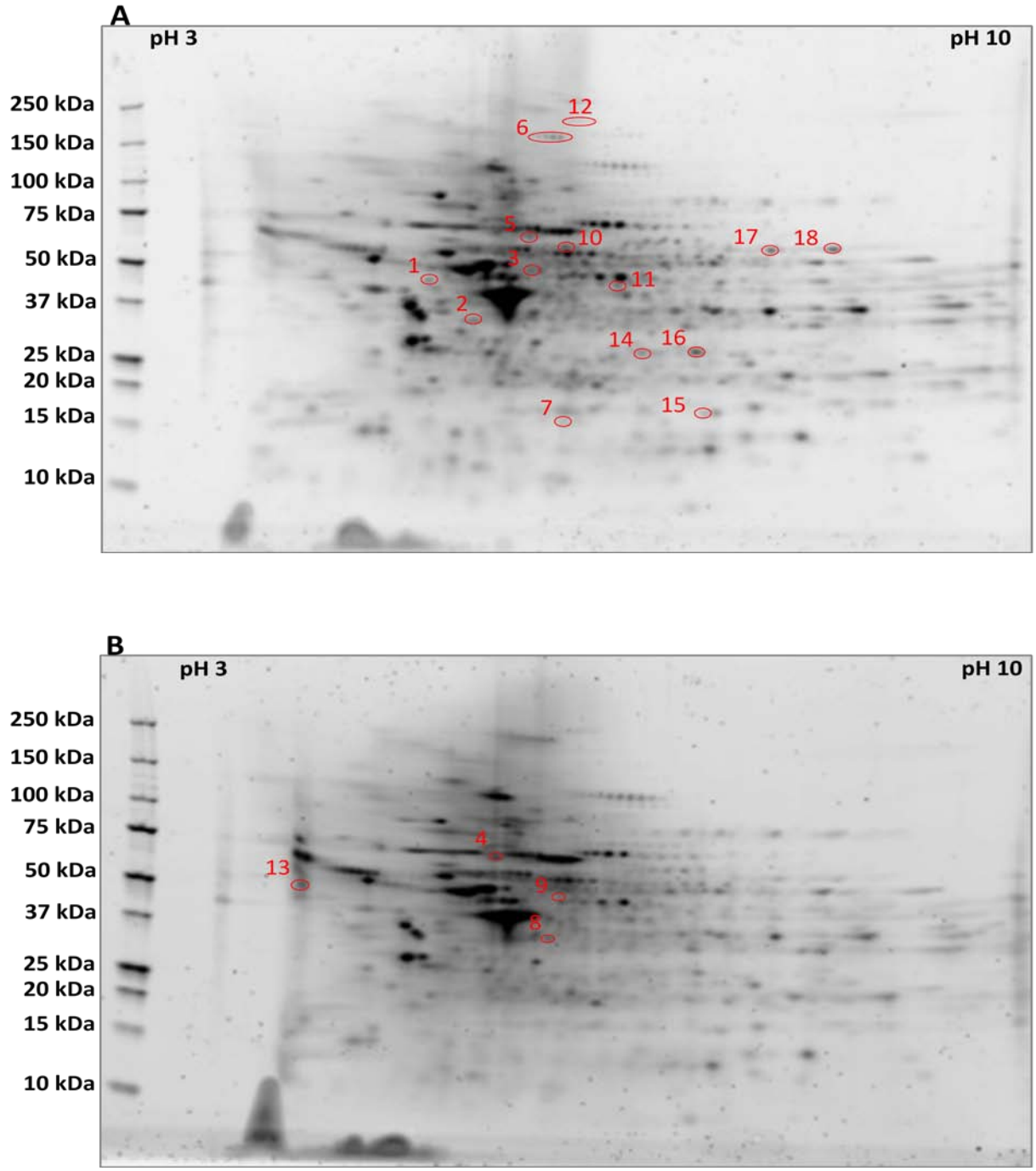

Figure 2.6 A and B: Primary renal cells treated with rat adipose tissue secretions: Typical 2-DE gel images for each set. Circled spots indicate those proteins increased in abundance by a factor of 2 or more in either control or treated cell cultures. (A) Control, non-treated PRCs grown in standard PRC culture medium. (B) PRCs treated with adipose tissue secretions. Gels were stained with the Flamingo™ fluorescent protein stain on a Pharos™ gel scanner using Quantity One® 1-D image acquisition and analysis software.

Table 2.1: Proteins identities from differentially displayed spots from **Figure 2.6 A** and **B**.

Spot Number:	Protein Name:	Mass (Daltons):	Probability MOWSE Score:	Accession number:	Function:
2	Thioredoxin-like protein 1	32229	37	Q920J4	Unknown
11	Alpha-enolase	47098	203	P04764	Glycolysis
15	Nucleoside diphosphate kinase B	17272	189	P19804	Nucleoside biosynthesis, Negative regulation of apoptosis
16	Peroxiredoxin-5, mitochondrial	22165	363	Q9R063	Oxidoreductase, Peroxidase, Antioxidant enzyme
17	Pyruvate kinase isozymes M1/M2	57781	769	P11980	Glycolysis
18	Pyruvate kinase isozymes M1/M2	57781	582	P11980	Glycolysis
8	F-actin capping protein subunit alpha-1	32889	70	B2GUZ5	Negative regulation of actin filament growth

Table 2.1: Proteins identified as two-fold (or more) increased in abundance in either the control or treated PRC cultures. Spot numbers refer to the proteins circled in **Figure 2.6 (A and B)**. Notably, only seven out of eighteen protein spots were successfully identified, due to low protein densities and lack of technical replicate gels (making only one attempt at each protein identification possible). Spot number cells that have been greyed indicate those proteins increased in abundance in the control PRC group, whereas the white indicates decreased abundance in the control group.

Figure 2.7: Western blot image of primary renal cells treated with biotinylated rat adipose tissue secretions, probed with ExtrAvidin®–HRP conjugated biotin specific probe.

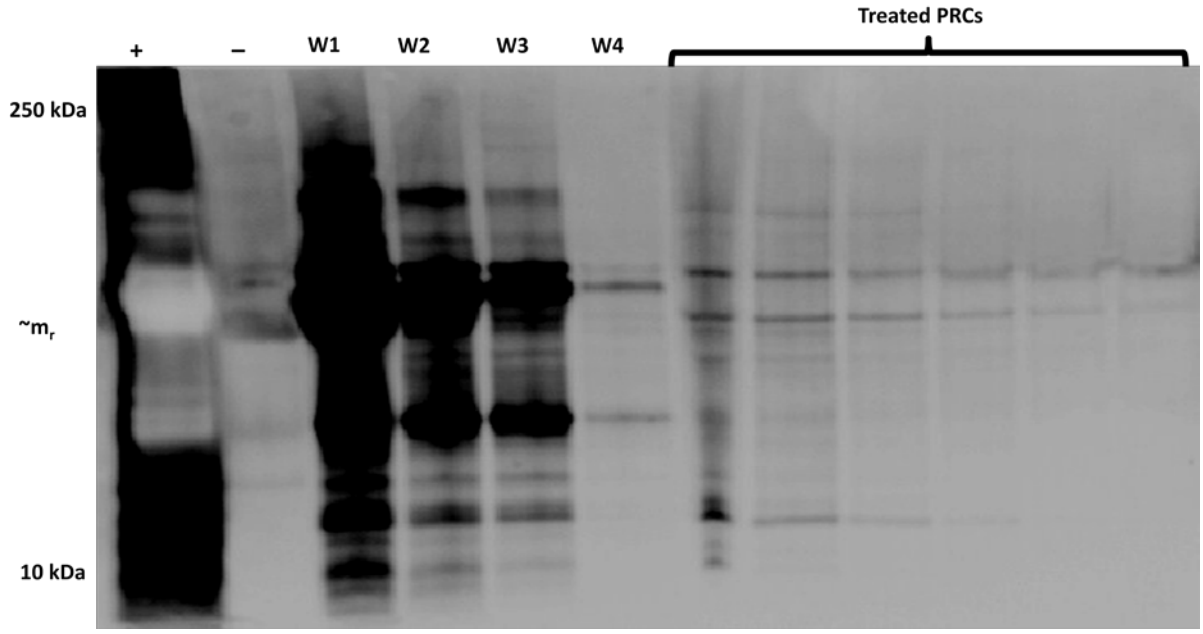

Figure 2.7: Western blot image of primary renal cells treated with biotinylated rat adipose tissue secretions, probed with streptavidin-HRP and developed using the ChemiDoc™ XRS fluorescence/chemiluminescence imager (Bio-Rad Pty. Ltd). (+) Positive control made from biotinylated adipose tissue secretions only. (-) Non-treated negative control PRC lysate, visible protein bands here were likely due to overflow of protein from the adjacent lanes which were heavily overloaded (W1-W4). Proteins present within the wash solutions after each wash step of the PRCs in sequential order. Five wash steps in total were performed, with the last one excluded from the blot. The decline in biotinylated proteins from wash-to-wash indicates very little presence in the 'W5' sample. (Treated PRCs) Biotinylated adipose secretion proteins present on the surface of, or within the treated PRCs present after five wash steps. This well contains biotinylated protein bands that suggest a pattern distinct from that of the unbound wash step fractions. This indicated that binding of some proteins from the secretions to the PRCs may be occurring through binding or up-take of specific secretion proteins on the surface of, or inside the PRCs. The distortion present within the (+) lane is likely due to the severe protein load within the sample placed into that particular well, given that it not only contains the biotinylated proteins from the adipose secretions, but the entire PRC lysate as well. This experiment was repeated twice in total.

Figure 2.8: The trial of CaptAvidin™ bead technology to capture and recover the biotinylated PRC interacting proteins.

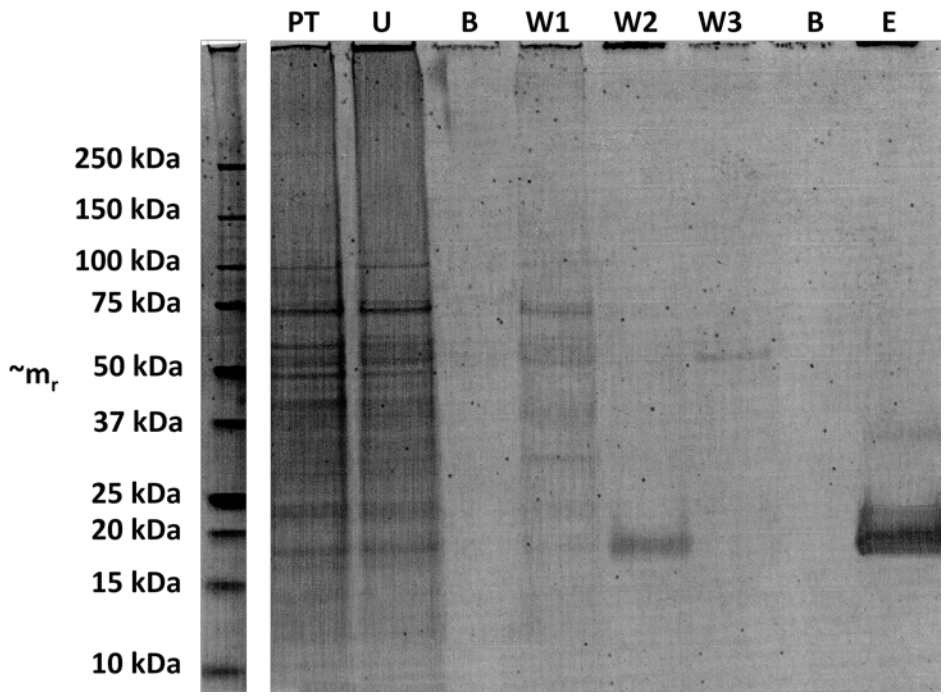

Figure 2.8: An attempt to recover and enrich the biotinylated proteins thought to interact with the PRCs from **Figure 2.7** using CaptAvidin™ agarose magnetic beads. The gel was stained with the Flamingo™ fluorescent protein stain on a Pharos™ gel scanner using Quantity One® 1-D image acquisition and analysis software. (PT) Pre-treatment sample, the mixture of PRC proteins and biotinylated fat secretion proteins placed onto the CaptAvidin™ beads. (U) Unbound protein fraction removed from the bead mixture after the recommended binding time. (B) Blank lanes. (W1 – W3) Wash steps of the bead slurry in sequential order showing a decrease in remaining unbound protein for each wash. (E) Elution fraction from the beads following a pH change from acidic to alkaline conditions and subsequent thirty-fold concentration using a centrifugal 3 MW cut-off filter. Very little protein was recovered in the elution fraction, indicating possible problems with the sample preparation or sample binding steps. Note: The gap in the gel image between the protein standards and the sample lanes is present in order to cut out other samples from the image that were resolved on the same gel belonging to other projects. This experiment was attempted three times with very similar results for each. The image displayed above is representative of the results obtained in each attempt.

Figure 2.9: 2-D western blot separation of primary renal cells treated with biotinylated adipose tissue secretions:

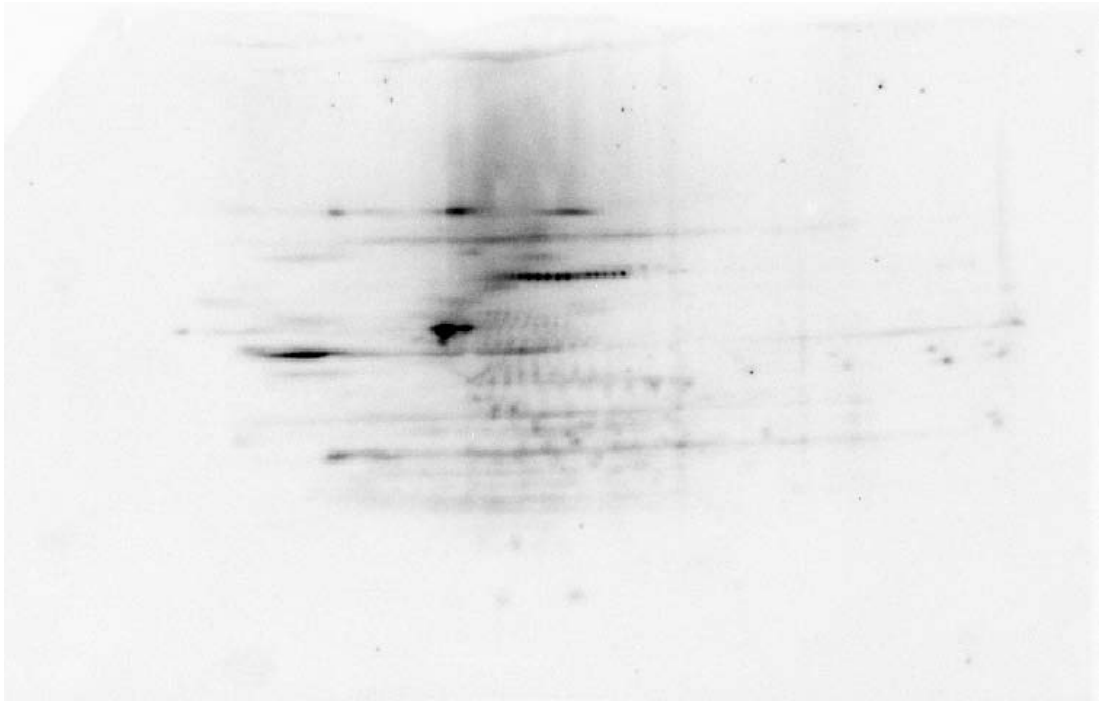

Figure 2.9: 2-D western blot separation of primary renal cells treated with biotinylated adipose tissue secretions in an attempt to identify the interacting biotinylated adipose secretion proteins. PRCs were treated with biotinylated adipose secretions and washed in the same manner as in **Figures 2.2** and **2.3** and the PRC lysate was separated using 2-DE preparation technique and then western blotted and probed with ExtrAvidin®-HRP. This experiment was completed once in an attempt to try to use this image as an overlay for a preparative 2-D gel of treated PRCs, possibly making recognition of the pattern in the image above visible within the PRC 2-DE gel. This would have theoretically allowed for the excision and spot identification of some of the biotinylated proteins. However, the preparative 2-D gel of the PRCs did not reveal a pattern that could be matched to the one above (data not shown).

Figure 2.10 A and B: Typical 2-D PAGE gel images of Vero cell cultures treated with rat adipose tissue secretions compared to non-treated controls. (A) Control Vero cells. (B) Treated Vero cells.

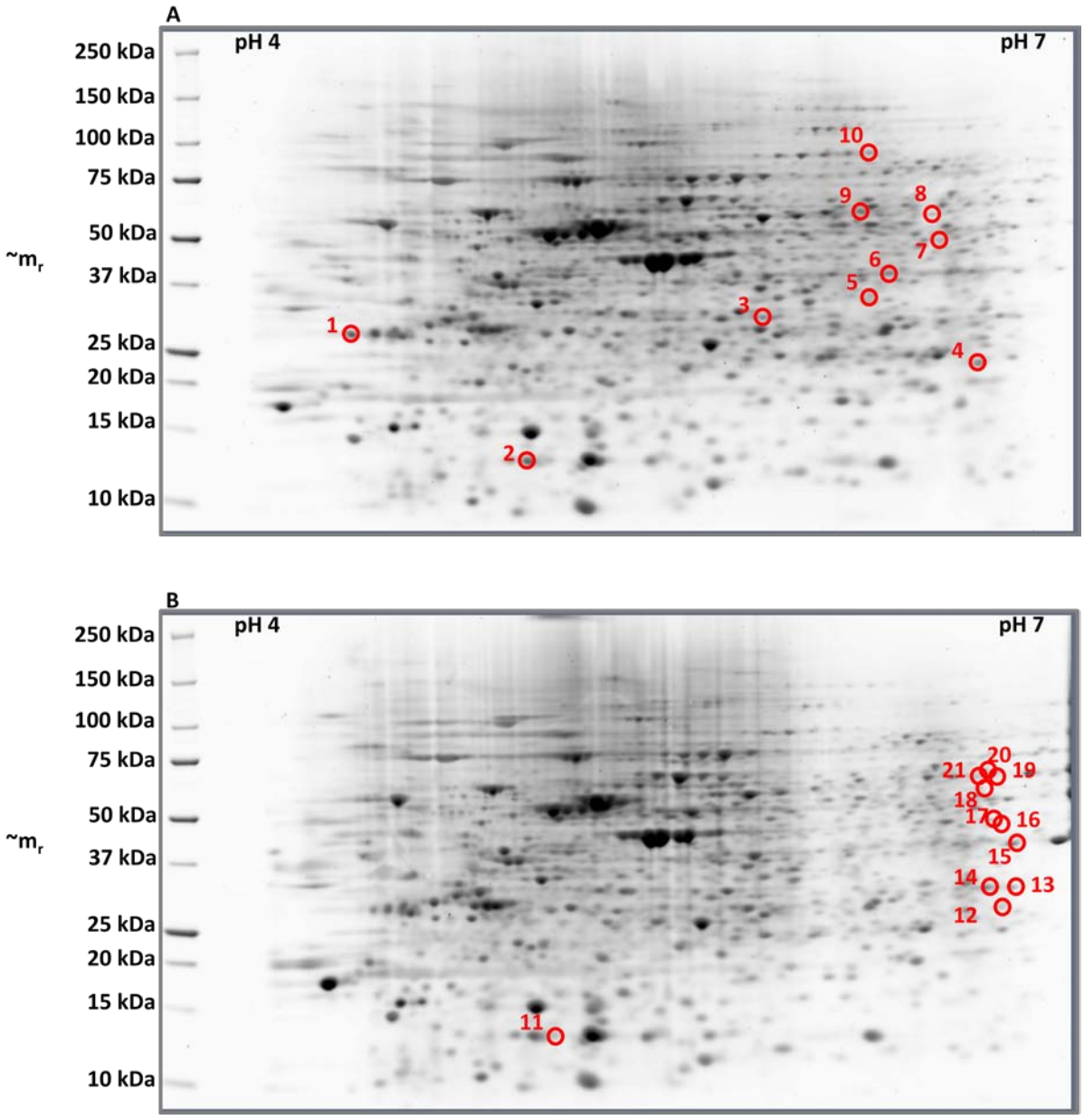

Figure 2.10 A and B: Typical 2-D PAGE gel images of Vero cell cultures treated with rat adipose tissue secretions compared to non-treated controls. (A) Control Vero cells. (B) Treated Vero cells. The gel was stained with the Flamingo™ fluorescent protein stain on a Pharos™ gel scanner using Quantity One® 1-D image acquisition and analysis software. Circled spots represent those proteins found to be differentially displayed between control and treated groups with a fold-change of ≥2 and a p-value of <0.05 using PDQuest™ image analysis software. The annotated spots were identified using LC/MS techniques and can be seen in **Table 2.2**.

Table 2.2: Protein annotation identifications from the Vero cell 2-D differential display experiment in **Figure 2.10**.

Spot Number:	Protein Name:	Mass (Daltons):	Probability MOWSE Score:	Accession number:	Function:
1	Cathepsin L1	37406	269	Q9GKL8	Proteolysis in lysosomes
2	Thioredoxin	11715	383	P29451	Cellular redox reactions, antioxidant
3	6-phosphogluconolactonase	27374	805	G7NMS1	Metabolic enzyme
4	Cofilin-1	18507	771	Q4R5C0	Cytoskeletal organisation
5	Nitrilase family, member 2	30621	1010	ENSMMUP00000026329	Metabolic enzyme
6	Serine/threonine protein phosphatase	67164	908	F7C4T3	Protein phosphorylation
7	Solute carrier family 22 member 6 (OAT1)	48430	608	ENSMMUP00000013742	Ion transmembrane transport
8	Aldehyde dehydrogenase X, mitochondrial [putative identification]	57240	837	ENSPTRP00000035841	Detoxification of alcohol derived acetaldehyde
9	Tryptophan--tRNA ligase, cytoplasmic [putative identification]	53251	947	ENSMMUP00000032575	Protein biosynthesis
10	Keratin, type II cytoskeletal 5 [putative identification]	65422	343	ENSCJAP00000033484	Cytoskeletal protein structural component
11	Thioredoxin	11715	344	P29451	Cellular redox reactions, antioxidant

12	Glutathione S-transferase theta-2 [putative identification]	14361	112	P30713	Metabolic enzyme
13	Triosephosphate isomerise [putative identification]	26694	1271	F7BWS5	Gluconeogenesis
14	Bisphosphoglycerate mutase [putative identification]	29996	265	Q4R6L7	Glycolysis
17	Alpha-centractin [putative identification]	42587	524	F6XCG8	Vesicle mediated transport, G2/M transition of mitotic cell cycle
18	RuvB-like 1 [putative identification]	50196	1014	F7GWQ2	Cell cycle, cell division, mitosis
20	T-complex protein 1 subunit zeta [putative identification]	58298	1033	F7DV12	Chaperone, protein folding
21	D-3-phosphoglycerate dehydrogenase [putative identification]	56482	1184	Q60HD7	Amino-acid biosynthesis

Table 2.2: Annotated spots from the 2-D Vero cell differential display gels (**Figure2.5**). Most of the spots were able to be successfully identified using spot excision, in-gel tryptic digestion and LC/MS identification. Accession numbers provided are predominantly from the UniProtKB electronic database (http://www.uniprot.org), those that begin with 'ENS' are derived from the Ensembl electronic genome database (http://asia.ensembl.org/index.html). Most protein information was derived from characterised proteins of other monkey species due to the lack of characterisation and annotation of the Vero cell line species of origin *Chlorocebus sabaeus*. The monkey species used primarily were *Macaca fascicularis, Macaca mulatta and Callithrix jacchus*. All proteins identified based on similarity to proteins from the aforementioned species were labeled with '[putative identification]'. Spot numbers with greyed cells indicate proteins that were increased in abundance in the control Vero cells, while white spot number cells (below the bold line) indicate proteins increased in abundance from the treated Vero set.

2.5 Discussion:

2.5.1 Changes to the PRC proteome in response to treatment with rat adipose secretions:

The limited PRC sample availability and the requirement for high protein loads affected the utility of the 2-D gel based experiment. These limitations led to the development of the strategies discussed in the next chapters. From the 2-D gel experiment, eighteen proteins were shown to be differentially expressed between the control and treated PRCs (**Figure 2.6**). I was able to obtain MS data for the identification of seven proteins from this group of eighteen (**Table 2.1**). Due to scarcity of sample, only two technical replicates from one biological replicate for each condition were possible. This smaller dataset provided only indicative information about the effects of adipose secretions on the PRCs, and has therefore been interpreted as such. In a normal, full 2-DE based differential display experiment comparing two cell populations, the two sample groups would typically consist of a minimum of three biological replicates and three technical replicates; that is, a minimum of nine controls and nine treated gels in total. Typically, any identified protein spots of interest that exhibit a low intensity can then be excised from multiple replicate gels and pooled, thereby enriching the tryptic digest and increasing the chances of successful protein identification.

From the limited information revealed through the protein identifications in **Table 2.1**, I was unable to draw any conclusions about the potential utility of adipose cell secretions for renal treatment. In fact, it can be seen that the treated cell population appear to decrease the abundance of some anti-apoptotic and pro-glycolysis proteins, although the significance of this is unclear. The identification of only one protein that was increased in abundance in the treated PRCs makes any kind of assertion as to the overall cellular activity of the cells impossible.

2.5.2 Detection of the interaction of rat adipose secretions with PRCs:

The rationale behind the use of biotin labelling in the attempts to identify an interaction between the adipose secretions and the PRCs was based on the wide knowledge base behind its chemistry, the availability of labelling kits and the specificity and strength of the biotin-avidin interaction. By treating the PRCs *in vitro* with biotinylated rat adipose tissue secretions, it was thought that the PRCs would bind to or internalise proteins from this

complex mixture and that this selection would result in a novel form of 'biological filtering' of the adipose secretions. The bound/internalised biotinylated proteins may then be separated from the non-biologically relevant proteins through repeated washing steps and then detected using an ExtrAvidin®-HRP probed semi-dry western blot system. The results shown in **Figure2.3** indicate that there seems to be some proteins that were internalised or bound to the cell surface in such a manner that they resisted unbinding during the four wash steps that the PRCs were subjected to. The 'treated PRC' lanes in **Figure 2.7** is a protein pattern distinct from that shown in the 'Wash' lanes, which represent the unbound labelled secretion protein fractions. To my knowledge, this is a novel use of the biotin-avidin system for the detection of interactions of a cell with a complex mixture of tissue secretions. Rats do not possess the avidin gene and so it is unlikely that the proteins displayed in the western blot of **Figure 2.7** are present on or within the renal cells due to binding of the biotin attachment on the labelled secretion proteins. The first 'Treated PRC' lane in **Figure 2.7** contains some distortion which is probably due to the very high level of total protein within the lane, as it contains the proteins visible due to the ExtrAvidin® probe and the entire water soluble proteome of the PRCs as well. The spread of proteins in the first 'Treated PRC' lane of **Figure 2.7** indicates that a large number of distinct secretion proteins may be taken-up by the PRCs. However, the lack of a large number of highly distinct protein bands in the 'Treated PRC' lanes indicates that these interacting proteins are either only present, or only required by the PRCs at relatively low levels. This is consistent with the action of cytokines, which are routinely present at picomolar concentrations and therefore bind to target cells at a relatively low level and exert their effects via second messengers and autocrine/paracrine signalling.

Experiments that reveal the identity of the proposed interacting proteins, like those described in **Figure 2.7**, are essential in elucidating possible mechanisms of interaction and would make sense of the PRC responses to treatment and also the mechanisms of action of these secretions on target cells. For these reasons, experiments were planned to try to identify the proteins proposed to be interacting with the PRCs in the 'Treated PRC' lanes of **Figure 2.7**.

2.5.3 Attempts to identify the proteins that may be interacting with the PRCs *in vitro*:

The identification of a likely interaction between the biotinylated adipose secretions and the rat PRCs *in vitro,* shown in **Figure 2.7**, was an exciting and novel adaptation of the biotin-avidin system for a broad scale cell-based assay system. However, identifying the possible interaction does not reveal information about the mechanisms taking place within the PRCs. The identification of the interacting adipose secretion proteins was presumed to be the most direct and logical way to find out how the secretion protein/PRC interaction takes place, what effects the secretions have on the PRCs and the biochemical mechanisms driving these processes. The attempts to identify these interacting proteins did not yield sufficient sample for successful identification. **Figure 2.8** details the results obtained through the use of a modified avidin system, CaptAvidin™, which features a reversible binding of biotinylated proteins through a pH shift which alters the binding site for biotin molecules during the elution phase, releasing the biotinylated material. Results using this system demonstrated a few problems in terms of adaptation of the technology for this project's uses. The very low levels of biotinylated material present within the PRC lysate samples was likely the key reason for the lack of protein observed in the Flamingo™ stained gel of **Figure 2.8**.

As the capture and isolation of the biotinylated secretion proteins was out of reach due to technical and experimental scale constraints, it was decided to take a different approach to the identification process. It was theorised that because the treated PRC lysate samples contained both endogenous PRC proteins and the biotinylated proteins taken up from the treatment with the adipose secretions, these proteins could be separated using a 2-D gel approach. The biotinylated proteins could be detected on a replicate 2-D gel which was submitted to Western blotting and probed for the biotin label, as in **Figure 2.7**; and then this 2-D Western blot pattern could form a map for feint protein spots present on the original 2-D gel which contained both PRC proteins and the biotinylated secretion proteins. If spots from the Western blot pattern were identified, they could have then been excised for LC/MS based protein identification. The 2-D Western blot image of the interacting secretion proteins can be seen in **Figure 2.9**. However, the original 2-D gel to be used for the spot identification step was required to be heavily overloaded in order to increase the possibility that some of the biotinylated secretion proteins would be visible on the gel among the far

more abundant endogenous PRC proteins. This resulted in a 2-D gel image which was essentially a poorly focused, heavily overloaded and unrecognisable pattern of protein spots.

It may have been naïve to expect these two techniques to produce significant amounts of biotinylated proteins at the scale of experiment possible in this type of study. The concentrations of cytokines required to produce biological effects is commonly very low and therefore very large cell numbers would have been required to obtain significant concentrations of biotinylated proteins. These constraints made further progress with these experiments impractical. While the possibility for future work in this area remains highly interesting, time and sample availability constraints meant that this project had to move on to other approaches that were thought to be able to yield other biologically significant data.

2.5.4 The use of Vero cells as a renal cell line for *in vitro* study of adipose secretion induced renal cell responses:

The differential display conducted using the Vero cells in this case included enough replicate gels of each sample to yield indicative data regarding the effects of the adipose tissue secretions on the Vero cells. The data indicates that the treatment with adipose secretions may induce a broad range of effects on the Vero cells including changes to metabolic activity, increased mitotic activity and a possible reduction in the organisation of the cytoskeleton. More biological and technical replicates would have been required for a statistically rigorous and significant analysis however.

Vero cells are an epithelial cell line derived from the kidney of a normal adult African green monkey. Vero cells are a hypodiploid, continuous cell line exhibiting apparently unlimited growth potential without the development of senescent characteristics. Use of Vero cells in the case of this project was brought about by our requirement for a greater source of sample renal cells and the need to propagate the renal cells quickly with high reproducibility. These cells were readily available through a kind donation by Dr Michael Johnson of UTS and were thus an easy choice as a renal cell replacement at the time. The use of an immortalised cell line came with the disadvantage of possible deviations in function, morphology or behaviour from the original epithelial cell function the cells would have had in the kidney *in vivo*. It is acknowledged that these cells may not have been ideal representatives of tubular cells of the mammalian kidney; however they fulfilled an

important purpose in allowing for the refinement of the future methods and desired experimental outcomes for this project and they were available at a time when primary tissue cell sources were at an all time low in the project just two months prior to the transfer of the Herbert laboratory members to Macquarie University.

2.6 Conclusions:

The 2-DE work using adipose secretion treated PRCs and Vero cells did not reveal consistent results that would indicate the effects of this adipose secretion preparation on cells of the kidney *in vitro*. The novel use of biotin labelled adipose secretions was an interesting avenue of investigation, but was also complicated by technical difficulties. The identification of some form of binding of the biotinylated secretion proteins to the PRCs is however an interesting finding and indicates that this would be a promising field of investigation for a future project, but required a level of optimisation that was outside the scope of this project overall.

While the work in this chapter did not reveal any statistically significant evidence for the effects of adipose tissue secretions on cells of the kidney, the work completed in this chapter of the PhD project was instrumental in the formation of the rest of the thesis and the design of the experiments that would follow after the move from UTS to Macquarie University.

Chapter 3 Prologue:

This chapter marks the start of my candidature at Macquarie University, after the transfer of much of the group from UTS. The many months of lab setup after the move allowed for time to reflect on the project at-large and formulate a cohesive plan for the rest of the project, involving the further use of primary rat kidneys and an immortalised renal cell line, the MDCKs discussed in Chapter 4. The 'down-time' also allowed time for wide-spread improvements to my basic culture technique and a fresh start on the project as a whole.

Work on both Chapter 3 and Chapter 4 progressed more or less simultaneously and often the lessons (sometimes harsh ones) from one were often translated from one chapter's work to the other straight away. This was a busy and exhilarating time where I finally saw the project coalesce into something I had once never considered myself capable of.

Access to the Macquarie University resident proteomic expertise at the Australian Proteome Analysis Facility (APAF) provided myself, Ben and the group as a whole, access to equipment like the Bio-Plex™ and analytical tools like iTRAQ. These would prove integral to our new plans for the project and its new direction.

Chapter 3: Treatment of Primary Renal Cells with Human Fat Secretions

3.1 Introduction:

The preliminary experiments detailed in Chapter 2 indicated some interesting and promising effects of adipose tissue secretions on cells of the mammalian kidney. Published data also states that adipose-derived mesenchymal stem cells, or adipose stem cells (ASCs) are secretors of a range of proteins, cytokines and growth factors capable of improving many disease states [12,30,129]. The work in Chapter 3 follows on from the preliminary investigations of the effects of adipose derived secretions in Chapter 2, with an improved renal cell culture method, an enrichment of ASCs during the production of the adipose tissue secretions and the further development of a more refined cell-based assay system utilising primary renal cells.

This chapter utilised improved cell culture techniques that allowed for the culture, growth and expansion of the renal cells to a greater level than detailed in Chapter 2. The change in university during the final 1.5 years of my PhD allowed me to start all experiments from fresh, utilising the knowledge I had gained along the way. This in turn, meant that the resulting experiments were very different in terms of design, technique, scale and complexity. The renal cell isolation technique itself remained largely unchanged; however the maintenance of the cells *in vitro* was altered by the introduction of sub-culturing techniques. The source of adipose tissue secretions selected for this chapter was human adipose tissue, obtained from waste liposuction material volunteered by consenting donors in accordance with Macquarie University Human Ethics Committee guidelines and approvals. The change from rat to human adipose tissue provided multiple advantages to the experimental design of downstream experiments. The use of waste liposuction material is less ethically problematic than dealing with fat derived from specifically bought animals that are euthanised prior to fat harvest. Waste liposuction material is obtainable in up to litre volumes and is relatively easy to obtain.

The processing of the human adipose tissue for the production of the adipose tissue secretions involved the partial digest of the tissue using a collagenase type I enzyme and the short-term culture of the remaining pieces of adipose tissue. This resulted in a cell

population with an enriched suspension of stromal vascular fraction (SVF) cells, which were liberated from the tissue pieces and the presence of small, intact fat pieces in the same culture vessel. Some of the free-floating SVF cells were able to make contact with the surface of the plastic culture flask, adhere and proliferate (depending on cell type). This partial digest and culture method thereby enabled the growth and survival of the entire cellular complement of the sample adipose tissue, while allowing for the enrichment of the ASCs once they adhered to the surface of the culture vessel and started to proliferate. Each cell type within the mix could then release their own array of protein secretions into the growth media over the course of the incubation. It was thought that this process should result in a conditioned media rich in a large number of adipokines, growth factors, immune-modulators and other trophic factors which may be suitable for the treatment of renal cells *in vitro* as a model for renal disease.

The change from rat adipose tissue secretions to human adipose tissue secretions meant that the treatment of rodent primary renal cells with the secretions was a xenogeneic treatment. Xenogeneic treatments in the field of ASC and BMSC regenerative medicine are well documented and generally show that transplanted mesenchymal stem cells from one species into another are able to simultaneously evade the host immune response and illicit a therapeutically beneficial effect to the host in a range of *in vivo* disease models [30]. The xenogeneic aspect to the experiments described in this chapter proved to be key to the detection of the secretory response of the rodent primary renal cells (PRCs) to treatment with human adipose secretions while also simultaneously allowing for the monitoring of the 'consumption' of some human adipose secretion cytokines by the PRCs over time in the same experimental set of replicates.

This chapter assessed the changes in the PRC proteome induced by treatment with a preparation of human adipose tissue secretions while simultaneously detecting alterations in the PRC secretion profile and the 'consumption' of human cytokines over the course of the treatment. This array of proteomic experiments was conducted on the same set of biological and technical replicates and thus, has allowed for direct correlation of the datasets. It is also, to my knowledge, a novel application of a xenogeneic treatment to simultaneously monitor changes in a cellular global proteome and 'both sides of the coin' of treatment cytokine – cellular secretory response interplay.

3.2 Aims:

1. To identify effects of human adipose tissue secretions on the proteome of primary cells of the rodent kidney using iTRAQ analysis.
2. To identify changes to the primary rodent kidney cell secretome using a multiplexed cytokine/growth factor assay.
3. To identify cytokines/growth factors that may be responsible for the therapeutic effects of adipose tissue secretions using a multiplexed cytokine/growth factor assay.

3.3 Materials and Methods:

The collection and use of waste human adipose tissue derived from elective cosmetic surgery procedures was completed in accordance with Macquarie University Human Research Ethics Committee (HREC) approval. Project reference number: 5201100385. Project title: *Investigation of the properties and secretions of adipose tissue and cells isolated from adipose tissue*. To view a copy of the project description, refer to **Appendix A**.

3.3.1 Combined materials for all experiments within this chapter:

Materials required:

- Steriflip filter unit, (custom) 400 µm pore size mesh insert -Millipore, Billerica MA USA.
- Collagenase enzyme - Sigma-Aldrich, St Louis MO USA.
- 75 cm^2 cell culture flasks
- 175 cm^2 cell culture flasks
- CO_2 incubator
- Class II biological safety cabinet
- 50 mL syringe, disposable, luer lock
- Syringe filters, 0.2 µm pore size. Millex-GP Filter unit 33 mm – Millipore Corporation. Billerica, MA USA.
- Steripak 0.2 µm filter - Millipore, Billerica MA USA.
- Peristaltic pump and two lengths of sterile silicone tubing
- Bio-Plex™ PRO Rat 23-plex Bio-Plex™ kit - Bio-Rad Laboratories Pty. Ltd. Hercules, CA, USA.
- Bio-Plex™ PRO Human 27-plex (group I) Bio-Plex™ kit - Bio-Rad Laboratories Pty. Ltd. Hercules, CA, USA.
- Bio-Plex™ plate reader - Bio-Rad Laboratories Pty. Ltd. Hercules, CA, USA.
- Bio-Plex™ magnetic bead plate wash-station - Bio-Rad Laboratories Pty. Ltd. Hercules, CA, USA.
- Bio-Plex™ data acquisition and analysis software
- Criterion™ 1-Dimensional Precast 18-well, 4 - 12% Bis-Tris 11 cm, 1.0 mm, polyacrylamide gels - Bio-Rad Pty. Ltd. Hercules CA USA.
- Criterion™ gel resolving apparatus - Bio-Rad Pty. Ltd. Hercules CA USA.

- Typhoon Trio™ gel imager - GE Healthcare Fairfield CT USA
- Typhoon Scanner Control (v5.0) image acquisition software - GE Healthcare Fairfield CT USA.
- Orbital shaker.

Solutions required:

- DMEM-HG (High glucose) media - Life Technologies Corporation, Wilmington DE USA.
- DMEM/F12 media (pre-mixed in a ratio of 1:1) - Life Technologies Corporation, Wilmington DE USA.
- Foetal bovine serum (FBS), heat inactivated, lot/batch # 8122821 - Life Technologies Corporation, Wilmington DE USA.

  NOTE: This is the same lot/batch # present in the preparation of human adipose secretions
- Kidney digestion solution: 0.2% Collagenase enzyme (w/v) in DMEM-HG filtered through a 0.2 µm filter.
- Fat digestion solution: 0.1% Collagenase enzyme (w/v) in DMEM/F12 media supplemented with 1% ABAM (*v/v*), filtered through a 0.2 µm filter.
- Renal cell culture media: DMEM-HG supplemented with 30% (v/v) Foetal bovine serum and 1% (v/v) antimycotic/antibiotic solution.
- PRC expansion media composed of: DMEM-HG supplemented with 10% Foetal bovine serum (*v/v*) and 1% Antibiotic/antimycotic (ABAM) (*v/v*).
- Trypsin / EDTA solution
- Human fat secretion media: DMEM/F12 supplemented with 10% Foetal bovine serum (*v/v*) (control batch # 8122821) and 1% antibiotic/antimycotic (*v/v*) solution.
- Sterile isotonic saline solution
- Human adipose tissue digestion solution composed of: Saline solution and 0.1% (*w/v*) Collagenase enzyme
- Bio-Plex™ plate reader sheath fluid - Bio-Rad Laboratories Pty. Ltd. Hercules, CA, USA.
- Bio-Plex™ standard diluent (standard PRC expansion media: DMEM-HG supplemented with 10% FBS 1% ABAM).
- Gel fixing solution – 40% Methanol, 10% Acetic acid (*v/v*).
- MES gel resolving buffer – 50 mM Tris-base pH 8.8, 50 mM 2-(N-morpholino)ethanesulfonic acid, 1 mM EDTA; 0.1% SDS.
- Precision Plus Protein™ unstained molecular weight markers - Bio-Rad Pty. Ltd. Hercules CA USA.
- Coomassie blue G250 staining solution 1.

- Coomassie blue G250 staining solution 2 (50% Ammonium sulphate).
- Coomassie destaining solution, 1% Acetic acid (*v/v*).

3.3.2 Primary renal cell culture establishment method:

Rat kidneys were obtained as donated tissue (waste) from an unrelated project undertaken by staff at Regeneus Ltd. under Regeneus animal ethics committee approval number: RE001. This method was adapted and simplified from methods previously described by Menè and Stoppacciaro [214].

Kidneys were taken from the animal inside a laminar flow hood after the animal's underbelly had been clipped of excess fur, sprayed down with ethanol and processed for use by Regeneus staff for the purposes of research under ethics number RE001. *Note:* All steps were performed within a laminar flow hood unless otherwise stated. Kidneys were then taken from the donor animals using a sterile scalpel and forceps. Once excised, they were placed into a sterile 50 mL tube containing 10 mL sterile DMEM-HG at room temperature until all kidneys from all donors had been extracted. The outer membrane of the kidneys were removed using forceps and discarded. Kidneys were then minced in separate mincing pots using sterile scissors until pieces were approximately 2-3 mm^3 in size. Kidneys were then digested in a new 50 mL tube containing 10 mL kidney digestion solution at 37°C for eighty minutes with manual agitation of the tubes every ten minutes to mix the kidney pieces. Once digested, the liberated cells were filtered away from the remaining kidney pieces using a Steriflip filter and hand pump apparatus. The filtrate was then centrifuged at 500 x g for ten minutes to pellet the cells and remove them from the collagenase within the digestion solution supernatant, which was discarded. The kidney cell pellet was then re-suspended in 20 mL DMEM solution to dilute any remaining collagenase enzyme and then the centrifugation was repeated at 500 x g for ten minutes. The cell pellet was then re-suspended in 50 mL primary renal culture medium and then pipetted into five T75 culture flasks labeled with the date, rat number of origin (rat 1, rat 2 etc), passage number ('passage 0' in this case) and culture type. A further 5 mL primary renal culture medium was added to each flask before incubating them at 37°C, 5% CO_2 for approximately one-and-a-half to two weeks until plastic adherent cells could be seen on the surface of the flasks. Flasks were checked for adherent cells, media colouration and contamination using a combination of macroscopic and microscopic inspection. Microscopic inspection was performed using an inverted light microscope. *Note:* Generally, flask success rates were low. About two in five primary setup flasks resulted in the characteristic plastic adherent cells desired. All other flasks were discarded for autoclaving if no evidence of these cells was seen within one-and-

a-half to two weeks after tissue digestion. Flask media was changed every three to four days after the first one-and-a-half to two week incubation period using the Primary renal cell culture expansion and maintenance method.

3.3.2 Primary renal cell culture expansion and maintenance method:

Only PRC culture flasks with a significant number of growing plastic adherent cells were used for the cultivation of PRCs *in vitro* from this point onwards. Once the cultures had reached approximately eighty-five to ninety-five percent confluency, as judged by microscopic examination, all the flasks derived from one rat were taken for trypsinisation, pooling and re-seeding for expansion. Briefly, the 75 cm^2 flask cultures were drained of all current media and washed using sterile DMEM solution pre-warmed to 37°C. 1.5 mL of Trypsin/EDTA solution was then added to each flask and mixed over the cells by gentle swirling and tipping. The flasks were incubated at 37°C for five to ten minutes until all cells were no longer plastic adherent. 8.5 mL PRC expansion media was then added to each flask and mixed over the flask growth surface to suspend all cells and dilute the trypsin. The contents of all stripped flasks from one rat were then pooled into a single flask and mixed again. 10 mL of the pooled PRC suspension was used to seed new 175 cm^2 sized culture flasks. Each newly seeded 175 cm^2 flask was then topped up to a final volume of 25 mL with PRC expansion media. Flasks were labelled with cell type (PRC), rat number, passage number and date and then incubated at 37°C 5% CO_2. Flask media was changed every three to four days and flasks were trypsinised, pooled and split again once eighty-five to ninety-five percent confluency was reached. PRCs were not cultured past passage 3, representing three rounds of trypsinisation, pooling and re-seeding, due to problems with senescence and growth characteristics after this point.

3.3.3 Production of human fat secretions using partial digest method:

Human adipose tissue was obtained from donors undergoing elective cosmetic surgery under Macquarie University Human Ethics Committee approval number: 5201100385. Human fat was transported to Macquarie University inside an insulated box containing pre-warmed bricks to maintain it at approximately 37°C. All procedures were completed inside a Class II Biological containment cabinet where applicable for personnel safety reasons. Using a 50 mL serological pipette tip, 4 x 220 mL centrifuge tubes were filled to 200 mL with the floating fat layer of the lipoaspirate sample. The tubes were centrifuged

at 1000 x g for ten minutes to remove tumescent fluid from the sample; the cell pellet and the fat layer were retained (roughly 100 mL volume per tube at this stage). Sterile, pre-warmed saline was then added to the tubes and mixed thoroughly but gently to wash the fat. Tubes were centrifuged again at 1000 x g for ten minutes and the wash saline was discarded. To each tube, fat digestion solution was added and mixed thoroughly; the tubes were then incubated in a water bath at 37°C for twenty minutes with regular checks and manual agitation to partially digest the fat. After the partial digest, the tubes were centrifuged at 1000 x g for ten minutes and the fat digest solution and any free lipid above the fat layer was discarded, leaving only the cell pellet and fat layer behind. Samples were washed twice with 80 mL of sterile pre-warmed saline solution to remove remaining collagenase enzyme. To each tube, 200 mL of human fat secretion medium was added and mixed thoroughly. 50 mL of the suspension of human fat pieces and human fat stromal vascular fraction (SVF) cells was then dispensed into a 175 cm^2 sized culture flask and incubated for three days at 37°C 5% CO_2.

The first harvest (harvest A) of the fat secretions took place at the three day timepoint. Flasks were checked under the microscope for the level of plastic adherent cells and the amount of floating, healthy looking fat pieces. The harvest A conditioned media from each flask was removed and placed into 50 mL tubes, washing down the surfaces of the flask as it was removed to ensure maximum removal of fat pieces and free lipid into the tubes. The culture flasks were then filled with 50 mL of fresh pre-warmed human fat secretion medium each, gently tipped to mix the media over the flask and then incubated for a further three days at 37°C 5% CO_2. The tubes were then centrifuged at 1000 x g for ten minutes and the floating fat and lipid layers both discarded. The remaining conditioned media samples were then pooled into a sterile 1 L container and frozen at -22°C.

The second harvest (harvest B) was then completed after the second three day incubation period. The flasks were checked for level of cell confluency and any overt signs of contamination. The flask contents were then removed into sterile 50 mL tubes and centrifuged at 1000 x g for ten minutes. All pieces of remaining fat and free lipid were removed and discarded, while the supernatant was carefully pooled into a 1 L sterile container and frozen at -22°C.

The two harvests were defrosted and pooled into a new sterile 2 L container ready for filtering through a Steripak 0.2 µm filter using sterile silicone tubing, a peristaltic pump and another sterile 2 L container to collect the filtrate. The filtered fat secretion preparation was then mixed thoroughly, aliquotted into 50 mL tubes and frozen at -22°C and stored for longer periods (>three months) at -80°C. The aliquots of human adipose tissue secretions produced here, from a single donor, were used in the work completed in chapters three and four. A single batch of secretions was produced in order to reduce the amount of variation in the data between the two bodies of work and enable a direct comparison of the results obtained. To optimise the procedure and familiarise the author with the handling of human fat, the digestion process and aid in scale-up, four smaller-scale human fat partial digests were completed prior to the production of the large 'master stock' of human adipose tissue secretions used in the work described here.

3.3.4 Treatment of rat PRC cultures with human fat secretions:

Primary rat renal cells that had been expanded *in vitro* to passage 3 were selected for treatment with human adipose tissue secretions. PRC cultures from one biological replicate, 'rat 1' for example, were expanded so that there were eight total flasks of PRCs from 'rat 1'. Each flask was grown until it had a confluency level of eighty to ninety percent before being treated with the human fat secretions. The eight flasks were split into two groups, four 'control' PRC cultures and four 'treated' PRC cultures. Each flask was drained of its current PRC expansion media and washed twice with 10 mL plain DMEM/F12 media. The control flasks then received 25 mL control PRC media preparation each and were incubated at 37°C 5% CO_2 for three days. The treated PRC flasks received 25 mL human adipose secretion media, composed of 50% human adipose tissue secretions (produced in section **3.3.3**) and 50% control PRC media. The treated PRC flasks were also incubated at 37°C 5% CO_2 for three days in the same incubator as the controls. During the three day incubation, 2 x 200 µL media samples were taken from each of the control and treated flasks at 0, 1, 3, 18, 24, 42, 48 and 72 hour timepoints.

Flasks containing no PRCs at all were also set up at the same time as the control and treated PRCs, containing 25 mL of either control PRC media or human adipose secretion media. These flasks were dubbed 'Control/Treated media blanks'. These flasks were also incubated in the same conditions as the PRC-containing flasks (37°C 5% CO_2, three days) in

order to assess the contribution of cytokine degradation over time at 37°C 5% CO_2 and also to assess the cross-reactivity of the human cytokines on the rat Bio-Plex™ assay and vice versa. Samples of the media from these blank flasks were also taken at each of the timepoints stated above.

All control media, human adipose secretion media and blank samples were collected into labeled 600 µL tubes and frozen at -22°C and then at -80°C for future analysis in the human and rat Bio-Plex™ multiplexed cytokine assays as described in later sections of this chapter. Control and treated PRCs were harvested from the flasks at the 72 hour timepoint for iTRAQ proteomic analysis as described in **3.3.5** and **3.3.6**.

3.3.5 Harvesting of PRCs for proteomic analyses:

At the 72 hour timepoint of the PRC treatment procedure, following collection of the final 72 hour timepoint samples, all media was removed from the control and treated PRC flasks and replaced with 25 mL plain, pre-warmed DMEM-HG media. The flasks were incubated at 37°C 5% CO_2 for ten minutes to wash the cells of excess protein in order to facilitate cell stripping from the flask surface. The DMEM-HG wash media was removed and discarded and 2 mL TrypLE solution was added to each PRC containing flask. The flasks were incubated at 37°C 5% CO_2 for five to ten minutes, until cell were no longer adherent to the flask surface. Once the cells were no longer adhered, 10 mL PBS solution was added to each flask with the solution being washed down the surface of the flask to ensure adequate suspension of the PRCs. The PRC cell suspension from one flask was then transferred to a 15 mL tube and topped up with PBS to a final volume of 14 mL and inverted to mix. The tubes were then centrifuged at 500 x g for ten minutes, the supernatant was discarded and the PRC pellet was re-suspended in 14 mL PBS solution. The tubes were centrifuged again at 500 x g for ten minutes. The supernatant was carefully removed as completely as possible and then the dry PRC pellets were frozen inside the 15 mL tubes at -80°C for future iTRAQ proteomic analysis.

3.3.6 Preparation of PRCs for iTRAQ quantitative proteomic analysis:

The frozen PRC cell pellets were defrosted, suspended in 1 mL 1% (*w/v*) SDS solution and transferred into a 1.7 mL tube. The samples were then sonicated inside an ultrasonic water bath for fifteen minutes and then boiled using a heating block for ten minutes. The

boiled samples were centrifuged at 21000 x g for ten minutes to pellet any cellular debris or contaminants. The supernatants were transferred into new 15 mL tubes and acetone precipitated with the addition of acetone to a final volume of 13 mL, the sample was then mixed thoroughly by inversion. Precipitation was aided by the addition of 80 mM citric acid until precipitation was initiated. The samples were incubated at room temperature for thirty minutes and then centrifuged at 3000 x g for ten minutes to pellet the protein precipitate. The supernatant was carefully discarded and the pellets were suspended in 0.1% SDS and sonicated in the ultrasonic bath for ten minutes. Total protein loads for each treated and control sample were then assessed using the method described in Chapter 2, section 2.3.11. Once the samples were all equalised to a total protein concentration of ~100 ng/mL, 10 µL of each sample was taken and placed into a 600 µL tube for confirmation of the equalisation; the remainder of each sample was frozen at -80°C.

The protein loads of each 10 µL sub-sample were then compared using 1-D electrophoresis. 10 µL of each sample was added to 3 µL of NuPAGE® LDS Sample Buffer (4x) and mixed thoroughly. The samples were then boiled for five minutes in a heating block and centrifuged at 21000 x g for ten minutes before the entire 13 µL of each sample was loaded into lanes of a Criterion™ 1-Dimensional Precast 18-well, polyacrylamide gel. The gel was resolved at 150 V (constant), inside the Criterion™ gel resolving apparatus using the MES gel resolving buffer until the tracking dye front reached the bottom of the gel. The gel was then fixed by placing it into 100 mL of the gel fixing solution for forty minutes on an orbital shaker and then placed into Coomassie G250 protein staining solution composed of a mix of Coomassie G250 solution 1 and solution 2 in a ratio of 4:1 respectively. The gel was incubated in the stain overnight on the orbital shaker. The gel was then destained using Coomassie destaining solution for one hour with regular changes of the solution to speed up the process. The gel was imaged using a desktop document scanner for direct visual confirmation of protein loads in each sample. **Figure 3.7** demonstrates the level of total protein load equalisation achieved between the samples.

Following confirmation of the presence of equal protein loads within each sample for iTRAQ processing at APAF, the frozen PRC protein samples for the comparison were then submitted to APAF for iTRAQ analysis under the request of an 'Advanced liquid chromatography electrospray ionisation analysis' at a protein concentration of

approximately 100 ng/mL. The labelling of each sample, subsequent preparation steps and the LC-MS runs were all performed by APAF staff according to standard operating procedures. These steps were the only procedures completed by people other than me unless otherwise stated.

3.3.7 iTRAQ analysis of treated and control PRCs:

For a brief overview of a typical iTRAQ experimental work-flow, please refer to **Figure 3.1**. This describes the labelling, combining and overall comparison methods used to compare different protein samples quantitatively. The figure has been adapted to include samples relevant to the work completed in this chapter. As four treated PRC samples and four control PRC samples were present in the full experiment described in this chapter, the four-plex iTRAQ experiment shown in **Figure 3.1** was completed twice. One 4-plex experiment contained samples from Rats 1 and 2 (treatment and control) and the second contained samples from Rats 3 and 4 (treatment and control).

The iTRAQ analysis was completed in the Australian proteome analysis facility (APAF), a national collaborative research infrastructure strategy facility (NCRIS) provided by the Australian Government, according to their pre-established standard operating procedures for iTRAQ analysis. Protein MS/MS data was identified as part of the iTRAQ analysis within the ProteinPilot™ software version 1.0.8085 using the Paragon algorithm (# 4.0.0.0, 148083). Quantitative protein analysis was then completed as per the ProteinPilot™ user manual.

3.3.7 Bio-Plex™ PRO Rat 23-plex Bio-Plex™ multiplexed assay and Bio-Plex™ PRO Human 27-plex (group I) Bio-Plex™ multiplexed assay procedures:

The samples selected for the two different types of multiplexed assay differ here in terms of timepoints and cytokines assessed, however the preparation for the assays themselves were identical in terms of the filtration steps and standard diluents used. The two protocols have therefore been described here in the one section. Differences with the assay protocols do exist, but are detailed within the respective assay manuals provided with each kit, which have been followed to the letter for each kit type. Each assay and all preparatory steps and procedures were performed by me, with the use of the Bio-Plex™ plate reader and plate washing apparatus inside the APAF facility.

A number of timepoint media samples derived from the three day treatment of PRCs with either control PRC media or human adipose secretion media were selected for the assessment of rat-derived cytokine levels over time. For the rat cytokine assay, the selected timepoints were 0, 3, 24 and 48 hours from the 'rat 1' biological replicate and were compared using the Bio-plex PRO rat 23-plex Bio-Plex cytokine assay kit. The preliminary human cytokine assay assessed the 0, 3, 24 and 48 hour timepoints, whereas the more comprehensive human cytokine assay completed afterwards included the 0, 3, 18, 24, 48 hour timepoints.

The samples were defrosted and 100 µL was taken for filtration using 0.2 µm centrifugal filters. The standard diluent used in the assay was composed of standard PRC culture expansion medium, as recommended by the Bio-Plex™ manual; the standard diluent was then filtered using a 0.2 µm syringe filter before use. The samples and standard diluent were then processed through the assay according to the provided assay protocol using facilities and equipment provided by APAF. The plate was washed during this procedure using the Bio-Plex™ magnetic bead plate wash-station and read using the Bio-Plex™ plate reader and Bio-Plex™ data acquisition and analysis software Version 5.0. Data output was exported to Microsoft Office Excel (2007) (Microsoft. Redmond, Washington USA) and then analysed using the statistical data analysis software package R and the code editor Tinn-R for analysis of mean cytokine levels, standard deviation, changes to the cytokine abundances over time, box-plot analysis and 1-way analysis of variance (ANOVA) for assessment of statistical significance between treatment and control groups. The statistical analysis program R is available free online at http://www.r-project.org/. The code-editor Tinn-R is also available free online at http://www.sciviews.org/Tinn-R/index.html.

Figure 3.1: iTRAQ experimental work-flow overview.

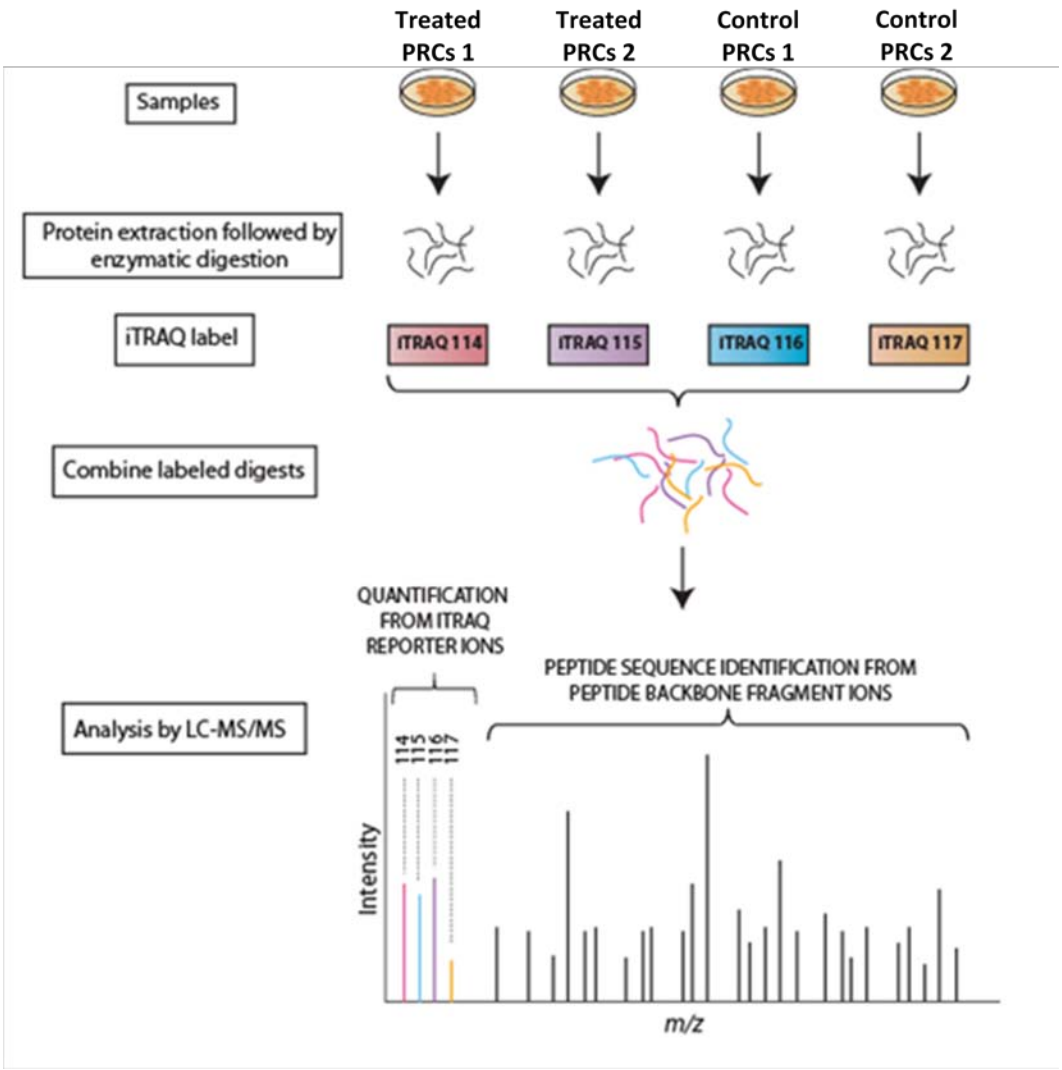

Figure 3.1: iTRAQ experimental work-flow overview, describing the digestion, labelling, combining and relative MS/MS data quantification for comparison of different samples using ProteinPilot™ software. Samples are prepared then tryptically digested and labelled separately with one of the distinct isobaric tags (114, 115 etc) before being combined into the one liquid sample and being subject to LC/MS procedure for analysis. Figure was adapted to include relevant sample labels from http://www.broadinstitute.org/scientific-community/science/platforms/proteomics/itraq.

3.4 Results:

Bio-Plex™ assay analysis of the adipose tissue secretions, the PRC secretome and changes to the adipose secretions via possible PRC-secretion interactions:

The preparation of the human adipose tissue secretions was quantitatively assayed for the levels of a selection of twenty-seven cytokines and growth factors using the Bio-Rad Bio-Plex™ 27-plex human group I magnetic bead based assay kit. The Bio-Plex™ human cytokine assay revealed potentially biologically active levels of eighteen of the twenty-seven cytokines/growth factors and also displayed the high level of reproducibility of the assay procedure as seen through the low standard deviation values for most analytes. Results can be seen in **Table 3.1**.

Samples of the growth media from the treated PRC flasks, control PRC flasks and blank treatment and control media flasks were taken at multiple timepoints during treatment of the PRCs with the human adipose tissue secretions for temporal analysis of cytokine changes. This was done to assess the relative increases and decreases in cytokine/growth factor levels in the control/treatment media over time. It was postulated that treatment with the human adipose secretions would cause changes to the secretions of the rat PRCs that could be measured using a rat cytokine/growth factor assay kit. It was also postulated that the rat PRCs would preferentially take-up certain human cytokines/growth factors from the treatment media over time and that this would be measurable using the human cytokine/growth factor assay kit system. It was thought that this would be observable as a decline in the concentration of a given human cytokine over time that was greater than the decline in concentration caused by simple degradation of the treatment media over the course of the incubation period.

To analyse the change in PRC secretion profile, the Bio-Rad Bio-Plex™ multiplex bead based assay system was utilised, allowing for the simultaneous assay of twenty-three different rat cytokine/growth factors over the course of the treatment as compared to PRCs treated with control media containing only FBS (10% *v/v*) and antibiotics (1% *v/v*). Blank treatment media and control media samples, not exposed to the PRCs were also assayed in order to ensure that no human-rat cross-reactivity had occurred and that no protein degradation products were causing false readings during the assay. These blank flasks were

incubated in the same culture conditions for the same time periods as all other samples to ensure that any changes to the cytokines/growth factors within a sample were due to the presence of the PRCs and not due to degradation during incubation at 37°C for up to seventy-two hours or cross-reactivity of human cytokines on the rat kit and *vice-versa*.

The theory behind this type of double-sided human-rat cytokine assay temporal analysis was strong, and previous experiences with the assay technology also suggested that the cross-reactivity between human and rat assay kits and samples was low. But as the assay Bio-Plex™ assay kits can be costly, it was decided to only assay the flask supernatants from the technical replicates derived from the first biological replicate, rat 1. These assay results for the rat PRC secretions in response to treatment are shown in **Table 3.2**. The decline in human factors from the treatment media over time can be seen in **Table 3.3**. In these preliminary results the PRC secretory response to treatment appeared to contain pro-inflammatory factors, highlighted in **Figure 3.2;** while the preliminary results of the human Bio-Plex™ indicate that PRCs appear to take up platelet-derived growth factor (PDGF-bb) and vascular endothelial growth factor (VEGF) from the treatment media over time, highlighted in **Figure 3.3**.

Following the promising results obtained from the initial smaller-scale human Bio-Plex™ experiment, it was decided that a larger scale experiment should be conducted in order to obtain statistically significant results using the other three biological replicate samples of the treatment timecourse. It would have been good to also complete a more comprehensive analysis of the initial rat Bio-Plex™ samples in the same fashion, however the results from the initial rat Bio-Plex™ experiment were in some ways not as novel as those obtainable by completing the analysis of the human cytokines (in our view). The project did not have sufficient time or funds available for the completion of both Bio-Plex™ analyses, as the kits are generally in excess of $3500.00 AUD each.

The more comprehensive human Bio-Plex™ analysis involved timepoint samples from 0, 3, 18, 24 and 48 hours during the treatment and included samples from the three remaining biological replicates, rat 2, rat 3 and rat 4 in duplicate. To add more statistical power, a pooled sample for each condition at each timepoint was included, also in duplicate. The inclusion of a pooled sample effectively provided the data with a synthetically produced

‘rat 5’ sample, from a statistical analysis perspective. The data for each condition across all four biological replicates and blank media controls were analysed using the software package, R and the code editor Tinn-R.

For each of the twenty-seven cytokines within the panel for each timepoint and condition, control cells at zero hours for example; data was averaged using the eight data points from all biological and technical replicates to produce a single mean (+/- standard deviation) for control and treatment timepoint for each cytokine. This information was then plotted against the control and treatment blank sample means for each cytokine to give the abundance of every cytokine over time in each sample. The bar graphs for each of the twenty-seven assayed human cytokines over the timecourse can be seen in **Figure 3.4** where cytokine abundance is expressed in picograms per millilitre over treatment time in hours.

Using the bar graph data in **Figure 3.4** as an indicator of cytokines/growth factors of interest, the analytes that exhibited an apparent decline in concentration over time in the presence of the PRCs (blue bars), but not in the blank samples (yellow bars) were selected for statistical analysis. Due to limited space on the assay ELISA plate (96-wells), it was only possible to obtain two data-points for the control blank and treatment blank pooled samples at each timepoint. This meant that there would not have been enough data points for the blank treatment at forty-eight hours (two in total) to complete a satisfactory statistical analysis. Therefore, an analysis of the difference between the blank treatment sample at zero hours and forty-eight hours was completed, shown in **Figure 3.5**. The box plot showed no significant difference between the concentrations of all analytes between the zero and forty-eight hour timepoints, allowing for the addition of the zero hour treatment blank analyte data to the forty-eight hour blank data; and thus a more statistically powerful comparison between treatment media (PRCs present) and media blank samples.

The statistical analysis of the nine selected analytes, based on the bar graph trends described above was completed using the software packages R and Tinn-R. Box plots were constructed to analyse the spread of data for the treated PRCs at forty-eight hours compared to the blank treatment media at forty-eight hours, with zero hour blank data supplemented in for the reasons described previously. These plots showed a marked difference for all nine analytes in terms of interquartile range and median concentration

values. In order to be sure of the significance of the differences between the levels of the nine cytokines/growth factors in the treated PRC forty-eight hour media samples and the treated blank forty-eight hour samples, a one-way Analysis of Variance (ANOVA) was performed, which is equivalent to a t-test. The results of this ANOVA are shown in **Table 3.4** and show that all nine analytes displayed a significantly lower concentration in the treated PRC samples at forty-eight hours compared to the secretion media blank sample. This indicated that the PRCs were likely involved in the up-take of these cytokines from the treatment media and that these cytokines may be some of the ones responsible for any differences between the cellular proteomes of the control and treated PRCs observed in the iTRAQ analysis conducted on these cells.

Quantitative proteomic analysis of treated and control PRCs:

Secretions are well documented to be a major method of cell function and activity modulation. It was highly likely that the adipose tissue secretions would change aspects of the PRCs in a manner that would yield information regarding the health, state and some activated or deactivated biological pathways. Proteomics is an effective way to compare two or more cell populations based on their protein expression profiles. As it was used in the previous chapter, the initial plan for the PRCs was to compare treated and non-treated (control) PRCs using a two-dimensional electrophoresis (2-DE) technique known as differential display. This would have involved the isolation and separation of treated and non-treated PRC proteins in a 2-DE format gel, followed by image analysis and finally, identification of protein spots shown to be differentially expressed using spot excision, tryptic digestion and LC/MS identification. This technique has a distinct advantage over many liquid digest LC/MS based techniques in that it is inherently able to separate and display multiple post-translational modifications (PTM) of the same protein on the one gel. This can be important when proteins that have multiple functions that are modulated based on their PTM state. However, the cell yields obtained from each flask of PRCs in either the treated or control flasks were too small for this type of technique to be applied (data not shown).

iTRAQ was selected as the technique for the comparison of the treated and control PRCs because it requires considerably less starting material than 2-DE. In addition, compared to 2-DE, iTRAQ has simple preparation requirements and the datasets obtained are large

with all proteins detected being quantified. There is considerable resident expertise available at Macquarie University through the Australian Proteome Analysis Facility (APAF). iTRAQ is an LC/MS based technique whereby up to eight mixed protein samples can be compared using an isobaric chemical derivatisation technique allowing for the comparison and identification of proteins from different samples within the one experiment. This reduces the need for technical replicates due to the fact that all the samples are resolved on the same mass spectrometer at the same time; thus no day-to-day variation in the mass spectrometry equipment can occur. LC/MS approaches can typically identify a larger number of proteins overall.

In order to conduct the iTRAQ analysis, control and treated PRC cell lysates were prepared and total protein concentrations were equalised and compared using 1-D SDS PAGE, as seen in **Figure 3.7**. The samples were equalised between control and treatment samples of one biological replicate, *i.e.* the rat 1 control sample was equalised only against the rat 1 treated sample. **Figure 3.7** demonstrated that the samples within one biological replicate were equalised satisfactorily for use in iTRAQ analysis. Following the iTRAQ analysis at APAF, proteins were selected from the raw data output based on the significance (p-value < 0.05) of the change in abundance between control and treated and a minimum fold-change cut-off of +/- 1.2 fold. The proteins shown to be decreased in abundance in the treated PRCs are shown in **Table 3.6 A**. The proteins increased in abundance in the treated PRCs are shown in **Table 3.6 B**. Selection of the relevant proteins from these two lists was refined by the use of Blast2GO software, which aided in the data-mining of the functions of each identified protein and was able to sort and group them based on gene ontology (GO) information. **Figures 3.8-3.10** show pie-graphs for the decreased and increased in abundance protein data sets based on GO information describing involvement in biological processes and protein functions; the size of each pie slice was dependant on the number of proteins in the dataset attributed to that function/process. The use of the Blast2GO software allowed for a faster method for protein GO analysis and also highlighted protein functions and processes for more in-depth investigation. Without using this kind of data processing it would have been necessary to manually analyse the GO functions, processes and possible links to renal physiology or pathophysiology for all forty-nine identified differentially expressed proteins. The pie-graph analysis in **Figures 3.8-10** highlighted some protein

functions and biological processes that have known relevance to renal physiology and pathophysiology. These functions or processes were then selected and investigated for the identified proteins involved from within the **Table 3.6 A and B** datasets. The biological processes and functions of interest and possible relevance to renal failure were then assessed more closely to see which proteins from the iTRAQ datasets were involved. The breakdown of the proteins found to be involved in the biological functions and processes of interest are provided in **Tables 3.6** to **3.8**.

Table 3.1: Human cytokine concentrations in the adipose tissue secretions media used in all cell treatment experiments.

Cytokine:	Concentration (pg/mL)	Standard deviation (+/-)	Cytokine:	Concentration (pg/mL)	Standard deviation (+/-)
PDGF-bb	27.60	3.23	**IL-17**	28.60	3.58
IL-1b	15.20	0.71	**Eotaxin**	125.06	10.56
IL-1ra	132.85	12.21	**FGF basic**	25.65	1.76
IL-2	20.23	1.32	**G-CSF**	92818.51	24644.34
IL-4	2.67	0.20	**GM-CSF**	70.72	5.85
IL-5	1.50	0.11	**IFN-g**	374.45	33.00
IL-6	>19500.00*	0**	**IP-10**	164.39	11.58
IL-7	14.59	1.54	**MCP-1 (MCAF)**	>24000*	0**
IL-8	>28000.00*	0**	**MIP-1a**	286.14	27.50
IL-9	41.68	4.28	**MIP-1b**	202.51	9.41
IL-10	26.70	2.34	**RANTES**	25.23	0.86
IL-12 (p70)	117.70	5.08	**TNF-a**	32.89	1.43
IL-13	11.55	1.51	**VEGF**	1794.90	112.61
IL-15	6.85	1.15			

Table 3.1: The levels of twenty-seven human cytokines in the preparation of human adipose tissue secretion media used in all cell treatment experiments; measured using the Human 27-plex group I Bio-Plex kit. Asterisked concentrations and standard deviations show cytokines that had concentrations far above those of the standard curve; proteins were assigned the concentration value of the highest standard for that cytokine in this case. Kit size restrictions meant that the inclusion of multiple dilutions of the treatment media to account for very high concentrations, were not able to be completed.

Table 3.2: Initial assessment of PRC secretion of rat cytokines/growth factors over time.

	Rat Cytokine/Growth factor observed concentration (pg/mL)																					
Sample:	**IL-1a (21)**	**IL-1b (28)**	**IL-2 (22)**	**IL-4 (33)**	**IL-5 (52)**	**IL-6 (56)**	**IL-7 (38)**	**IL-10 (19)**	**IL-12 (p70) (78)**	**IL-13 (15)**	**IL-17 (72)**	**IL-18 (20)**	**EPO (14)**	**G-CSF (54)**	**GM-CSF (37)**	**GRO/KC (57)**	**IFN-g (34)**	**M-CSF (26)**	**MIP-1a (77)**	**MIP-3a (36)**	**RANTES (55)**	**TNF-a (43)**	**VEG-F (47)**
C1 0hr	0	2.5	0	2.19	7.21	0	0	0	1.05	1.19	0	0	0	0	0	0	0	0	5.56	0	0	0	0.25
C1 3hr	4.96	0	10.53	4.13	15.62	843.89	3.82	121.3	1.93	2.4	0	0	0	0	0	109.36	2.03	4.16	0	298.61	0	15.74	241.91
C1 24hr	18.55	6.21	23.01	6.78	19.4	1520.48	9.55	201.28	4.68	3.33	2.63	0	23.98	0	3.1	143.84	4.42	24.5	0	388.27	20.67	30.38	847.1
C1 48hr	9.4	6.21	17.59	6.31	13.84	2017.94	6.6	257.45	2.92	3.33	0	0	0	0	2.57	187.05	4.81	46.11	0	592.17	12.97	30.9	1859.17
T1 0hr	0	9.06	0	1.11	8.85	13.16	0	0	1.79	1.53	0	0	0	0	1.01	12.47	1.52	0	274.76	0	0	0	27.16
T1 3hr	4.96	9.06	5.29	2.58	5.21	1522.92	3.47	0	1.47	1.08	0	0	0	0	0.7	140.18	1.52	4.64	300.34	271.42	0	0	413.27
T1 24hr	10.51	18.47	19.28	6.31	15.87	5861.66	9.73	155.53	3.3	4.34	0.83	0	8.77	0	2	337.09	6.39	35.39	254.22	709.58	14.87	27.69	2071.29
T1 48hr	12.73	17.9	23.01	7.71	17.03	10885.88	13.53	201.28	4.02	4.6	1.63	0	13.41	0	2.32	597.95	6.61	58.82	238.68	953.71	13.62	29.84	2515.8
Blank C 0hr	0	0	0	0	5.21	5.26	0	8.36	0	0.63	0	0	0	0	0	0	0	0	0	0	0	0	0
Blank C 48hr	6.07	0	0	0	5.21	21.14	0	18.88	1.12	1.26	0	0	0	0	0.8	0.65	1.26	1.01	35.45	0	0	0	0
Blank T 0hr	6.49	13.91	0	2.97	6.28	21.14	0	8.36	0	1.8	0	0	0	0	0.8	14.08	3.48	0.94	277.48	0	0	0	30.47
Blank T 48hr	4.12	11.91	0	2.27	4.61	5.26	0	45.81	1.12	2.17	0	0	8.77	0	1.28	13.21	0	0.66	283.45	0.44	0	0	29.7

Table 3.2: Levels of rat cytokines detected in the control and treated cell culture supernatants of the PRCs from Rat 1 biological replicates during time-course culture, using the Bio-Plex™ Pro Rat 23-plex assay. This was used as a small-scale test for validation of our experimental plan. The majority of cytokines/growth factors within the panel displayed no changes in concentration (greyed boxes); with the exception of IL-6, IL-10, GRO/KC-like protein, MIP-3a and VEGF. MIP-1a displayed a high level of cross-reactivity with the human cytokines present within the blank secretion media samples.

Figure 3.2 (A to E): Proteins that may be secreted by the PRCs over time during the treatment with adipose tissue secretions.

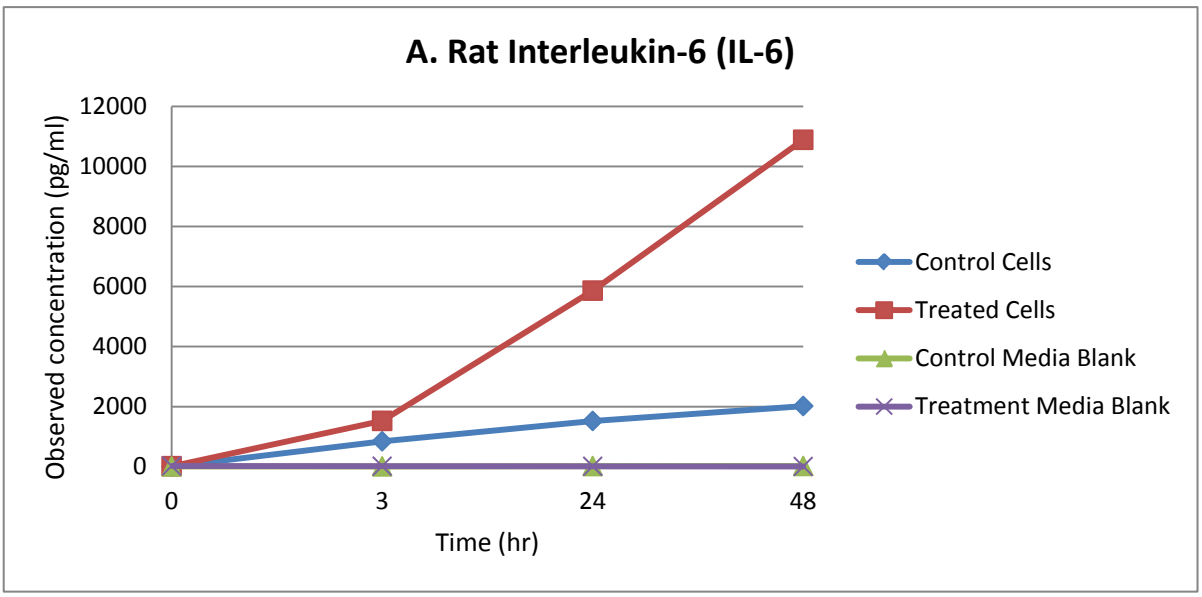

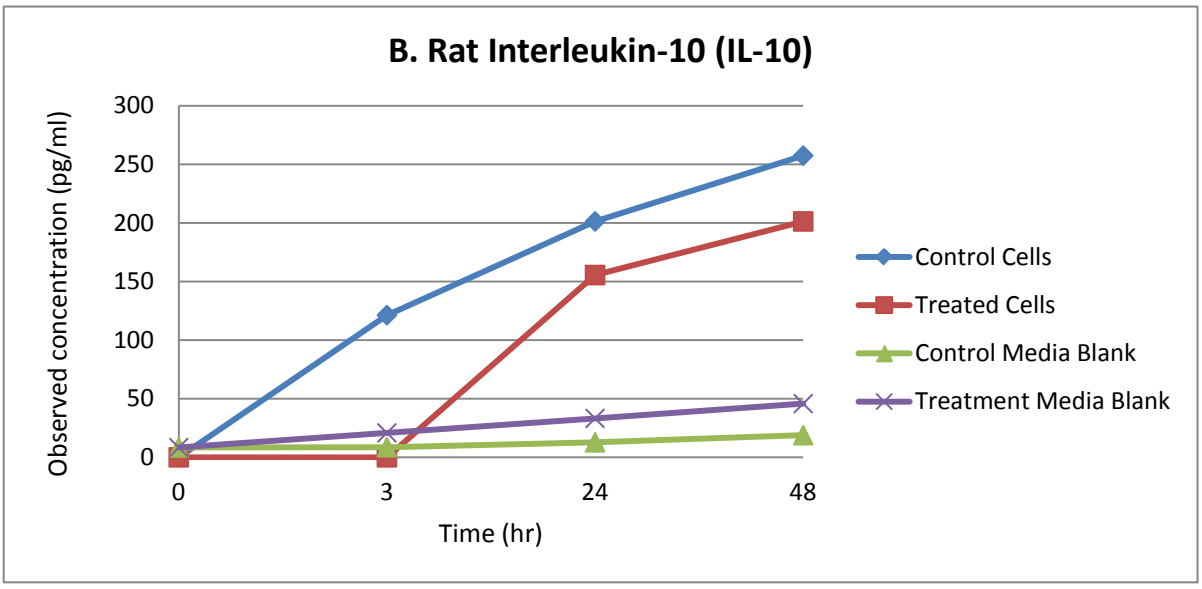

Figure 3.2 (A to E): Rat cytokine/growth factor levels for the five analytes in **Table 3.2** that displayed changes in abundance over time in response to the treatment with human adipose tissue secretion media. **A)** IL-6 with a 539% increase in abundance in the treated PRC media over controls. **B)** IL-10 displayed a 10% decreased abundance in treated PRC media compared to control PRCs. **C)** GRO/KC-like protein was increased by 319% in treated PRCs. **D)** MIP-3a abundance was increased by 161% in treated PRC flasks. **E)** VEGF abundance was increased in treated PRC flasks by 35%. These data indicate a change in the secretion profile of the PRCs over time in response to the presence of the adipose secretions compared to non-treated controls.

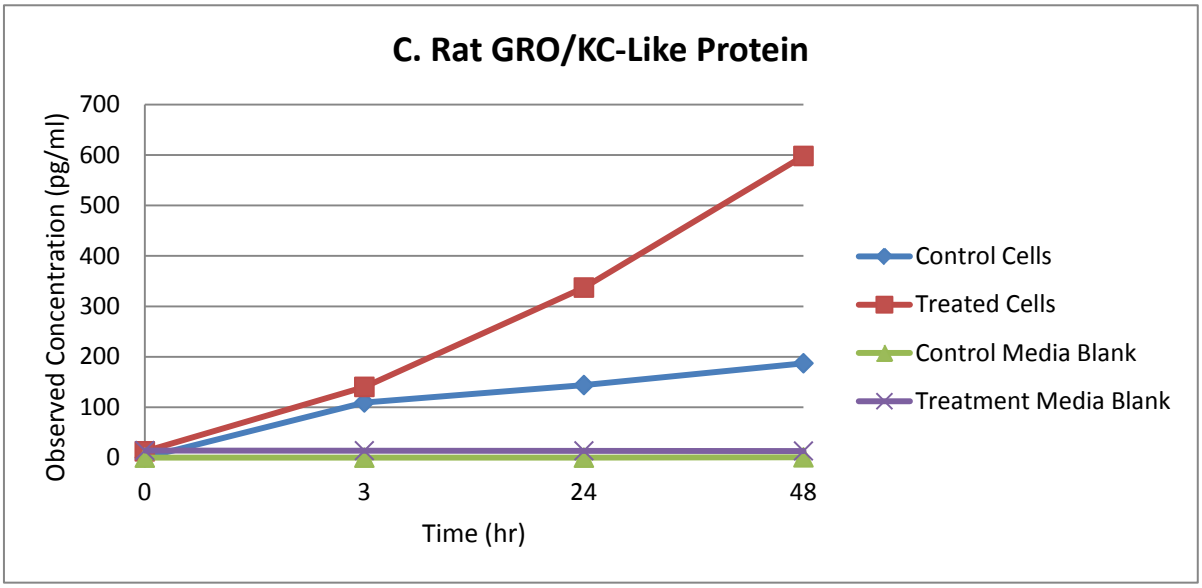
C. Rat GRO/KC-Like Protein
Observed Concentration (pg/ml)
700
600
500
400
300
200
100
0
0
3
24
48
Time (hr)
Control Cells
Treated Cells
Control Media Blank
Treatment Media Blank

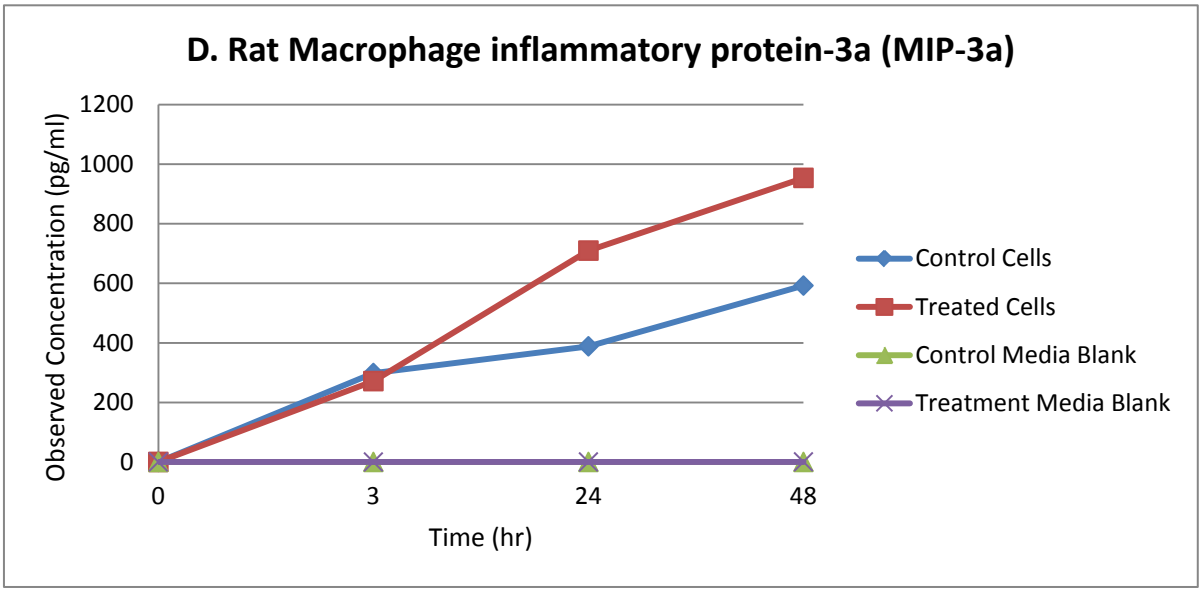
D. Rat Macrophage inflammatory protein-3a (MIP-3a)
Observed Concentration (pg/ml)
1200
1000
800
600
400
200
0
0
3
24
48
Time (hr)
Control Cells
Treated Cells
Control Media Blank
Treatment Media Blank

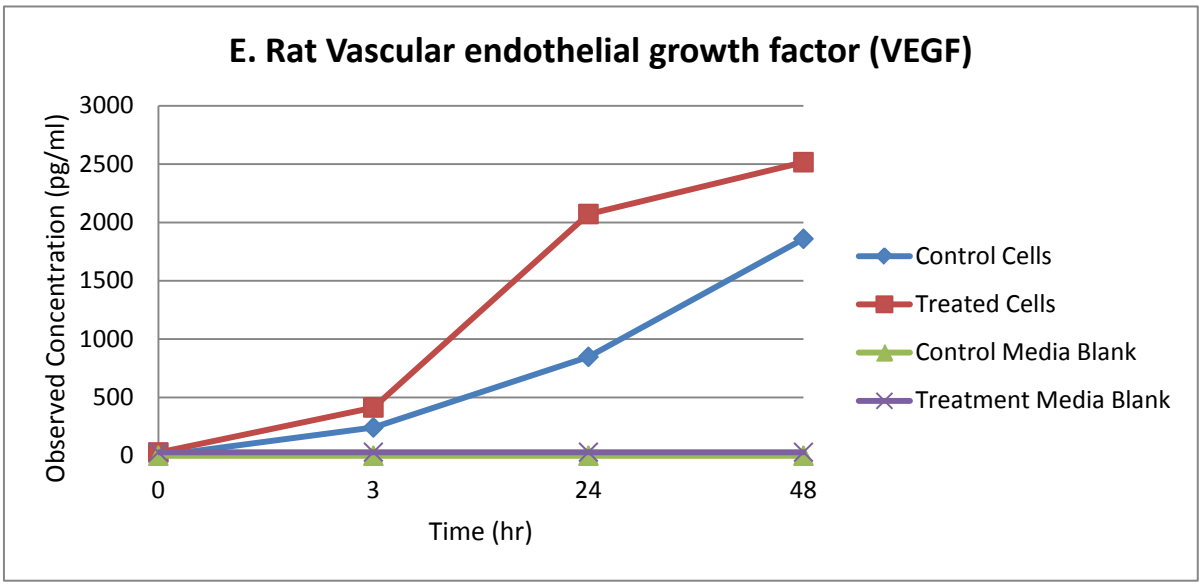
E. Rat Vascular endothelial growth factor (VEGF)
Observed Concentration (pg/ml)
3000
2500
2000
1500
1000
500
0
0
3
24
48
Time (hr)
Control Cells
Treated Cells
Control Media Blank
Treatment Media Blank

Table 3.3: Initial assessment of the human cytokine/growth factor levels over time during treatment of the PRCs with human adipose secretions.

	Human cytokine/growth factor observed concentrations (pg/mL)													
Sample:	**IL-1b**	**IL-1ra**	**IL-2**	**IL-4**	**IL-5**	**IL-6**	**IL-7**	**IL-8**	**IL-9**	**IL-10**	**IL-12(p70)**	**IL-13**	**IL-15**	**IL-17**
C1 0hr	0.37	0	0	*0.10	0	0	0	0	0	0	0	0.53	0	1.4
C1 3hr	0.37	2.36	0	0	0	0	0	0	0	0	0	0.31	0	0.31
C1 24hr	0	5.27	0	0	0	0	0	0	0	0	3.44	0.29	0	0
C1 48hr	0.44	7.37	0	0.37	0	0	0	0	0	0	0	0.41	0	0
T1 0hr	20.46	128.71	9.42	4.44	0	*20871.11	1.73	*29015.14	45.58	26.18	40.97	1.58	18.05	27.58
T1 3hr	20.57	113.73	9.17	4.22	0	*20871.11	1.73	*29015.14	44.36	24.29	28.89	1.32	16.26	28.62
T1 24hr	16.12	95.06	3.82	3.24	0	*20871.11	0.64	*29015.14	29.63	19.14	36.95	1.42	9.59	16.13
T1 48hr	15.07	103.11	3.44	3.28	0	*20871.11	1.93	*29015.14	19.54	15.35	27.88	2.99	10.44	14.05
Blank C 0hr	0.41	1.49	0	0	0	0	0	0	4.11	0	0	0.25	0	0
Blank C 3hr	0.48	0.32	1.2	0	0	0	0	0	11.38	0	0	0.23	0	13
Blank C 24hr	0	2.36	2.05	0	0	0	0	0	9.67	0	0	0.18	0	8.81
Blank C 48hr	0.37	4.76	1.2	0	0	0	0	0	5.56	0	0	0.25	2.29	1.93
Blank T 0hr	22.36	105.55	6.48	3.99	0	*20871.11	0.38	*29015.14	45.06	18.15	40.52	1.7	12.37	18.74
Blank T 3hr	19.49	146.57	6.32	3.58	0	*20871.11	2.12	*29015.14	37.89	21.42	44.1	2.69	5.68	21.34
Blank T 24hr	19.2	115.38	8.6	3.62	0	*20871.11	2.12	*29015.14	54.2	22.4	40.75	1.28	13.3	19.26
Blank T 48hr	21.32	100.69	7.02	3.35	0	*20871.11	0.64	*29015.14	39.92	18.51	35.38	2.99	10.15	19.52

Table 3.3 (continued):

	Human cytokine/growth factor observed concentrations (pg/mL)												
Sample:	**Eotaxin**	**FGF basic**	**G-CSF**	**GM-CSF**	**IFN-g**	**IP-10**	**MCP-1(MCAF)**	**MIP-1a**	**MIP-1b**	**PDGF-bb**	**RANTES**	**TNF-a**	**VEGF**
C1 0hr	6.57	5.23	2.96	0	0	0	0	0	0	0	0	0.98	0
C1 3hr	0	0	0.42	0	3.65	0	0	0	0	0	0	0	11.75
C1 24hr	0	0	1.33	0	11.24	0	0	0	0	0	0	0.98	25.42
C1 48hr	0	0	0	0	24.52	0	0	0	0	0	0	0	66.68
T1 0hr	20.21	30.7	15151.67	77.44	142.16	83.24	*19769.92	203.83	209.86	15.79	23.75	51.62	2548.88
T1 3hr	37.35	33.17	*32596.54	69.49	146.46	84.23	*19769.92	174.62	171.38	12.76	22.03	52.74	2244.66
T1 24hr	16.86	13.63	30250.15	34.23	114.84	75.22	*19769.92	216.08	171.71	0	24.29	50.78	1874.32
T1 48hr	14.48	12.47	21884.31	22.4	111.96	58.51	*19769.92	114.53	147.71	0	20.46	41.78	1798.15
Blank C 0hr	0	4.43	2.16	3.25	7.62	0	0	0	0	0	0	0	1.56
Blank C 3hr	0	0	0	14.69	0	0	0	0	0.14	0	0	0	5.27
Blank C 24hr	0	6.77	2.96	18.03	3.65	0	0	0	1.28	0	0	0	5.86
Blank C 48hr	0	6.28	0	21.93	3.65	8.6	0.3	0	0	0	0	0	13.68
Blank T 0hr	14.48	38.32	*32596.54	66.22	127.79	72.12	*19769.92	198.77	167.93	20.83	19.32	49.94	2485.77
Blank T 3hr	0	31.53	*32596.54	66.62	133.54	72.12	*19769.92	224.17	209.28	16.89	19.38	49.1	2693.1
Blank T 24hr	37.1	29.44	*32596.54	78.73	122.04	76.75	*19769.92	297.31	203.83	17.25	15.57	50.78	2451.68
Blank T 48hr	13.54	28.37	*32596.54	59.44	97.52	77.25	*19769.92	171.79	154.7	15.04	18.83	45.73	2563.34

Table 3.3: The levels of human cytokines present within the cell culture supernatant of the control and treated primary renal cells over time-course intervals of 0 hr, 3 hr, 24 hr and 48 hr in one biological replicate (Rat 1) as a preliminary proof-of concept experiment. Cytokines were quantified using the Bio-Plex™ Pro Human 27-plex group I kit in the APAF facility. Data obtained shows that two of the twenty-seven assayed factors (PDGF-bb and VEGF) displayed trends toward preferential up-take from the media by the PRCs. This can be observed by looking at the decline in concentration over time compared to the blank media controls over time. Both PDGF-bb and VEGF show greater decline in the presence of PRCs.

Figure 3.3: Initial data for PDGF-bb and VEGF concentrations over time in biological replicate 'rat 1' samples.

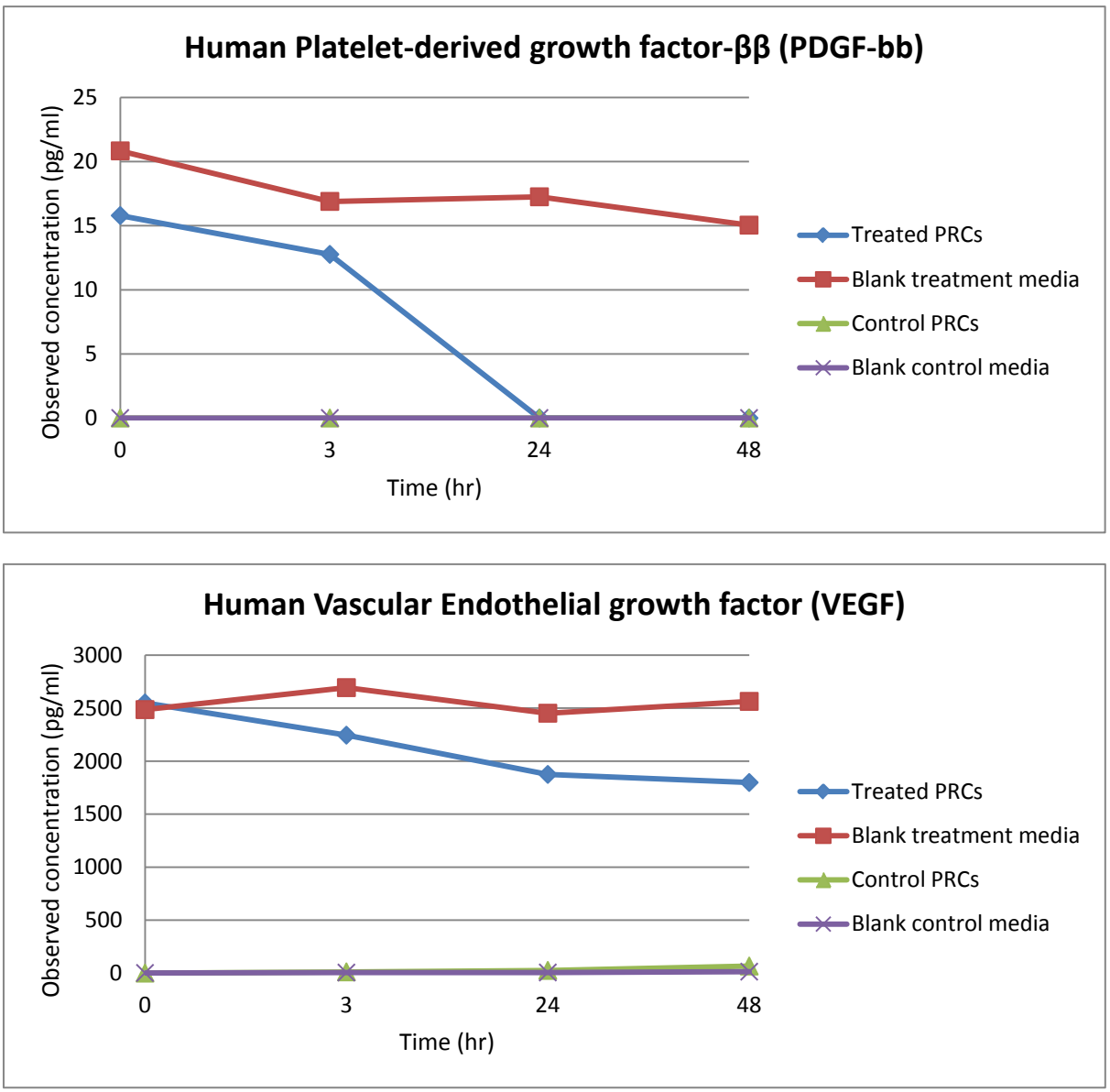

Figure 3.3: Human PDGF-bb and VEGF concentrations over time. These two graphs better depict the changes in the concentration of PDGF-bb and VEGF in the treatment media exposed to the PRCs. A clear trend in both graphs shows a decrease in concentration of the analytes over time when compared to the blank (no PRC) treatment media controls. PDGF-ββ displayed a 100% decrease in abundance over forty-eight hours while VEGF abundance declined 30% in the same period. This indicates a potential mechanism of preferential uptake of these factors from the treatment media by the PRCs, implicating them in any effects that the treatment may have on the cells.

Figure 3.4: Detected changes in cytokine levels over time compared to control and treatment media blanks.

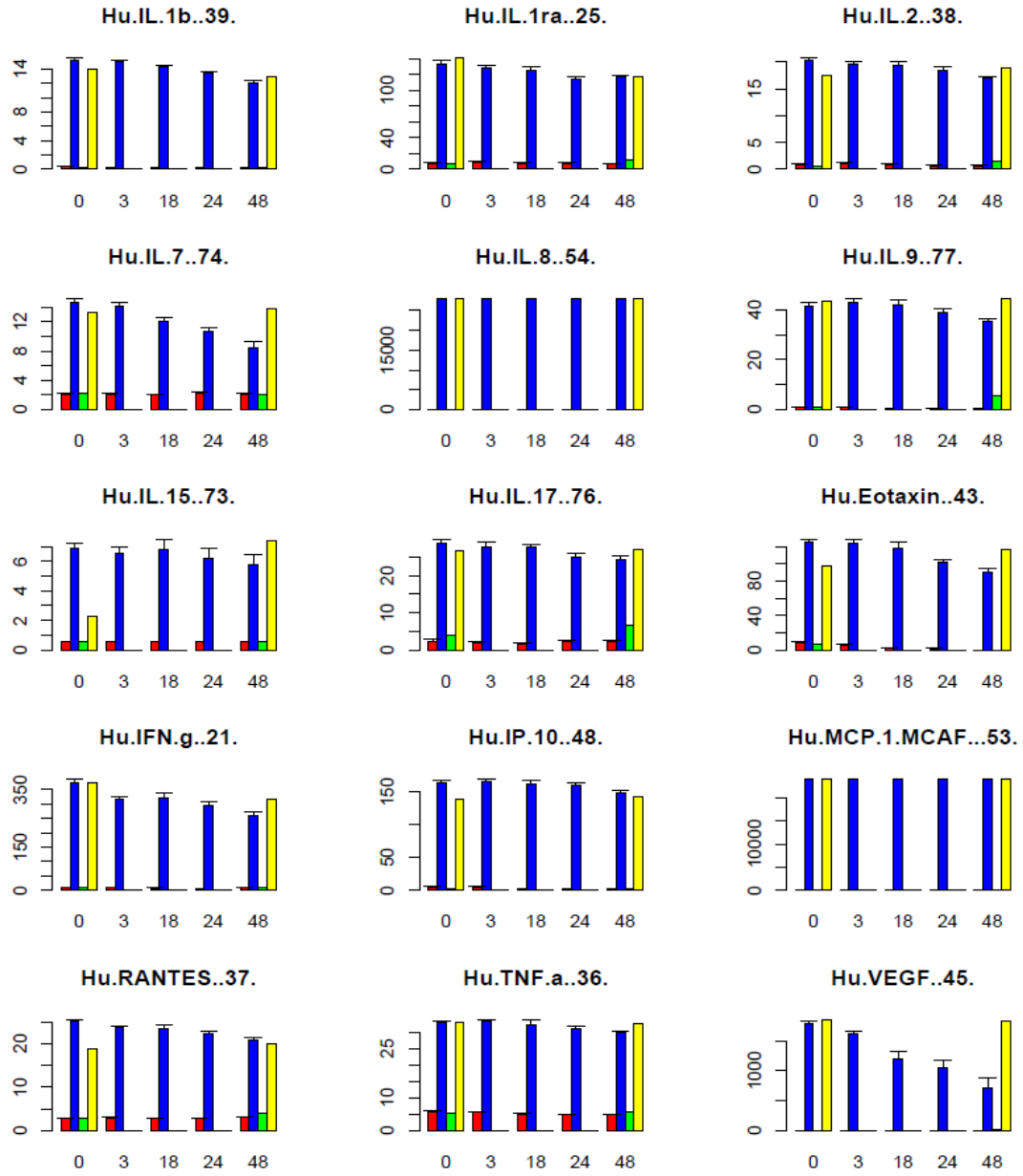

KEY

Red: Control media PRCs

Blue: Treatment/secretion media PRCs

Green: Control media blank

Yellow: Treatment media blank

Y-axis: Cytokine concentration (pg/mL)

X-axis: Treatment time (hours)

Figure 3.4 (continued):

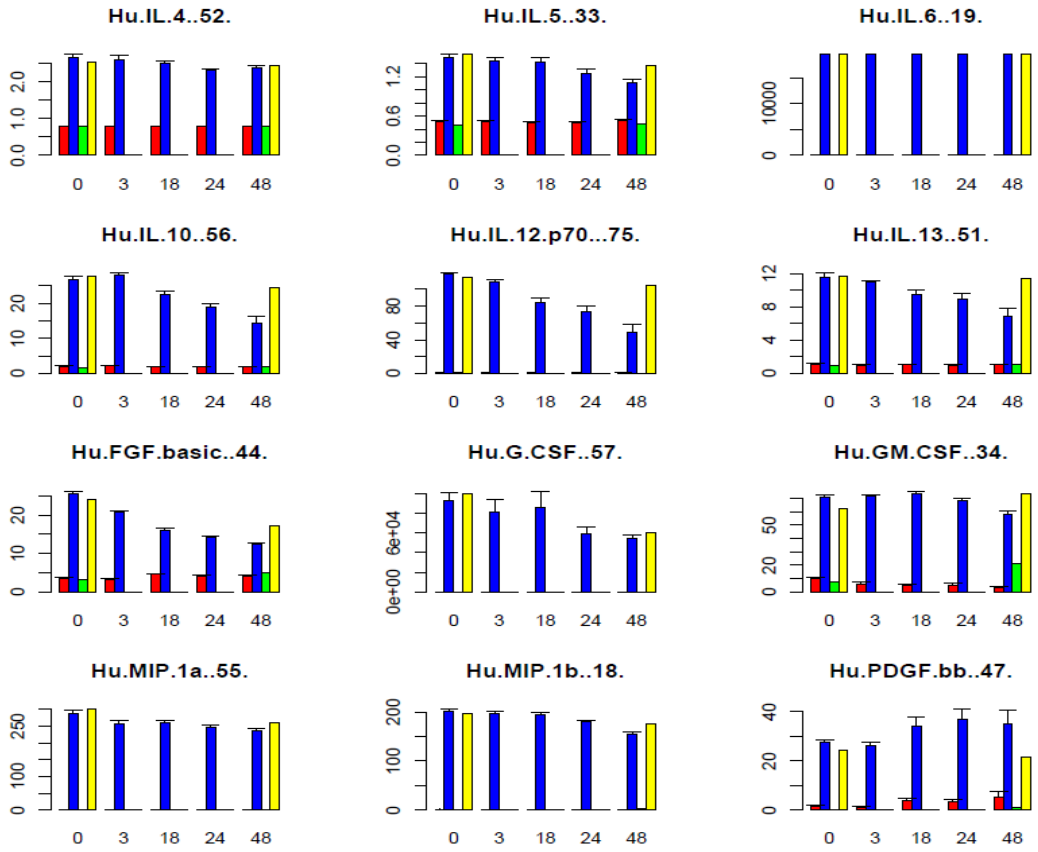

KEY

Red: Control media PRCs

Blue: Treatment/secretion media PRCs

Green: Control media blank

Yellow: Treatment media blank

Y-axis: Cytokine concentration (pg/mL)

X-axis: Treatment time (hours)

Figure 3.4: Changes in human cytokine levels during treatment of PRCs with human adipose tissue secretions as measured using the Bio-Plex™ human 27-plex group I cytokine detection kit. The concentration of human cytokines is much greater in the treated PRC (blue) and the treatment blank (yellow) samples than the control media PRCs (red) or the control media blank (green), indicated low cross-reactivity of the Bio-Plex™ assay used. In general, degradation in cytokine concentration was observed over time when comparing the yellow zero hour and forty-eight hour bars in each plot. Plots of interest were those that displayed greater degradation in human cytokine level over time in the treated PRC bars (blue) than that seen in the corresponding treatment blank bars (yellow) for each cytokine. These included IL-7, IL-9, IFN-gamma, VEGF, IL-5, IL-10, IL-12, IL-13 and FGF-b. The data from these cytokines was selected for more detailed statistical analysis to test for significant differences between treated PRC samples versus treatment blanks.

Figure 3.5: Box plot representation of treatment blank samples at zero hours and forty-eight hours in the human Bio-Plex™ assay.

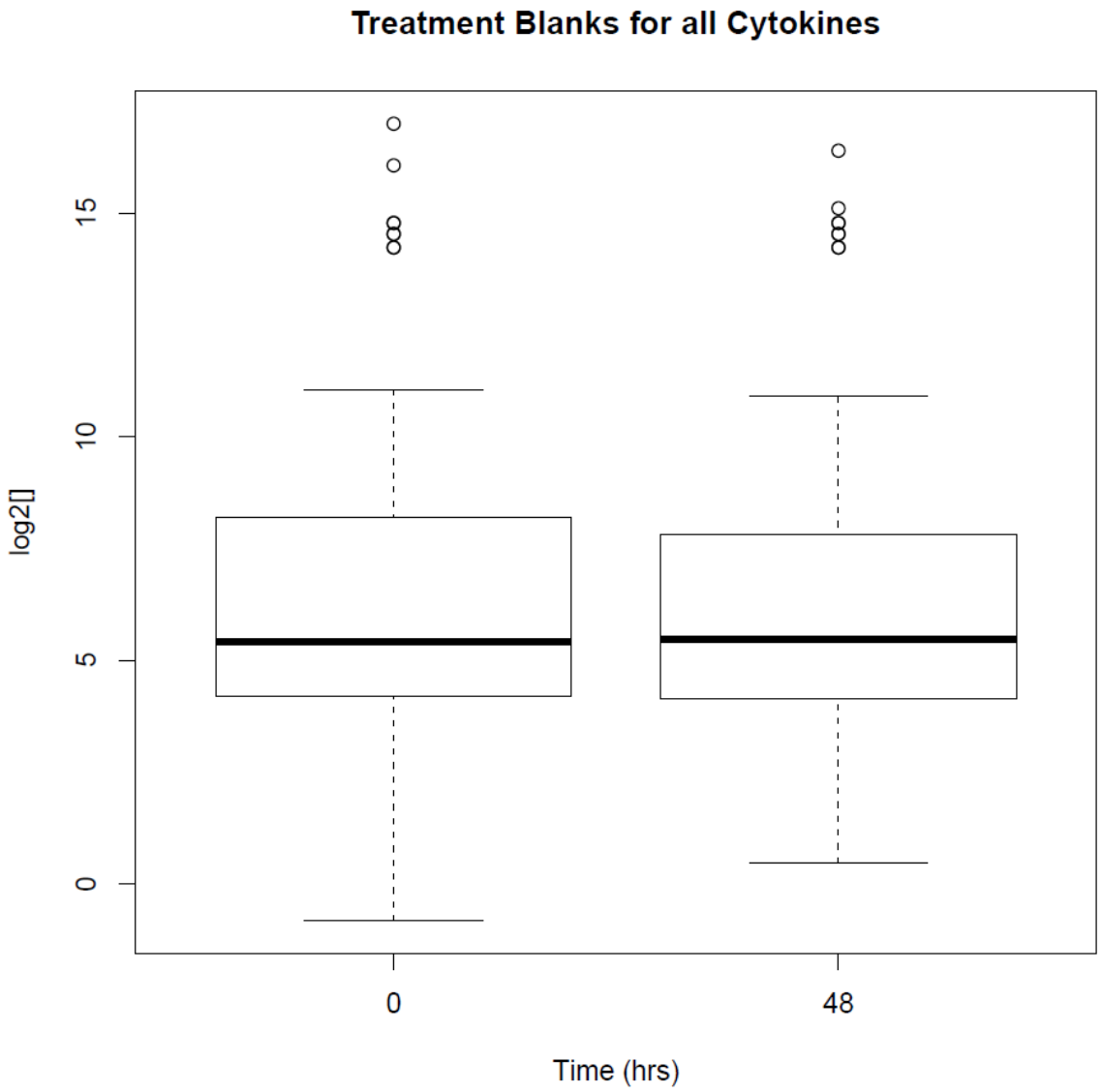

Figure 3.5: Box plot representation of treatment blank samples at zero hours and forty-eight hours in the human Bio-Plex™ assay. The data represented here shows that for all twenty-seven cytokines assayed for in the treatment blank samples (no cells present), no significant difference between the zero hour and forty-eight hour timepoints exist. This means that little to no degradation in cytokine levels overall was observed and that the zero hour and forty-eight hour timepoint sample data points could be combined for comparison to the forty-eight hour treatment samples (with PRCs present).

Figure 3.6: Box plots of the nine human cytokines from the treatment media that may be taken up by the PRCs during the treatment time. Cytokine concentration is measured in pg/mL for all plots. (BT) Blank treatment media incubated for forty-eight hours without PRCs present, designed to display the concentration of human cytokines within the media after any degradation due to the incubation conditions. (T) Treatment media samples from flasks containing PRCs after forty-eight hours incubation. From the different boxes within each plot, it can be seen that these selected cytokines differ in regards to their interquartile range and medians. The same data that was used to construct these box plots was then utilised in a one-way ANOVA statistical analysis comparing the BT and T groups at forty-eight hours to test for significance in the differences observed (see **Table 3.4**). Data analysis was completed using the R and Tinn-R statistical data analysis software packages as described in **section 3.3.7**.

Figure 3.6: Box plots of the nine human cytokines from the treatment media that may be taken up by the PRCs during the treatment time.

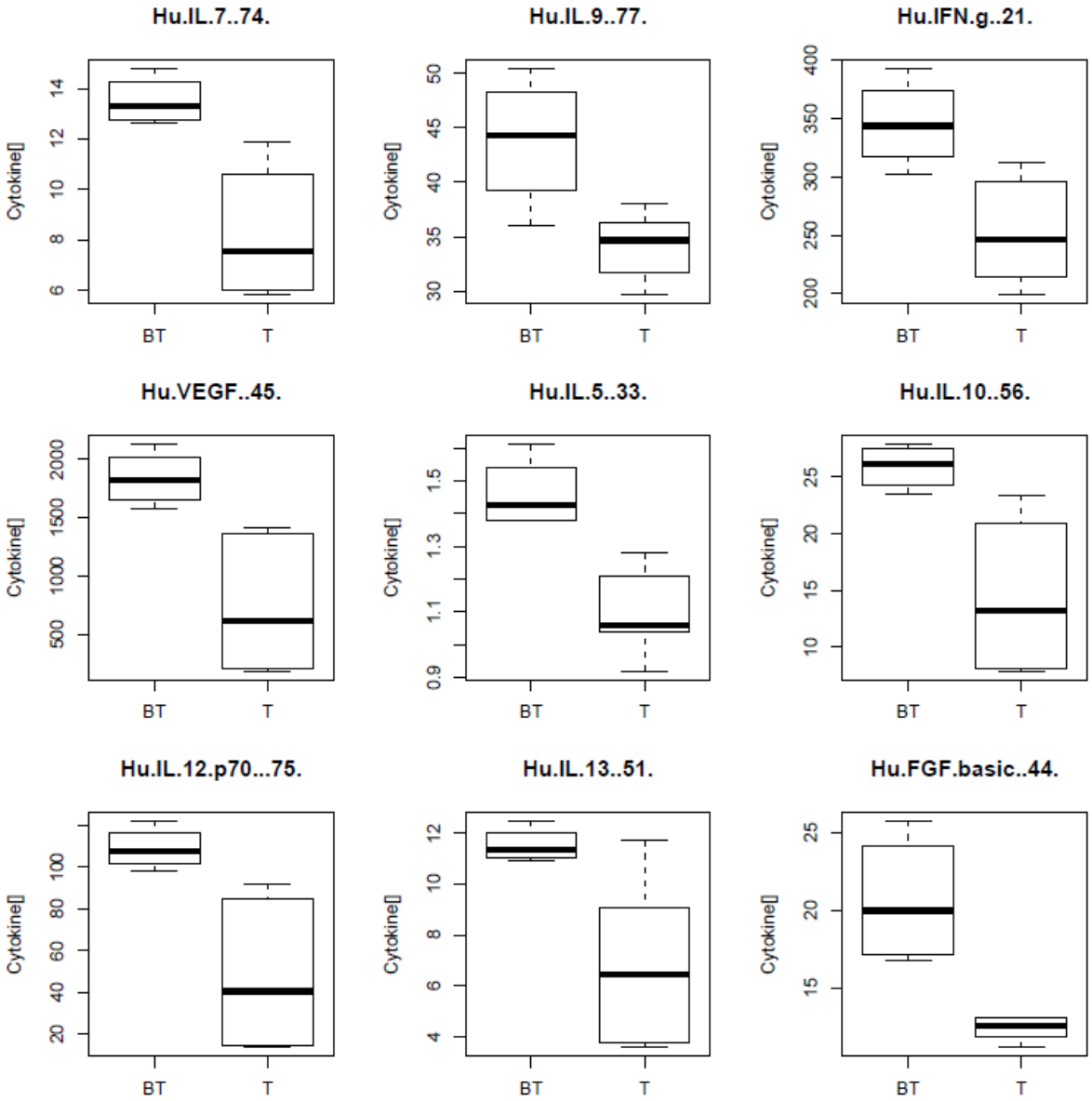

Table 3.4: Statistical data for the nine human cytokines displayed in **Figure 3.6** indicating significant differences between treatment media exposed to PRCs and treatment media blanks.

Cytokine:	*p*-value:	Concentration Δ (pg/mL):
IL-7	0.004	5.02
IL-9	0.001	8.55
IFN-g	0.010	87.53
VEGF	0.005	1120.40
IL-5	0.002	0.34
IL-10	0.010	11.75
IL-12	0.009	60.4
IL-13	0.021	4.69
FGF-basic	0.001	8.14

Table 3.4: Statistical data analysis of the nine selected cytokines/growth factors from **Figure 3.4**. A 1-way ANOVA analysis was used to compare the treatment blank samples to the treatment PRC samples for each individual cytokine/growth factor. A comparison that gave a *p*-value of <0.05 was deemed to have a significant difference between treatment blank and treated PRC. Changes in concentration between the treatment blank samples and the treatment PRC samples are also shown, revealing quite small changes in most of the cytokines assessed. Statistical analysis was completed using the R and Tinn-R statistical analysis programs.

Figure 3.7: Demonstration of protein load equalisation between each control and treated sample in preparation for iTRAQ proteomic analysis.

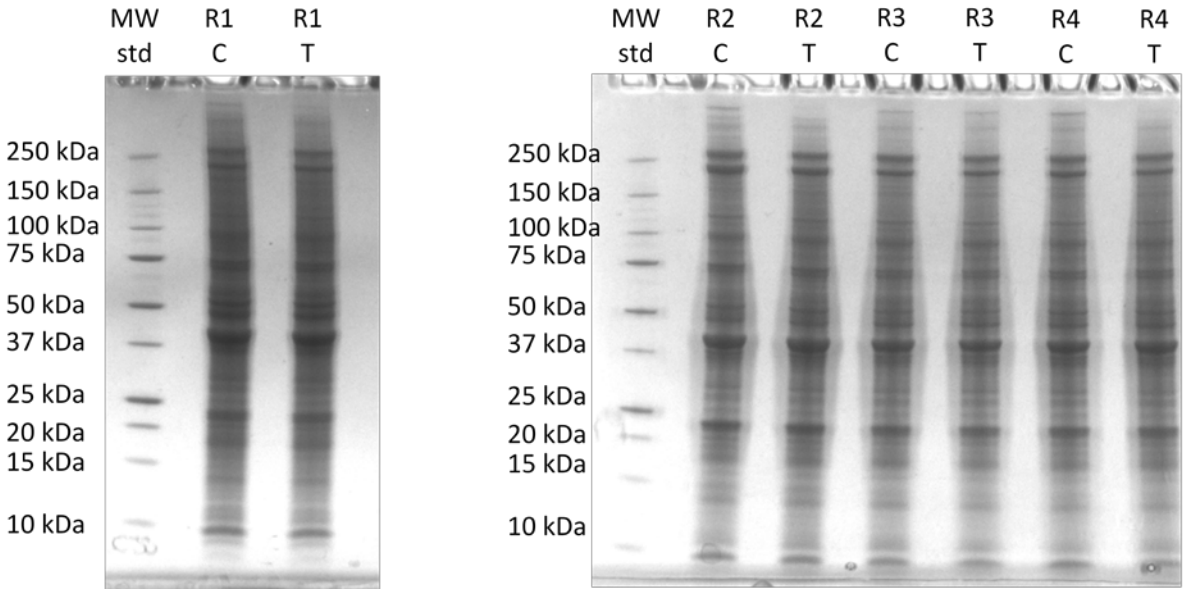

Figure 3.7: 1-D SDS PAGE gel of control (C) and treated (T) samples prepared for iTRAQ analysis confirming the level of equalisation achieved in each biological replicate sample (rat 1 [R1], rat 2 [R2], etc). Each lane displays the total protein content in 10 µL of each sample. The control and treated samples for each biological replicate were equalised against each other, not against the samples from a different biological replicate. This was because the planned iTRAQ comparisons for each sample were only between samples within a single biological replicate. Rat 1 samples were resolved on a separate gel prior to the preparation and resolving of the other biological replicates this was to ensure no un-anticipated problems with the sample preparation had arose before using up all the samples. The gels used here were Criterion™ pre-cast 18-well 1-dimensional polyacrylamide gel, with Precision Plus Protein™ unstained molecular weight markers, stained with Flamingo™ protein stain, imaged on a Typhoon Trio™ gel imager using Typhoon Scanner Control (v5.0) image acquisition software.

Table 3.5: Summary reports for the two 4-plex iTRAQ analyses of treated and control PRCs.

Software version:	ProteinPilot™ software version 4.0
Revision number:	148085
Paragon algorithm	4.0.0.0, 148083
Confidence interval applied to MS data:	95%
4-plex run #1:	
Spectra identified:	95255
Distinct peptides:	31420
Proteins detected:	1724
Background correction used:	Yes
4-plex run #2:	
Spectra identified:	94438
Distinct peptides:	32075
Proteins detected:	1555
Background correction used:	Yes

Table 3.5: Summary report table output obtained from the two 4-plex iTRAQ analyses from APAF. This indicates the total number of proteins and spectra identified and a brief overview of the run parameters used in the ProteinPilot™ software during the database searching of the MS data from the two 4-plex analyses.

Table 3.6 A: Proteins found to have decreased abundance in the treated PRCs identified using iTRAQ analysis.

Protein name	Protein accession / Gene accession	%Cov(95)	Peptides (95%)	Treated:Control	*p*-value Treated:Control	Frequency
Acetyl-CoA acetyltransferase, cytosolic	Q5XI22 / THIC_RAT	35.77	8	0.64	0.0125	*
Acylamino-acid-releasing enzyme	P13676 / ACPH_RAT	12.57	6	0.79	0.0049	*
Annexin A5	P14668 / ANXA5_RAT	71.47	38	0.63	0.0198	*
Annexin A6	P48037 / ANXA6_RAT	61.81	49	0.80	0.0123	*
Collagen alpha-1(I) chain	P02454 / CO1A1_RAT	50.38	120	0.32	2.45E-10	**
Collagen alpha-1(III) chain	P13941 / CO3A1_RAT	28.64	50	0.31	7.35E-05	**
Collagen alpha-2(I) chain	P02466 / CO1A2_RAT	45.55	74	0.44	5.15E-06	**
Cytoplasmic dynein 1 heavy chain 1	P38650 / DYHC1_RAT	35.38	121	0.7	1.31E-06	***
Cytoplasmic dynein 1 intermediate chain 2	Q62871 / DC1I2_RAT	23.67	9	0.56	0.0464	*
Destrin	Q7M0E3 / DEST_RAT	78.18	27	0.65	0.0304	*
Ectonucleotide pyrophosphatase/phosphodiesterase family member 1	Q924C3 / ENPP1_RAT	36.87	29	0.64	0.0180	*
Elongation factor 1-alpha 1	P62630 / EF1A1_RAT	68.4	91	0.79	0.0352	*
Fatty acid synthase	P12785 / FAS_RAT	27.35	44	0.70	0.0195	*
Galectin-1	P11762 / LEG1_RAT	85.19	35	0.67	0.0497	*
Integrin alpha-1	P18614 / ITA1_RAT	17.12	18	0.61	0.0303	*
Microtubule-associated protein 4	Q5M7W5 / MAP4_RAT	44.47	31	0.61	0.0248	*
Myosin-10 OS=Rattus norvegicus GN=Myh10 PE=1 SV=1	sp|Q9JLT0|MYH10_RAT	49.09	129	0.79	0.0077	***
Myosin-9	Q62812 / MYH9_RAT	58.44	286	0.67	0.0138	*
Myosin-Id	Q63357 / MYO1D_RAT	33.3	30	0.69	0.0438	**
Myristoylated alanine-rich C-kinase substrate	P30009 / MARCS_RAT	54.37	12	0.09	0.0011	***
Nestin	P21263 / NEST_RAT	40.41	65	0.73	0.0065	*

Table 3.6 A (continued):

Protein name	Protein accession / Gene accession	%Cov(95)	Peptides (95%)	Treated:Control	*p*-value Treated:Control	Frequency
Non-muscle caldesmon	Q62736 / CALD1_RAT	60.08	86	0.58	0.0069	*
Nucleobindin-2	Q9JI85 / NUCB2_RAT	41.43	15	0.65	0.0313	*
Plastin-3	Q63598 / PLST_RAT	65.24	49	0.67	0.0129	**
Procollagen C-endopeptidase enhancer 1	O08628 / PCOC1_RAT	33.55	10	0.60	0.0153	**
Procollagen-lysine,2-oxoglutarate 5-dioxygenase 2	Q811A3 / PLOD2_RAT	38.4	29	0.81	0.0026	**
Prolyl 4-hydroxylase subunit alpha-1	P54001 / P4HA1_RAT	39.7	22	0.69	0.0393	*
Protein Niban	Q9ESN0 / NIBAN_RAT	37.78	25	0.72	0.0259	*
REVERSED Glucoside xylosyltransferase 1	RRRRRsp / Q6GX83 / GXLT1_RAT	3.448	2	0.02	0.0167	*
Transgelin	P31232 / TAGL_RAT	89.55	115	0.59	0.0092	*
Tropomyosin alpha-1 chain	P04692 / TPM1_RAT	58.1	53	0.59	0.0170	*
Tropomyosin alpha-4 chain	P09495 / TPM4_RAT	68.15	51	0.63	0.0301	*
Vimentin	P31000 / VIME_RAT	83.48	162	0.54	0.0248	*

Table 3.6 A and B (3 pages): Proteins found to be differentially expressed between control and treated primary renal cell cultures using iTRAQ quantitative analysis and data analysis using Protein Pilot software and Microsoft Excel. **(A)** Proteins found to be of decreased abundance in the treated PRCs; **(B)** proteins found to be of increased abundance in the treated PRCs. A fold-change cut-off of 0.8 – 1.2 was applied for screening the data. Proteins were selected as significantly increased or decreased in abundance if the fold-change ratio was below 0.8 or above 1.2 and the ratio had a *p*-value of <0.05. The iTRAQ analysis was conducted using services provided by the Australian Government through APAF.

Table 3.6 B: Proteins found to be of increased abundance in the treated PRCs detected using iTRAQ analysis.

Protein name	Protein accession / Gene accession	%Cov(95)	Peptides (95%)	Treated:Control	p-value Treated:Control	Frequency
A-kinase anchor protein 2	Q5U301 / AKAP2_RAT	38.85	27	1.45	0.0288	*
Calponin-1	Q08290 / CNN1_RAT	71.72	54	1.79	0.0247	*
Cytochrome P450 1B1	Q64678 / CP1B1_RAT	23.76	8	2.11	0.0479	*
Fibronectin	P04937 / FINC_RAT	45.50	83	1.91	1.18E-11	*
Guanine deaminase	Q9WTT6 / GUAD_RAT	63.88	39	3.19	0.0009	*
Hexokinase-1	P05708 / HXK1_RAT	37.58	30	1.36	0.0190	*
Intercellular adhesion molecule 1	Q00238 / ICAM1_RAT	17.98	9	1.87	0.0339	**
Oxidized low-density lipoprotein receptor 1	O70156 / OLR1_RAT	27.75	7	1.49	0.0283	*
Plasminogen activator inhibitor 1	P20961 / PAI1_RAT	47.26	13	1.42	0.0376	**
Prostaglandin G/H synthase 1	Q63921 / PGH1_RAT	30.73	13	1.47	0.0416	*
Retinoid-inducible serine carboxypeptidase	Q920A6 / RISC_RAT	28.76	13	1.64	0.0482	*
Sarcoplasmic/endoplasmic reticulum calcium ATPase 2	P11507 / AT2A2_RAT	30.78	28	1.45	0.0103	*
Superoxide dismutase [Mn], mitochondrial	P07895 / SODM_RAT	47.30	13	1.64	0.0489	*
Tissue factor	P42533 / TF_RAT	24.07	8	2.40	0.0480	*
UDP-glucose 6-dehydrogenase	O70199 / UGDH_RAT	66.33	36	2.15	0.0002	***
Vascular cell adhesion protein 1	P29534 / VCAM1_RAT	44.25	26	1.27	0.0302	*

Table 3.6 A and B (3 pages): Proteins found to be differentially expressed between control and treated primary renal cell cultures using iTRAQ quantitative analysis and data analysis using Protein Pilot software and Microsoft Excel™. **(A)** Proteins found to be of decreased abundance in the treated PRCs; **(B)** proteins found to be of increased abundance in the treated PRCs. A fold-change cut-off of 0.8 – 1.2 was applied for screening the data. Proteins were selected as significantly increased or decreased in abundance if the fold-change ratio was below 0.8 or above 1.2 and the ratio had a *p*-value of <0.05. The iTRAQ analysis was conducted using services provided by the Australian Government through APAF.

Figure 3.8: Pie-chart of the protein identifications (featured in **Table 3.6 A**) found to be decreased in abundance in the treated sample group, sorted by gene ontology information based on biological process annotations. This pie-chart takes into account all the known biological process involvements for all proteins shown in **Table 3.6 A**. Numbers next to each biological process indicate the number of proteins attributed to this process from the dataset. Data analysis was conducted using Blast2GO data analysis software tool, available free online at: http://www.blast2go.com/b2glaunch.

Figure 3.8: Pie-chart of the protein identifications found to be decreased abundance in the treated sample group, sorted by gene ontology biological process annotations.

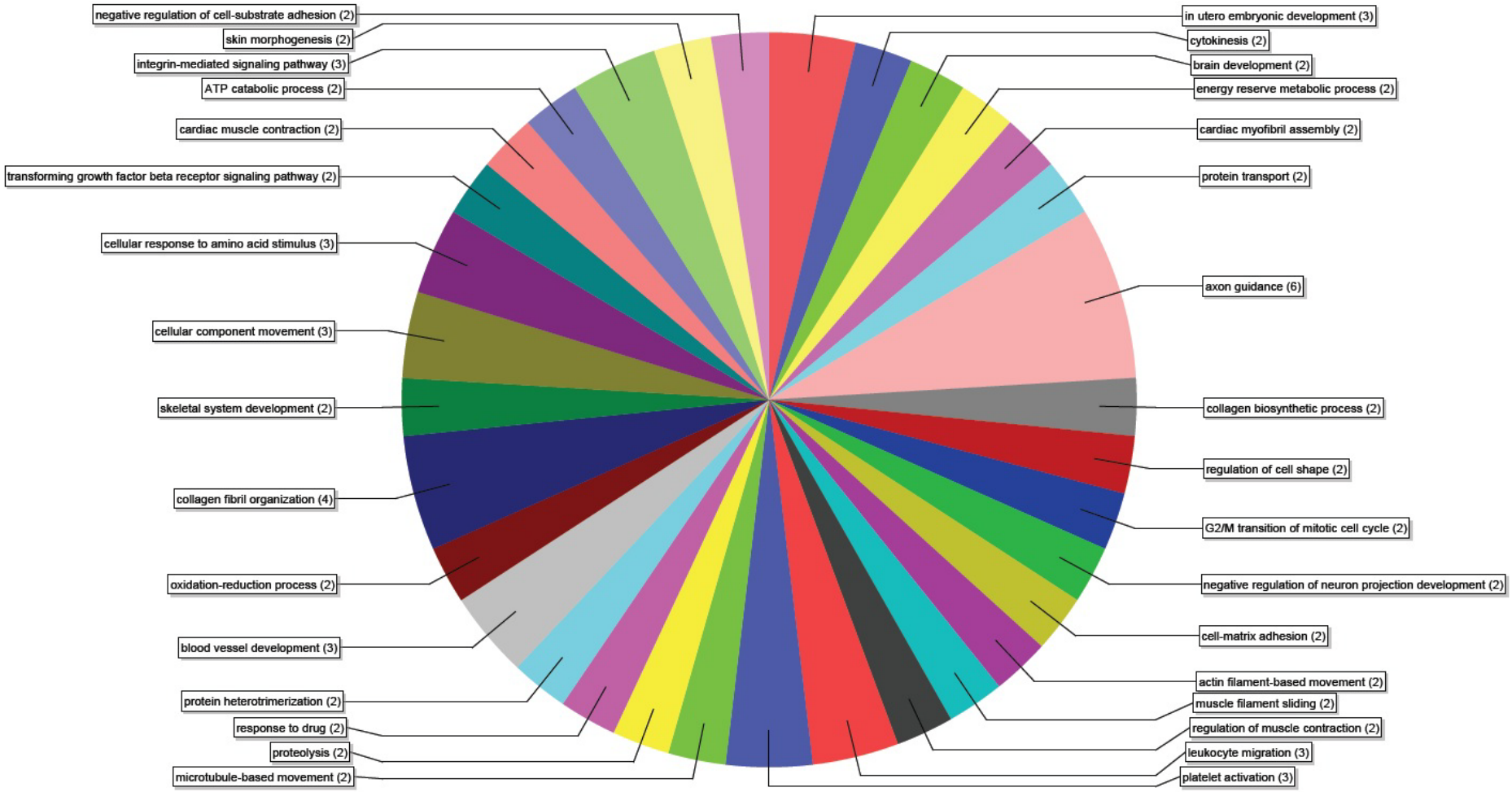

Table 3.7 details the breakdown of selected GO biological processes from **Figure 3.8** against the proteins attributed to these processes. Noticeably, the featured biological processes are dominated by collagen and myosin isoforms in many cases. However the presence of other proteins within some functional category may validate the significance of some of the selected biological functions as a true response of the primary renal cells to treatment with human adipose tissue secretions. These results indicate changes to the utilisation and production of collagen fibres, changes to cell shape and the distribution of cells and cellular contents on the cytoskeleton as a result of treatment.

Table 3.7: Biological processes of proteins shown to be present at decreased abundances from **Figure 3.8** and the individual proteins attributed to each process.

GO annotated biological process:	Proteins attributed to process from dataset
Transforming growth factor beta receptor signalling pathway	Collagen alpha-1(III) chain
	Collagen alpha-2(I) chain
Collagen fibril organisation	Collagen alpha-1(I) chain
	Collagen alpha-2(I) chain
	Collagen alpha-1(III) chain
	Prolyl 4-hydroxylase subunit alpha-1
Collagen biosynthetic process	Collagen alpha-1(I) chain
	Collagen alpha-1(III) chain
Blood vessel development	Collagen alpha-1(III) chain
	Collagen alpha-1(I) chain
	Collagen alpha-2(I) chain
In utero embryonic development	Tropomyosin alpha-1 chain
	Myosin-9
	Myosin-10
Cytokinesis	Myosin-9
	Myosin-10
Brain development	Nestin
	Acetyl-CoA acetyltransferase, cytosolic
Regulation of cell shape	Myosin-9
	Myosin-10
Cell-matrix adhesion	Collagen alpha-1(III) chain
	Integrin alpha-1
Leukocyte migration	Collagen alpha-1(I) chain
	Collagen alpha-2(I) chain
	Myosin-9
Platelet activation	Collagen alpha-1(I) chain
	Collagen alpha-1(III) chain
	Collagen alpha-2(I) chain
Skeletal system development	Collagen alpha-1(III) chain
	Collagen alpha-2(I) chain
Negative regulation of cell-substrate adhesion	Collagen alpha-1(I) chain
	Galectin-1
Integrin-mediated signalling pathway	Collagen alpha-1(III) chain
	Integrin alpha-1
	Myosin-9
Cellular component movement	Destrin
	Non-muscle caldesmon
	Tropomyosin alpha-4 chain
Actin filament-based movement	Myosin-9
	Myosin-10

Figure 3.9: Pie-chart of the protein identifications (featured in **Table 3.6 A**) found to be decreased in abundance in the treated sample group, sorted by gene ontology information based on protein functional annotations. This pie-chart takes into account all the known biological functions for all thirty-three proteins shown in **Table 3.6 A**. Data analysis was conducted using Blast2GO data analysis software tool, available free online at: http://www.blast2go.com/b2glaunch.

Figure 3.9: Pie-chart of the protein identifications found to be decreased in abundance in the treated sample group, sorted by GO functional annotations.

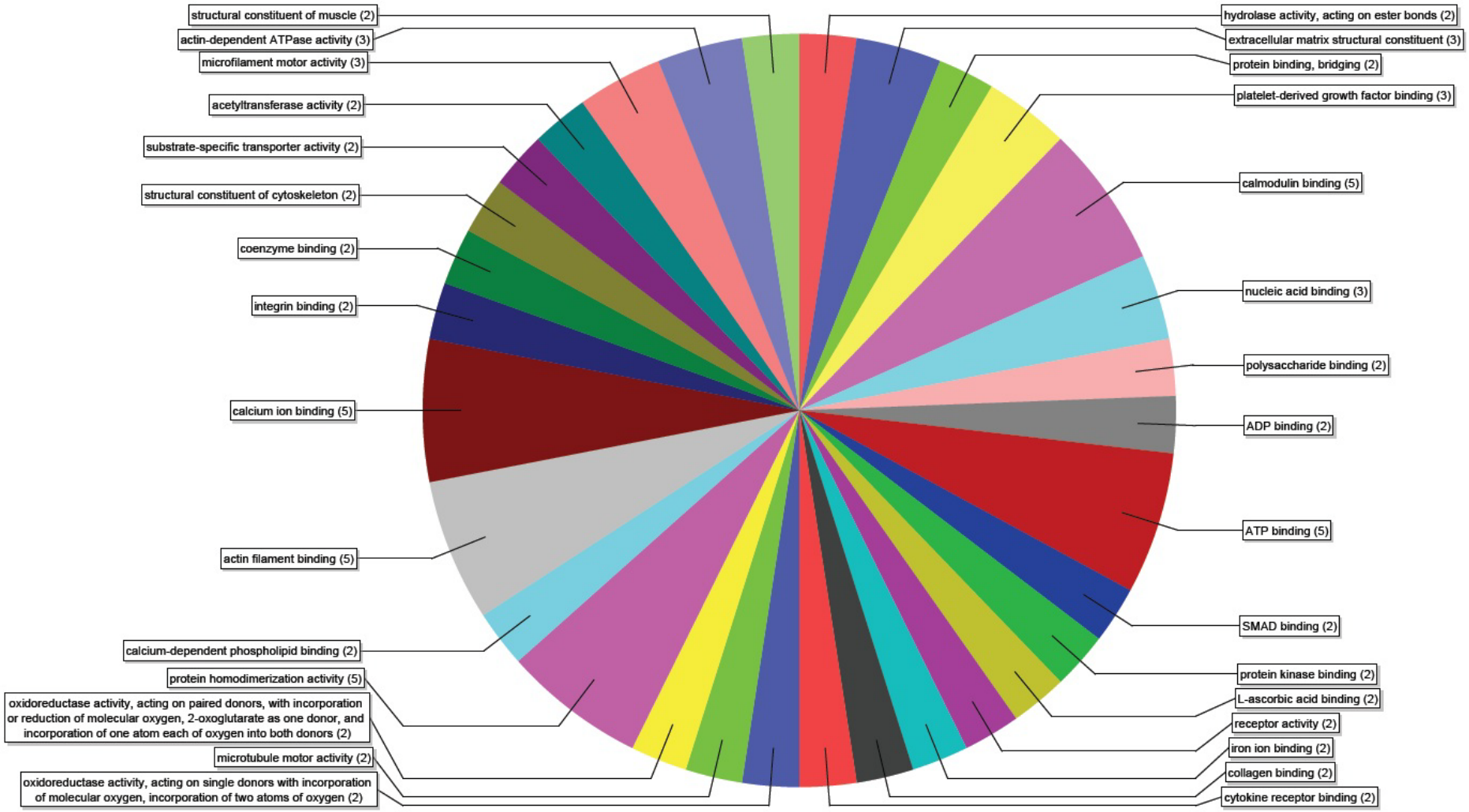

Table 3.8: Decreased abundance protein functions selected from **Figure 3.9** and the proteins that constitute these functions that may be relevant in the context of renal failure.

Protein function:	**Protein name:**
Actin dependant ATPase activity	Myosin-Id
	Myosin-10
	Myosin-9
Actin filament binding	Myosin-9
	Myosin-Id
	Myosin-10
	Transgelin
	Tropomyosin alpha-1 chain
Structural constituent of cytoskeleton	Vimentin
	Tropomyosin alpha-1 chain
Calcium ion binding	Nucleobindin-2
	Tropomyosin alpha-4 chain
	Plastin-3
	Annexin A5
	Annexin A6
Calmodulin binding	Myosin-9
	Myosin-Id
	Myosin-10
	Non-muscle caldesmon
	Myristoylated alanine-rich C-kinase substrate
Collagen binding	Procollagen C-endopeptidase enhancer 1
	Integrin alpha-1
Extracellular matrix structural constituent	Collagen alpha-1(I) chain
	Collagen alpha-1(III) chain
	Collagen alpha-2(I) chain
ATP binding	Ectonucleotide pyrophosphatase/phosphodiesterase family member 1
	Cytoplasmic dynein 1 heavy chain 1
	Myosin-9
	Myosin-Id
	Myosin-10
Platelet-derived growth factor binding	Collagen alpha-1(I) chain
	Collagen alpha-1(III) chain
	Collagen alpha-2(I) chain

Table 3.8 Decreased abundance protein functions selected from **Figure 3.9** and the proteins that constitute these functions from the dataset in **Table 3.6 A** that may be relevant in the context of renal failure. As in **Table 3.7**, collagen and myosin isoforms are the predominant proteins. Green cells indicate protein functions that may be important in a renal disease setting. These results indicate broad changes to the actin cytoskeleton, calcium binding and utilisation capacity, extracellular matrix deposition and anchoring of the cells to the extracellular matrix as a result of treatment.

Figure 3.10: Pie-chart of the protein identifications (featured in **Table 3.6 B**) found to be increased in abundance in the treated sample group, sorted by gene ontology information based on biological process annotations. This graph takes into account all the known biological involvements for all proteins shown in **Table 3.6 B** numbers next to each biological process name indicate the number of proteins assigned to this process. Data analysis was conducted using Blast2GO data analysis software tool, available free online at: http://www.blast2go.com/b2glaunch.

Figure 3.10: Pie-chart of the protein identifications found to be increased in abundance d in the treated sample group, sorted by GO information biological process annotations.

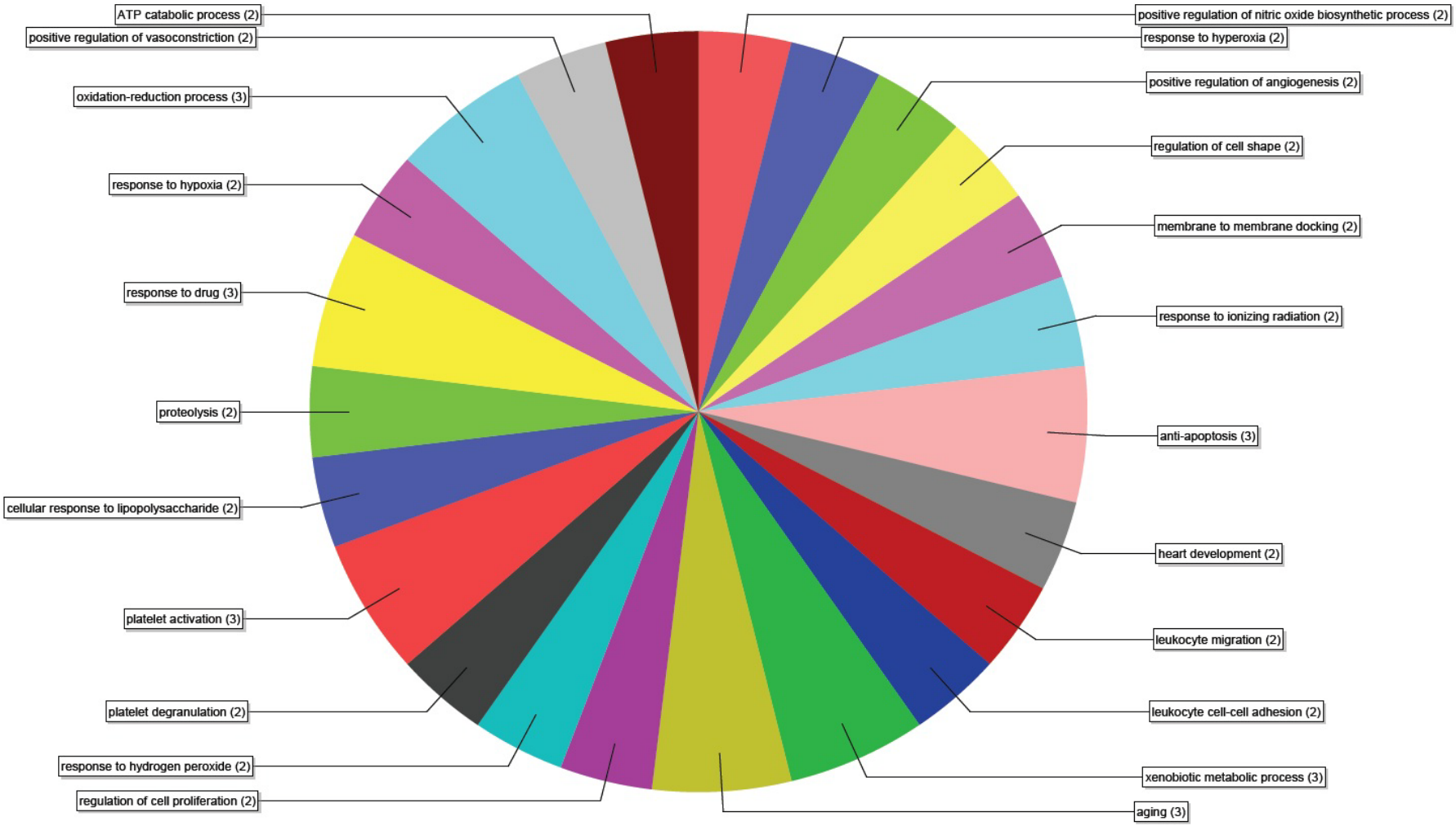

Table 3.9 details the biological processes of interest from **Figure 3.10**. Items in italics are proteins that were given slightly different GO annotation names. They were not included in the pie-slices for each function in **Figure 3.10**. It can be seen that a the treated cells appear to induce a range of proteins involved in broad biological processes, including suppression of apoptosis, inflammatory cell adhesion, promotion of angiogenesis, and protection from free radicals. The italicised proteins highlight the need for manual revision of any data that has been batch processed using GO annotation software.

Table 3.9: Up regulated biological processes of interest from **Figure 3.10** and the proteins that constitute these processes.

Oxidation-reduction process	Cytochrome P450 1B1
	Prostaglandin G/H synthase 1
	UDP-glucose 6-dehydrogenase
Response to hypoxia	Vascular cell adhesion protein 1
	Superoxide dismutase [Mn], mitochondrial
	Intercellular adhesion molecule 1 (cellular response to hypoxia)
Platelet activation	Plasminogen activator inhibitor 1
	Sarcoplasmic/endoplasmic reticulum calcium ATPase 2
	Fibronectin
Platelet degranulation	Fibronectin
	Plasminogen activator inhibitor 1
Response to hydrogen peroxide	Tissue factor
	Oxidized low-density lipoprotein receptor 1
Regulation of cell proliferation	Prostaglandin G/H synthase 1
	Plasminogen activator inhibitor 1
Positive regulation of nitric oxide biosynthetic process	Intercellular adhesion molecule 1
	Superoxide dismutase [Mn], mitochondrial
Response to hyperoxia	Superoxide dismutase [Mn], mitochondrial
	Plasminogen activator inhibitor 1
Positive regulation of angiogenesis	Tissue factor
	Plasminogen activator inhibitor 1
	Fibronectin (angiogenesis)
Regulation of cell shape	Fibronectin
	Intercellular adhesion molecule 1
Anti-apoptosis	Fibronectin
	Superoxide dismutase [Mn], mitochondrial
	Tissue factor
	Hexokinase-1 (negative regulation of apoptosis)
	Plasminogen activator inhibitor 1 (negative regulation of apoptosis)
Heart development	Superoxide dismutase [Mn], mitochondrial
	Vascular cell adhesion protein 1
Leukocyte migration	Fibronectin
	Oxidized low-density lipoprotein receptor 1
Leukocyte cell-cell adhesion	Intercellular adhesion molecule 1
	Oxidized low-density lipoprotein receptor 1
Aging	Prostaglandin G/H synthase 1
	Vascular cell adhesion protein 1
	Tissue factor
Positive regulation of vasocontriction	Prostaglandin G/H synthase 1
	Intercellular adhesion molecule 1

3.5 Discussion:

The work completed here in Chapter 3 utilised adapted and evolved forms of some of the techniques used in the previous chapter, mainly in relation to primary renal cell (PRC) culture and the production of the adipose tissue secretion preparation batch. Previous attempts at PRC culture in Chapter 2 were completed on a small-scale with little technical experience and guidance in modern cell culture techniques. After learning more about cell senescence, culture confluency and culture expansion, my increased competency in these techniques allowed for the more successful generation of PRCs from donor rat kidneys, a greater number of cells in culture to begin with and a greater ability to expand the cells once obtained. With the new-found ability to obtain and expand cultures and previous experiences with 2-DE techniques; the initial aims were to treat the PRCs with adipose secretions and compare treated and non-treated cultures using 2-DE differential display. As indicated however, sample sizes were still too small for adequate technical replicates for 2-DE analysis and iTRAQ was then selected as the replacement method. The protein identification data obtained from the treated Vs control PRC iTRAQ analysis was of a large size and allowed for a thorough comparison of the treated PRC and control PRC proteomes; thus providing a solid basis for the discovery of the effects of the adipose secretions on primary cells of the kidney *in vitro*.

Previous techniques for adipose tissue secretion preparation were crude and did not allow adequate time or environmental conditions for enrichment and expansion of the plastic adherent stromal vascular fraction cells from within the adipose tissue. The introduction to a partial digestion method allowed for the partial break-down of the tissue thereby releasing stromal vascular fraction cells from the tissue matrix and allowing them to adhere to the plastic flask surface during a longer incubation period. The tissue digestion also inevitably resulted in the loss of some adipocytes, observed through the release of free lipid into the digestion milieu, which further served to enrich the SVF cell proportions *in vitro*. Choice of donor adipose tissue was crucial in this experiment in particular and the change from the use of rat fat derived from the same donor animals as were used to obtain the PRCs to human adipose tissue provided the basis for the xenogeneic cytokine/growth factor analysis used successfully in this chapter. Xenogeneic transplants and use of xenogeneic secretions for successful treatment of some diseases is well documented and

provided the inspiration behind the experiments completed here. The xenogeneic nature of this experiment allowed for the examination of 'both sides of the coin' in terms of the secretory response of the PRCs to the treatment media and changes to the treatment media in the presence of the PRCs; not to mention the changes in the PRC intracellular proteome after treatment through the iTRAQ analysis. The use of species-specific cytokine/growth factor assays enabled the differentiation between the rat-derived PRC secretions *into* the media and the decline in human-derived adipose secretions *out* of the media over time; an observation technique and experimental design that is to my knowledge, novel.

The cells utilised in the experiments described in this chapter are uncharacterised primary cultures of rat kidney cells that are likely kidney mesangial cells based on *in vitro* growth characteristics, morphology and similarity in isolation technique as previously described in the literature [216,217]. Furthermore, the results obtained in this chapter in relation to increased and decreased iTRAQ protein identifications and the cytokines/growth factors found to bind to and be secreted by the PRCs are all consistent with key proteins in mesangial cell function, pathogenesis and disease resolution.

3.5.1 Intracellular PRC protein changes due to adipose secretion treatment measured using iTRAQ analysis:

The iTRAQ analysis revealed a large number of proteins for the treated and control PRC intracellular proteomes, allowing for a solid comparison of the treated and control cells. Those proteins that were found to be significantly decreased in abundance in the treated PRC population depict a cell population with a kind of decreased differentiation state demonstrated by deregulation of the cytoskeletal structure and sub-cellular localisation, decreased capacity for pro-fibrotic actions and some suppression of apoptosis. Up regulated proteins in the treated PRC population indicate anti-apoptotic effects, increased nitric oxide (NO) synthesis capability and proteins associated with the repair of renal tissues after injury. Aspects of both the decreased and increased abundance protein datasets infer a positive effect on the PRCs and are explored in greater detail in the following sections.

iTRAQ proteins of interest showing decreased abundance:

The importance of Transforming Growth Factor-beta (TGF-β) and relevance to this dataset:

Many proteins that have been decreased in abundance in the iTRAQ dataset (**Table 3.8**) have been shown to be regulated by of involved in TGF-β signalling pathways. TGF-β signalling controls a range of cellular responses to stimuli relating to apoptosis, proliferation and differentiation [218]. TGF-β signalling is also responsible for much of the errant extracellular matrix deposition that results in tissue fibrosis in some diseases [219]. Over-expression of TGF-β in transgenic mice was shown to result in fibrosis of the liver, kidney and adipose tissue [220]. Cellular responses to TGF-β are many and varied, include changes to cytoskeletal structure/proteins, apoptosis, anti-apoptosis (depending on co-signalling protein presence), cell proliferation and extracellular matrix deposition. For a broad review of the context dependant actions of TGF-β, see Bottinger and Bitzer, 2002 [221].

TGF-β signalling is mediated by intracellular SMAD proteins that convert TGF-β receptor binding into a directed cellular response [222]. TGF-β is known to cause large-scale changes in the cytoskeletal structures of epithelial cells, commonly characterised by the re-arrangements of actin microfilaments into stress fibres [223,224]. In this experiment, the observed decrease in the abundance of actin filament binding proteins, structural components of the cytoskeleton, calcium ion binding and calmodulin binding proteins are all related due to their common interactions with the cytoskeleton; and in many cases, the TGF-β signalling pathway. This indicates a large-scale down-regulation of proteins involved in regulation of cell shape, sub-cellular localisation and movement of intracellular components, has taken place in the treated PRCs. These cytoskeletal interactions are commonly mediated by calmodulin complexed to Ca^{2+}, known as Ca^{2+}/calmodulin. Changes to the actin cytoskeleton of renal epithelial tubular cells have been found to occur in response to renal ischemia [225], resulting in severe changes to epithelial cellular morphology [226]. The proteins identified to have changed in the treated PRCs that are associated with the actin cytoskeleton are not actins themselves (**Table 3.6 A**). These proteins are actin-binding proteins responsible for either motility of cellular components or are implicated in changes to the actin cytoskeletal composition/structure, commonly resulting in phenotypic changes to the cell [226]. The primary renal cells used in these experiments did not display an epithelial cell phenotype when expanded *in vitro* and are likely to be mesangial cells due to their

growth characteristics and cellular morphology. Therefore, changes to the proteins interacting with the actin cytoskeleton are likely to have different effects than those observed in tubular epithelial cells where cell polarity is integral to the maintenance of proper renal function.

Transgelin, also called SM22α, is a highly conserved actin binding protein and proposed tumour suppressor used as a marker of cell differentiation and transformation. Transgelin expression has been identified in vascular smooth muscle cells, fibroblasts and some epithelial cells [227]. This protein has been shown to be up-regulated during early and late stages of an anti-glomerular basement membrane nephritis model in rat kidney podocytes, crescentic cells and podocytes of the Bowman's capsule [228]. A further study by Inomata *et al* [229] also revealed differential transgelin expression between different models of renal failure. The functional significance of changes to transgelin expression in the pathogenesis of renal disease is currently unknown. Decreases in renal cellular transgelin level may be indicative of a decreased stress or inflammatory response in the treated primary renal cells.

Vimentin levels are maintained at relatively constant levels in mesangial and epithelial cells of the glomeruli of both healthy and diseased kidneys, however levels have been found to increase in the renal interstitium of kidneys with glomerulonephritis, associated with increased levels of renal fibrosis [230]. Bravo *et al* [231] showed that vimentin levels are increased in kidneys experiencing renal inflammation and oxidative stress when induced using angiotensin II infusion and inhibition of nitric oxide (NO) production with N^{ω}–nitro-L-arginine-methylester . This may be significant as the iTRAQ analysis presented in this chapter shows the levels of vimentin expression in the treated PRCs to be decreased, along with an increase in proteins known to promote NO production (**Table 3.8**). The effects of NO production on cells of the kidney are discussed in a later section of this discussion.

Calcium (Ca^{2+}) has many broad ranging effects on the functions of a cell and on protein interactions as a cofactor to many enzymatic processes. Disruption to homeostasis of intracellular Ca^{2+} is seen as a key up-stream promoter of apoptosis in mammalian cells [232]. Calcium is also a well-known important cofactor in the function of contractile motor proteins like myosins [233] that aid in movement of whole cells (cytokinesis), intracellular structures and

in cellular contractions. Calcium is also integral to the progression of the coagulation cascade, mediating cellular responses to hormones, neurotransmitters and growth hormones like TGF-β [234].

Annexins are a group of proteins named because of their ability to bind negatively charged phospholipids in a Ca^{2+}-dependant manner and the possession of an 'annexin repeat' domain which is approximately 70 amino acids in length [235]. Annexins are thought to have functions linked to cytoskeletal binding to the plasma membrane, cell differentiation and apoptosis through phospholipid binding and Ca^{2+} signalling mechanisms [236]. The protein annexin A5 was found to be decreased in abundance in the treated PRCs (**Table 3.8**). Current knowledge of the functions of annexin A5 is still being expanded, studies show that it may be important in repair of plasma membrane disruptions and regulation/formation of a Ca^{2+} ion channels [235,237]. Down regulation of this protein may indicate a decreased requirement for membrane repair due to the treatment with adipose secretions; or conversely a decreased capacity to perform membrane repair due to the adipose secretion treatment. Down regulation of annexin A5 may also infer a decreased intracellular Ca^{2+} availability which could lead to down-stream effects on the abundance of other a Ca^{2+} utilising proteins; potentially explaining the decrease in other a Ca^{2+} binding proteins and calmodulin binding proteins observed in the treated PRCs. The annexin A5 apoptosis assay (or annexin V assay) is a well-established method for measuring annexin A5 binding on the surface of apoptotic cells and can be used to quantify the level of apoptotic cells within a sample [238]. The down-regulation of annexin A5 infers an anti-apoptotic phenotype the treated cells, reducing local cell-loss in a renal failure scenario. Little information is currently available for the effects of annexin A5 on intracellular myosin levels. Annexin A6, another member of the annexin family, was also found to be decreased in abundance in the treated PRCs. Annexin A6 has been shown to inhibit Ras signalling pathways through its interactions with membrane-bound signal modulator p120GAP [236]. Ras signalling is linked to increased cell proliferation, survival and differentiation, but also has an ability to promote apoptosis in some circumstances [239]. Down-regulation of annexin A6 is linked to increased cell proliferation and has been observed in many cancers. However, annexin A6 knockout mice appear normal and do not develop tumours [236].

Myristoylated alanine-rich C-kinase substrate (MARCKS) has functions that may implicate it in the stabilisation of cytoskeletal elements during differentiation [240]. Non-muscle caldesmon is involved in the regulation of actin-myosin interactions through a Ca^{2+}/calmodulin system [241]. The decrease in abundance of this protein mirrors the concomitant decrease in other actin binding proteins like myosin 9, 10 and Id; and is likely a further sign of the cytoskeletal deregulation that appears to have occurred in the treated PRCs. There are known to be up to eighteen classes of myosin protein types, each having different patterns of expression, many of which are known to interact with Ca^{2+}/calmodulin. The decrease in abundance of the myosin types that were identified in this study are all classed as 'unconventional myosins', a term given to myosin types that function as monomers rather than many of the skeletal muscle myosins that form complex fibres to perform contractile functions. Unconventional myosins have differing tail sequences, suggesting unique functions for each type; however relatively little is known about the specific functions of each type at this stage.

The treated PRCs exhibited decreased levels of proteins that function as part of the extracellular matrix during fibrosis or as proteins that bind these components of the extracellular matrix in some way. The decreased abundance of type 1 and type 3 collagens indicate a decreased deposition of two major structural pro-fibrotic proteins, indicating a potential anti-fibrotic effect induced by treatment with the adipose secretions. The decreased abundance of collagen binding proteins integrin alpha-1 and procollagen C-endopeptidase enhancer-1 indicate changes to the ability of the treated cells to modify and stabilise extracellular matrix proteins, further decreasing the ability of these cells to contribute to fibrosis [242]. Collagen α-1 (chain 1) (also called type I collagen), is a major constituent of the extracellular matrix in mammalian tissue; it is also the major collagen component in fibrotic tissue [242]. Increased expression of type I collagen in diseased tissues has been associated with fibrosis and scar tissue development, processes which are permanent and detrimental to the regaining of function in resolution of myocardial infarction [243] and glomerulosclerosis [244] among many other diseases. Collagen α-1 (chain 3) (also called type 3 collagen) is also present in the extracellular matrix of most mammalian internal organs and skin, commonly associated with type 1 collagen within mature collagen fibrils [245]. A major inducer of both type 1 and type 3 collagen synthesis has been shown to be

transforming growth factor-beta (TGF-β) [246]. The TGF-β signalling pathway is a well-known protagonist of tissue fibrosis in many diseases including renal failure [220,247,248]. This is explained diagrammatically in **Figure 3.11** where when the fine balance of TGF-β expression is maintained within a damaged glomerulus, full repair is an achievable outcome. However when the TGF-β signal becomes stronger, the glomerular cellular responses can shift towards an aberrant pro-fibrotic phenotype resulting in scar tissue formation and loss of glomerular function.

Figure 3.11: TGF-β signalling outcomes during glomerulus injury

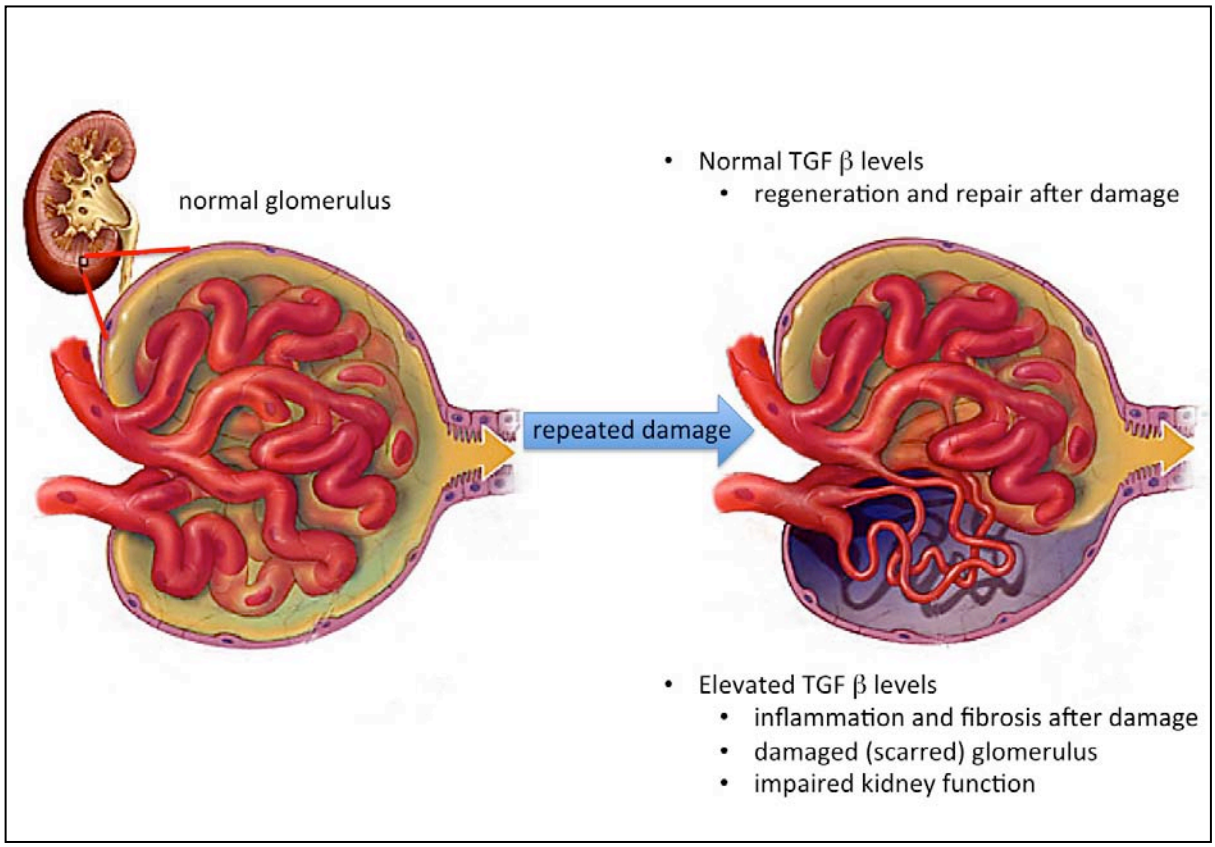

Figure 3.11: TGF-β signalling outcomes during glomerulus injury. TGF- β is constitutively expressed in some cells of the mammalian kidney, maintenance of normal TGF- β levels after insult commonly results in the glomerulus being able to regenerate and return to normal functional levels. Elevated TGF- β levels promote extracellular matrix deposition (fibronectin, type I- and type III- collagens) ending in scar formation and loss of glomerular function.

iTRAQ proteins of interest found to have increased abundance:

The proteins detected in the iTRAQ experiment showing increased abundance (**Table 3.9**) show that the cells may display an increased ability to survive the pro-apoptotic stimuli that may be encountered in a renal disease scenario. The observed increase in abundance of anti-apoptotic proteins, immune cell adhesion molecules, nitric oxide synthetic processes and haemoregulation proteins can all infer a positive effect on cells of the kidney, particularly in the glomerulus during renal disease. In many cases of glomerular injury, deposition of extracellular proteins such as type I and III collagens and fibronectin are closely tied to increased mesangial cell proliferation [249]. The increased abundance of fibronectin, but not other interstitial extracellular matrix proteins (collagen I and III) and the lack of identification of signs of increased cell proliferation, may indicate the activation of a specific anti-apoptotic pathway within the cells during treatment that is separate from the pathway responsible for tissue fibrosis and increased cell proliferation.

Superoxide dismutase is an anti-oxidant enzyme found to be important in the protection of cells from pro-apoptotic processes. Superoxide molecules have been shown to be toxic to cells and production of superoxides is elevated during diabetic nephropathy pathogenesis due to a down-regulation of superoxide dismutase [250]. Superoxide dismutase can also enhance or restore the vasodilatory actions of nitric oxide (NO) on renal arterioles, providing better renal blood flow during type II diabetes on-set [251]. Manganese superoxide dismutase (MnSOD) has been shown to be reno-protective in an experimental model of cisplatin induced renal injury [238]. In a study by Davis, Nick and Agarwal (2001) [238], it was found that cells over-expressing MnSOD had lower apoptotic indices and significantly less cell detachment than controls. Interestingly, the up regulati of MnSOD did not result in an increase in annexin A5 binding in these cells [238]; a result similar to those obtained in this chapter where annexin A5 was shown to be decreased in abundance. The increased abundance of cell-cell and cell-matrix adhesion molecules in the PRCs after treatment may also be explained by the presence of increased MnSOD, as MnSOD over-expression also resulted in increased cell attachment [238], however this remains speculative.

Investigations regarding the inflammatory response associated with forms of renal failure predominantly centre on the development of an excessive inflammatory response associated with loss of organ function and fibrogenesis. However, the inflammatory

response is essential for the removal of excess, damaged or apoptotic cells throughout the body under normal and disease states. Fibronectin is a well documented component of the extracellular matrix with roles in cell-cell and cell-matrix adhesions and implications in the structural composition of fibrosed tissue [252]. The expression of fibronectin has been positively tied to cellular responses to TGF-β, which is the most well known inducer of fibronectin and collagen expression; and has an important role in the incorporation of fibronectin and collagen into the extracellular matrix [253]. The increased abundance of fibronectin in the treated PRCs in this case conflicts with the large-scale decrease in abundance of many other TGF-β induced proteins like Collagen type I and III and proteins involved in TGF-β signal transduction pathways. This may be explained by the possibility that fibronectin expression could be induced by other unknown cytokines/growth factors within the adipose tissue secretion treatment. Fibronectin has also been shown to hold anti-apoptotic effects in some cell-types [254], which may confer additional beneficial effects to the PRCs and potentially to other cells of the kidney in a renal disease scenario. The increased expression of proteins involved in the promotion of the synthesis of nitric oxide (NO) has also been observed (**Table 3.9**).

The cytotoxic and cytoprotective effects of NO on various cell and tissue types are extensively documented and very complex [255]. The increased abundance of proteins that promote NO production could be a result of the presence of oxidised low-density lipoprotein (OxLDL) within the treatment media, because the treatment media is derived from processed adipose tissue. NO has been shown to protect endothelial cells from the cytotoxic effects of OxLDL [256]. In the kidney, NO is intrinsically expressed as part of the mechanism of homeostasis, regulating glomerular and renal arteriolar blood pressure and blood flow and suppression of NO commonly occurs in chronic renal disease, further decreasing glomerular filtration rates by decreasing renal vasodilatation [257,258].

Renal homeostasis is an important aspect of the regulation of renal function, dictating the level of vasoconstriction and thus blood flow, oxygen availability and glomerular filtration rate. The protein prostaglandin G/H synthase 1, also called cyclooxygenase-1 (Cox-1) or prostaglandin H2 synthase 1, has a role in the normal functioning of the mammalian kidney and cells of other organs in the body as a house-keeping protein [259]. Prostaglandins, the products of the Cox-1 and Cox-2 enzymes, have been

shown to increase renal blood flow and glomerular filtration rate in a dose-dependent manner [260]. Data suggests that Cox-1 may be important in the maintenance of renal haemodynamics and water/salt balance in the kidney and that increased expression of Cox-1; and not Cox-2, is associated with the repair phase of glomerulonephritis [261]. This indicates a positive effect on the PRCs after treatment with the adipose tissue secretions compared to control cells.

3.5.2 Preliminary temporal analysis of changes to the PRC secretome and human adipose secretions during adipose tissue secretion treatment using the Bio-Plex™ bead-based assay platform:

The results shown in **Figure 3.2 (A to E)** were derived from samples taken from a single biological replicate, known as 'Rat 1'. This rat cytokine/growth factor Bio-Plex™ experiment was conducted on a smaller scale for cost purposes. The experiment was completed in order to assess the ability of the rat Bio-Plex™ assay to distinguish between human and rat cytokines and also to assess whether our idea of using a xenogeneic treatment regimen combined with a xenogeneic assay system would even work, before wasting an entire assay kit. Of the twenty-three analytes assayed, only one displayed any significant cross reactivity with the human cytokine/growth factors present within the samples as seen in **Table 3.2** in the Macrophage inflammatory protein-1a (MIP-1a) concentration data where the treatment media blank samples (Blank T) show a similar MIP-1a level to the treated cells (T1 samples). This indicated that the Bio-Plex™ assay system could be used effectively to test for rat cytokines/growth factors in the presence of a large mix of human cytokines with minimal cross-reactivity. It also indicated that the secretion media appeared to stimulate the PRCs to secrete more IL-6, GRO/KC-like protein, MIP-3a and VEGF than controls PRCs, whilst appearing to decrease secretion of IL-10.

Accurate inferences from the preliminary data about the reasons and mechanisms behind the changed secretion patterns of the treated PRCs were difficult to make because a more comprehensive examination of the secretomes of the other three biological replicates (Rats 2, 3 and 4) were not able to be completed due to time and budget constraints. This type of analysis will be completed in the future as funding and time becomes available for future statistical analysis and peer-reviewed publishing of the results. A more comprehensive analysis, using the other biological replicate samples, may reveal a different

set of results due to a combination of technical and biological variation. This can be seen clearly in the human cytokine analysis experiment data (**Figure 3.3** and **Figure 3.4**), where two human cytokines were observed to have changed in the preliminary data from the 'rat 1' samples, but upon the more comprehensive analysis, a total of nine cytokines were shown to be present at significantly lower levels in the PRC forty-eight hour samples than the blank treatment samples. More specifically, in the case of PDGF-bb, preliminary results indicated a sharp decrease in concentration over time in the presence of the PRCs. However, when PDGF-bb levels across the other three biological replicates were examined, with duplicates and more thorough statistical assessment; no significant decrease was identified (**Figure 3.4**). This change in findings in this case is likely due to a combination of technical variation, biological variation and the fact that the concentrations being measured in both sets of analyses for PDGF-bb were effectively at the lower limit of detection for the assay. To draw any solid conclusions about the actions of the adipose secretions on the PRC secretome at this stage would be premature based on the level of change possible once all three biological replicates have been assayed. However, the premise of the experiment has been shown to be plausible; that the monitoring of two different species analytes can occur simultaneously within the one culture with little cross-reactivity between the two species analytes. This is a novel application of the Bio-Plex™ assay technology when combined with the human cytokine data from the same samples.

3.5.3 Temporal analysis of changes to the concentration of human cytokines/growth factors in the presence of PRCs:

This subset of experiments represents the other side of the coin in this xenogeneic treatment between rat cells and human cytokines. The rationale applied here was aimed at identifying some of the cytokines that may be responsible for any changes observed in the proteome of the treated PRCs as detected by the iTRAQ analysis (discussed earlier in section 3.5.1) and changes to the PRC secretome (discussed in section 3.5.2). However, once the preliminary human Bio-Plex™ results were analysed, they took precedence over the rat Bio-Plex™ results and it was decided to devote the remaining resources into investigation of the human analyte 'consumption' by the PRCs as it was a more novel observation. Figure 3.4 displays the levels of each of the twenty-seven human analytes within the Bio-Plex™ assay used including standard deviation (+/-). The potential for finding a mechanistic cause to the

changes in the PRC proteome post-treatment; and the fact that this type of xenogeneic iTRAQ and Bio-Plex™ combination is completely novel (to our knowledge). This was the motivation behind choosing the human Bio-Plex™ assay as the one for a more comprehensive assay and statistical analysis. A decline in concentration over time greater than that of the treatment media blanks indicated that the presence of the PRCs was the determining factor that decided which cytokines would be more closely investigated. Degradation over time in the blank treatment media samples across all cytokines on average was shown to be negligible (Figure 3.5), but nine of the human cytokines assayed for were found to decline over time when in the presence of the PRCs, implicating the PRCs in the selective uptake of these cytokines from the media. Table 3.4 details the nine human analytes that significantly declined in concentration over time in the presence of PRCs. This data indicates the potential involvement of nine cytokines/growth factors from the twenty seven in the assay in binding to the PRCs. This data does not necessarily mean that these analytes are causative of the changes in the treated PRCs that were observed by the iTRAQ analysis. However, some parallels between the known effects of the nine analytes identified in the Bio-Plex™ assay can be drawn and are important factors to consider when choosing specific targets for future investigation.

Interleukin 12 (IL-12):

Interleukin 12 receptors have been identified on renal mesangial cells and IL-12 has been shown to regulate some functions associated with mesangial cell contraction [262]. This provides some rationale behind the apparent up-take of IL-12 from the treatment media by the PRCs, given that they are likely mesangial cells and therefore are likely to have the ability to bind free IL-12 from the media. Documented effects of IL-12 include changes to the cytoskeleton of mesangial cells, causing a change in filamentous actin distribution toward the cell periphery indicating greater propensity to cell contraction [262]. The binding of IL-12 by the PRCs may be linked to the changes to the PRC cytoskeletal proteins observed in the iTRAQ analysis previously discussed; with the observed decrease in abundance of myosin 9, 10 and Id, transgelin, tropomyosin alpha-1 chain and vimentin. However, it is unclear how the observed down-regulation of the different myosin chains in the PRCs would have affected the cells ability to contract in this experiment. The lack of the identification of myosin II chains in the iTRAQ experiment however, indicates that perhaps the contractile

ability of the PRCs has remained unchanged after treatment. Myosin II chains are the predominant myosin chain type in smooth muscle and mesangial cells [263]. It is unclear at this stage whether the changes in the PRC myosin levels are linked to an IL-12 response, or whether this represents a novel finding on the interaction between IL-12 and other myosin chain types.

Interferon-gamma (IFN-g):

Interferon gamma (IFN-g) plays multiple roles in cell-mediated immunity including monocyte recruitment, monocyte activation, antiviral activity, intracellular parasitic infection, T-helper 1 lymphocyte responses, immune regulation for disease resolution and modulation of T-helper and T-regulatory lymphocyte differentiation [264-267]. Cultured human mesangial cells have been shown to respond to IFN-g presence with the secretion of the macrophage chemoattractant MCP-1 and complement C4 induction [264,268]. The effects of MCP-1 have been discussed in Chapter 1. Cultured rat mesangial cells have been shown to decrease proliferation rates in the presence of IFN-g and can continue to inhibit mitosis in the presence of PDGF and interleukin 1, but not epidermal growth factor [269]. The documented responsiveness of mesangial cells to IFN-g provides credence to the theory behind this part of the experiment that the treated PRCs actively bound IFN-g from the treatment media, causing a detectable change in concentration over time.

The pro-inflammatory effects of IFN-g on mesangial cells may at least partially explain the apparent increases in the secretion of pro-inflammatory cytokines that was shown in the preliminary assessment of the treated PRC secretions (preliminary rat Bio-Plex™ assay results shown in **Figure 3.2**). The documented anti-mitotic effects of IFN-g on mesangial cells also correlates with the PRC iTRAQ data analysis presented here which indicated no evidence of increased cell division in the treated PRCs. Unlike the results of Chapter 4, where proliferation of treated MDCK cells can be observed through the increased abundances of mitotic and cell-cycle related proteins.

It is currently not clear whether the secretion of pro-inflammatory cytokines and monocyte chemoattractants by the treated PRCs would yield a beneficial or detrimental effect on a regenerating kidney. However, the anti-proliferative effects of IFN-g on cultured mesangial cells and by extension, the PRCs used here; may suggest that the adipose

secretions could improve diseases where proliferation of glomerular mesangial cells is undesirable, like proliferative glomerulonephritis; this is pure speculation however. The apparent up-take of IFN-g by the PRCs and the fact that mesangial cells express the IFN-g receptor also provides extra evidence that the PRCs are likely to be primary rat mesangial cells.

Vascular Endothelial Growth Factor (VEGF):

The pleiotropic effects of VEGF in relation to the kidney have been discussed in detail in Chapter 1. Human and rat mesangial cells have been shown to express VEGF constitutively and in response to a range of stimuli [270-272]. Human and rat mesangial cells also express the VEGF receptors flt-1 and flk [270,271,273]. The preliminary assessment of the treated PRC secretions using the rat Bio-Plex (**Figure 3.2**) indicated an increase in the secretion of VEGF by the treated PRCs by 35%, which correlates to the ability of mesangial cells to secrete VEGF. Furthermore, the apparent up-take of VEGF from the treatment media by the PRCs indicates the presence of a VEGF receptor, which also correlates to reported mesangial cell characteristics. These findings further enhance the view that the PRCs are likely to be mesangial cells.

VEGF has been shown to increase rat mesangial cell collagen synthesis *in vitro* at a concentration of 200 ng/mL [271], a concentration approximately 111-fold greater than that present in the adipose tissue secretions used to treat the PRCs (**Table 3.1**). The apparent up-take of VEGF by the PRCs occurred to a level far above the other cytokines measured using the Bio-plex assay system, with a net change on average of over 1000 pg/mL of media at the forty-eight hour timepoint. The exact cause for this up-take and a hypothesis on its effects is difficult to form at this stage due to the increasingly complex and somewhat unknown effects of VEGF on the mammalian kidney. For a review of this complexity, see Schrijvers, Flyvbjerg and Vriese, 2004 [197].

Interleukin 6 (IL-6):

Interleukin 6 (IL-6) was not featured in **Table 3.4** because it did not exhibit the desired pattern of accelerated decline in abundance in the presence of PRCs. However, this may have been due to the fact that the concentration of IL-6 in the treatment media was so high that it was consistently above the accurate detectable range in every treated PRC and treated media blank well of the human Bio-Plex, >19500 pg/mL (see **Figure 3.4**, IL-6 plot and

Table 3.3, IL-6 column). IL-6 is worth a short exploration because it has known effects on mesangial cells as an autocrine factor which can act to increase cell proliferation and also cause an increase in the secretion of IL-6 by other mesangial cells [274,275]. However as previously discussed in the IFN-g section of this chapter, no changes to cell proliferation related processes were observed in the iTRAQ analysis of the treated PRCs, indicating no net increase or decrease in cell proliferation activity. It may be that the anti-proliferative effects of IFN-g counter-act the proliferative effects of IL-6; however the differences in concentration between the two cytokines are stark (~374 pg/mL for IFN-g compared to >19500 pg/mL for IL-6) so this is not likely to be the case. At this stage it is unclear what effect the large concentration of IL-6 within the treatment media has had on the PRCs due to the complexity of the treatment media. This is one pitfall of a target discovery approach, yielding a complex web of effects and conflicts between the observed results and results obtained by other groups using more defined, simple, 'single cytokine/growth factor' experiments.

Changes in human cytokines not likely to be causative of protein changes in the PRCs:

The remaining five analytes featured in **Table 3.4** but not discussed above, were thought unlikely to be the causative agents behind the changes observed in the treated PRC population. These proteins have been found to be more depleted at forty-eight hours in the treated PRC flasks than the treatment blank media flasks; however the changes in concentration observed were very small, between approximately 0.34 and 11.75 pg/mL (**Table 3.4**). The low abundances and small changes observed in these cytokines raises the question for each analyte: would the uptake of this amount of cytokine be enough to illicit an observable biological response in the treated PRCs? Those cytokines that exhibited observed changes in abundance between 0.34 pg/mL and 11.75 pg/mL in **Table 3.4** were not deemed likely to have changed the PRCs significantly from a biological perspective and so will not be discussed further.

3.6 Conclusions:

The iTRAQ analysis of the treated *vs* control PRC cellular proteomes identified thousands of proteins across all four biological replicates for quantitative protein comparisons between the groups. The portion of proteins shown to be decreased in abundance in the treated PRC group of the iTRAQ analysis contained proteins with functions

involved in TGF-β signalling pathways, apoptotic processes and the production of extracellular matrix, *i.e*, fibrosis. TGF-β signalling is known to be involved in a variety of aspects of renal pathogenesis [221]. Suppression of TGF-β pathways has been shown to be beneficial to the recovery of the glomerulus and the nephron after renal injury, with reduced glomerular fibrosis observed in experimental animals [112,219]. The decreased presence of ECM proteins observed in this iTRAQ dataset corroborates this data. The reduction in apoptosis associated proteins in the treated PRCs show that they are likely more resistant to pro-apoptotic stimuli and may be able to better survive renal insult *in vivo*. Those proteins shown to be increased in abundance in the treated PRCs indicate that the treatment likely increased the PRC resistance to oxidant stress, increased the NO production capacity of the PRCs and potentially increased the glomerular repair capacity due to an increase in COX-1. Taken together, the results indicate a decreased susceptibility to general cellular injury processes and cell death while also increasing the ability of the PRCs to respond and repair to such insults.

The iTRAQ data alone discussed here suggests that the use of adipose tissue derived protein secretions may be useful in aiding the recovery of renal cells after insult. The application of such preparations is worthy of further investigations either through more defined *in vitro* cell-model experiments or in an *in vivo* renal failure animal model. Additionally, further experiments will be required for the development and optimisation of an administration method for the adipose secretions to a damaged kidney *in vivo*. Assays for known TGF-β pathway suppressors such as decorin could be used in future experiments to detect levels in the human adipose secretion preparation pre- and post treatment and to also assess the expression of such TGF-β suppressors by the PRCs in response to treatment *in vitro*. While no quantitative changes to the levels of actin itself were observed between treated and control cells, significant alterations of actin-associated proteins were identified, indicating that investigation of changes to the actin cytoskeletal structure and organisation would be worthwhile. Temporal measurement of cellular morphology during treatment using antibodies for immunocytochemistry to measure changes in the composition of the treated PRC cytoskeletal composition and distribution over time. Possible antigens would include vimentin, tropomyosin alpha-1 chain, fibronectin, intercellular adhesion molecule 1 and myosin -9, -10 and 1D. Monitoring changes to the cytoskeleton in the treated cells over

time would likely visually demonstrate the previously discussed evidence of cytoskeletal reorganisation.

The novel use of the Bio-Plex™ assay systems to simultaneously measure changes to the human treatment media analyte abundance and the effects the treatment had on the rat PRC secretome coupled with the iTRAQ analysis of the global PRC proteome provided a solid basis for the further development of this type of xenogeneic cell-based assay system in the future. In the data presented here, the rat PRC response to treatment was observed by changes to the secretion profile between control and treated cells. The treatment induced changes to five of the twenty-three rat analytes in the samples from biological replicate 'rat 1' indicating an apparently pro-inflammatory secretory profile; however this may change after analysis of the other biological replicates, as was the case in the human analyte analysis. The abundances of the human analytes put onto the rat PRCs were measured from the same biological replicates as the rat analytes, providing directly comparable sets of data. Statistical analysis revealed that nine human cytokines were decreased in abundance in the treatment media in the presence of PRCs compared to non-PRC containing flasks. This indicated that the PRCs were involved in the preferential uptake of these analytes from the treatment media and the decline in the concentration observed was not due to degradation because of incubation at 37°C 5% CO_2 over seventy-two hours. Therefore, the apparent uptake of these proteins from the media by the PRCs implicates these nine analytes in the net proteomic effects of the treatment media on the PRCs as seen in the iTRAQ analysis dataset. One point of note is that the twenty-seven human analytes in the human Bio-Plex™ assay only represent a snapshot of the total profile of secretions present within the human adipose secretions used here. It is possible therefore that other proteins may also be taken up from the treatment media by the PRCs in the same fashion and that other major drivers of the effects observed through changes to the PRC proteome in the iTRAQ analysis could be identified in the future. Work to confirm the exciting observation of the apparent uptake of human growth factors or cytokines from the treatment media would be necessary and would most likely involve immunocytochemistry techniques to detect the binding or internalisation of the human analytes onto or inside of the PRCs. This would demonstrate that the observed decrease in human cytokines found here is, or is not, due to the PRC binding and response to these cytokines *in vitro* over the treatment period.

The novel use of the human and rat Bio-Plex™ platforms in this chapter also have future implications for the further development of other cell-based assay systems. This type of xenogeneic secretion-cell-based assay system could be potentially applied to a wide variety of cell lines used as *in vitro* models for other diseases. One potential example includes asthma, where T-cell activation assays and cultured airway epithelial cells model the inflammatory and mucosal responses to various stimulants [276].

Chapter 4 Prologue:

The work completed in this chapter was driven by a requirement for more kidney-derived cell samples. All previous work in this thesis was performed using primary tissues obtained through our own animal ethics applications or through kind donations from control animals from non-related projects where kidneys were surplus unwanted tissues. These two methods of obtaining sample for my own project were problematic at times, limiting my access to adequate materials and leaving me with some significant down-time. Due to this, it was decided to take a step back from primary kidney tissue and utilise an immortalised cell line of the kidney tubule, the MDCK cells. We had to trade-off moving away from the use of a primary tissue (and the relative closeness to the in vivo kidney) with the advantages of having an almost inexhaustible number of MDCK cells and the relative ease of culturing them for use.

Looking back, the primary motivations for switching to an immortalised line were also driven by a desire to have enough treated/control cell sample within each replicate to compare the treated and control populations using 2-DE techniques. Again, the samples obtained were limited by my cell culture knowledge at the time and I was not aware of, nor did I have the budget for large-scale multilayer flasks in order to achieve the numbers of MDCK cells required for 2-DE and the analysis was changed to iTRAQ. However, it is important to note that the experiments in Chapter 3 and Chapter 4 were not performed one-after the other in an exclusive manner. Both experiments were being performed in various stages at the same time period in the project. I would be a slow learner indeed if this were not the case.

Chapter 4: The effects of adipose tissue secretions on Madin-Darby Canine Kidney (MDCK) cells

4.1 Introduction:

This chapter details the treatment of an immortalised renal cell line with the same preparation of adipose tissue secretions described in Chapter 3. The cell line selected was the Madin-Darby canine kidney (MDCK) cell line, derived from the epithelium of the canine distal tubule [277]. MDCK cells have been commonly used as a model cell system of the mammalian kidney to study the toxic or beneficial effects of a range of drugs, foodstuffs and other reagents. This cell line was selected for use in this study due to this history in renal research, and also because these cells represent a spatially distinct portion of the nephron compared to the primary renal cells of Chapter 3. As discussed previously, the PRCs of Chapter 3 were likely mesangial cells derived from the glomerular end of the nephron, whereas the MDCK cells are distal tubule cells of an epithelial origin. This means the two cell types are not only situated at opposite ends of the nephron, but also have distinct functional and phenotypic characteristics which aid in their respective functions. It was thought that these cell-specific differences may be reflected in the response of the MDCK cells to the adipose tissue secretions. While MDCK cells are an immortalised cell line, they have retained a phenotype which is still very close to that of cells of the normal mammalian renal tubule [278]. MDCK cells are able to form an asymmetrical membrane *in vitro* similar to the functional tubular epithelium of a normal kidney and have many properties required for the functioning of a transporting epithelia [278]. MDCK cells are able to form structural and functional cell polarity [278], meaning that the organisation of intracellular components of the cytoskeleton and associated solute transport components are consistent with that of a normal mammalian tubule epithelial surface. This makes MDCK cells a suitable choice for *in vitro* studies of the effects of adipose tissue secretions on the tubules of the mammalian kidney.

There are many types of renal diseases, which tend to affect distinct portions of the nephron. Therefore, to more completely assess the possibility that adipose tissue secretions may have therapeutic potential for treatment of renal disease, we decided to use a different cell line derived from the opposite end of the kidney to that used in Chapter 3. Another

important advantage in using a cell line very different from the PRCs of Chapter 3 is that the results may have revealed a different set of effects from the same preparation of adipose tissue secretions. Previous reports of the use of MSC and ASC conditioned media on a range of different diseases, cell types and tissues has shown potential applicability for these secretions in conditions ranging from retinopathies and wound repair to heart failure, with very little variation in secretion preparation methods [11,13,30]. Differences in the necessary steps for the repair of different tissues and pathologies exist, however MSC secretions have been shown to promote effective disease resolution in many cases. It is possible that this could occur due to the large number of different cytokines, growth factors and adipokines present within the secretion preparation. The complexity of the adipose tissue secretions used and the possibility that the same preparation of secretions can have different effects on different cell populations is an exciting prospect for the use of adipose tissue secretions in 'complex biological' therapeutic agents in the future.

Cell-based assays, like the ones described in Chapter 3 and here in Chapter 4, are one key to understanding some of the complex interactions that the adipose tissue secretions may have with cells of the kidney. Identifying the potential for different effects on distinct segments of the nephron may be important in our understanding of the applicability of these secretion products to different diseases in general and may also provide key mechanistic information on how these different effects are induced from the same complex set of stimuli.

The initial approach used in the work in this chapter was to take advantage of the proliferative ability of the MDCK cells to expand them to such a number that they could be used in a 2-D PAGE differential display proteomics experiment. This involved the expansion of the cells to a large number within each flask, treatment with the adipose secretions (or control media), purification of the proteins from the treated and control cells and a comparison of these protein expression profiles using a 2-D gel based differential display technique. However, the cell yield obtained from the MDCK cultures was still too low for the rather sample-hungry 2-DE technique initially planned out. Typically, a 2-D gel based comparison of this type would require a minimum of three 2-D gels (four is ideal) from each flask of cells, but this was not possible without using more sensitive methods such as Difference gel electrophoresis (DIGE) which shows the same number of proteins as a typical

2-D gel preparation, but requires much less sample and technical replicates. As a technique, DIGE is also more expensive than a typical 2-D gel differential display. Following on from the previous chapter, iTRAQ was then selected as the method of choice for the comparison of adipose secretion treated MDCK cultures *versus* control media treated MDCKs.

4.2 Aims:

1. To identify the effects of the adipose tissue secretions on MDCK cells using a global proteomic iTRAQ approach.
2. To infer possible therapeutic or toxic effects of the adipose tissue secretion preparation on the mammalian kidney.

4.3 Materials and Methods:

4.3.1 Combined materials list for all experiments performed within this chapter:

Materials required:

- -20° C freezer
- -80° C freezer
- Centrifuge
- Micro Bio-Spin columns with Bio-Gel P-6 in SSC buffer - Bio-Rad Pty. Ltd. Hercules CA USA.
- Criterion™ 1-D SDS PAGE pre-cast gels, 11 cm, 4-12% gradient, bis-tris buffered, 18-well - Bio-Rad Pty. Ltd. Hercules CA USA.
- Criterion™ 1-D SDS PAGE pre-cast gels, 11 cm, 4-12% gradient, bis-tris buffered, 12-well - Bio-Rad Pty. Ltd. Hercules CA USA.
- Criterion™ gel resolving apparatus - Bio-Rad Pty. Ltd. Hercules CA USA.
- Flat-bed scanner
- Typhoon gel scanning apparatus -
- Steriflip filter unit, custom-made filter unit fitted with 400 µm pore size mesh insert - Millipore, Billerica MA USA.
- Collagenase enzyme - Sigma-Aldrich, St Louis MO USA.
- 75 cm^2 cell culture flasks filter cap - Nalge Nunc International. Rochester NY USA.
- 175 cm^2 cell culture flasks filter cap - Nalge Nunc International. Rochester NY USA.
- CO_2 incubator (maintained at 5% CO_2, 37°C).
- Class II biological safety cabinet
- 50 mL syringe, disposable, luer lock
- Syringe filters, 0.2 µm pore size. Millex-GP Filter unit 33 mm – Millipore Corporation. Billerica, MA USA.
- Steripak 0.2 µm filter - Millipore, Billerica MA USA.
- Peristaltic pump and two lengths of sterile silicone tubing
- Orbital shaker.
- MDCK type I cell line – American Type Culture Collection (ATCC). Manassas VA USA

Solutions required:

- DMEM/F12 (1:1 *v/v*) GlutaMAX™ growth medium - Life Technologies Corporation, Wilmington DE USA.
- DMEM- HG (High glucose) media - Life Technologies Corporation, Wilmington DE USA.
- Foetal bovine serum (FBS), heat inactivated, lot/batch # 8122821 - Life Technologies Corporation, Wilmington DE USA.

  NOTE: This is the same lot/batch # present in the preparation of human adipose secretions
- Antibiotic/antimycotic, 100x (ABAM) additive - Life Technologies Corporation, Wilmington DE USA.
- MDCK cell expansion medium: DMEM-HG supplemented with 5 % FBS (*v/v*) and 1 % ABAM solution (*v/v*).
- MDCK cell Control media: DMEM/F12 supplemented with 5% FBS (lot # 8122821) (*v/v*) and 1% ABAM (*v/v*)
- MDCK cell Treatment media: A 1:1 ratio of the human adipose tissue secretion preparation and DMEM/F12 supplemented with 1% ABAM (no FBS added).
- Trypsin / EDTA solution, 0.25% (*w/v*) - Life Technologies Corporation, Wilmington DE USA.
- TrypLE Select 1x solution - Life Technologies Corporation, Wilmington DE USA.
- 1 x Phosphate buffered saline (PBS) solution
- Triethylammonium bicarbonate (TEAB) - Sigma-Aldrich, St Louis MO USA.
- 1% (*w/v*) Sodium dodecyl sulphate (SDS) solution
- 4x Lithium dodecyl sulphate solution resolving buffer (4 x LDS resolving buffer) - Life Technologies Corporation, Wilmington DE USA.
- Precision Plus Protein™ unstained molecular weight markers - Bio-Rad Pty. Ltd. Hercules CA USA.
- MES resolving buffer - Bio-Rad Pty. Ltd. Hercules CA USA.
- Gel fixing solution made up of 40% (v/v) methanol and 10% (v/v) acetic acid.
- Coomassie (G250) protein stain
- NuPAGE® LDS Sample Buffer (4x) - Life Technologies Corporation, Wilmington DE USA.

4.3.2 Protocol for the production of human adipose tissue secretion sample:

The preparation of human adipose tissue secretions used in this chapter was the same as that used in Chapter 3. For the methodology utilised, please see section **3.3.3**. Samples of the adipose secretions used here in Chapter 4 were stored at -80°C in aliquots of 1 mL and 40 mL each until required; freeze-thaw cycles were limited to two per aliquot to prevent possible loss of cytokine activity over the course of the experiments.

4.3.3 MDCK cell culture procedure:

For the culture and propagation of the MDCK cells in preparation for treatment with the adipose secretions, the MDCK cells were grown in MDCK cell expansion media. The cells were cultured in T175 flasks (175 cm^2) with 25 mL media per flask. The media was changed every two to three days and the cells were monitored using an inverted light microscope for cell morphology, signs of contamination and for the monitoring of culture confluence level. Once cultures reached approximately ninety percent confluence, the flasks were stripped, pooled together and re-seeded into new flasks in a ratio of 1:4 (*i.e.* one flask is split into 4 new ones). Briefly, the flasks were drained of their current media and washed for five minutes with 10 mL of plain DMEM-HG, pre-warmed to 37°C. The wash DMEM-HG was then removed and to each 175 cm2 flask, 2 mL Trypsin/EDTA solution was added; each flask was tipped to ensure coverage of the enzyme over the cell monolayer. The flasks were then incubated at 37°C for five to ten minutes until the cells were detached. At this time, 8 mL of MDCK expansion media was added to each flask and washed over the flask growth surface extensively to ensure suspension of the cells. All the MDCK cell suspensions were then pooled into a single flask and mixed thoroughly to ensure a homogeneous cell suspension. The cell suspension was then used to seed new 175 cm^2 flasks by adding 2.5 mL of cell suspension to each new flask. The new flasks were then topped up with 22.5 mL of MDCK expansion media and mixed before being placed back into the incubator at 37°C, 5% CO_2.

4.3.4 Treatment of MDCK cells with adipose tissue secretions:

Once there were enough MDCK cell cultures for treatment with the human adipose secretions, cultures were selected for stripping and re-seeding into new flasks with either control media or human adipose secretion media as follows. The selected MDCK cultures were drained of all media and washed for five minutes with 10 mL DMEM-HG pre-warmed to 37°C. The wash media was then removed and 2 mL of trypsin/EDTA solution was added

and mixed over the cells thoroughly. The cultures were incubated for five to ten minutes at 37°C 5% CO_2 until all cells had detached from the flask surface. Once complete, 8 mL MDCK expansion media was added to each flask and washed down the surface of the flasks multiple times to ensure suspension of the MDCK cells and the break-up of any cell clumps. The cell suspensions were then combined and mixed thoroughly to create a homogeneous cell suspension. At this point, a small aliquot of the cell suspension was taken for cell counting using a haemocytometer. Two equal aliquots of the cell suspension were taken and placed into two new sterile 15 mL tubes and centrifuged at 500 x g for five minutes. One cell pellet was re-suspended in 10 mL MDCK cell Control media and seeded into four new labelled flasks at a density of 9 x 10^3 cells/cm^2. While the second tube cell pellet was suspended in 10 mL MDCK cell Treatment media and seeded into new labelled flasks at the same cell density. The flasks were then incubated for twenty-four hours at 37°C 5% CO_2 until they were ready for harvesting for iTRAQ proteomic analysis.

4.3.5 Harvesting MDCK cells for iTRAQ analysis:

Once the MDCK cells had been incubated for twenty-four hours in the control or treatment media, they were observed under the inverted light microscope to assess cell morphology, signs of contamination and confluency level. The MDCK cells were harvested once confluency had reached eighty percent (*i.e.* approximately eighty percent of the flask surface was covered in cell growth). The media was drained from all flasks and 20 mL of 37°C DMEM-HG was added to each flask to wash the cultures for five minutes. The wash media was then removed and replaced with 2 mL TrypLE Select stripping reagent which was mixed over the cell monolayers carefully before the flasks were incubated at 37°C, 5% CO_2 for five to ten minutes until the cells had fully detached. To the flasks, 10 mL of pre-warmed 1x PBS solution was then added and used to suspend the cells. The contents of each flask were transferred into separate 15 mL tubes and then topped up to the 14 mL mark with more PBS solution. The tubes were then centrifuged at 500 x g for five minutes. The supernatants were carefully removed completely and discarded while the cell pellets were re-suspended in a further 14 mL PBS and centrifuged again at 500 x g for five minutes. The supernatants were fully removed again, with care taken not to disturb the cell pellets, and discarded. The control and treated MDCK cell pellets were then frozen inside the 15 mL tubes as dry pellets at -80°C until required for preparation for iTRAQ analysis.

4.3.6 MDCK cell protein extraction technique for iTRAQ analysis:

The treated and control MDCK cell pellets were defrosted to room temperature and then suspended in 3 mL 1% SDS (*w/v*), 100 mM TEAB solution. The samples were sonicated in an ultrasonic bath for fifteen minutes and then transferred into 2 mL tubes (two per sample) and incubated at 100°C in a heating block for ten minutes. The samples were centrifuged at 21000 x g for ten minutes, the supernatants for each sample were transferred into 15 mL tubes and acetone precipitated by the addition of 12 mL acetone. Precipitation was aided by the addition of citric acid to the samples once mixed with the acetone. The samples were incubated for thirty minutes at room temperature and then centrifuged for ten minutes at 3000 x g. The supernatants were discarded carefully and the pellets were re-suspended in 110 µL of 1% SDS solution and boiled for five to ten minutes. The samples were then buffer exchanged into 0.1% SDS solution using Bio-Spin™ Micro-Bio-Spin 6 columns.

The total protein loads of each sample were determined and equalised using the method described in Section 2.3.11. As a confirmatory step to ensure adequate equalisation had been achieved, a 10 µL aliquot of each sample was taken for resolving on a 1-D gel in order to assess the relative protein loads of each sample. Briefly, 3 µL of NuPAGE® LDS Sample Buffer (4x) and 1.5 µL of TBP was added to each of the 10 µL sample aliquots and mixed well. The aliquots were then boiled for five minutes and centrifuged at 21000 x g for ten minutes. The entire 13 µL volume of each sample was loaded into lanes of a Criterion™ 1-Dimensional Precast 18-well, polyacrylamide gel. The gel was resolved at 150 V (constant), inside the Criterion™ gel resolving apparatus using the MES gel resolving buffer until the tracking dye front reached the bottom of the gel. The gel was then fixed by placing it into 100 mL of the gel fixing solution for forty minutes on an orbital shaker and then placed into Coomassie G250 protein staining solution composed of a mix of Coomassie G250 solution 1 and solution 2 in a ratio of 4:1 respectively. The gel was incubated in the stain overnight on the orbital shaker. The gel was then destained using Coomassie destaining solution for one hour with regular changes of the solution to speed up the process. The gel was imaged using a desktop document scanner for direct visual confirmation of protein load equalisation in each sample. Following confirmation of the presence of equal protein loads within each sample for iTRAQ processing at APAF, the frozen treated and control MDCK cell protein samples were then submitted to APAF for iTRAQ analysis under the request of an 'Advanced

liquid chromatography electrospray ionisation analysis' at a protein concentration of approximately 150 ng/mL. The labelling of each sample, subsequent preparation steps and the LC-MS runs were all performed by APAF staff according to standard operating procedures. These steps were the only procedures completed by people other than me unless otherwise stated.

4.3.7 MDCK cell iTRAQ analysis:

The iTRAQ analysis performed on treated and control MDCK cells was conducted by APAF staff through the use of an in-house specialised LC-MS service. The MDCK cell protein samples that were prepared and equalised using the method described in section 4.3.6, were submitted to APAF frozen in 600 µL tubes in a total volume of 100 µL at a protein concentration of approximately 150 ng/mL. Samples were labelled with 'C1, C2, T1, T2'. The samples were prepared, labelled and resolved using APAF standard operating procedures. A final report was then obtained from APAF technical staff detailing the conditions of the analysis. The data from the iTRAQ analysis was obtained from APAF in the form of Notepad documents for each isobaric tag label, *i.e.*: 114, 115, 116 and 117. The data for these tags were imported into Microsoft Office Excel (2007) and filtered and sorted according to both *p*-value and control: treated relative ratios. The proteins found to be increased or decreased in abundance in the treated samples compared to the controls were selected based on a relative fold-change cut off of +/- 1.2 and a *p*-value of less than 0.05.

4.4 Results:

Chapter 3 displayed changes in the PRC proteome due to treatment with the adipose tissue secretions using iTRAQ analysis. The same principles from Chapter 3 were also applied here to the MDCK cells. One advantage gained by the use of these cells rather than primary cells is the homogeneity of the population, meaning that the treated and control cultures are as close to each other as possible with no additional biological variation due to donor animals. The differences between the treated and control MDCKs observed in this chapter were expected to be more reproducible and more closely tied to the specific functions of the secretions.

Once the MDCK cells had been cultured, treated and harvested for iTRAQ analysis; the samples were equalised based on total protein load using a 1-D gel based approach described in Chapter 3. **Figure 4.1** demonstrates that each sample had been equalised to an adequate level for iTRAQ analysis. The iTRAQ analysis report has been summarised in **Table 4.1** displaying the version of ProteinPilot^{TM} used and the parameters of the database search. Almost three thousand proteins were identified in total across all four samples, indicating that the protein isolation and preparation technique used was sound. This also indicates a high quality assessment of the proteomes of the treated and control MDCK cells was possible.

Following the iTRAQ analysis at APAF, proteins were selected from the raw data output based on the significance (p-value < 0.05) of the change in abundance between control and treated and a minimum fold-change cut-off of +/- 1.2 fold. The proteins shown to be decreased in abundance in the treated MDCK cells are shown in **Table 4.2**, indicating thirty proteins that had decreased in relative abundance in the treated cells. The proteins found to be increased in abundance in the treated MDCK cells are featured in **Table 4.3**, with a total of forty-one proteins increased. In order to efficiently process this data and identify trends in the functions and biological process involvement of each protein, the java-based program Blast2GO was utilised. Blast2GO sorted the proteins in each based on the gene ontology (GO) information around the biological process involvement of each protein. The program was also used to apply an algorithm to the data in order to score the prevalence of each biological process that each protein is annotated to take part in; the greater the score, the greater the biological significance in relation to the data sets. **Figure 4.1** details the

breakdown of the proteins decreased in abundance categorised by biological process only, without prevalence scoring. This provided an insight into the complexity of the changes observed in the treated cells. The fact that many proteins have multiple annotated functions means they appear in multiple GO categories, thus complicating the dataset. **Figure 4.2** shows the same data as **Figure 4.1**, but after the application of the prevalence scoring algorithm, enabling the identification of the processes relevant to renal health that has been further explored in **Table 4.4**. **Table 4.4** shows the decreased abundance protein processes likely to be of relevance to renal health and the proteins attributed to these processes based on GO annotation. These proteins were selected manually by the author from the data based on the literature search data for each protein identified.

The same process of mass data analysis and refinement using Blast2GO was also employed for the increased abundance protein data shown in **Table 4.3**. **Figures 4.3** and **4.4** show the increased abundance protein datasets sorted by biological process and by biological process and score respectively. They indicate a very broad range of effects on the treated MDCK cells. The biological processes relevant to renal health have been collated into **Table 4.5**, which displays the proteins from the increased abundance data set attributed to those processes. The use of the Blast2GO software was an initial filter that enabled the refinement of the data into a more manageable form and provided information on common functions and processes. An alternate method would have been to manually cross check multiple GO databases for every protein identified in **Tables 4.2** and **4.3**, collate the data, remove redundancies and then sort through the data for the common threads based on protein function and biological process.

Due to the diversity in GO terms over various databases, some biological processes are featured several times in the data under slightly different names, 'Cell cycle process' and 'Mitotic spindle organisation, G2/M transition of mitotic cell cycle' or 'S phase of mitotic cell cycle, M/G1 phase of mitotic cell cycle' for example. As is always necessary with any automated large-scale analysis, manual verification is occasionally required. **Table 4.6** displays manually selected increased abundance proteins that have been assigned to different but related biological processes; or have functions which could be related to renal function.

Figure 4.1: Verification of the MDCK cell total protein load equalisation using a 1-D gel.

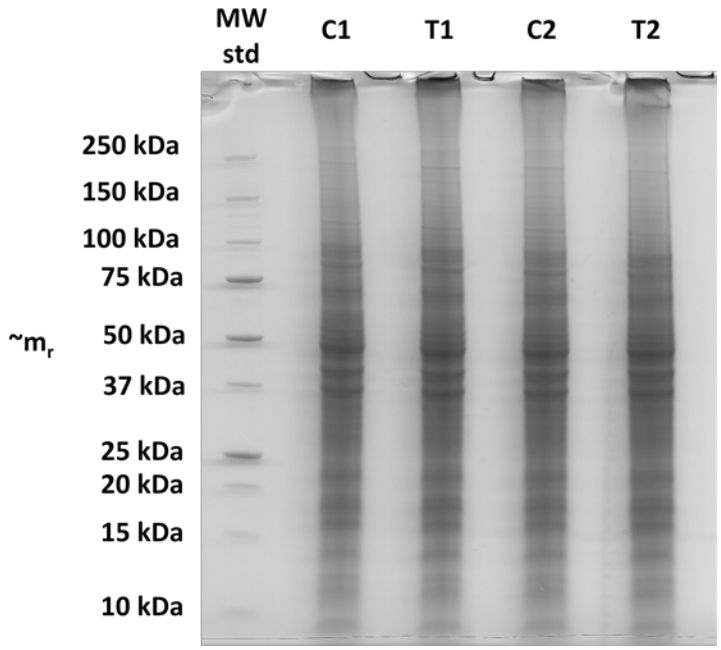

Figure 4.1: Confirmation of the equalisation of total protein loads between each sample prior to iTRAQ analysis. Treated and Control MDCK cell protein fractions separated on a pre-cast Criterion™ pre-cast 18-well 1-dimensional polyacrylamide gel, stained with Coomassie blue G250 protein stain. Molecular weight standards (MW std) used were Precision Plus Protein™ unstained molecular weight markers. Control samples are shown in lanes marked "C1" and "C2" while treated MDCK samples are in the "T1" and "T2" lanes. The total protein loads between the four samples were equal and suitable for iTRAQ analysis.

Table 4.1: ProteinPilot™ software summary statistics and result parameters output for the comparison of treated and non treated MDCK cells using iTRAQ.

Software version:	ProteinPilot™ software version 4.0
Revision number:	148085
Paragon algorithm	4.0.0.0, 148083
Confidence interval applied to MS data:	95%
Spectra identified:	75200
Distinct peptides:	30308
Proteins detected:	2952
Background correction used:	Yes

Table 4.1: ProteinPilot™ software summary statistics output for the comparison of treated and non treated MDCK cells using iTRAQ. A large number of total proteins were detected using this method, almost 3000, indicating the effective purification of the MDCK cell proteome and labelling with the iTRAQ reagents.

Table 4.2: Down regulated proteins due to adipose tissue secretion treatment.

Protein name	Protein accession / Gene accession	%Cov(95)	Peptides (95%)	Treated:Control (Mean)	*p*-value Treated:Control	Frequency (out of 4)
plasminogen activator inhibitor 1	gi|308193314	11.94	4	0.48537598	0.0336	4
PREDICTED: paxillin	gi|345791188	7.08	6	0.21656156	0.0095	4
PREDICTED: ephrin type-A receptor 2 isoform 1	gi|73950854	23.08	20	0.60322422	0.0006	4
PREDICTED: talin-1 isoform 2	gi|73971306	57.69	124	0.68073122	0.0035	4
transferrin receptor protein 1	gi|50978812	23.25	15	0.64391504	0.0043	4
PREDICTED: nucleolar RNA helicase 2	gi|345798963	31.59	24	0.56056517	0.0080	4
PREDICTED: myb-binding protein 1A isoform 4	gi|345800504	39.26	33	0.51127176	0.0036	4
PREDICTED: importin subunit alpha-2 isoform 2	gi|73965247	38.75	15	0.58645073	0.0022	4
PREDICTED: tRNA (cytosine(34)-C(5))-methyltransferase isoform 1	gi|74003041	20.64	10	0.60381237	0.0183	2
PREDICTED: mitochondrial-processing peptidase subunit beta	gi|345783001	20.32	7	0.56532043	0.0283	2
PREDICTED: elongation factor 2	gi|359322142	68.48	107	0.67309085	0.0339	2
PREDICTED: lupus La protein homolog	gi|74004835	57.39	23	0.64598972	0.0141	2
PREDICTED: polypyrimidine tract-binding protein 1 isoform 8	gi|73987401	52.54	32	0.36897406	0.0065	2
PREDICTED: eukaryotic translation initiation factor 5 isoform 4	gi|73964067	18.84	7	0.52500781	0.0322	2
PREDICTED: xin actin-binding repeat-containing protein 1	gi|73990261	8.72	10	0.49661337	0.0390	2

Protein name	Protein accession / Gene accession	%Cov (95)	Peptides (95%)	Treated:Control (Mean)	*p*-value Treated:Control	Frequency (out of 4)
PREDICTED: prostacyclin synthase	gi|345789704	43.84	24	0.68560454	0.0349	2
PREDICTED: integrin alpha-2	gi|345799149	13.62	14	0.61022553	0.0085	2
PREDICTED: zyxin	gi|345781474	27.99	11	0.68883488	0.0137	2
PREDICTED: ribonuclease inhibitor	gi|345783337	45.91	19	0.21698594	0.0034	2
PREDICTED: glutaminase kidney isoform, mitochondrial isoform 1	gi|74005002	25.77	13	0.64268774	0.0293	1
myosin, heavy polypeptide 9, non-muscle	gi|89994139	56.07	163	0.7798301	0.0241	1
PREDICTED: filamin-A isoform 1	gi|74008829	61.22	164	0.79432821	0.0261	1
PREDICTED: N-myc down regulated gene 1 (NDRG1)	gi|345779489	33.64	16	0.62517267	0.0288	1
PREDICTED: ATP-dependent RNA helicase DDX3X isoform 3	gi|74006722	47.89	31	0.60255957	0.0177	1
PREDICTED: plasma membrane calcium-transporting ATPase 4 isoform 5	gi|74005833	20.98	21	0.61376202	0.0468	1
thioredoxin reductase 1, cytoplasmic	gi|169881283	30.23	15	0.47424197	0.0220	1
PREDICTED: threonyl-tRNA synthetase, cytoplasmic	gi|345798924	30.57	19	0.79432821	0.0399	1
PREDICTED: 60S ribosomal protein L10a isoform 5	gi|356460978	41.47	12	0.57543993	0.0297	1
PREDICTED: 60S ribosomal protein L37a-like	gi|73975534	41.30	3	0.15135613	0.0402	1
PREDICTED: multifunctional protein ADE2 isoform 1	gi|73975047	39.06	18	0.57016426	0.0177	1

Table 4.2: Proteins showing decreased abundance in the treated cells after treatment of the MDCK cells with adipose secretions, identified using iTRAQ analysis. A larger number of proteins were shown to be increased in abundance rather than decreased in abundance. These proteins have diverse functions and cellular origins, making direct conclusions from the dataset difficult.

Figure 4.1: Pie-chart representation of proteins shown to be decreased in abundance in the iTRAQ analysis categorised by the GO annotation biological process. This chart takes into account all the known biological process involvements for all proteins shown in **Table 4.2**. Numbers next to each biological process indicate the number of proteins attributed to this process from the dataset. Data analysis was conducted using Blast2GO data analysis software tool, available free online at: http://www.blast2go.com/b2glaunch.

Figure 4.1: Pie-chart of proteins decreased in abundance categorised by biological process

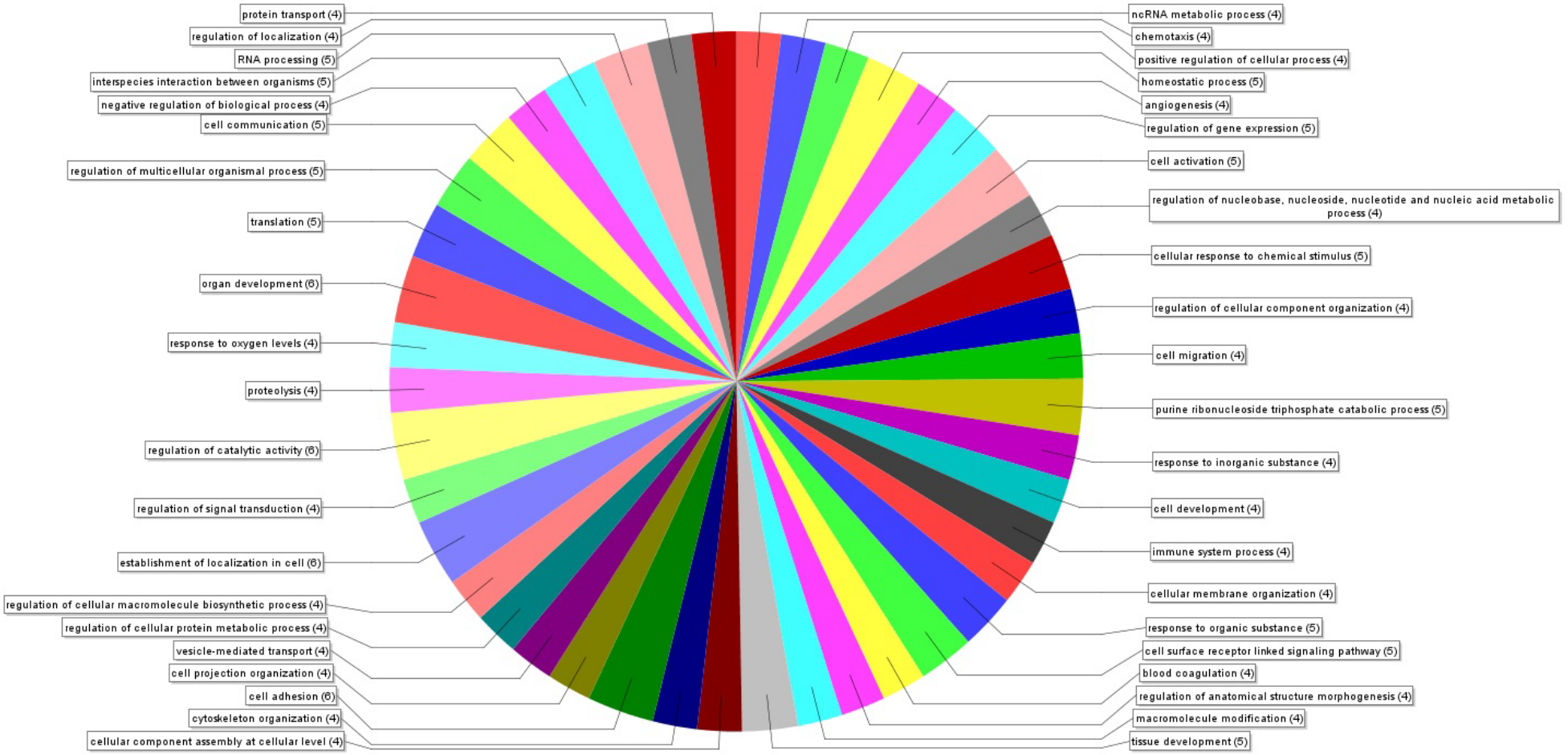

Figure 4.2: Decreased in abundance proteins from **Table 4.1** sorted by biological process and presented based on prevalence scores as derived by Blast2GO software. Numbers besides each biological process indicate the number of proteins from **Table 4.1** that compose each pie slice. These biological processes were selected by Blast2GO software based on a scoring system which calculated the relative importance of all biological functions within a dataset. The more proteins involved in a given process, the higher the relative importance and therefore the higher the score. Data analysis was conducted using Blast2GO data analysis software tool, available free online at: http://www.blast2go.com/b2glaunch.

Figure 4.2: Proteins shown to be decreased in abundance as sorted by biological process and filtered based on prevalence score.

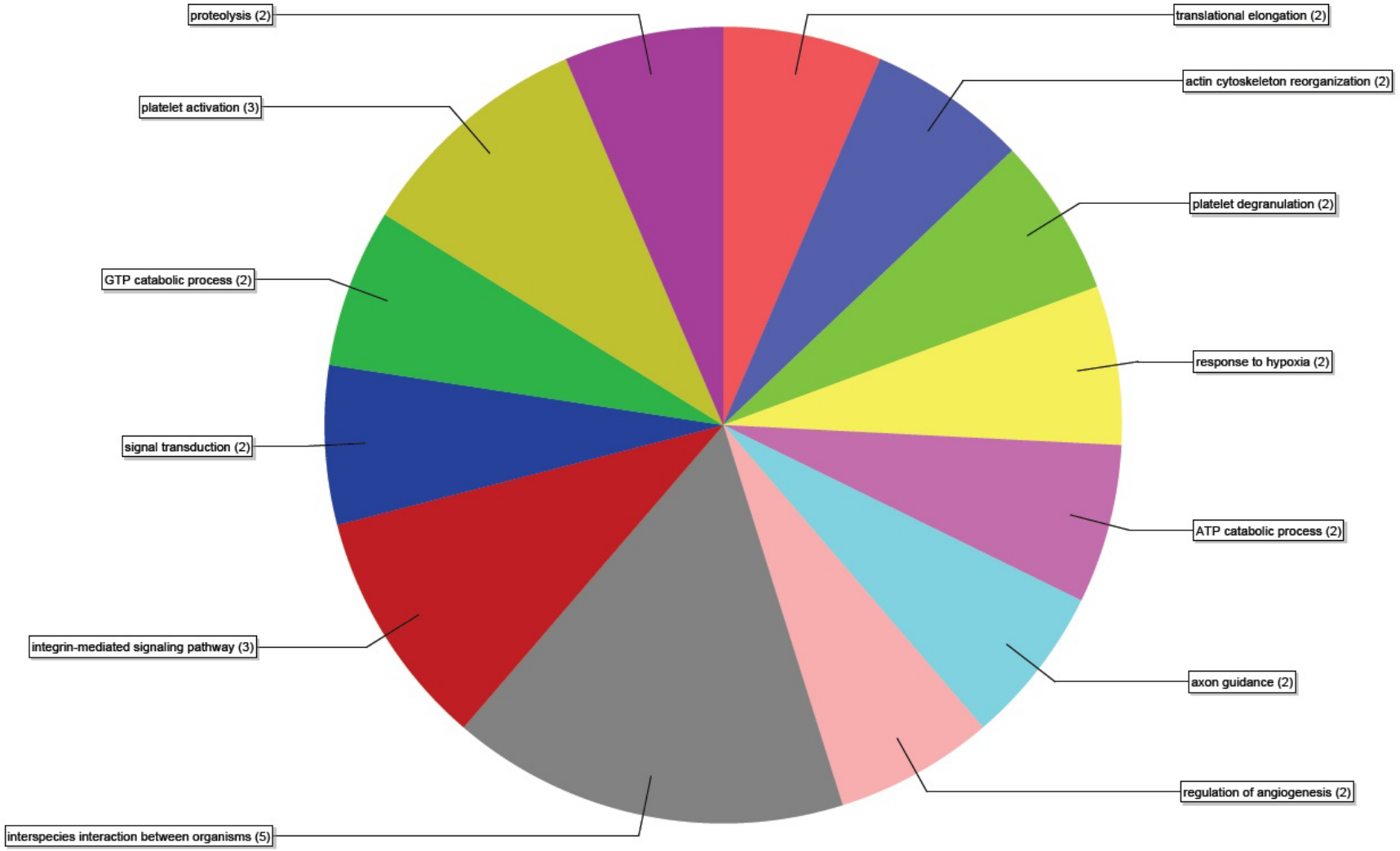

Table 4.3: Proteins shown to be increased in abundance after treatment with adipose derived secretions.

Protein name:	Protein accession:	%Cov(95)	Peptides(95%)	Treated:Control (mean)	*p*-value:	Frequency:
PREDICTED: clathrin heavy chain 1 isoform 1	gi|73966629	49.85	99	1.461	0.00090	4
PREDICTED: pyruvate kinase isozymes M1/M2 isoform 1	gi|74000677	75.71	108	1.585	0.00356	4
PREDICTED: ATP-citrate synthase isoform 2	gi|73965857	47.05	41	1.839	0.00001	4
ribosome receptor	gi|984114	32.72	28	1.348	0.00014	4
PREDICTED: UDP-glucose 6-dehydrogenase isoform 1	gi|73951555	63.97	29	1.562	0.00791	4
PREDICTED: glucose-6-phosphate isomerase isoform 1	gi|73947982	47.67	57	1.707	0.01214	4
Collagen alpha-1(I) chain	gi|8134354	28.15	39	2.611	0.00010	4
PREDICTED: procollagen-lysine,2-oxoglutarate 5-dioxygenase 2	gi|345789311	31.15	20	1.581	0.00129	4
PREDICTED: UDP-N-acetylhexosamine pyrophosphorylase isoform 3	gi|345797803	32.67	13	1.779	0.00746	4
PREDICTED: fibronectin	gi|345797318	7.624	12	2.849	0.00071	4
PREDICTED: pyruvate carboxylase, mitochondrial isoform 1	gi|73982897	12.56	11	2.630	0.01266	4
PREDICTED: purine nucleoside phosphorylase isoform 1	gi|73977271	26.64	6	4.682	0.00111	4
PREDICTED: 6-phosphogluconate dehydrogenase, decarboxylating isoform 1	gi|73950940	59.01	30	1.607	0.00743	3
PREDICTED: cytoplasmic dynein 1 heavy chain 1-like isoform 1	gi|73964009	38.92	138	1.225	0.03452	2
PREDICTED: coatomer subunit beta	gi|345787834	43.86	32	1.331	0.01408	2

Protein name:	Protein accession:	%Cov(95)	Peptides(95%)	Treated:Control (mean)	*p*-value:	Frequency:
PREDICTED: phosphoglycerate kinase 1 isoform 2	gi|74007807	67.87	45	1.242	0.00877	2
PREDICTED: glucose-6-phosphate 1-dehydrogenase	gi|74009187	52.48	35	1.387	0.03753	2
PREDICTED: Golgi apparatus protein 1 isoform 1	gi|73957014	25.72	26	3.005	0.00025	2
calnexin precursor	gi|50979014	44.35	34	1.316	0.01442	2
PREDICTED: prolyl 4-hydroxylase subunit alpha-1 isoform 3	gi|73952886	38.2	19	1.407	0.01367	2
PREDICTED: bifunctional 3'-phosphoadenosine 5'-phosphosulfate synthase 1 isoform 2	gi|74002083	36.8	17	1.386	0.01466	2
PREDICTED: integrin alpha-V isoform 2	gi|74004771	20.43	17	1.770	0.02407	2
PREDICTED: V-type proton ATPase catalytic subunit A isoform 1	gi|57109638	34.14	16	1.524	0.01060	2
PREDICTED: Na(+)/H(+) exchange regulatory cofactor NHE-RF1	gi|359320259	28.69	8	1.565	0.01790	2
Endoplasmin	gi|729425	56.22	67	1.282	0.02830	1
PREDICTED: L-lactate dehydrogenase A chain isoform 2	gi|73988675	72.89	93	1.675	0.02607	1
PREDICTED: coatomer subunit alpha, partial	gi|345797687	37.62	39	1.225	0.04205	1
glyceraldehyde-3-phosphate dehydrogenase	gi|6983847	77.78	96	1.318	0.04367	1
PREDICTED: ATP synthase subunit alpha, mitochondrial isoform 2	gi|345802726	55.33	45	1.923	0.01291	1
PREDICTED: dihydropyrimidinase-related protein 3	gi|345793957	65.09	41	1.432	0.03605	1
PREDICTED: keratin, type I cytoskeletal 18 isoform 1	gi|57106334	66.59	46	1.486	0.02758	1

Protein name:	Protein accession:	%Cov(95)	Peptides(95%)	Treated:Control (mean)	*p*-value:	Frequency:
PREDICTED: trifunctional enzyme subunit alpha, mitochondrial isoform 2	gi|57098165	47.11	33	1.318	0.04404	1
PREDICTED: prostaglandin reductase 1 isoform 1	gi|73971560	70.52	38	1.459	0.03117	1
PREDICTED: puromycin-sensitive aminopeptidase	gi|345805467	37.33	24	1.445	0.04283	1
PREDICTED: ERO1-like protein alpha	gi|73963815	53.85	24	2.148	0.00552	1
PREDICTED: 26S proteasome non-ATPase regulatory subunit 6 isoform 1	gi|73985103	42.67	14	1.570	0.01457	1
PREDICTED: signal transducer and activator of transcription 3 isoform 1	gi|73965766	10.27	4	2.831	0.04335	1
PREDICTED: epidermal growth factor receptor pathway substrate 15-like 1 isoform 4	gi|345787653	2.418	2	1.355	0.00740	1
***PREDICTED: LOW QUALITY PROTEIN: microtubule-associated protein 4 isoform 1	gi|345787491	42.63	36	1.306	0.04268	1
***REVERSED PREDICTED: dedicator of cytokinesis protein 8 isoform 1	RRRRRgi|345785280	0.4498	1	21.938	0.03187	2
***PREDICTED: thioredoxin domain-containing protein 5-like	gi|345796700	38.23	22	1.364	0.00031	3

Table 4.3: Up regulated proteins after treatment of the MDCK cells with adipose secretions, identified using iTRAQ analysis. A larger number of proteins were shown to be increased in abundance rather than decreased. These proteins have diverse functions and cellular origins, making direct conclusions difficult and emphasising the need for further data analysis using a gene ontology data analyser like Blast2GO.

Figure 4.3: Proteins found to be increased in abundance in the treated MDCK cells, sorted by GO biological process annotation only. The range of biological processes altered in the treated cells shown here indicates a complex set of responses to the treatment with human adipose secretions. Data was categorised and sorted using the free Java-based software tool Blast2GO, available free online at: http://www.blast2go.com/b2glaunch.

Figure 4.3: Proteins shown to be increased in abundance in the treated MDCK cells categorised by biological process.

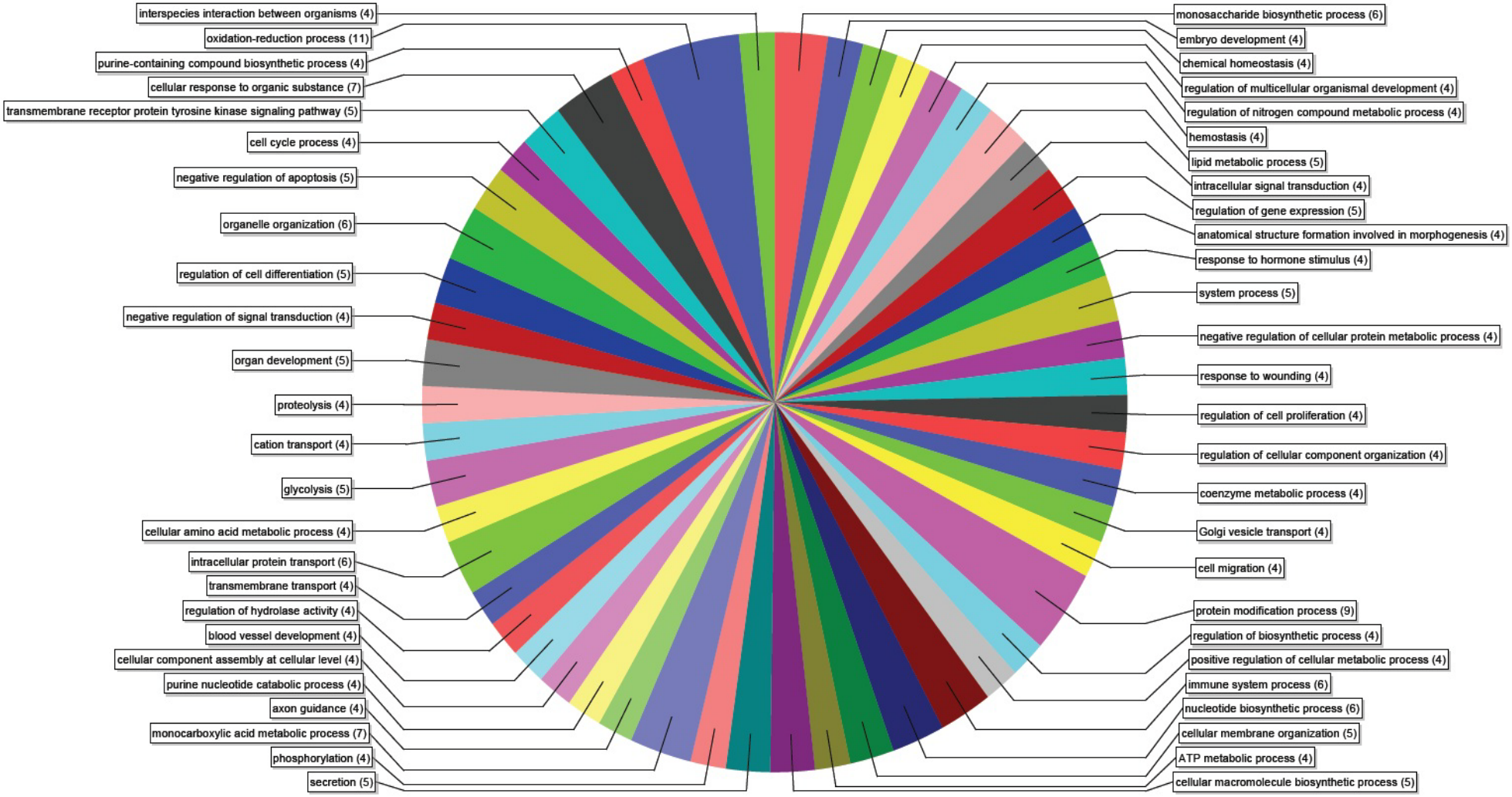

Figure 4.4: Proteins of increased abundance in the treated MDCK cells based on biological process GO annotation and score. The range of biological processes has been reduced with the addition of the scoring filter, enabling for the selection of processes from the data set relevant to renal health. Data was categorised and sorted using the free Java-based software tool Blast2GO, available free online at: http://www.blast2go.com/b2glaunch.

Figure 4.4: Proteins of increased abundance in the treated MDCK cells based on biological process GO annotation and score.

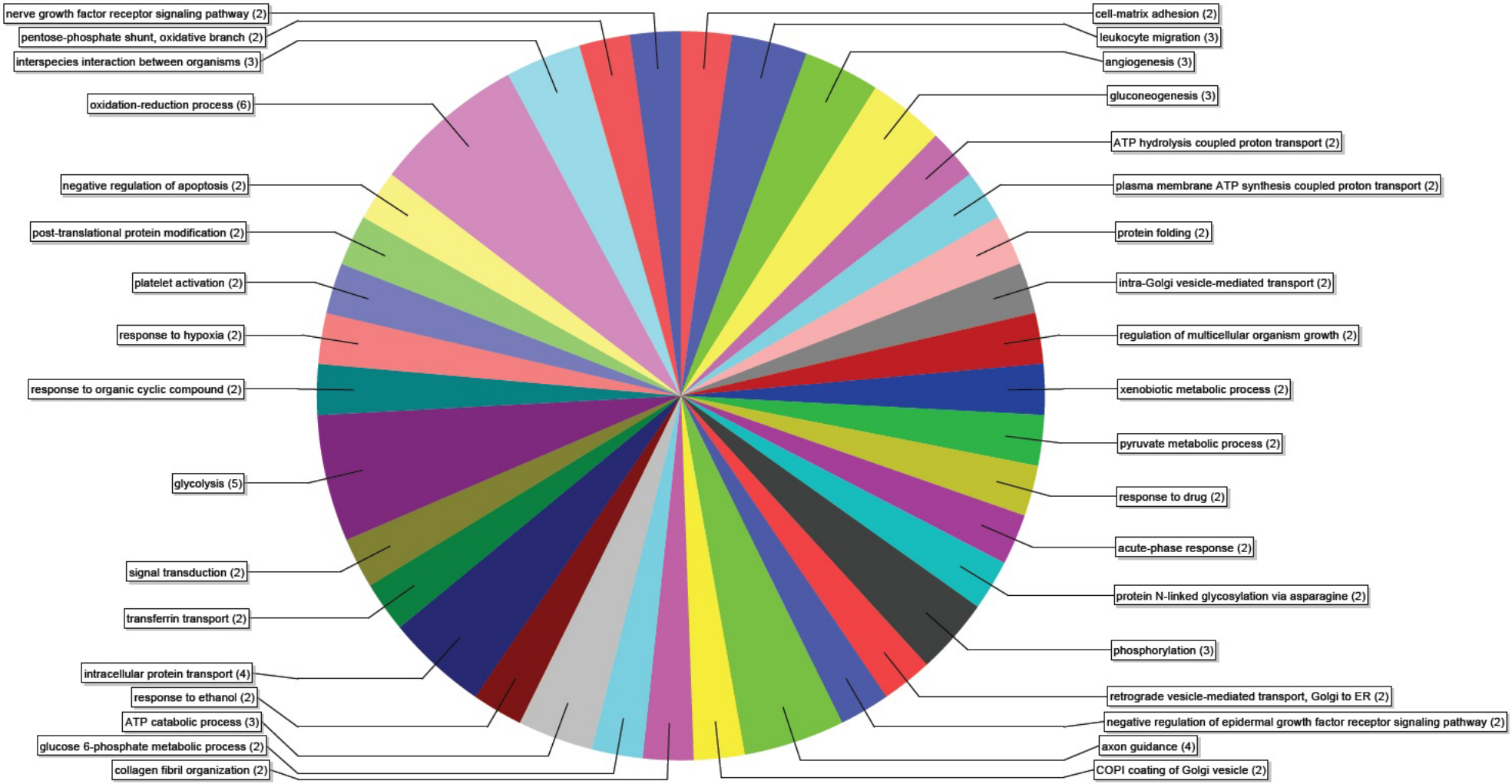

Table 4.4: Biologically significant decreased abundance processes and proteins derived from **Figure 4.2**.

Biological process:	**Down regulated proteins involved:**
Platelet activation	Plasminogen activator inhibitor 1
	Plasma membrane calcium-transporting ATPase 4 isoform 5
	Filamin-A isoform 1
Platelet degranulation	Plasminogen activator inhibitor 1
	Filamin-A isoform 1
Actin cytoskeleton reorganisation	Filamin-A isoform 1
	Myosin, heavy polypeptide 9, non-muscle
Response to hypoxia	N-myc down regulated gene 1 (NDRG1)
	Integrin alpha-2
	Transferrin receptor protein 1
Regulation of angiogenesis	Ribonuclease inhibitor
	Myosin, heavy polypeptide 9, non-muscle
Integrin-mediated signalling pathway	Paxillin
	Myosin, heavy polypeptide 9, non-muscle
	Integrin alpha-2
Interspecies interaction between organisms	Zyxin
	Integrin alpha-2
	ATP-dependent RNA helicase DDX3X isoform 3
	Importin subunit alpha-2 isoform 2
	Transferrin receptor protein 1

Table 4.4: Potentially biologically significant decreased abundance processes and proteins, derived from **Figure 4.2**. These processes were selected from the score-based pie graph in **Fig 4.2** based on possible relevance to epithelial cell function and thus potential significance during a renal disease setting. This shows that integrin alpha-2, filamin-A and myosin heavy polpeptide 9, non muscle; all potentially have multiple roles in the observed changes in the treated MDCK cells.

Table 4.5: Biologically significant processes and proteins that are increased in abundance derived from **Figure 4.4**. These processes are dominated with the theme of increased energy expenditure, energy production and increased MDCK cell mitosis. Two growth factor pathways were also identified to be potentially important in the effects of the adipose tissue secretions on the MDCK cells. Unlike in Chapter 3, these processes are not dominated by a small handful of key individual proteins like collagens or myosins. Italicised GO process information has been placed after proteins that were not included in the process pie slice in **Figure 4.4** due to GO terminology redundancy and the failure of the Blast2GO software to identify these proteins as part of the same GO process. These proteins were manually identified and verified and have thus been included in the table as part of the complement of proteins that were increased in abundance and attributed to performing each process.

Table 4.5: Biologically significant processes and proteins that are increased in abundance derived from **Figure 4.4**

Biological process:	**Proteins of increased abundance involved:**
Nerve growth factor signalling pathway	Signal transducer and activator of transcription 3 isoform 1 (STAT 3)
	Clathrin heavy chain 1 isoform 1 (*also involved in mitosis*)
Negative regulation of apoptosis	Keratin, type I cytoskeletal 18 isoform 1
	Integrin alpha-V isoform 2
	Endoplasmin *(anti-apoptosis)*
	Glucose-6-phosphate isomerase isoform 1 *(negative regulation of neuron apoptosis)*
	26S proteasome non-ATPase regulatory subunit 6 isoform 1 *(regulation of apoptosis)*
Acute phase response	Signal transducer and activator of transcription 3 isoform 1 (STAT 3)
	Fibronectin
Negative regulation of epidermal growth factor receptor signalling pathway	Clathrin heavy chain 1 isoform 1
	Epidermal growth factor receptor pathway substrate 15-like 1 isoform 4
Angiogenesis	Glucose-6-phosphate isomerase isoform 1
	Integrin alpha-V isoform 2
	Fibronectin
Glycolysis	Glyceraldehyde-3-phosphate dehydrogenase
	L-lactate dehydrogenase A chain isoform 2
	Pyruvate kinase isozymes M1/M2 isoform 1
	Phosphoglycerate kinase 1 isoform 2
	glucose-6-phosphate isomerase isoform 1
Gluconeogenesis	Glucose-6-phosphate isomerase isoform 1
	Pyruvate carboxylase, mitochondrial isoform 1
	Phosphoglycerate kinase 1 isoform 2
ATP catabolic process	ATP synthase subunit alpha, mitochondrial isoform 2
	ATP-citrate synthase isoform 2
	26S proteasome non-ATPase regulatory subunit 6 isoform 1
ATP hydrolysis coupled proton transport	V-type proton ATPase catalytic subunit A isoform 1
	ATP synthase subunit alpha, mitochondrial isoform 2
Plasma membrane ATP synthesis coupled proton transport	V-type proton ATPase catalytic subunit A isoform 1
	ATP synthase subunit alpha, mitochondrial isoform 2

Table 4.6: Other proteins that were shown to be increased in abundance with relevance to previous work and other protein expression trends in this chapter.

Protein name:	**Annotated relevant biological process involvement:**
6-phosphogluconate dehydrogenase, decarboxylating isoform 1	Cell cycle process
Keratin, type I cytoskeletal 18 isoform 1 (*alternate name*: Cell proliferation-inducing gene 46 protein)	Cell cycle process
cytoplasmic dynein 1 heavy chain 1-like isoform 1	Mitotic spindle organisation, G2/M transition of mitotic cell cycle
26S proteasome non-ATPase regulatory subunit 6 isoform 1	S phase of mitotic cell cycle, M/G1 phase of mitotic cell cycle
Golgi apparatus protein 1 isoform 1	Negative regulation of TGF-β receptor signalling pathway
Na(+)/H(+) exchange regulatory cofactor NHE-RF1	Renal absorption, renal sodium ion transport

Table 4.6 Other proteins that were shown to be increased in abundance with relevance to previous work and other protein expression trends in this chapter. These proteins have been included in the table because the either have ancillary functions that may be relevant to renal failure, or they have been shown to have interactions with pathways found to be important in the action of the adipose tissue secretions in previous work (Chapter 3).

4.5 Discussion:

MDCK cells are an immortalised canine renal epithelial cell line derived from the distal convoluted tubule [277]. Epithelial cells of the nephron perform various physiological functions by mediating solute and water uptake and excretion into the urine. Distal tubule epithelial cells are primarily responsible for the active reabsorption of salts from the nephron lumen in order to retain sodium and calcium homeostasis in response to different signalling hormones like aldosterone [279]. These functions rely on the presence of ion transporters on the luminal face of the epithelial cells to actively reabsorb these ions and the presence of transporters on the basement membrane face of the cells to secrete the desired ions back into circulation. The difference in function of the two faces of the epithelial cells is known as cell polarity and is reflected by the distinct composition of the two polar plasma membranes and associated actin cytoskeletal components [278]. Polarity is integral to the function of tubular epithelial cells. Despite being immortalised and passaged extensively, MDCK cells have not lost the ability to form asymmetric cell monolayers with polar intracellular configurations [278]. MDCK cell monolayers *in vitro* are also capable of forming a membrane with similar permeability and transporting properties as *in vivo* epithelia [280]. This means that they have retained many of the functional characteristics of normal mammalian tubular epithelial cells and are thus a suitable model to assess the effects of the prepared adipose secretions on the kidney tubule. The immortalisation of the MDCK cells and *in vitro* expansion meant that each flask essentially contained clones. This cut the biological variation of the experiments in this chapter, making reproducibility much higher than would be possible with most primary cell-based experiments. The canine origin of the MDCK cells however, did mean that large-scale multi-plexed analysis of the xenogeneic adipose secretions-MDCK cell interaction in a similar style to those of Chapter 3 were not ideal. That is, the analysis of the secretory response of the MDCK cells to treatment with the adipose secretions was not possible. An analysis of the 'uptake' of human adipose cytokines by the MDCK cells would have been very interesting, however was not completed here because of known cross-reactivity of canine cytokines/growth factors to the human Bio-Plex™ kit, based on unpublished data from experiments using canine samples on the human kits completed by colleagues.

The use of iTRAQ analysis to compare treated and non-treated MDCK cells resulted in a very large dataset of almost 3000 proteins in total identified (**Table 4.1**). This indicates an extensive overview of the proteomes of these cells at the time of harvest and provides confidence in the sample preparation and protein purification steps taken prior to sample submission to the APAF facility for iTRAQ sample labelling and LC/MS analysis. The large number of identified proteins also indicates that the view of the MDCK cell proteome was sensitive enough to scratch below the surface of the most highly abundant cellular proteins and give some view of the less abundant and perhaps more transiently expressed proteins. Thus likely providing a deeper insight into the workings of the control and treated MDCK cell populations, giving more meaningful data. The dataset for the MDCK cell proteome yielded higher total protein identifications and a larger hit rate than the dataset for the PRCs of Chapter 3 as seen in **Table 3.5**. This may be due to inherent differences in the cell types and the complement of protein expressed in each. Both datasets provided a large number of total proteins identified, indicating broad coverage of the proteomes of each type of cell. The hit rate of both iTRAQ runs, that is, the percentage value of proteins identified compared to distinct peptides, were also within the normal ranges for an LC-MS run.

The **Tables 4.4**, **4.5** and **4.6** show processes that have been found to be potentially important to the function of the renal tubule or its health or repair. These processes have been explored further in the following sections in order to explain the relevance of each in the context of the individual proteins from the iTRAQ analysis shown to be involved.

4.5.1 Down regulated protein processes:

4.5.1.1 Decreased platelet activation and degranulation:

Platelet activation in gene ontology terms is the process of the binding of platelets to sub-endothelial tissues and the initiation of the formation of a haemostatic plug (or blood clot). Platelet degranulation is the regulated exocytosis of granules by a platelet after activation. The platelet activation process can be induced by a large variety of factors [281,282], including selected proteins decreased in abundance shown in **Table 4.4**. A state of increased platelet activation measured by blood markers has been shown to be associated with chronic renal disease [283] and acute renal failure [284]. Plasminogen activator inhibitor 1 (PAI-1) was decreased in abundance by a factor of approximately 2.1 fold in the adipose secretion

treated MDCK cells. PAI-1 is a key protein in the regulation and maintenance of the fibrin clot and has roles in the inhibition of plasminogen activation into plasmin [285]. This leads to fibrinolysis (blood clot breakdown) and plasmin-linked activation of other matrix metalloproteinases [178,285]. According to Rerolle *et al* [178], PAI-1 is not constitutively expressed in the normal human kidney, but is highly induced in a range of kidney diseases and may be associated with renal fibrogenesis; PAI-1 expression in the canine kidney is yet to be determined but may follow the same expression patterns as in humans. Decreased abundance of this protein in the treated MDCK cells likely indicates a decrease in the stress-state of the treated cells in comparison to the control cells. PAI-1 expression in the treated PRCs (Chapter 3) and MDCK cells appear to show opposing results; PAI-1 is increased in abundance in the PRCs, but is decreased in abundance in the treated MDCK cells. This may be due to the difference in cell type and species; and thus a difference in cell-surface receptor expression patterns. The effect may also be due in part, to the complexity of the adipose tissue secretions activating and suppressing a variety of pathways within each cell type, depending on the receptors present on the surface of each cell.

Filamin A isoform 1, is a protein involved in actin cytoskeleton cross linking and provides a docking site for some cell surface receptors and intracellular signal transducers [286]. It was decreased in abundance in the treated MDCK cells on average by 1.26 fold. It has also been shown to be involved in the regulation of platelet activation (and thus blood clotting) by binding to the cytoplasmic tail of glycoprotein Ibα, thereby regulating von Willebrand factor activities; a key mediator of platelet activation [287].

4.5.1.2 Decreased actin cytoskeleton reorganisation:

This gene ontology (GO) process term is given to any process that leads to changes in the actin cytoskeletal structure or composition of cytoskeleton structures comprised of actin filaments or associated proteins. During the repair of acute renal injury, it is thought that tubular epithelial cells undergo a process known as dedifferentiation [288]. This is thought to involve the depolarisation of the epithelial cell actin cytoskeleton and detachment of the surviving epithelial cells from the basement membrane; followed by migration into zones of lost epithelium and rapid proliferation which can restore renal function [288]. Changes to the actin cytoskeletal structure or composition, or both, are required for all of these cellular functions.

Filamin A has roles in actin filament cross linking, is a docking site for cell surface receptors and intracellular signalling proteins and has been shown to aid in cell migration through filopodia formation [286]. Filopodia are cellular micro-projections thought to be used by migrating cells to sense environmental cues to direct movement and adhere to the extracellular matrix [289]. Down regulation of filamin A shown in these experiments may be a result of the increased metabolic activity and cell division of the treated MDCK cells compared to the controls, which will be discussed in a later section regarding the proteins that were identified to be increased in abundance. Even though the culture flasks at the time of harvest were at sub-confluence (eighty percent confluence); it is possible that the increased cell growth meant that cell migration over the flask surface during expansion was no longer necessary as much of the surface area had already been grown over with cells. Another possibility behind the decreased in abundance of filamin A is that it is connected to the decreased in abundance of proteins connected to the TGF-β signalling pathway. In Chapter 3, results indicated a broad-scale decreased in abundance of many proteins connected with cellular TGF-β signalling and function. It is possible that some of the same effects have occurred in the treated MDCK cells. Filamin A has been shown to be integral to the signalling of TGF-β; with filamin deficient cells shown to be un-responsive to TGF-β stimulation [290]. In primary renal proximal tubule cells, TGF-β was shown to promote cell adhesion and migration, as well as an increase in the organisation of the actin cytoskeleton to a state similar to that of the normal, functioning kidney epithelium [223]. This is likely an integral part of the final stages of tissue regeneration when the dedifferentiated epithelial cells have proliferated to an adequate level and have replaced the lost tissue and are now ready to re-differentiate into normal renal epithelial cells. However, this re-differentiation would probably not be advantageous at times when the dedifferentiated epithelial cells are still required to proliferate and fill the spaces left on the basement membrane left by dead cells.

It is unclear as to whether the decrease in abundance of filamin A would be advantageous or deleterious to the kidney after renal injury, however the possibility that the decrease in abundance observed here is connected to some form of TGF-β signalling disruption may indicate that the decrease in abundance of filamin A is connected to a

suppression of proteins linked to epithelial cell maturation designed to allow for the regeneration of lost tissue prior to the return of full re-differentiated epithelial cell function.

4.5.1.3 Response to hypoxia:

Hypoxia in *in vitro* cell culture is seen as any situation where the oxygen tension is between 0.1% and 5.0%. In the kidney *in vivo*, the oxygen tension is quite low compared to the amount of blood supplied to the kidneys [291]. The significance of the decreased in abundance of hypoxia response proteins in the treated MDCK flasks is not fully clear; as the treated and control MDCK cultures were incubated in the same incubator at the same time in identical external conditions. However, when proteins from **Table 4.4** attributed to this process are examined more closely, some interesting correlations with other processes can be observed.

N-myc down regulated gene 1 (NDRG1), is a protein with functions that are still being investigated in the literature. NRDG1 was shown to be decreased in abundance in the treated MDCK cells by 1.6 fold on average. NDRG1 levels have been shown to be increased in growth arrested differentiating cells and in situations of cell stress like DNA damage and hypoxia [292]. NDRG1 mRNA and protein is decreased in cells that have undergone transformation and increased during colon epithelial cell differentiation [293,294]. The decrease in abundance of this protein in the treated MDCK cells may reflect other changes to the differentiation state of the treated MDCK cells. The finding of the decrease in abundance of filamin A and its links to the TGF-β pathway regarding actin cytoskeletal organisation tethered with the decrease in abundance of NDRG1 both serve to promote a view that the treated cells may in some way be dedifferentiated. This therefore could be beneficial in a renal disease situation, whereby the dedifferentiation and proliferation of renal epithelial cells is vital to tubular recovery [288].

4.5.1.4 Integrin mediated signalling pathway:

Integrins are a family of cell surface receptors that exist in up to twenty heterodimeric forms in mammals [295,296]. The receptor functions as a dimer of a single α and a single β subunit, with classification of integrin receptor function most commonly categorised by the type of β subunit isoform present [295,297]. The most common type of integrin within the mammalian kidney is the β_1 integrin receptor type, with the α_2-, α_3- and α_6- β1, receptors identified in the distal tubule segment of the normal adult nephron [295]. Integrins function as

cell surface receptors that mediate cell-cell and cell-extracellular matrix adhesion and interactions. They are able to signal across the plasma membrane in both directions and have links to the actin cytoskeleton for intracellular signal transduction [296,298]. Expression of β1 integrins has been found to increase in some cases of renal disease like gomerulonephritis and diabetic nephropathy [295,297]. It is curious that in this experiment, changes to two different alpha integrin types were observed, but no change to any beta integrin subunits was identified. Integrin alpha-2 was decreased in abundance by approximately 1.64 times in the treated cells, whereas another subunit, integrin alpha-V was increased in abundance by approximately 1.77 times in the same set of treated cells. The similarity in the level of change in the two alpha integrin subunits without an observed change in any beta subunit levels may suggest that the expression of the two subunits are linked in some way and that removal of the integrin alpha-2 may be followed by its replacement in the cytoskeleton by integrin alpha-V. Confirmation of this possibility could be performed using immunofluorescent staining over time for the two alpha subunit types to monitor changes in expression and cellular localisation over time during treatment with the adipose tissue secretions. Integrin alpha-2 is a known collagen adhesion molecule on the surface of platelets involved in platelet aggregation [299]; this finding is consistent with previously discussed results regarding other platelet activation proteins decrease in abundance in the treated MDCK cells.

Paxillin is a focal adhesion molecule that functions primarily in the interaction with integrins and growth factor receptors to encourage cell migration [300]. Paxillin was shown to be decrease in abundance by 4.6 times on average in treated MDCK cells. Previously, increased paxillin expression in MDCK cells has been shown to be associated with the induction of cell scattering [301]. The decreased paxillin expression in the treated MDCK cells shown in this iTRAQ experiment is in concert with the previously discussed decrease in abundance of filamin A, both shown to be important in cell migration. This suggests, along with other decreases in actin cytoskeletal modification proteins (**Table 4.4**), that the MDCK cells motility may be broadly suppressed by treatment with the adipose tissue secretion preparation.

4.5.2 Up regulated protein processes:

4.5.2.1 Negative regulation of apoptosis:

Apoptosis describes the process of ordered, self-induced cell death. Apoptosis is an integral biological function of all cells within multicellular organisms, allowing for the proper control of tissue cell density, the removal of damaged cells and the elimination of cells liable for malignant transformation. The inhibition of apoptosis can be a beneficial way to prevent cell loss at the onset of a disease insult, particularly in the recovery from a disease like renal failure where it is known that post-injury, the remaining tubular epithelial cells proliferate rapidly to replace lost tubular epithelium and return the nephron to full functionality [288]. In the early stages of renal failure glomerular and tubular cell damage and stress is high, resulting in high apoptosis levels. Not all cells that initiate apoptotic pathways are damaged irreversibly; and the inhibition of apoptosis pathways in reversibly stressed or damaged cells can result in full recovery of the affected tissues/cells [288,302]. The treatment of the MDCK cells with this preparation of adipose tissue secretions has increased the abundance of a range of anti-apoptosis proteins (**Table 4.5**), indicating that in a renal failure scenario, epithelial cells (at least of the distal tubule) may be better able to recover from the initial insult. This could likely lead to faster tubule recovery due to a reduction in the level of tubular regeneration required to replace lost cells, as there are fewer requiring replacement.

The use of iTRAQ as the proteomic technique in this experiment produced a very large dataset. The initial desired approach intended was the use of 2-D electrophoresis based, differential display; as described in Chapter 3. However, the ability to generate sufficient cells was again the deciding factor in the determination of the final technique chosen, for many of the same reasons as those in Chapter 3. Keratin, type I cytoskeletal 18, highlights one of the reasons a 2-DE gel based approach was initially desired. The functions of Keratin, type I cytoskeletal 18 are broad and are highly dependent on post-translational modifications like phosphorylation and glycosylation [303]. A 2-DE based differential display experiment is capable of not only identifying gross relative changes in the abundances of different proteins, but is also capable of highlighting the relative abundances of different isoforms of the same protein that have undergone post-translational modification. The caveat however, is that the number of proteins identified in total would likely have been lower in a gel-based experiment and so identification of Keratin, type I cytoskeletal 18 may

not have been present on the sample gels. In addition, 2-DE preparations can be problematic when attempting to analyse very large or small proteins; iTRAQ is less limited in this regard. Clathrin heavy chain 1 for example, was identified in this iTRAQ experiment and has a molecular weight of approximately 191 kDa, which may not have been possible to detect or at least properly resolve in a 2-DE approach. Every proteomic technique has pros and cons at this time; iTRAQ was selected due to confidence in the technique to provide large datasets and a comprehensive overview of the MDCK cell proteome, the lack of distinction between protein isoforms due to post-translational modification was one necessary concession in this case due to sample size.

4.5.2.2 Acute phase response (APR):

The acute phase response (APR) refers to the complex series of actions that are induced immediately after cellular or tissue injury, insult or disease and constitute the earliest stages of the onset of inflammation [304]. The broad range of acute responses rapidly clear dead or damaged cells, eliminate infective agents responsible for the damage and initiate regenerative processes in the affected area. As is the case in many disease states, renal diseases exhibit signs of the acute phase response, particularly in cases of acute renal failure where the damage or disease process damages the kidney on a large scale, in a short amount of time. The proteins attributed to the APR identified in this research (**Table 4.5**), are not just APR-specific proteins but have broad roles in many mammalian biological processes.

Signal transducer and activator of transcription 3 isoform 1 (STAT 3), was increased in abundance in the treated cells by an average of 2.83 fold and is an important transcription factor implicated in tumorigenesis, wound healing and cellular responses to a wide range of growth factors [305]. STAT3 has been identified as a key part of cellular responses to IL-6 and epidermal growth factor receptor signalling [306,307] and has been shown to promote VEGF production [308] and is integral to production of anti-apoptotic proteins Bcl-2 and survivin [309,310]. Suppression of STAT3 activity can induce apoptosis in some cell populations [310]. The increased expression of STAT3 in the treated MDCK cells indicates an increased resistance to cell death by apoptosis consistent with the strong, broad anti-apoptosis response already discussed in this chapter.

As shown in Chapter 3, **Table 3.1**, there is a very high level of IL-6 present in the adipose tissue secretion media used to treat the MDCK cells (over 20 ng/mL, which is ~700 pM). Normal levels of IL-6 in humans are between 1 and 2 pg/mL (0.07 pM) [311-313]. The level of IL-6 present in the human adipose tissue secretions used in Chapter 3 and 4 is 10,000 times higher than the normal human serum concentration (**Table 3.3**). The studies presented in this thesis have focused on cell-based assays and analysing panels of protein markers. Whilst this is a powerful strategy when large datasets are generated and analysed as a whole, there can be significant shortcomings, especially where multiple gene products are produced from a single gene. IL-6 is a classic example of that scenario, where post-translational modifications and various protein complexes result in many different forms, with different functions, dependent on cell type, injury or disease status and immune response [314]. The antibody for IL-6 in the Bio-Plex™ assay is likely to recognise many forms of the protein, thus providing a total level rather than a functional assay. The network effect of complex mixtures of cytokines and other proteins in the secretion media is clearly more powerful than any individual cytokine which is present at abnormal concentrations. Although I discuss the potential effects of individual proteins based on the literature, the network effect of the complex mixture should be kept in mind. As IL-6 is a known inducer of STAT3, the high IL-6 level may be the cause of the increased STAT3 level observed in the treated cell population. However, many growth factors and cytokines have been implicated in activation of STAT3 and only a relatively small selection of twenty-seven cytokines and growth factors were assayed for using the Bio-Plex™ human cytokine assay. This means that given the known complexity of the adipose tissue and ASC secretomes, there may be more than one activator of STAT3 within the treatment media that is present at levels sufficient to cause STAT3 activation. To test the importance of IL-6 to increased STAT3 abundance in this system, it may be necessary to selectively remove or inactivate the IL-6 from the treatment media and assay specifically for changes to STAT3 expression. This may also reveal an alternate activation of STAT3, if the increase in STAT3 occurs regardless of IL-6 presence. Interestingly leptin, a well known adipokine, has also been identified as a specific activator of STAT3 in hypothalamic cells of mice *in vivo* [315]; indicating one possible alternate mechanism of STAT3 activation assuming that MDCK cells express the proper leptin receptor required, which is currently an area not fully explored.

Fibronectin is a well known protein constituent of the extracellular matrix with roles in cell-cell adhesion, cell-matrix adhesion, cell migration and differentiation; and matrix stabilisation [316]. Fibronectin is also a well known interacting partner with a variety of integrins, including the integrin alpha-V subunit [317]; which may indicate a relationship with the observed increased abundance of this subunit (**Table 4.5**). Another partner of fibronectin that was found to be increased in abundance was the collagen alpha-1(I) chain protein, known for its structural role in the extracellular matrix with fibronectin and their combined role in wound healing and fibrogenesis [318]. This may suggest that treatment with the adipose secretions has lead to a pro-fibrotic phenotype in the MDCK cells. However, fibronectin is also cited as a critical protein in tubulogenesis by MDCK cells *in vitro* and thus may be integral to the formation and indeed re-formation of the kidney tubule after insult [319].

The increased abundance of fibronectin was identified in all treated: control comparisons made in the analysis of this experiment, with a mean fold-change of ~2.8 times. This indicates a strong and specific response of the treated MDCK cells to the treatment may be taking place with regards to fibronectin expression. The reasons or mechanisms behind this response are currently unclear as fibronectin isoform expression shifts have been shown to occur in the presence of different cytokines and at different cell densities, including in MDCK cells [320]. Theoretically, up to twenty fibronectin isoforms exist in humans [321]. Briefly, cytokines like epidermal growth factor, HGF and TGF-β have been shown to change the isoform expression patterns of fibronectin in fibroblasts and in MDCK cells in culture. Both epidermal growth factor and TGF-β induce the EDA-fibronectin isoform which is known to be expressed by cells during pathological conditions where tissue remodelling, cell proliferation and cell migration is required [320]. HGF can also induce this EDA-fibronectin isoform, but can also encourage the production of non-EDA fibronectin in MDCK cells. At lower cell densities, HGF has been shown to be more effective at encouraging the EDA-fibronectin isoform in MDCK cells, but at higher cell densities, like those used in the culturing of the MDCK cells in this chapter, HGF does not highly induce the EDA isoform [320]. Alternatively, TGF-β was shown to be most potent at inducing the EDA isoform at higher cell densities [320]. For these reasons, the identification of the distinct isoforms of fibronectin within each sample would have been greatly advantageous. Changes in the isoform expression of fibronectin in this manner may have been better elucidated through the use of a 2-DE approach. Without identification of

the actual isoform(s) that were increased in abundance in this experiment in the treated MDCK cells, it is not clear whether the increased presence of fibronectin would be detrimental or beneficial in a renal care scenario.

4.5.2.3 Negative regulation of epidermal growth factor signalling pathway:

The involvement and significance of the two proteins identified to be part of the negative regulation of epidermal growth factor signalling is currently unclear as epidermal growth factor signalling is potentially highly important to the regeneration of the kidney after insult [322]. Clathrin heavy chain 1 isoform 1 (also called CHC17) is known in the Uniprot protein database (www.uniprot.org) to have functions in the normal signalling and the negative regulation of signalling in the epidermal growth factor signalling pathway. CHC17 is ubiquitously expressed in human cells and has been extensively studied for its roles in endocytosis and mitosis, for which it is essential [323]. Increased abundance of this protein may not be connected with its roles in any form of epidermal growth factor signalling, but with its roles in mitosis. This would be consistent with the concomitant increase in other proteins linked to mitotic functions discussed later in this chapter.

The protein known as epidermal growth factor receptor pathway substrate 15-like 1 isoform 4 (eps15R isoform 4) is a protein that is likely to be a component of clathrin-coated pits required for receptor-mediated endocytosis [324]. There are currently four known isoforms of the eps15R protein that are formed through alternative splicing of the eps15R gene, each of them are proposed to have distinct, but as-yet unknown functions within the cell associated with endocytic processes involving clathrin pits and epidermal growth factor receptor signalling [324,325]. Evidence for the negative regulation of the epidermal growth factor pathway in the literature concerning eps15R is difficult to find. The identification of eps15R in this experiment may identify a possible role for this protein in aiding the functioning of CHC17 in a pro-mitotic capacity, this is purely speculation however.

The functional ambiguity of the two proteins identified as part of the epidermal growth factor signalling biological process may indicate that these proteins are involved in either negative or positive regulation of epidermal growth factor signalling in a purely mechanistic way, meaning that other proteins are responsible for the true regulatory steps that decide the outcome of eps15R and CHC17 functions.

4.5.2.4 Evidence for increased metabolic activity in the treated MDCK cells:

Many of the remaining proteins shown to be present in increased in abundance in **Table 4.5** are associated with the production or use of energy in the form of either glucose or ATP. These proteins indicate a large-scale, broad increase in the energy production and requirement for the treated MDCK cells and are probably (or at least in part) associated with the functions of the proteins featured in **Table 4.6** that indicate a concomitant increase in the mitotic activity of the treated cells. The increased metabolic activity of the treated cells is consistent with the possibility of a dedifferentiated cellular state in the treated MDCK cells, as discussed in section **4.5.1.2**, connected to the decrease in abundance of filamin A and the increased mitotic proteins identified in **Table 4.6**. In short, the decrease in abundance of filamin A and other cytoskeletal organising proteins makes the treated cell cytoskeleton less organised, more plastic and more amenable to increased mitosis. The metabolic proteins discussed here provide the energy for these processes, including the likely cell division being encouraged by the adipose secretion media.

4.5.2.5 Evidence for increased mitosis in the treated MDCK cells:

The proteins featured in **Table 4.6** all have functions associated with the progression of cell division and the cell cycle. The increased expression of these proteins indicates a greater level of mitosis in the treated MDCK cells over the controls. As previously discussed, this is consistent with the decreased cytoskeletal organisation and increased metabolic activity in the treated cells. This would likely be advantageous in a renal failure scenario as the tubular epithelial cells would be further encouraged to divide and replace lost cells and may aid in a faster tubular recovery.

4.6 Conclusions:

As discussed in the PRC results of Chapter 3, blocking TGF-β signalling may be integral to the proteomic changes observed in the treated MDCK population. The work in this chapter identified significant decreases in the abundance of proteins involved in cytoskeletal organisation, a process critical to fully differentiated distal and proximal tubular epithelium. If the potential for the importance TGF-β had been known earlier, another set of treated MDCK cells treated with a specific TGF-β signalling blocker would have been included in the iTRAQ analysis. This would have allowed for an assessment of how many changes induced by the adipose secretions were due to TGF-β signal blockade, if any.

In future or related experiments testing the effects of human adipose secretions on cell populations, changes to the treated MDCK cell cytoskeleton could be more directly observed using immunocytochemistry staining . Temporal changes to the expression of integrin alpha 2, integrin alpha V and filamin A are suggested targets for observation.

The apparent increase in metabolic rate in the treated MDCK cells could be verified directly using an assay for intracellular ATP levels. One example is the ATP Determination kit by Life Technologies (Catalogue # A22066), which uses a bioluminescence assay for quantitative determination of ATP with recombinant firefly luciferase and its substrate D-luciferin down to 0.1 picomole.

This chapter has shown that adipose derived secretions may have a beneficial effect on tubular recovery after renal injury. The results indicate that the treated MDCK cells exhibited a cytoskeletal structure that was less organised due to the decreased presence of filamin A and NDRG1. These results are consistent with the increased expression of mitotic and metabolic proteins in the treated cells. The treated cells also exhibited signs of a greater resistance to apoptotic stimuli than the controls. Taken together, the treated MDCK cells appear to represent a cell population capable of efficient cell division with a higher resistance to apoptotic stimuli. As the dedifferentiation and division of tubular epithelia has been shown to be essential to tubular recovery after renal insult, it is likely that the effects induced in the treated MDCK cells would be beneficial to aiding the recovery of the kidney after such an event.

Chapter 5: Final conclusions and future directions

This project was the first adipose derived cell project conducted within the laboratories of Dr Ben Herbert at both UTS and Macquarie University. The work performed here represents part of the maturation of our groups' and particularly my own understanding of cell culture, renal failure, adipose derived cells, cell therapy, regenerative medicine, adipokines and mesenchymal stem cell secretions. The 'waterfront' was very wide with regards to the application of adipose cell and secretion-based therapies. This project represents the first set of experiments designed to test the potential for application of adipose derived secretions to renal failure in a broad sense. The work shown here has displayed a novel combination of the proteomic tools iTRAQ and Bio-Plex™, and cell-based assays in order to gain meaningful data on the usefulness of adipose tissue secretions to the amelioration of renal failure.

Cell-based assays are important *in vitro* tools for assessing the effects of a biologically active compound or a complex biological product on a target population of cells. They have been broadly used in cancer research, early pharmaceutical screening, immunology, and other research fields [326,327]. Cell based assays are important because they provide information on the biological activity or toxicity of a given drug or treatment regime, not just characterisation by presence or abundance. Appropriate cell-based assays can demonstrate the complex downstream effects of the sample on the target cell, assuming the user has an analysis method for the cell. The use of the PRCs and MDCKs in the cell-based assays described here enabled for an analysis of the effect of a single complex adipose secretion mixture on the target cells. The xenogeneic approach described in these studies extended the cell-based assay approach and enabled the changes in the treatment mixture to be determined in the same experiment as any changes in the treated cells and their secretions were determined. The large scale relative quantification of the treated and control cell proteomes as well as analysis of the secretion profiles provided a comprehensive view of the biological effect of adipose tissue secretions. These data form an important first step towards a secretion based therapeutic trial in an animal model of renal disease.

As discussed previously, the use of the Bio-Plex™ multiplexed assays in Chapter 3 to temporally analyse both human adipose secretion uptake and rat PRC secretion production was a novel application of this technology to this type of cell-based assay. The panels used

for the analysis of twenty-seven human and twenty-three rat cytokines provided a snap-shot of the cytokine changes across many biologically relevant pathways. Many proteins and cytokines have a broad range of biological functions and thus measuring single analytes as a surrogate marker for cell health or activity can yield confounding results. In the past, single biomarkers were searched for in order to facilitate faster and cheaper detections systems *in vitro* and because biomarker discovery technologies were poorly developed. Multiplexed analysis systems are becoming increasingly utilised due to advances in both discovery technology and multiplex analyses platforms, leading to reduced cost. The use of panels of biomarkers, rather than assays for single analytes is increasing and these are now understood to be a more comprehensive form of biological analysis [328]. Examples include early cancer [329] and sepsis [330] detection. The use of Bio-Plex™ multiplex assays has allowed for the monitoring of many biologically active cytokines in the same culture system simultaneously, giving comprehensive information on the levels of each analyte down to picogram quantities and providing a more rounded view of the actions of the adipose secretions on the PRCs.

Adipose stem cell therapies and secretion-based therapies have been proposed as a potential treatment for a growing number of diseases by many groups worldwide. Arthritis [3], myocardial infarction [4-6], stroke [7], multiple sclerosis [8], acute ischemic renal failure [9], liver cirrhosis [10], hair growth [11] and wound healing [12-14] studies have all been conducted to investigate the therapeutic benefits of the application of BMSCs and ASCs. Investigations into the use of adipose derived cell therapies has heavily implicated the secretion of proteins, hormones, growth factors and cytokines in the therapeutic benefits observed [12,13,30]. This is also seen to be the case in acute renal failure models through the work of Togel *et al* [9,29] and even more recently in a chronic renal failure model in work done by van Koppen *et al* [331]. My supervisor and I both hypothesised that a complex mixture of secretions from ASCs and other cells from adipose tissue could be therapeutically beneficial to the kidney in a renal disease setting. These published studies provide further evidence for our hypotheses.

This project utilised *in vitro* models of the mammalian kidney in experiments designed to assess the application of adipose derived secretions to renal failure. The preparation of adipose derived secretions used for the main two chapters of this thesis

(Chapters 3 and 4) were optimised specifically for the enhancement of the ASC portion of the adipose cell population *in vitro* while also containing proteins secreted by the other cellular constituents of the tissue.

As previously discussed, these experiments were intended as a set of broad-scale analyses to provide indications for the usefulness of adipose tissue derived secretions in the treatment of renal disease. This project has provided a list of protein pathways that are candidates for a set of more in-depth future investigations into the potential for the applications of adipose tissue secretions in the treatment of renal disease. The two cell-based *in vitro* models described were selected to provide an overview of the mammalian kidney. However, the use of cells in culture can provide results that would not be obtained *in vivo* due to a range of potential issues. Changes undergone by cells *in vitro* are well documented and can alter the outcomes of a particular treatment so that they no longer match the *in vivo* scenario. The loss of cell-cell contacts, three dimensional structure, broad temperature variation, feast and famine feeding cycles, treatment with trypsin (or other cell stripping reagents) can all affect cells in culture and contribute to potential deviation from *in vivo* behaviour. The use of *in vitro* models in this project has provided some advantages over the use of *in vivo* experiments in this early stage of investigation. This project began with a broad hypothesis on the likely renoprotective effects of adipose tissue secretions. This hypothesis was well supported by the available literature on the treatment of renal failure with mesenchymal stem cells [9]. However there was not a specific hypothesis as to the targets or pathways that would be affected by the treatment of the renal cells with the secretions. The use of cultured cells allowed for a less complex cellular sub-section of the kidney to be explored so that specific target proteins and pathways might be identified prior to the use of *in vivo* models in subsequent projects. This approach has prevented animal subjects from the suffering associated with the surgical or chemical induction of renal disease while these targets have been identified. The use of MDCK cells for example, has provided this project with results specifically relating to the renal epithelium, allowing for the planning of more refined *in vivo* future experiments. The following sections detail the findings of each chapter and highlight future directions that can be applied to new projects in a targeted fashion to further elucidate the effects of adipose secretion treatment on renal cells *in vitro* and *in vivo*.

Thoughts from Chapter 2:

Chapter 2 did not reveal definitive results that clearly indicated whether adipose derived secretions would positively or negatively affect renal cells *in vitro*. There were a number of technical challenges associated with the 2-DE approaches taken at the time that affected the obtaining of statistically significant datasets. The novel use of the PRCs *in vitro* as a type of 'biological filter' to select biotinylated adipose secretions was an interesting avenue of exploration and should be investigated further, potentially with high sensitivity MS analysis. The identification of a detectable apparent interaction of the biotinylated secretions with the PRCs indicates that this sort of system could be transposed to other experiments where the biologically relevant proteins within a complex mixture need to be identified. Of course, this would require a large amount of optimisation and experimentation before being a viable cell assay option for this type of application. Key aspects of the optimisation would involve the concentration of biotinylated proteins to be put on the cells and the required exposure time for optimal binding.

Common findings from Chapters 3 and 4:

The multiplexed cytokine analysis presented in Chapter 3, sections **3.5.2** and **3.5.3** presented novel applications of the Bio-Plex™ platforms to measure the potential cytokine up-take by the PRCs and cytokine output of the cells in response to the adipose secretion treatment within the one *in vitro* system. The novel nature of the temporal human cytokine experiment (section **3.5.3**) meant that this results set was explored more fully than the temporal analysis of the PRC secretory response (**3.5.2**). The human Bio-Plex™ analysis revealed that nine of twenty-seven human cytokines assayed for exhibited a decrease in concentration over time in the presence of the PRCs that was greater than the controls. Many of the human cytokines found to be decreased in the presence of the PRCs over time could be related to the changes in the treated PRCs observed in the iTRAQ analysis as discussed in section **3.5.3**. Through this novel application of the Bio-Plex™ technology, the identification of some of the proteins that may be responsible for the proteomic changes in the treated PRCs was achieved. This fulfilled the aims of the experiment and has provided IL-12, IL-16, IFN-g and VEGF as targets for further investigation. Confirmation of the uptake, utilisation or binding of these proteins by the PRCs from the secretions could be completed using immunocytochemistry techniques and specific fluorescent monoclonal antibodies to

the analytes. In this way, temporal visual analysis of the localisation of these cytokines may be observed using repeated live cell fluorescence microscopy or flow cytometry. For a more detailed analysis on the effects of specific analytes, the treatment of the PRCs with human adipose tissue secretions may be repeated using secretions that contain a competing antibody of a selected human analyte, VEGF for example. This will replicate the conditions of the PRC treatment demonstrated here, but will negate the function of VEGF. A comparison of the results from the 'anti-VEGF' secretions on the PRCs to a normal secretion control will provide more evidence of the effects of VEGF (or any other selected analyte) on the system as a whole.

The iTRAQ analyses performed were aimed at illuminating the effects of the adipose secretion preparation on cells of the mammalian kidney. Uncharacterised mesangial cells of the glomerulus (PRCs) and tubular epithelial cells of the distal convoluted tubule (MDCK cells) were utilised, providing a more rounded view of the possible effects of the adipose secretions on the kidney overall. Through iTRAQ analysis, Chapters 3 and 4 highlighted a broad range of proteins that had increased or decreased abundance in the treated renal cells compared to non-treated controls. The same adipose secretion preparation was used to treat the PRCs of Chapter 3 and the MDCKs of Chapter 4. Having a single homogenous human adipose secretions batch for both chapters meant that the results of Chapter 3 and 4 could be directly compared in terms of the effects of the secretions on different cell types.

The treated cell populations of Chapter 3 and Chapter 4 both expressed proteins known to suppress apoptosis. Given the difference in function and species between the two cell types, it is very likely that the PRCs and MDCK cells express a distinct array of surface receptors, making them sensitive to different sets of signals from the adipose secretions. The identification of proteins with anti-apoptotic activity that are distinct between the PRC and MDCK cell proteomes indicates that the adipose secretions may possess broad anti-apoptotic activity through a range of different pathways. The indications that adipose secretions prepared using the partial digest method may be able to suppress apoptosis in a variety of cell types are promising for prospective use as a treatment to renal failure *in vivo*.

Proteins involved in TGF-β signalling pathways were observed to be decreased in abundance in both the treated PRC and MDCK cell populations. Proteins found to be

influenced by the actions of TGF-β, like cytoskeletal organisation proteins were also found to be similarly altered in both the PRCs and MDCK cells. This indicates a key role for TGF-β suppression in the mode of action of the secretion mixture. As discussed in detail in section **3.5.1**, TGF-β can induce a very complex array of cellular responses [332] and is a known proponent of renal fibrosis in diabetes models [219] and other forms of renal dysfunction [333]. Suppression of TGF-β signalling in renal failure models can significantly reduce the level of glomerular scarring and extracellular matrix deposition post injury [333,334]. TGF-β is not only a prominent feature of renal fibrosis, but is heavily involved in the progression of almost all chronic and fibrotic diseases [221,334]. The blockade of TGF-β observed in this thesis warrants more in-depth investigations of the actions of these secretions and potential for application to treat a wide range of TGF-β affected diseases. Assays for known suppressors of TGF-β signalling like decorin, Smad 6 and Smad 7 should be completed on the adipose secretions in order to assess whether the TGF-β suppression may be due to the presence of known or novel suppressors. Assays for the production of TGF-β suppressors in treated cell populations may also be completed in order to see if the suppression is direct or through the induction of a cellular response. For this purpose, a xenogeneic experiment using non-human cells treated with human-derived adipose secretions may be advantageous in order to simultaneously assess the levels of known human TGF-β inhibitors within the secretions and the levels of non-human inhibitors potentially produced by the treated cells.

Final thoughts:

The large datasets obtained in Chapters 3 and 4 have provided broad overview of the range of actions induced by treatment with adipose tissue secretions on rat primary renal cells and Madin Darby Canine Kidney cells. It has been shown that between the two treated cell types, the major modes of action of the secretion mixture appear to broadly suppress apoptotic stimuli and inhibit the signalling of transforming growth factor beta. Both of these effects have been shown to be beneficial to the recovery of the kidney after renal insult. Thus the experiments described here have provided important and informative results that indicate a strong potential for the use of adipose derived secretions as a treatment for renal diseases in the future. In order to address the possibility that the observed PRC and MDCK results were artefact caused by a cellular reaction to the xenogeneic treatment, it is suggested that a follow-up assay be conducted using primary or immortalised human renal

cells treated with human adipose secretions. Primary human tissue can be obtained commercially through companies like Capital Biosciences Inc. The human renal cells can then be assessed using iTRAQ and Bio-Plex™ analysis in a similar manner as previously described here in order to ensure that the same or similar effects are observed. Once this has been shown, it is suggested that these results become the foundation of the justification for an *in vivo* animal trial designed to test the effects of adipose derived secretions on an animal model of renal failure. Follow-up *in vitro* based studies could also be completed in order to more fully explore the TGF-β signal blocking activity of the adipose secretions as described earlier.

References:

1. Tiraby, C*., et al.* Acquirement of brown fat cell features by human white adipocytes. *The Journal of biological chemistry* **278**, 33370-33376 (2003).
2. Zuk, P.A*., et al.* Multilineage cells from human adipose tissue: implications for cell-based therapies. *Tissue Eng* **7**, 211-228 (2001).
3. Jorgensen, C*., et al.* Mesenchymal stem cells and rheumatoid arthritis. *Joint Bone Spine* **70**, 483-485 (2003).
4. Kawada, H*., et al.* Nonhematopoietic mesenchymal stem cells can be mobilized and differentiate into cardiomyocytes after myocardial infarction. *Blood* **104**, 3581-3587 (2004).
5. Miyahara, Y*., et al.* Monolayered mesenchymal stem cells repair scarred myocardium after myocardial infarction. *Nat Med* **12**, 459-465 (2006).
6. Mangi, A.A*., et al.* Mesenchymal stem cells modified with Akt prevent remodeling and restore performance of infarcted hearts. *Nat Med* **9**, 1195-1201 (2003).
7. Ohtaki, H*., et al.* Stem/progenitor cells from bone marrow decrease neuronal death in global ischemia by modulation of inflammatory/immune responses. *Proc Natl Acad Sci U S A* **105**, 14638-14643 (2008).
8. Riordan, N.H*., et al.* Non-expanded adipose stromal vascular fraction cell therapy for multiple sclerosis. *J Transl Med* **7**, 29 (2009).
9. Togel, F*., et al.* Administered mesenchymal stem cells protect against ischemic acute renal failure through differentiation-independent mechanisms. *Am J Physiol Renal Physiol* **289**, F31-42 (2005).
10. Kharaziha, P*., et al.* Improvement of liver function in liver cirrhosis patients after autologous mesenchymal stem cell injection: a phase I-II clinical trial. *Eur J Gastroenterol Hepatol* **21**, 1199-1205 (2009).
11. Park, B.S*., et al.* Hair growth stimulated by conditioned medium of adipose-derived stem cells is enhanced by hypoxia: evidence of increased growth factor secretion. *Biomed Res* **31**, 27-34 (2010).
12. Kim, W.S*., et al.* Wound healing effect of adipose-derived stem cells: a critical role of secretory factors on human dermal fibroblasts. *J Dermatol Sci* **48**, 15-24 (2007).
13. Oh, J.Y*., et al.* The anti-inflammatory and anti-angiogenic role of mesenchymal stem cells in corneal wound healing following chemical injury. *Stem Cells* **26**, 1047-1055 (2008).
14. Falanga, V*., et al.* Autologous bone marrow-derived cultured mesenchymal stem cells delivered in a fibrin spray accelerate healing in murine and human cutaneous wounds. *Tissue engineering* **13**, 1299-1312 (2007).
15. Fain, J.N., Madan, A.K., Hiler, M.L., Cheema, P. & Bahouth, S.W. Comparison of the release of adipokines by adipose tissue, adipose tissue matrix, and adipocytes from visceral and subcutaneous abdominal adipose tissues of obese humans. *Endocrinology* **145**, 2273-2282 (2004).
16. Alvarez-Llamas, G*., et al.* Characterization of the human visceral adipose tissue secretome. *Molecular & Cellular Proteomics* **6**, 589-600 (2007).
17. Maury, E*., et al.* Adipokines oversecreted by omental adipose tissue in human obesity. *American Journal of Physiology-Endocrinology and Metabolism* **293**, E656-E665 (2007).
18. Lau, D.C., Dhillon, B., Yan, H., Szmitko, P.E. & Verma, S. Adipokines: molecular links between obesity and atheroslcerosis. *Am J Physiol Heart Circ Physiol* **288**, H2031-2041 (2005).
19. Steppan, C.M., Bailey, S. T., Bhat, S., Brown, E. J., Banerjee, R. R., Wright, C. M., Patel, H. R., Ahima, R. S., Lazar, M. A. The hormone resistin links obesity to diabetes. *Nature* **409**, 307 (2001).
20. Fukuhara, A*., et al.* Visfatin: a protein secreted by visceral fat that mimics the effects of insulin. *Science* **307**, 426-430 (2005).

21. Hida, K.*, et al.* Visceral adipose tissue-derived serine protease inhibitor: A unique insulin-sensitizing adipocytokine in obesity. *Proceedings of the National Academy of Sciences of the United States of America* **102**, 10610-10615 (2005).
22. Hauner, H. Secretory factors from human adipose tissue and their functional role. *Proceedings of the Nutrition Society* **64**, 163-169 (2005).
23. Mohamed-Ali, V., Pinkney, J.H. & Coppack, S.W. Adipose tissue as an endocrine and paracrine organ. *International Journal of Obesity & Related Metabolic Disorders* **22**, 1145 (1998).
24. Margetic, S., Gazzola, C., Pegg, G. G., Hill, R. A. Leptin: a review of its peripheral actions and interactions. *Int J Obes Relat Metab Disord* **26**, 1407-1433 (2002).
25. Frayn, K.N., Karpe, F., Fielding, B.A., Macdonald, I.A. & Coppack, S.W. Integrative physiology of human adipose tissue. *Int J Obes Relat Metab Disord* **27**, 875-888 (2003).
26. Lembo, G.*, et al.* Leptin induces direct vasodilation through distinct endothelial mechanisms. *Diabetes* **49**, 293-297 (2000).
27. Tanida, M., Iwashita, S., Ootsuka, Y., Terui, N., Suzuki, M. Leptin injection into white adipose tissue elevates renal sympathetic nerve activity dose-dependently through the afferent nerves pathway in rats. *Neuroscience Letters* **293**, 107-110 (2000).
28. McMahon, G.A.*, et al.* Plasminogen Activator Inhibitor-1 Regulates Tumor Growth and Angiogenesis. *Journal of Biological Chemistry* **276**, 33964-33968 (2001).
29. Togel, F.*, et al.* Vasculotropic, paracrine actions of infused mesenchymal stem cells are important to the recovery from acute kidney injury. *American journal of physiology. Renal physiology* **292**, F1626-1635 (2007).
30. Shabbir, A., Zisa, D., Suzuki, G. & Lee, T. Heart failure therapy mediated by the trophic activities of bone marrow mesenchymal stem cells: a noninvasive therapeutic regimen. *Am J Physiol Heart Circ Physiol* **296**, H1888-1897 (2009).
31. Sommer, G.*, et al.* Secretory products from human adipocytes stimulate proinflammatory cytokine secretion from human endothelial cells. *J Cell Biochem* **106**, 729-737 (2009).
32. Bokarewa, M., Nagaev, I., Dahlberg, L., Smith, U. & Tarkowski, A. Resistin, an adipokine with potent proinflammatory properties. *J Immunol* **174**, 5789-5795 (2005).
33. Kos, K.*, et al.* Adiponectin and resistin in human cerebrospinal fluid and expression of adiponectin receptors in the human hypothalamus. *The Journal of clinical endocrinology and metabolism* **92**, 1129-1136 (2007).
34. Van Harmelen, V.*, et al.* Leptin secretion from subcutaneous and visceral adipose tissue in women. *Diabetes* **47**, 913-917 (1998).
35. Trayhurn, P. & Beattie, J.H. Physiological role of adipose tissue: white adipose tissue as an endocrine and secretory organ. *Proceedings of the Nutrition Society* **60**, 329-339 (2001).
36. Spranger, J.*, et al.* Adiponectin and protection against type 2 diabetes mellitus. *Lancet* **361**, 226-228 (2003).
37. Trayhurn, P. & Wood, I.S. Adipokines: inflammation and the pleiotropic role of white adipose tissue. *British Journal of Nutrition* **92**, 347-355 (2004).
38. Harmancey, R.*, et al.* The vasoactive peptide adrenomedullin is secreted by adipocytes and inhibits lipolysis through NO-mediated beta-adrenergic agonist oxidation. *FASEB J* **19**, 1045-1047 (2005).
39. Chopp, M. & Li, Y. Treatment of neural injury with marrow stromal cells. *The Lancet Neurology* **1**, 92-100 (2002).
40. Koc, O.N.*, et al.* Rapid hematopoietic recovery after coinfusion of autologous-blood stem cells and culture-expanded marrow mesenchymal stem cells in advanced breast cancer patients receiving high-dose chemotherapy. *J Clin Oncol* **18**, 307-316 (2000).
41. Kunter, U.*, et al.* Transplanted mesenchymal stem cells accelerate glomerular healing in experimental glomerulonephritis. *J Am Soc Nephrol* **17**, 2202-2212 (2006).

42. Lange, C.*, et al.* Administered mesenchymal stem cells enhance recovery from ischemia/reperfusion-induced acute renal failure in rats. *Kidney Int* **68**, 1613-1617 (2005).
43. Majumdar, M.K., Thiede, M.A., Mosca, J.D., Moorman, M. & Gerson, S.L. Phenotypic and functional comparison of cultures of marrow-derived mesenchymal stem cells (MSCs) and stromal cells. *J Cell Physiol* **176**, 57-66 (1998).
44. Caplan, A.I. & Dennis, J.E. Mesenchymal stem cells as trophic mediators. *J Cell Biochem* **98**, 1076-1084 (2006).
45. Caplan, A.I. & Correa, D. The MSC: an injury drugstore. *Cell Stem Cell* **9**, 11-15 (2011).
46. Caplan, A.I. 2010 lifetime achievement award of Tissue Engineering and Regenerative Medicine International Society--north America: Arnold I. Caplan, Ph.D. *Tissue Eng Part A* **17**, 267 (2011).
47. Caplan, A.I. Why are MSCs therapeutic? New data: new insight. *The Journal of Pathology* **217**, 318-324 (2009).
48. Van Gaal, L.F., Mertens, I.L. & De Block, C.E. Mechanisms linking obesity with cardiovascular disease. *Nature* **444**, 875-880 (2006).
49. Bahia, L.*, et al.* Relationship between adipokines, inflammation, and vascular reactivity in lean controls and obese subjects with metabolic syndrome. *Clinics (Sao Paulo)* **61**, 433-440 (2006).
50. Ryan, J.M., Barry, F., Murphy, J.M. & Mahon, B.P. Interferon-gamma does not break, but promotes the immunosuppressive capacity of adult human mesenchymal stem cells. *Clin Exp Immunol* **149**, 353-363 (2007).
51. Kim, K.W.*, et al.* Relationship between adipokines and manifestations of childhood asthma. *Pediatr Allergy Immunol* **19**, 535-540 (2008).
52. Radon, K.*, et al.* Serum leptin and adiponectin levels and their association with allergic sensitization. *Allergy* **63**, 1448-1454 (2008).
53. Halleux, C.M.*, et al.* Secretion of adiponectin and regulation of apM1 gene expression in human visceral adipose tissue. *Biochem Biophys Res Commun* **288**, 1102-1107 (2001).
54. Lin, F. Stem cells in kidney regeneration following acute renal injury. *Pediatr Res* **59**, 74R-78R (2006).
55. Morigi, M.*, et al.* Mesenchymal stem cells are renotropic, helping to repair the kidney and improve function in acute renal failure. *J Am Soc Nephrol* **15**, 1794-1804 (2004).
56. Arriero, M., Brodsky, S.V., Gealekman, O., Lucas, P.A. & Goligorsky, M.S. Adult skeletal muscle stem cells differentiate into endothelial lineage and ameliorate renal dysfunction after acute ischemia. *Am J Physiol Renal Physiol* **287**, F621-627 (2004).
57. Black, L.L.*, et al.* Effect of intraarticular injection of autologous adipose-derived mesenchymal stem and regenerative cells on clinical signs of chronic osteoarthritis of the elbow joint in dogs. *Vet Ther* **9**, 192-200 (2008).
58. Nakagami, H.*, et al.* Novel autologous cell therapy in ischemic limb disease through growth factor secretion by cultured adipose tissue-derived stromal cells. *Arterioscler Thromb Vasc Biol* **25**, 2542-2547 (2005).
59. Fantuzzi, G. Adipose tissue, adipokines, and inflammation. *Journal of Allergy and Clinical Immunology* **115**, 911-919 (2005).
60. Kershaw, E.E. & Flier, J.S. Adipose Tissue as an Endocrine Organ. *J Clin Endocrinol Metab* **89**, 2548-2556 (2004).
61. Weisberg, S.P., McCann, D., Desai, M., Rosenbaum, M., Leibel, R. L., Ferrante, A. W., Jr. Obesity is associated with macrophage accumulation in adipose tissue. *J Clin Invest* **112**, 1796-1808 (2003).
62. Curat, C.A., Miranville, A., Sengenes, C., Diehl, M., Tonus, C., Busse, R., Bouloumie, A. From blood monocytes to adipose tissue-resident macrophages: induction of diapedesis by human mature adipocytes. *Diabetes* **53**, 1285-1292 (2004).

63. Ouchi, N., Kihara, S., Arita, Y., Maeda, K., Kuriyama, H., Okamoto, Y., Hotta, K., Nishida, M., Takahashi, M., Nakamura, T., Yamashita, S., Funahashi, T., Matsuzawa, Y. Novel Modulator for Endothelial Adhesion Molecules : Adipocyte-Derived Plasma Protein Adiponectin. *Circulation* **100**, 2473-2476 (1999).
64. Yamauchi, T., Kamon, J., Waki, H., Terauchi, Y., Kubota, N., Hara, K., Mori, Y., Ide, T., Murakami, K., Tsuboyama-Kasaoka, N., Ezaki, O., Akanuma, Y., Gavrilova, O., Vinson, C., Reitman, M. L., Kagechika, H., Shudo, K., Yoda, M., Nakano, Y., Tobe, K., Nagai, R., Kimura, S., Tomita, M., Froguel, P., Kadowaki, T. The fat-derived hormone adiponectin reverses insulin resistance associated with both lipoatrophy and obesity. *Nat Med* **7**, 941-946 (2001).
65. Kojima, S*., et al.* Levels of the adipocyte-derived plasma protein, adiponectin, have a close relationship with atheroma. *Thrombosis Research* **115**, 483-490 (2005).
66. Yamamoto, C., Urano, A., Fujiwara, Y., Kaji, T. Adiponectin as an inducer of decorin synthesis in cultured vascular smooth muscle cells. *Life Sciences* **83**, 447-452 (2008).
67. Montague, C.T. & Farooqi, I.S. Congenital leptin deficiency is associated with severe early-onset obesity in humans. *Nature* **387**, 903 (1997).
68. Considine, R.V., Sinha, M. K., Heiman, M. L., Kriauciunas, A., Stephens, T. W., Nyce, M. R., Ohannesian, J. P., Marco, C. C., McKee, L. J., Bauer, T. L., Caro, J. F. Serum Immunoreactive-Leptin Concentrations in Normal-Weight and Obese Humans. *N Engl J Med* **334**, 292-295 (1996).
69. Kimura, K*., et al.* Involvement of Nitric Oxide in Endothelium-Dependent Arterial Relaxation by Leptin. *Biochemical and Biophysical Research Communications* **273**, 745-749 (2000).
70. Lord, G.M., Matarese, G., Howard, J. K., Baker, R. J., Bloom, S. R., Lechler, R. I. Leptin modulates the T-cell immune response and reverses starvation-induced immunosuppression. *Nature* **394**, 897-901 (1998).
71. Ring, B.D*., et al.* Systemically and topically administered leptin both accelerate wound healing in diabetic ob/ob mice. *Endocrinology* **141**, 446-449 (2000).
72. Patel, L., Buckels, A. C., Kinghorn, I. J., Murdock, P. R., Holbrook, J. D., Plumpton, C., Macphee, C. H., Smith, S. A. . Resistin is expressed in human macrophages and directly regulated by PPAR[gamma] activators. *Biochemical and Biophysical Research Communications* **300**, 472-476 (2003).
73. Kim, K.H., Lee, K., Moon, Y.S. & Sul, H.S. A cysteine-rich adipose tissue-specific secretory factor inhibits adipocyte differentiation. *J Biol Chem* **276**, 11252-11256 (2001).
74. Holcomb, I.N*., et al.* FIZZ1, a novel cysteine-rich secreted protein associated with pulmonary inflammation, defines a new gene family. *EMBO J* **19**, 4046-4055 (2000).
75. Park, H.S., Park, J.Y. & Yu, R. Relationship of obesity and visceral adiposity with serum concentrations of CRP, TNF-[alpha] and IL-6. *Diabetes Research and Clinical Practice* **69**, 29-35 (2005).
76. Yudkin, J.S., Kumari, M., Humphries, S.E. & Mohamed-Ali, V. Inflammation, obesity, stress and coronary heart disease: is interleukin-6 the link? *Atherosclerosis* **148**, 209-214 (2000).
77. Gieling, R.G., Wallace, K. & Han, Y. Interleukin-1 participates in the progression from liver injury to fibrosis. *Am J Physiol Gastrointest Liver Physiol* **296**, G1324-1331 (2009).
78. Garcia-Welsh, A., Schneiderman, J.S. & Baly, D.L. Interleukin-1 stimulates glucose transport in rat adipose cells: Evidence for receptor discrimination between IL-1[beta] and IL-1[alpha]. *FEBS Letters* **269**, 421-424 (1990).
79. Dinarello, C.A. Biologic basis for interleukin-1 in disease. *Blood* **87**, 2095-2147 (1996).
80. Kitamura, K*., et al.* Adrenomedullin: A Novel Hypotensive Peptide Isolated from Human Pheochromocytoma. *Biochemical and Biophysical Research Communications* **192**, 553-560 (1993).
81. Hino, M*., et al.* Expression and regulation of adrenomedullin in renal glomerular podocytes. *Biochemical and Biophysical Research Communications* **330**, 178-185 (2005).

82. Hamid, S.A. & Baxter, G.F. Adrenomedullin: regulator of systemic and cardiac homeostasis in acute myocardial infarction. *Pharmacology & Therapeutics* **105**, 95-112 (2005).
83. Ishimitsu, T., Ono, H., Minami, J., Matsuoka, H. Pathophysiologic and therapeutic implications of adrenomedullin in cardiovascular disorders. *Pharmacology & Therapeutics* **111**, 909-927 (2006).
84. Temmesfeld-Wollbruck, B., Hocke, A.C., Suttorp, N. & Hippenstiel, S. Adrenomedullin and endothelial barrier function. *Thromb Haemost* **98**, 944-951 (2007).
85. Groux, H. & Cottrez, F. The complex role of interleukin-10 in autoimmunity. *Journal of Autoimmunity* **20**, 281-285 (2003).
86. Heyen, J.R.R., Ye, S., Finck, B.N. & Johnson, R.W. Interleukin (IL)-10 inhibits IL-6 production in microglia by preventing activation of NF-[kappa]B. *Molecular Brain Research* **77**, 138-147 (2000).
87. Tagashira, Y.*, et al.* Interleukin-10 attenuates TNF-[alpha]-induced interleukin-6 production in endometriotic stromal cells. *Fertility and Sterility* **91**, 2185-2192 (2009).
88. Siegmund, B.*, et al.* Suppression of tumor necrosis factor-[alpha] production by interleukin-10 is enhanced by cAMP-elevating agents. *European Journal of Pharmacology* **321**, 231-239 (1997).
89. Gerhardt, C.C., Romero, I.A., Cancello, R., Camoin, L. & Strosberg, A.D. Chemokines control fat accumulation and leptin secretion by cultured human adipocytes. *Mol Cell Endocrinol* **175**, 81-92 (2001).
90. Christiansen, T., Richelsen, B. & Bruun, J.M. Monocyte chemoattractant protein-1 is produced in isolated adipocytes, associated with adiposity and reduced after weight loss in morbid obese subjects. *Int J Obes Relat Metab Disord* **29**, 146-150 (2004).
91. Carr, M.W., Roth, S.J., Luther, E., Rose, S.S. & Springer, T.A. Monocyte chemoattractant protein 1 acts as a T-lymphocyte chemoattractant. *Proceedings of the National Academy of Sciences* **91**, 3652-3656 (1994).
92. Stefansson, S. & Lawrence, D.A. The serpin PAI-1 inhibits cell migration by blocking integrin alpha V beta 3 binding to vitronectin. *Nature* **383**, 441-443 (1996).
93. Moschen, A.R.*, et al.* Visfatin, an adipocytokine with proinflammatory and immunomodulating properties. *Journal of immunology* **178**, 1748-1758 (2007).
94. Kralisch, S.*, et al.* Interleukin-6 is a negative regulator of visfatin gene expression in 3T3-L1 adipocytes. *Am J Physiol Endocrinol Metab* **289**, E586-590 (2005).
95. Kralisch, S.*, et al.* Hormonal regulation of the novel adipocytokine visfatin in 3T3-L1 adipocytes. *The Journal of endocrinology* **185**, R1-8 (2005).
96. Zarnegar, R. & Michalopoulos, G.K. The many faces of hepatocyte growth factor: from hepatopoiesis to hematopoiesis. *J Cell Biol* **129**, 1177-1180 (1995).
97. Bussolino, F.*, et al.* Hepatocyte growth factor is a potent angiogenic factor which stimulates endothelial cell motility and growth. *J Cell Biol* **119**, 629-641 (1992).
98. Santos, O.F.*, et al.* Involvement of hepatocyte growth factor in kidney development. *Developmental Biology* **163**, 525-529 (1994).
99. Kawaida, K., Matsumoto, K., Shimazu, H. & Nakamura, T. Hepatocyte growth factor prevents acute renal failure and accelerates renal regeneration in mice. *Proceedings of the National Academy of Sciences of the United States of America* **91**, 4357-4361 (1994).
100. Mizuno, S.*, et al.* Hepatocyte growth factor prevents renal fibrosis and dysfunction in a mouse model of chronic renal disease. *The Journal of Clinical Investigation* **101**, 1827-1834 (1998).
101. Neufeld, G., Cohen, T., Gengrinovitch, S. & Poltorak, Z. Vascular endothelial growth factor (VEGF) and its receptors. *Faseb Journal* **13**, 9-22 (1999).
102. Oyama, T.*, et al.* Vascular endothelial growth factor affects dendritic cell maturation through the inhibition of nuclear factor-kappa B activation in hemopoietic progenitor cells. *Journal of immunology* **160**, 1224-1232 (1998).

103. Benjamin, L.E., Hemo, I. & Keshet, E. A plasticity window for blood vessel remodelling is defined by pericyte coverage of the preformed endothelial network and is regulated by PDGF-B and VEGF. *Development* **125**, 1591-1598 (1998).
104. Seeger, J.*, et al.* Serum levels of the adipokine vaspin in relation to metabolic and renal parameters. *J Clin Endocrinol Metab* **93**, 247-251 (2008).
105. Fasshauer, M., Paschke, R. & Stumvoll, M. Adiponectin, obesity, and cardiovascular disease. *Biochimie* **86**, 779-784 (2004).
106. Hotta, K.*, et al.* Plasma concentrations of a novel, adipose-specific protein, adiponectin, in type 2 diabetic patients. *Arterioscler Thromb Vasc Biol* **20**, 1595-1599 (2000).
107. Jartti, T.*, et al.* Obesity, adipokines and asthma. *Allergy* **64**, 770-777 (2009).
108. Radon, K., Schulze, A., Schierl, R., Dietrich-Gumperlein, G., Nowak, D., Jorres, R. A. Serum leptin and adiponectin levels and their association with allergic sensitization. *Allergy* **63**, 1448-1454 (2008).
109. Ouchi, N., Kihara, S., Arita, Y., Nishida, M., Matsuyama, A., Okamoto, Y., shigami, M., Kuriyama, H., Kishida, K., Nishizawa, H., Hotta, K., Muraguchi, M., Ohmoto, Y., Yamashita, S., Funahashi, T., Matsuzawa, Y. Adipocyte-derived plasma protein, adiponectin, suppresses lipid accumulation and class A scavenger receptor expression in human monocyte-derived macrophages. *Circulation* **103**, 1057-1063 (2001).
110. Okamoto, Y., Kihara, S., Ouchi, N., Nishida, M., Arita, Y., Kumada, M., Ohashi, K., Sakai, N., Shimomura, I., Kobayashi, H., Terasaka, N., Inaba, T., Funahashi, T., Matsuzawa, Y. Adiponectin reduces atherosclerosis in apolipoprotein E-deficient mice. *Circulation* **106**, 2767-2770 (2002).
111. Endemann, G.*, et al.* CD36 is a receptor for oxidized low density lipoprotein. *J Biol Chem* **268**, 11811-11816 (1993).
112. Border, W.A.*, et al.* Natural inhibitor of transforming growth factor-beta protects against scarring in experimental kidney disease. *Nature* **360**, 361-364 (1992).
113. Arici, M. & Walls, J. End-stage renal disease, atherosclerosis, and cardiovascular mortality: Is C-reactive protein the missing link? *Kidney International* **59**, 407 (2001).
114. Zoccali, C., Mallamaci, F., Tripepi, G., Benedetto, F. A., Cutrupi, S., Parlongo, S., Malatino, L. S., Bonanno, G., Seminara, G., Rapisarda, F., Fatuzzo, P., Buemi, M., Nicocia, G., Tanaka, S., Ouchi, N., Kihara, S., Funahashi, T., Matsuzawa, Y. Adiponectin, Metabolic Risk Factors, and Cardiovascular Events among Patients with End-Stage Renal Disease. *J Am Soc Nephrol* **13**, 134-141 (2002).
115. Shen, Y.Y., Charlesworth, J. A., Kelly, J. J., Loi, K. W., Peake, P. W. Up-regulation of adiponectin, its isoforms and receptors in end-stage kidney disease. *Nephrol Dial Transplant* **22**, 171-178 (2007).
116. Pischon, T., Girman, C. J., Hotamisligil, G. S., Rifai, N., Hu, F. B., Rimm, E. B. Plasma adiponectin levels and risk of myocardial infarction in men. *JAMA* **291**, 1730-1737 (2004).
117. Fasshauer, M.*, et al.* Adiponectin gene expression and secretion is inhibited by interleukin-6 in 3T3-L1 adipocytes. *Biochemical and Biophysical Research Communications* **301**, 1045-1050 (2003).
118. Fasshauer, M., Klein, J., Neumann, S., Eszlinger, M., Paschke, R. Hormonal regulation of adiponectin gene expression in 3T3-L1 adipocytes. *Biochem Biophys Res Commun* **290**, 1084-1089 (2002).
119. Fasshauer, M., Klein, J., Neumann, S., Eszlinger, M. & Paschke, R. Adiponectin gene expression is inhibited by [beta]-adrenergic stimulation via protein kinase A in 3T3-L1 adipocytes. *FEBS Letters* **507**, 142-146 (2001).
120. Delporte, M.L., Funahashi, T., Takahashi, M., Matsuzawa, Y., Brichard, S. M. Pre- and post-translational negative effect of beta-adrenoceptor agonists on adiponectin secretion: in vitro and in vivo studies. *Biochem J* **367**, 677-685 (2002).

121. Hausberg, M.*, et al.* Sympathetic Nerve Activity in End-Stage Renal Disease. *Circulation* **106**, 1974-1979 (2002).
122. Tilg, H., Moschen, A. R. Adipocytokines: mediators linking adipose tissue, inflammation and immunity. *Nature Reviews Immunology* **6**, 772-783 (2006).
123. Pelleymounter, M.A., Cullen, M. J., Baker, M. B., Hecht, R., Winters, D., Boone, T., Collins, F. Effects of the obese gene product on body weight regulation in ob/ob mice. *Science* **269**, 540-543 (1995).
124. Sharma, K. & Considine, R.V. The Ob protein (leptin) and the kidney. *Kidney Int* **53**, 1483-1487 (1998).
125. Stephens, T.W., Basinski, M., Bristow, P. K., Bue-Valleskey, J. M., Burgett, S. G., Craft, L., Hale, J., Hoffmann, J., Hsiung, H. M., Kriauciunas, A. MacKellar, W., Rosteck, P.J., Schoner, B., Smith, D., Tinsley, F., Zhang, X., Heiman, M. The role of neuropeptide Y in the antiobesity action of the obese gene product. *Nature* **377**, 530-532 (1995).
126. Kougias, P.*, et al.* Effects of Adipocyte-Derived Cytokines on Endothelial Functions: Implication of Vascular Disease. *Journal of Surgical Research* **126**, 121-129 (2005).
127. Serradeil-Le Gal, C., Raufaste, D., Brossard, G., Pouzet, B., Marty, E., Maffrand, J-P., Le Fur, G. . Characterization and localization of leptin receptors in the rat kidney. *FEBS Letters* **404**, 185-191 (1997).
128. Margetic, S., Gazzola, C., Pegg, G. G., Hill, R. A. Characterization of leptin binding in bovine kidney membranes. *Domest Anim Endocrinol* **23**, 411-424 (2002).
129. Murad, A.*, et al.* Leptin is an autocrine/paracrine regulator of wound healing. *The FASEB journal : official publication of the Federation of American Societies for Experimental Biology* **17**, 1895-1897 (2003).
130. Kralisch, S.*, et al.* Secretory products from human adipocytes impair endothelial function via nuclear factor [kappa]B. *Atherosclerosis* **196**, 523-531 (2008).
131. Panzer, U., Steinmetz, O. M., Turner, J-E., Meyer-Schwesinger, C., von Ruffer, C., Meyer, T. N., Zahner, G., Gomez-Guerrero, C., Schmid, R. M., Helmchen, U., Moeckel, G. W., Wolf, G., Stahl, R. A. K., Thaiss, F. Resolution of renal inflammation: a new role for NF-{kappa}B1 (p50) in inflammatory kidney diseases. *Am J Physiol Renal Physiol* **297**, F429-439 (2009).
132. Banerjee, R.R.*, et al.* Regulation of fasted blood glucose by resistin. *Science* **303**, 1195-1198 (2004).
133. Reilly, M.P., Lehrke, M., Wolfe, M. L., Rohatgi, A., Lazar, M. A., Rader, D. J., . Resistin Is an Inflammatory Marker of Atherosclerosis in Humans. *Circulation* **111**, 932-939 (2005).
134. Verma, S., Li, S., Wang, C., Fedak, P. W. M., Li, R., Weisel, R. D., Mickle, D. A. G. Resistin Promotes Endothelial Cell Activation: Further Evidence of Adipokine-Endothelial Interaction. *Circulation* **108**, 736-740 (2003).
135. Steppan, C.M. & Lazar, M.A. REVIEW The current biology of resistin. *Journal of Internal Medicine* **255**, 439-447 (2004).
136. Rea, R. & Donnelly, R. Resistin: an adipocyte-derived hormone. Has it a role in diabetes and obesity? *Diabetes Obes Metab* **6**, 163-170 (2004).
137. Roubicek, T., Bartlova, M., Krajickova, J., Haluzikova, D., Mraz, M., Lacinova, Z., Kudla, M., Teplan, V., Haluzik, M. Increased production of proinflammatory cytokines in adipose tissue of patients with end-stage renal disease. *Nutrition* **25**, 762-768 (2009).
138. Axelsson, J.*, et al.* Elevated resistin levels in chronic kidney disease are associated with decreased glomerular filtration rate and inflammation, but not with insulin resistance. *Kidney Int* **69**, 596-604 (2006).
139. Flynn, J.L.*, et al.* Tumor necrosis factor-[alpha] is required in the protective immune response against mycobacterium tuberculosis in mice. *Immunity* **2**, 561-572 (1995).
140. Hotamisligil, G.S. & Spiegelman, B.M. Tumor necrosis factor alpha: a key component of the obesity-diabetes link. *Diabetes* **43**, 1271-1278 (1994).

141. Cawthorn, W.P. & Sethi, J.K. TNF-[alpha] and adipocyte biology. *FEBS Letters* **582**, 117-131 (2008).
142. Park, H.S., Park, J. Y., Yu, R. Relationship of obesity and visceral adiposity with serum concentrations of CRP, TNF-[alpha] and IL-6. *Diabetes Research and Clinical Practice* **69**, 29-35 (2005).
143. Descamps-Latscha, B., Herbelin, A., Nguyen, A. T., Roux-Lombard, P., Zingraff, J., Moynot, A., Verger, C., Dahmane, D., de Groote, D., Jungers, P. Balance between IL-1 beta, TNF-alpha, and their specific inhibitors in chronic renal failure and maintenance dialysis. Relationships with activation markers of T cells, B cells, and monocytes. *J Immunol* **154**, 882-892 (1995).
144. Pereira, B.J.G., Shapiro, L., King, A. J., Falagas, M. E., Strom, J. A., Dinarello, C. A. Plasma levels of IL-1[beta], TNF[alpha] and their specific inhibitors in undialyzed chronic renal failure, CAPD and hemodialysis patients. *Kidney Int* **45**, 890-896 (1994).
145. Marino, M.W., Dunn, A., Grail, D., Inglese, M., Noguchi, Y., Richards, E., Jungbluth, A., Wada, H., Moore, M., Williamson, B., Basu, S., Old, L. J. Characterization of tumor necrosis factor-deficientâ€‰mice. *Proceedings of the National Academy of Sciences of the United States of America* **94**, 8093-8098 (1997).
146. Mohamed-Ali, V., Goodrick, S., Rawesh, A., Katz, D. R., Miles, J. M., Yudkin, J. S., Klein, S., Coppack, S. W. Subcutaneous Adipose Tissue Releases Interleukin-6, But Not Tumor Necrosis Factor-{alpha}, in Vivo. *J Clin Endocrinol Metab* **82**, 4196-4200 (1997).
147. Wallenius, V., Wallenius, K., Ahren, B., Rudling, M., Carlsten, H., Dickson, S. L., Ohlsson, C., Jansson, J. Interleukin-6-deficient mice develop mature-onset obesity. *Nature Medicine* **8**, 75 (2002).
148. Sakata, J., Shimokubo, T., Kitamura, K., Nakamura, S., Kangawa, K., Matsuo, H., Eto, T. Molecular Cloning and Biological Activities of Rat Adrenomedullin, a Hypotensive Peptide. *Biochemical and Biophysical Research Communications* **195**, 921-927 (1993).
149. Julián, M*., et al.* Adrenomedullin: a new target for the design of small molecule modulators with promising pharmacological activities. *European Journal of Medicinal Chemistry* **40**, 737-750 (2005).
150. Zuk, P.A., Zhu, Min, Ashjian, Peter, De Ugarte, Daniel A., Huang, Jerry I., Mizuno, Hiroshi, Alfonso, Zeni C., Fraser, John K., Benhaim, Prosper, Hedrick, Marc H. Human Adipose Tissue Is a Source of Multipotent Stem Cells. *Mol. Biol. Cell* **13**, 4279-4295 (2002).
151. Caplan, A.I. & Bruder, S.P. Mesenchymal stem cells: building blocks for molecular medicine in the 21st century. *Trends Mol Med* **7**, 259-264 (2001).
152. Zhang, F., Wu, R., Zhou, M., Blau, .S. A., Wang, P. Human adrenomedullin combined with human adrenomedullin binding protein-1 is protective in gut ischemia and reperfusion injury in the rat. *Regulatory Peptides* **152**, 82-87 (2009).
153. Xia, C., Yin, H., Borlongan, C. V., Chao, J., Chao, L., . Postischemic infusion of adrenomedullin protects against ischemic stroke by inhibiting apoptosis and promoting angiogenesis. *Experimental Neurology* **197**, 521-530 (2006).
154. Park, S.C., Yoon, J., Lee, J., Yu, S. J., Myung, S. J., Kim, W., Gwak, G., Lee, S., Lee, S., Jang, J. J., Suh, K., Lee, H. Hypoxia-inducible adrenomedullin accelerates hepatocellular carcinoma cell growth. *Cancer Letters* **271**, 314-322 (2008).
155. Sandner, P., Hofbauer, K. H., Tinel, H., Kurtz, A., Thiesson, H. C., Ottosen, P. D., Walter, S., Skott, O., Jensen, B. L. Expression of adrenomedullin in hypoxic and ischemic rat kidneys and human kidneys with arterial stenosis. *Am J Physiol Regul Integr Comp Physiol* **286**, R942-951 (2004).
156. Temmesfeld-Wollbruck, B*., et al.* Adrenomedullin reduces vascular hyperpermeability and improves survival in rat septic shock. *Intensive Care Med* **33**, 703-710 (2007).
157. Chini, E.N*., et al.* Cytoprotective effects of adrenomedullin in glomerular cell injury: Central role of cAMP signaling pathway. *Kidney Int* **52**, 917-925 (1997).

158. Nishimatsu, H., Hirata, Y., Shindo, T., Kurihara, H., Kakoki, M., Nagata, D., Hayakawa, H., Satonaka, H., Sata, M., Tojo, A., Suzuki, E., Kangawa, K., Matsuo, H., Kitamura, T., Nagai, R. Role of Endogenous Adrenomedullin in the Regulation of Vascular Tone and Ischemic Renal Injury: Studies on Transgenic/Knockout Mice of Adrenomedullin Gene. *Circ Res* **90**, 657-663 (2002).
159. Ishimitsu, T*., et al.* Plasma levels of adrenomedullin, a newly identified hypotensive peptide, in patients with hypertension and renal failure. *The Journal of Clinical Investigation* **94**, 2158-2161 (1994).
160. Loisa, P., Rinne, T., Laine, S., Hurme, M. & Kaukinen, S. Anti-inflammatory cytokine response and the development of multiple organ failure in severe sepsis. *Acta Anaesthesiol Scand* **47**, 319-325 (2003).
161. Simmons, E.M., Himmelfarb, .J., Sezer, M. T., Chertow, G. M., Mehta, R. L., Paganini, E. P., Soroko, S., Freedman, S., Becker, K., Spratt, D., Shyr, Y., Ikizler, T. A. Plasma cytokine levels predict mortality in patients with acute renal failure. *Kidney International* **65**, 1357-1365 (2004).
162. Choi, Y.K*., et al.* Suppression of glomerulosclerosis by adenovirus-mediated IL-10 expression in the kidney. *Gene Therapy* **10**, 559 (2003).
163. Mu, W*., et al.* IL-10 Suppresses Chemokines, Inflammation, and Fibrosis in a Model of Chronic Renal Disease. *J Am Soc Nephrol* **16**, 3651-3660 (2005).
164. Rollins, B.J., Morrison, E.D. & Stiles, C.D. Cloning and expression of JE, a gene inducible by platelet-derived growth factor and whose product has cytokine-like properties. *Proceedings of the National Academy of Sciences of the United States of America* **85**, 3738-3742 (1988).
165. Jiang, Y., Beller, D.I., Frendl, G. & Graves, D.T. Monocyte chemoattractant protein-1 regulates adhesion molecule expression and cytokine production in human monocytes. *Journal of immunology* **148**, 2423-2428 (1992).
166. Sartipy, P. & Loskutoff, D.J. Monocyte chemoattractant protein 1 in obesity and insulin resistance. *Proceedings of the National Academy of Sciences of the United States of America* **100**, 7265-7270 (2003).
167. Gunn, M., Nelken, N., Liao, X. & Williams, L. Monocyte chemoattractant protein-1 is sufficient for the chemotaxis of monocytes and lymphocytes in transgenic mice but requires an additional stimulus for inflammatory activation. *The Journal of Immunology* **158**, 376-383 (1997).
168. Gu, L*., et al.* In vivo properties of monocyte chemoattractant protein-1. *J Leukoc Biol* **62**, 577-580 (1997).
169. Yla-Herttuala, S*., et al.* Expression of monocyte chemoattractant protein 1 in macrophage-rich areas of human and rabbit atherosclerotic lesions. *Proceedings of the National Academy of Sciences of the United States of America* **88**, 5252-5256 (1991).
170. Wang, Y*., et al.* Induction of monocyte chemoattractant protein-1 in proximal tubule cells by urinary protein. *Journal of the American Society of Nephrology : JASN* **8**, 1537-1545 (1997).
171. Banba, N*., et al.* Possible relationship of monocyte chemoattractant protein-1 with diabetic nephropathy. *Kidney International* **58**, 684-690 (2000).
172. Lloyd, C.M*., et al.* RANTES and monocyte chemoattractant protein-1 (MCP-1) play an important role in the inflammatory phase of crescentic nephritis, but only MCP-1 is involved in crescent formation and interstitial fibrosis. *J Exp Med* **185**, 1371-1380 (1997).
173. Dellas, C. & Loskutoff, D.J. Historical analysis of PAI-1 from its discovery to its potential role in cell motility and disease. *Thrombosis and haemostasis* **93**, 631-640 (2005).
174. Gils, A. & Declerck, P.J. Plasminogen activator inhibitor-1. *Curr Med Chem* **11**, 2323-2334 (2004).
175. Samad, F., Yamamoto, K. & Loskutoff, D.J. Distribution and regulation of plasminogen activator inhibitor-1 in murine adipose tissue in vivo. Induction by tumor necrosis factor-alpha and lipopolysaccharide. *The Journal of Clinical Investigation* **97**, 37-46 (1996).

176. Alessi, M.C*., et al.* Plasminogen activator inhibitor 1, transforming growth factor-beta1, and BMI are closely associated in human adipose tissue during morbid obesity. *Diabetes* **49**, 1374-1380 (2000).
177. Eddy, A.A. & Fogo, A.B. Plasminogen activator inhibitor-1 in chronic kidney disease: evidence and mechanisms of action. *Journal of the American Society of Nephrology : JASN* **17**, 2999-3012 (2006).
178. Rerolle, J.-P., Hertig, A., Nguyen, G., Sraer, J.-D. & Rondeau, E.P. Plasminogen activator inhibitor type 1 is a potential target in renal fibrogenesis. *Kidney Int* **58**, 1841-1850 (2000).
179. Samal, B*., et al.* Cloning and characterization of the cDNA encoding a novel human pre-B-cell colony-enhancing factor. *Mol Cell Biol* **14**, 1431-1437 (1994).
180. Haider, D.G*., et al.* The release of the adipocytokine visfatin is regulated by glucose and insulin. *Diabetologia* **49**, 1909-1914 (2006).
181. Berndt, J*., et al.* Plasma visfatin concentrations and fat depot-specific mRNA expression in humans. *Diabetes* **54**, 2911-2916 (2005).
182. Chen, M.P*., et al.* Elevated plasma level of visfatin/pre-B cell colony-enhancing factor in patients with type 2 diabetes mellitus. *The Journal of clinical endocrinology and metabolism* **91**, 295-299 (2006).
183. Curat, C.A*., et al.* Macrophages in human visceral adipose tissue: increased accumulation in obesity and a source of resistin and visfatin. *Diabetologia* **49**, 744-747 (2006).
184. Hammarstedt, A*., et al.* Visfatin is an adipokine, but it is not regulated by thiazolidinediones. *The Journal of clinical endocrinology and metabolism* **91**, 1181-1184 (2006).
185. Yilmaz, M.I*., et al.* Serum visfatin concentration and endothelial dysfunction in chronic kidney disease. *Nephrology, dialysis, transplantation : official publication of the European Dialysis and Transplant Association - European Renal Association* **23**, 959-965 (2008).
186. Weidner, K.M*., et al.* Evidence for the identity of human scatter factor and human hepatocyte growth factor. *Proceedings of the National Academy of Sciences of the United States of America* **88**, 7001-7005 (1991).
187. Sonnenberg, E., Meyer, D., Weidner, K.M. & Birchmeier, C. Scatter factor/hepatocyte growth factor and its receptor, the c-met tyrosine kinase, can mediate a signal exchange between mesenchyme and epithelia during mouse development. *J Cell Biol* **123**, 223-235 (1993).
188. Naldini, L*., et al.* Extracellular proteolytic cleavage by urokinase is required for activation of hepatocyte growth factor/scatter factor. *The EMBO journal* **11**, 4825-4833 (1992).
189. Schmidt, C*., et al.* Scatter factor/hepatocyte growth factor is essential for liver development. *Nature* **373**, 699-702 (1995).
190. Ueki, T*., et al.* Hepatocyte growth factor gene therapy of liver cirrhosis in rats. *Nature Medicine* **5**, 226-230 (1999).
191. Montesano, R., Schaller, G. & Orci, L. Induction of epithelial tubular morphogenesis in vitro by fibroblast-derived soluble factors. *Cell* **66**, 697-711 (1991).
192. Montesano, R., Matsumoto, K., Nakamura, T. & Orci, L. Identification of a fibroblast-derived epithelial morphogen as hepatocyte growth factor. *Cell* **67**, 901-908 (1991).
193. Liu, Y*., et al.* Up-regulation of hepatocyte growth factor receptor: an amplification and targeting mechanism for hepatocyte growth factor action in acute renal failure. *Kidney International* **55**, 442-453 (1999).
194. Yang, J. & Liu, Y. Blockage of tubular epithelial to myofibroblast transition by hepatocyte growth factor prevents renal interstitial fibrosis. *Journal of the American Society of Nephrology : JASN* **13**, 96-107 (2002).
195. Shalaby, F*., et al.* A requirement for Flk1 in primitive and definitive hematopoiesis and vasculogenesis. *Cell* **89**, 981-990 (1997).
196. Carmeliet, P*., et al.* Abnormal blood vessel development and lethality in embryos lacking a single VEGF allele. *Nature* **380**, 435-439 (1996).

197. Schrijvers, B.F., Flyvbjerg, A. & De Vriese, A.S. The role of vascular endothelial growth factor (VEGF) in renal pathophysiology. *Kidney International* **65**, 2003-2017 (2004).
198. Ishida, A.*, et al.* Expression of vascular endothelial growth factor receptors in smooth muscle cells. *Journal of Cellular Physiology* **188**, 359-368 (2001).
199. Tran, J.*, et al.* Marked induction of the IAP family antiapoptotic proteins survivin and XIAP by VEGF in vascular endothelial cells. *Biochemical and Biophysical Research Communications* **264**, 781-788 (1999).
200. Gabrilovich, D.I., Ishida, T., Nadaf, S., Ohm, J.E. & Carbone, D.P. Antibodies to vascular endothelial growth factor enhance the efficacy of cancer immunotherapy by improving endogenous dendritic cell function. *Clin Cancer Res* **5**, 2963-2970 (1999).
201. Robinson, C.J. & Stringer, S.E. The splice variants of vascular endothelial growth factor (VEGF) and their receptors. *Journal of cell science* **114**, 853-865 (2001).
202. Eremina, V.*, et al.* Glomerular-specific alterations of VEGF-A expression lead to distinct congenital and acquired renal diseases. *The Journal of Clinical Investigation* **111**, 707-716 (2003).
203. Kretzler, M.*, et al.* Detection of multiple vascular endothelial growth factor splice isoforms in single glomerular podocytes. *Kidney Int Suppl* **67**, S159-161 (1998).
204. Cooper, M.E.*, et al.* Increased renal expression of vascular endothelial growth factor (VEGF) and its receptor VEGFR-2 in experimental diabetes. *Diabetes* **48**, 2229-2239 (1999).
205. Simon, M.*, et al.* Expression of vascular endothelial growth factor and its receptors in human renal ontogenesis and in adult kidney. *The American journal of physiology* **268**, F240-250 (1995).
206. Youn, B.S.*, et al.* Serum vaspin concentrations in human obesity and type 2 diabetes. *Diabetes* **57**, 372-377 (2008).
207. Kloting, N.*, et al.* Vaspin gene expression in human adipose tissue: association with obesity and type 2 diabetes. *Biochemical and Biophysical Research Communications* **339**, 430-436 (2006).
208. Aggarwal, K., Choe, L.H. & Lee, K.H. Shotgun proteomics using the iTRAQ isobaric tags. *Brief Funct Genomic Proteomic* **5**, 112-120 (2006).
209. Wu, W.W., Wang, G., Baek, S.J. & Shen, R.F. Comparative study of three proteomic quantitative methods, DIGE, cICAT, and iTRAQ, using 2D gel- or LC-MALDI TOF/TOF. *Journal of Proteome Research* **5**, 651-658 (2006).
210. Chevalier, F. Highlights on the capacities of "Gel-based" proteomics. *Proteome Sci* **8**, 23 (2010).
211. Zuk, P.A.*, et al.* Human adipose tissue is a source of multipotent stem cells. *Mol Biol Cell* **13**, 4279-4295 (2002).
212. Aggarwal, S. & Pittenger, M.F. Human mesenchymal stem cells modulate allogeneic immune cell responses. *Blood* **105**, 1815-1822 (2005).
213. Dominici, M.*, et al.* Minimal criteria for defining multipotent mesenchymal stromal cells. The International Society for Cellular Therapy position statement. *Cytotherapy* **8**, 315-317 (2006).
214. Mene, P. & Stoppacciaro, A. Isolation and propagation of glomerular mesangial cells. *Methods Mol Biol* **466**, 3-17 (2009).
215. Kyhse-Andersen, J. Electroblotting of multiple gels: a simple apparatus without buffer tank for rapid transfer of proteins from polyacrylamide to nitrocellulose. *J Biochem Biophys Methods* **10**, 203-209 (1984).
216. Davies, M. The mesangial cell: a tissue culture view. *Kidney International* **45**, 320-327 (1994).
217. Ennulat, D. & Brown, S.A. Canine and equine mesangial cells in vitro. *In Vitro Cell Dev Biol Anim* **31**, 574-578 (1995).
218. Shi, Y. & Massague, J. Mechanisms of TGF-beta signaling from cell membrane to the nucleus. *Cell* **113**, 685-700 (2003).

219. Sharma, K., Jin, Y., Guo, J. & Ziyadeh, F.N. Neutralization of TGF-beta by anti-TGF-beta antibody attenuates kidney hypertrophy and the enhanced extracellular matrix gene expression in STZ-induced diabetic mice. *Diabetes* **45**, 522-530 (1996).
220. Clouthier, D.E., Comerford, S.A. & Hammer, R.E. Hepatic fibrosis, glomerulosclerosis, and a lipodystrophy-like syndrome in PEPCK-TGF-beta1 transgenic mice. *The Journal of Clinical Investigation* **100**, 2697-2713 (1997).
221. Bottinger, E.P. & Bitzer, M. TGF-beta signaling in renal disease. *Journal of the American Society of Nephrology : JASN* **13**, 2600-2610 (2002).
222. Massague, J., Seoane, J. & Wotton, D. Smad transcription factors. *Genes Dev* **19**, 2783-2810 (2005).
223. Humes, H.D*., et al.* Role of proteoglycans and cytoskeleton in the effects of TGF-beta 1 on renal proximal tubule cells. *Kidney International* **43**, 575-584 (1993).
224. Boland, S*., et al.* TGF beta 1 promotes actin cytoskeleton reorganization and migratory phenotype in epithelial tracheal cells in primary culture. *Journal of cell science* **109 (Pt 9)**, 2207-2219 (1996).
225. Molitoris, B.A., Leiser, J. & Wagner, M.C. Role of the actin cytoskeleton in ischemia-induced cell injury and repair. *Pediatric Nephrology* **11**, 761-767 (1997).
226. Kellerman, P.S. & Bogusky, R.T. Microfilament disruption occurs very early in ischemic proximal tubule cell injury. *Kidney International* **42**, 896-902 (1992).
227. Assinder, S.J., Stanton, J.A. & Prasad, P.D. Transgelin: an actin-binding protein and tumour suppressor. *Int J Biochem Cell Biol* **41**, 482-486 (2009).
228. Sakamaki, Y*., et al.* Injured kidney cells express SM22alpha (transgelin): Unique features distinct from alpha-smooth muscle actin (alphaSMA). *Nephrology (Carlton)* **16**, 211-218 (2011).
229. Inomata, S*., et al.* Expression of SM22alpha (transgelin) in glomerular and interstitial renal injury. *Nephron Exp Nephrol* **117**, e104-113 (2011).
230. Gonlusen, G., Ergin, M., Paydas, S. & Tunali, N. The expression of cytoskeletal proteins (alpha-SMA, vimentin, desmin) in kidney tissue: a comparison of fetal, normal kidneys, and glomerulonephritis. *Int Urol Nephrol* **33**, 299-305 (2001).
231. Bravo, J*., et al.* Vimentin and heat shock protein expression are induced in the kidney by angiotensin and by nitric oxide inhibition. *Kidney Int Suppl*, S46-51 (2003).
232. Shibasaki, F. & McKeon, F. Calcineurin functions in Ca(2+)-activated cell death in mammalian cells. *J Cell Biol* **131**, 735-743 (1995).
233. Robertson, S.P., Johnson, J.D. & Potter, J.D. The time-course of Ca2+ exchange with calmodulin, troponin, parvalbumin, and myosin in response to transient increases in Ca2+. *Biophys J* **34**, 559-569 (1981).
234. Chang, N*., et al.* Identification of a novel interaction between the Ca(2+)-binding protein S100A11 and the Ca(2+)- and phospholipid-binding protein annexin A6. *Am J Physiol Cell Physiol* **292**, C1417-1430 (2007).
235. Gerke, V. & Moss, S.E. Annexins: from structure to function. *Physiol Rev* **82**, 331-371 (2002).
236. Grewal, T*., et al.* Annexin A6 stimulates the membrane recruitment of p120GAP to modulate Ras and Raf-1 activity. *Oncogene* **24**, 5809-5820 (2005).
237. Bouter, A*., et al.* Annexin-A5 assembled into two-dimensional arrays promotes cell membrane repair. *Nat Commun* **2**, 270 (2011).
238. Davis, C.A., Nick, H.S. & Agarwal, A. Manganese superoxide dismutase attenuates Cisplatin-induced renal injury: importance of superoxide. *Journal of the American Society of Nephrology : JASN* **12**, 2683-2690 (2001).
239. Downward, J. Ras signalling and apoptosis. *Current Opinion in Genetics & Development* **8**, 49-54 (1998).

240. Dulong, S*., et al.* Myristoylated alanine-rich C kinase substrate (MARCKS) is involved in myoblast fusion through its regulation by protein kinase Calpha and calpain proteolytic cleavage. *The Biochemical journal* **382**, 1015-1023 (2004).
241. Ishikawa, R., Kagami, O., Hayashi, C. & Kohama, K. The binding of nonmuscle caldesmon from brain to microtubules. Regulations by Ca(2+)-calmodulin and cdc2 kinase. *FEBS Letters* **299**, 54-56 (1992).
242. Shalitin, N., Schlesinger, H., Levy, M.J., Kessler, E. & Kessler-Icekson, G. Expression of procollagen C-proteinase enhancer in cultured rat heart fibroblasts: evidence for co-regulation with type I collagen. *Journal of Cellular Biochemistry* **90**, 397-407 (2003).
243. Dean, R.G*., et al.* Connective tissue growth factor and cardiac fibrosis after myocardial infarction. *J Histochem Cytochem* **53**, 1245-1256 (2005).
244. Gupta, S., Clarkson, M.R., Duggan, J. & Brady, H.R. Connective tissue growth factor: potential role in glomerulosclerosis and tubulointerstitial fibrosis. *Kidney International* **58**, 1389-1399 (2000).
245. Liu, X., Wu, H., Byrne, M., Krane, S. & Jaenisch, R. Type III collagen is crucial for collagen I fibrillogenesis and for normal cardiovascular development. *Proceedings of the National Academy of Sciences of the United States of America* **94**, 1852-1856 (1997).
246. Eghbali, M., Tomek, R., Sukhatme, V.P., Woods, C. & Bhambi, B. Differential effects of transforming growth factor-beta 1 and phorbol myristate acetate on cardiac fibroblasts. Regulation of fibrillar collagen mRNAs and expression of early transcription factors. *Circulation Research* **69**, 483-490 (1991).
247. Garcia-Sanchez, O., Lopez-Hernandez, F.J. & Lopez-Novoa, J.M. An integrative view on the role of TGF-beta in the progressive tubular deletion associated with chronic kidney disease. *Kidney International* **77**, 950-955 (2010).
248. Varga, J., Rosenbloom, J. & Jimenez, S.A. Transforming growth factor beta (TGF beta) causes a persistent increase in steady-state amounts of type I and type III collagen and fibronectin mRNAs in normal human dermal fibroblasts. *The Biochemical journal* **247**, 597-604 (1987).
249. Wu, D*., et al.* Knockdown of fibronectin induces mitochondria-dependent apoptosis in rat mesangial cells. *Journal of the American Society of Nephrology : JASN* **16**, 646-657 (2005).
250. Fujita, H*., et al.* Reduction of renal superoxide dismutase in progressive diabetic nephropathy. *Journal of the American Society of Nephrology : JASN* **20**, 1303-1313 (2009).
251. Ohishi, K. & Carmines, P.K. Superoxide dismutase restores the influence of nitric oxide on renal arterioles in diabetes mellitus. *Journal of the American Society of Nephrology : JASN* **5**, 1559-1566 (1995).
252. Sakai, T., Larsen, M. & Yamada, K.M. Fibronectin requirement in branching morphogenesis. *Nature* **423**, 876-881 (2003).
253. Ignotz, R.A. & Massague, J. Transforming growth factor-beta stimulates the expression of fibronectin and collagen and their incorporation into the extracellular matrix. *The Journal of biological chemistry* **261**, 4337-4345 (1986).
254. Han, S.W. & Roman, J. Fibronectin induces cell proliferation and inhibits apoptosis in human bronchial epithelial cells: pro-oncogenic effects mediated by PI3-kinase and NF-kappa B. *Oncogene* **25**, 4341-4349 (2006).
255. Kroncke, K.D., Fehsel, K. & Kolb-Bachofen, V. Nitric oxide: cytotoxicity versus cytoprotection--how, why, when, and where? *Nitric Oxide* **1**, 107-120 (1997).
256. Struck, A.T., Hogg, N., Thomas, J.P. & Kalyanaraman, B. Nitric oxide donor compounds inhibit the toxicity of oxidized low-density lipoprotein to endothelial cells. *FEBS Letters* **361**, 291-294 (1995).
257. Vallance, P., Leone, A., Calver, A., Collier, J. & Moncada, S. Accumulation of an endogenous inhibitor of nitric oxide synthesis in chronic renal failure. *Lancet* **339**, 572-575 (1992).

258. Wilcox, C.S. Oxidative stress and nitric oxide deficiency in the kidney: a critical link to hypertension? *American journal of physiology. Regulatory, integrative and comparative physiology* **289**, R913-935 (2005).
259. Morita, I. Distinct functions of COX-1 and COX-2. *Prostaglandins Other Lipid Mediat* **68-69**, 165-175 (2002).
260. Dunn, M.J. Nonsteroidal antiinflammatory drugs and renal function. *Annu Rev Med* **35**, 411-428 (1984).
261. Hartner, A., Pahl, A., Brune, K. & Goppelt-Struebe, M. Upregulation of cyclooxygenase-1 and the PGE2 receptor EP2 in rat and human mesangioproliferative glomerulonephritis. *Inflamm Res* **49**, 345-354 (2000).
262. Bussolati, B.*, et al.* Interleukin-12 is synthesized by mesangial cells and stimulates platelet-activating factor synthesis, cytoskeletal reorganization, and cell shape change. *Am J Pathol* **154**, 623-632 (1999).
263. Aguilar, H.N. & Mitchell, B.F. Physiological pathways and molecular mechanisms regulating uterine contractility. *Hum Reprod Update* **16**, 725-744 (2010).
264. Grandaliano, G., Valente, A.J., Rozek, M.M. & Abboud, H.E. Gamma interferon stimulates monocyte chemotactic protein (MCP-1) in human mesangial cells. *J Lab Clin Med* **123**, 282-289 (1994).
265. Hu, X. & Ivashkiv, L.B. Cross-regulation of signaling pathways by interferon-gamma: implications for immune responses and autoimmune diseases. *Immunity* **31**, 539-550 (2009).
266. Huang, S.*, et al.* Immune response in mice that lack the interferon-gamma receptor. *Science* **259**, 1742-1745 (1993).
267. Wood, K.J. & Sawitzki, B. Interferon gamma: a crucial role in the function of induced regulatory T cells in vivo. *Trends in Immunology* **27**, 183-187 (2006).
268. Sacks, S., Zhou, W., Campbell, R.D. & Martin, J. C3 and C4 gene expression and interferon-gamma-mediated regulation in human glomerular mesangial cells. *Clinical and Experimental Immunology* **93**, 411-417 (1993).
269. Kakizaki, Y., Kraft, N. & Atkins, R.C. Differential control of mesangial cell proliferation by interferon-gamma. *Clinical and Experimental Immunology* **85**, 157-163 (1991).
270. Takahashi, T.*, et al.* Protein tyrosine kinases expressed in glomeruli and cultured glomerular cells: Flt-1 and VEGF expression in renal mesangial cells. *Biochemical and Biophysical Research Communications* **209**, 218-226 (1995).
271. Amemiya, T.*, et al.* Vascular endothelial growth factor activates MAP kinase and enhances collagen synthesis in human mesangial cells. *Kidney International* **56**, 2055-2063 (1999).
272. Iijima, K., Yoshikawa, N., Connolly, D.T. & Nakamura, H. Human mesangial cells and peripheral blood mononuclear cells produce vascular permeability factor. *Kidney International* **44**, 959-966 (1993).
273. Trachtman, H., Futterweit, S., Franki, N. & Singhal, P.C. Effect of vascular endothelial growth factor on nitric oxide production by cultured rat mesangial cells. *Biochemical and Biophysical Research Communications* **245**, 443-446 (1998).
274. Ruef, C.*, et al.* Interleukin 6 is an autocrine growth factor for mesangial cells. *Kidney International* **38**, 249-257 (1990).
275. Horii, Y.*, et al.* Involvement of IL-6 in mesangial proliferative glomerulonephritis. *Journal of immunology* **143**, 3949-3955 (1989).
276. Dabbagh, K.*, et al.* IL-4 induces mucin gene expression and goblet cell metaplasia in vitro and in vivo. *Journal of immunology* **162**, 6233-6237 (1999).
277. Gaush, C.R., Hard, W.L. & Smith, T.F. Characterization of an established line of canine kidney cells (MDCK). *Proc Soc Exp Biol Med* **122**, 931-935 (1966).
278. Cereijido, M., Ehrenfeld, J., Meza, I. & Martinez-Palomo, A. Structural and functional membrane polarity in cultured monolayers of MDCK cells. *J Membr Biol* **52**, 147-159 (1980).

279. Arroyo, J.P., Ronzaud, C., Lagnaz, D., Staub, O. & Gamba, G. Aldosterone paradox: differential regulation of ion transport in distal nephron. *Physiology (Bethesda)* **26**, 115-123 (2011).
280. Misfeldt, D.S., Hamamoto, S.T. & Pitelka, D.R. Transepithelial transport in cell culture. *Proceedings of the National Academy of Sciences of the United States of America* **73**, 1212-1216 (1976).
281. Siess, W. Molecular mechanisms of platelet activation. *Physiol Rev* **69**, 58-178 (1989).
282. Kamath, S., Blann, A.D. & Lip, G.Y. Platelet activation: assessment and quantification. *Eur Heart J* **22**, 1561-1571 (2001).
283. Landray, M.J*., et al.* Inflammation, endothelial dysfunction, and platelet activation in patients with chronic kidney disease: the chronic renal impairment in Birmingham (CRIB) study. *Am J Kidney Dis* **43**, 244-253 (2004).
284. Malyszko, J*., et al.* Hemostasis, platelet function and serotonin in acute and chronic renal failure. *Thrombosis Research* **83**, 351-361 (1996).
285. Vassalli, J.D., Sappino, A.P. & Belin, D. The plasminogen activator/plasmin system. *The Journal of Clinical Investigation* **88**, 1067-1072 (1991).
286. Ohta, Y., Suzuki, N., Nakamura, S., Hartwig, J.H. & Stossel, T.P. The small GTPase RalA targets filamin to induce filopodia. *Proceedings of the National Academy of Sciences of the United States of America* **96**, 2122-2128 (1999).
287. Feng, S., Resendiz, J.C., Lu, X. & Kroll, M.H. Filamin A binding to the cytoplasmic tail of glycoprotein Ibalpha regulates von Willebrand factor-induced platelet activation. *Blood* **102**, 2122-2129 (2003).
288. Bonventre, J.V. Dedifferentiation and proliferation of surviving epithelial cells in acute renal failure. *Journal of the American Society of Nephrology : JASN* **14 Suppl 1**, S55-61 (2003).
289. Gupton, S.L. & Gertler, F.B. Filopodia: the fingers that do the walking. *Sci STKE* **2007**, re5 (2007).
290. Sasaki, A., Masuda, Y., Ohta, Y., Ikeda, K. & Watanabe, K. Filamin associates with Smads and regulates transforming growth factor-beta signaling. *The Journal of biological chemistry* **276**, 17871-17877 (2001).
291. Eckardt, K.U*., et al.* Role of hypoxia in the pathogenesis of renal disease. *Kidney Int Suppl*, S46-51 (2005).
292. Wakisaka, Y*., et al.* Cellular distribution of NDRG1 protein in the rat kidney and brain during normal postnatal development. *J Histochem Cytochem* **51**, 1515-1525 (2003).
293. van Belzen, N*., et al.* A novel gene which is up-regulated during colon epithelial cell differentiation and down-regulated in colorectal neoplasms. *Lab Invest* **77**, 85-92 (1997).
294. Chua, M.S*., et al.* Overexpression of NDRG1 is an indicator of poor prognosis in hepatocellular carcinoma. *Mod Pathol* **20**, 76-83 (2007).
295. Kreidberg, J.A. & Symons, J.M. Integrins in kidney development, function, and disease. *American journal of physiology. Renal physiology* **279**, F233-242 (2000).
296. Hynes, R.O. Integrins: bidirectional, allosteric signaling machines. *Cell* **110**, 673-687 (2002).
297. Goligorsky, M.S., Lieberthal, W., Racusen, L. & Simon, E.E. Integrin receptors in renal tubular epithelium: new insights into pathophysiology of acute renal failure. *The American journal of physiology* **264**, F1-8 (1993).
298. Ginsberg, M.H., Du, X. & Plow, E.F. Inside-out integrin signalling. *Curr Opin Cell Biol* **4**, 766-771 (1992).
299. Kunicki, T.J., Orchekowski, R., Annis, D. & Honda, Y. Variability of integrin alpha 2 beta 1 activity on human platelets. *Blood* **82**, 2693-2703 (1993).
300. Brown, M.C. & Turner, C.E. Paxillin: adapting to change. *Physiol Rev* **84**, 1315-1339 (2004).
301. Lamorte, L., Rodrigues, S., Sangwan, V., Turner, C.E. & Park, M. Crk associates with a multimolecular Paxillin/GIT2/beta-PIX complex and promotes Rac-dependent relocalization of Paxillin to focal contacts. *Molecular biology of the cell* **14**, 2818-2831 (2003).

302. Rana, A., Sathyanarayana, P. & Lieberthal, W. Role of apoptosis of renal tubular cells in acute renal failure: therapeutic implications. *Apoptosis* **6**, 83-102 (2001).
303. Omary, M.B., Ku, N.O., Liao, J. & Price, D. Keratin modifications and solubility properties in epithelial cells and in vitro. *Subcell Biochem* **31**, 105-140 (1998).
304. Baumann, H. & Gauldie, J. The acute phase response. *Immunol Today* **15**, 74-80 (1994).
305. Aggarwal, B.B.*, et al.* Targeting signal-transducer-and-activator-of-transcription-3 for prevention and therapy of cancer: modern target but ancient solution. *Annals of the New York Academy of Sciences* **1091**, 151-169 (2006).
306. Hirano, T., Ishihara, K. & Hibi, M. Roles of STAT3 in mediating the cell growth, differentiation and survival signals relayed through the IL-6 family of cytokine receptors. *Oncogene* **19**, 2548-2556 (2000).
307. Zhong, Z., Wen, Z. & Darnell, J.E., Jr. Stat3: a STAT family member activated by tyrosine phosphorylation in response to epidermal growth factor and interleukin-6. *Science* **264**, 95-98 (1994).
308. Niu, G.*, et al.* Constitutive Stat3 activity up-regulates VEGF expression and tumor angiogenesis. *Oncogene* **21**, 2000-2008 (2002).
309. Real, P.J.*, et al.* Resistance to chemotherapy via Stat3-dependent overexpression of Bcl-2 in metastatic breast cancer cells. *Oncogene* **21**, 7611-7618 (2002).
310. Aoki, Y., Feldman, G.M. & Tosato, G. Inhibition of STAT3 signaling induces apoptosis and decreases survivin expression in primary effusion lymphoma. *Blood* **101**, 1535-1542 (2003).
311. Roytblat, L.*, et al.* Raised interleukin-6 levels in obese patients. *Obes Res* **8**, 673-675 (2000).
312. Khan, A. Detection and quantitation of forty eight cytokines, chemokines, growth factors and nine acute phase proteins in healthy human plasma, saliva and urine. *J Proteomics* (2012).
313. Wilson, L.D., Al-Majid, S., Rakovsky, C. & Schwindt, C.D. Higher IL-6 and IL6:IGF Ratio in Patients with Barth Syndrome. *J Inflamm (Lond)* **9**, 25 (2012).
314. Sehgal, P.B. Interleukin-6: molecular pathophysiology. *J Invest Dermatol* **94**, 2S-6S (1990).
315. Vaisse, C.*, et al.* Leptin activation of Stat3 in the hypothalamus of wild-type and ob/ob mice but not db/db mice. *Nature genetics* **14**, 95-97 (1996).
316. Pankov, R. & Yamada, K.M. Fibronectin at a glance. *Journal of cell science* **115**, 3861-3863 (2002).
317. Roy-Chaudhury, P., Hillis, G., McDonald, S., Simpson, J.G. & Power, D.A. Importance of the tubulointerstitium in human glomerulonephritis. II. Distribution of integrin chains beta 1, alpha 1 to 6 and alpha V. *Kidney International* **52**, 103-110 (1997).
318. Yokoi, H.*, et al.* Role of connective tissue growth factor in fibronectin expression and tubulointerstitial fibrosis. *American journal of physiology. Renal physiology* **282**, F933-942 (2002).
319. Liu, Z.*, et al.* Intracellular signaling via ERK/MAPK completes the pathway for tubulogenic fibronectin in MDCK cells. *Biochemical and Biophysical Research Communications* **353**, 793-798 (2007).
320. Inoue, T., Nabeshima, K., Shimao, Y. & Koono, M. Hepatocyte growth Factor/Scatter factor (HGF/SF) is a regulator of fibronectin splicing in MDCK cells: comparison between the effects of HGF/SF and TGF-beta1 on fibronectin splicing at the EDA region. *Biochemical and Biophysical Research Communications* **260**, 225-231 (1999).
321. Ruoslahti, E. Structure and biology of proteoglycans. *Annu Rev Cell Biol* **4**, 229-255 (1988).
322. Humes, H.D., Cieslinski, D.A., Coimbra, T.M., Messana, J.M. & Galvao, C. Epidermal growth factor enhances renal tubule cell regeneration and repair and accelerates the recovery of renal function in postischemic acute renal failure. *The Journal of Clinical Investigation* **84**, 1757-1761 (1989).
323. Hood, F.E. & Royle, S.J. Functional equivalence of the clathrin heavy chains CHC17 and CHC22 in endocytosis and mitosis. *Journal of cell science* **122**, 2185-2190 (2009).

324. Coda, L.*, et al.* Eps15R is a tyrosine kinase substrate with characteristics of a docking protein possibly involved in coated pits-mediated internalization. *The Journal of biological chemistry* **273**, 3003-3012 (1998).
325. Carbone, R.*, et al.* eps15 and eps15R are essential components of the endocytic pathway. *Cancer research* **57**, 5498-5504 (1997).
326. Indelicato, S.R., Bradshaw, S.L., Chapman, J.W. & Weiner, S.H. Evaluation of standard and state of the art analytical technology-bioassays. *Dev Biol (Basel)* **122**, 103-114 (2005).
327. Gonzalez, J.E., Oades, K., Leychkis, Y., Harootunian, A. & Negulescu, P.A. Cell-based assays and instrumentation for screening ion-channel targets. *Drug Discov Today* **4**, 431-439 (1999).
328. Zhou, H., Hewitt, S.M., Yuen, P.S. & Star, R.A. Acute Kidney Injury Biomarkers - Needs, Present Status, and Future Promise. *Nephrol Self Assess Program* **5**, 63-71 (2006).
329. Nossov, V.*, et al.* The early detection of ovarian cancer: from traditional methods to proteomics. Can we really do better than serum CA-125? *Am J Obstet Gynecol* **199**, 215-223 (2008).
330. Kofoed, K., Schneider, U.V., Scheel, T., Andersen, O. & Eugen-Olsen, J. Development and validation of a multiplex add-on assay for sepsis biomarkers using xMAP technology. *Clin Chem* **52**, 1284-1293 (2006).
331. van Koppen, A.*, et al.* Human Embryonic Mesenchymal Stem Cell-Derived Conditioned Medium Rescues Kidney Function in Rats with Established Chronic Kidney Disease. *PLoS One* **7**, e38746 (2012).
332. Shi, Y. & Massagué, J. Mechanisms of TGF-[beta] Signaling from Cell Membrane to the Nucleus. *Cell* **113**, 685-700 (2003).
333. Border, W.A. & Noble, N.A. TGF-beta in kidney fibrosis: a target for gene therapy. *Kidney International* **51**, 1388-1396 (1997).
334. Peters, H., Border, W.A. & Noble, N.A. Targeting TGF-beta overexpression in renal disease: maximizing the antifibrotic action of angiotensin II blockade. *Kidney International* **54**, 1570-1580 (1998).

Appendix A

Human research ethics committee final approval letter for project reference # 5201100385

Dear Dr Herbert

Re: "Investigation of the properties and secretions of adipose tissue and cells isolated from adipose tissue" (Ethics Ref: 5201100385)

Thank you for your recent correspondence. Your response has addressed the issues raised by the Human Research Ethics Committee and you may now commence your research.

Regarding your query in your response to point 4, the committee recommends that for completeness of research the dataset can ethically be retained (unless specifically requested by the participant when they withdraw from the study)

The following personnel are authorised to conduct this research:

Dr Benjamin Herbert- Chief Investigator/Supervisor
Mr Cameron Hill, Mr Michael Medynskyj, Mr Sinead Blaber, Ms Katherine Wongtrakul-kish
& Ms Rebecca Webster- Co-Investigators

NB. STUDENTS: IT IS YOUR RESPONSIBILITY TO KEEP A COPY OF THIS APPROVAL EMAIL TO SUBMIT WITH YOUR THESIS.

Please note the following standard requirements of approval:

1. The approval of this project is conditional upon your continuing compliance with the National Statement on Ethical Conduct in Human Research (2007).

2. Approval will be for a period of five (5) years subject to the provision of annual reports. Your first progress report is due on 28 June 2012.

If you complete the work earlier than you had planned you must submit a Final Report as soon as the work is completed. If the project has been discontinued or not commenced for any reason, you are also required to submit a Final Report for the project.

Progress reports and Final Reports are available at the following website:

http://www.research.mq.edu.au/for/researchers/how_to_obtain_ethics_approval/human_research_ethics/forms

3. If the project has run for more than five (5) years you cannot renew approval for the project. You will need to complete and submit a Final Report and submit a new application for the project. (The five year limit on renewal of approvals allows the Committee to fully re-review research in an environment where legislation, guidelines and requirements are continually changing, for example, new child protection and privacy laws).

4. All amendments to the project must be reviewed and approved by the Committee before implementation. Please complete and submit a Request for Amendment Form available at the following website:

http://www.research.mq.edu.au/for/researchers/how_to_obtain_ethics_approval/human_research_ethics/forms

5. Please notify the Committee immediately in the event of any adverse effects on participants or of any unforeseen events that affect the continued ethical acceptability of the project.

6. At all times you are responsible for the ethical conduct of your research in accordance with the guidelines established by the University. This information is available at the following websites:

http://www.mq.edu.au/policy/

http://www.research.mq.edu.au/for/researchers/how_to_obtain_ethics_approval/human_research_ethics/policy

If you will be applying for or have applied for internal or external funding for the above project it is your responsibility to provide the Macquarie University's Research Grants Management Assistant with a copy of this email as soon as possible. Internal and External funding agencies will not be informed that you have final approval for your project and funds will not be released until the Research Grants Management Assistant has received a copy of this email.

If you need to provide a hard copy letter of Final Approval to an external organisation as evidence that you have Final Approval, please do not hesitate to contact the Ethics Secretariat at the address below.

Please retain a copy of this email as this is your official notification of final ethics approval.

Yours sincerely
Dr Karolyn White
Director of Research Ethics
Chair, Human Research Ethics Committee